



Ratten iNKT Zellen: Phänotyp und Funktion

Rat iNKT Cells: Phenotype and Function

Doctoral thesis for a doctoral degree at the Graduate School of
Life Sciences, Julius-Maximilians-Universität Würzburg,
Section of Infection and Immunity

Submitted by
Elisa Monzón Casanova
from
Huesca, Spain

Würzburg, 2010

Submitted on:
Office stamp

Members of the *Promotionskomitee*:

Chairperson: Prof. Dr. Thomas Hünig

Primary Supervisor: Prof. Dr. Thomas Herrmann

Supervisor (Second): Prof. Dr. Thomas Müller

Supervisor (Third): Prof. Dr. Thomas Dandekar

Date of Public Defence:

Date of receipt of Certificates:

A mi madre y a mi hermano

Lo orgullosos que están de mí es la mejor recompensa de todas

ACKNOWLEDGMENTS

Foremost I am very thankful to Prof. Dr. Thomas Herrmann for giving me the opportunity to perform my PhD thesis under his supervision. I am very grateful for his support, his encouragement, the freedom he gave me and the stimulating discussions we had. All this was fundamental for overcoming the challenges which appeared during the course of this work.

I am also deeply grateful to Prof. Dr. Thomas Hünig for all his support and for the possibility to be part of the Graduate College Immunomodulation. The ongoing exchange of knowledge between Graduate Students and Project Leaders was very inspiring, constructive and joyful.

I also want to thank Prof. Dr. Birte Steiniger for her tremendous help in addressing the distribution of CD1d and the members of my Supervisory Committee: Prof. Dr. Thomas Müller and Prof. Dr. Thomas Dandekar for their support and suggestions.

I would also like to express my gratitude to the members of the Herrmann's laboratory. Especially to Ingrid Müller, from whom I learnt so much, and also to Lisa Starick; their work is a big part of this thesis. Thanks as well to Jianqiang, Stefanie, Martina, Mohindar, Daniel, Ronald, Tian and all the people who I met during the last six years at the institute. I always experienced a very nice working atmosphere and I especially appreciate the patience that everyone had with me when I had a "rat day".

Finally, I want to use the last sentences to thank my family and friends for their love and support. Unfortunately, there is not enough space to write every name. Nonetheless, I want to especially thank Maria and Ivan, for their friendship and pointing the North when I cannot find it; Ronald, for his support, understanding and company and my mother and my brother, simply, this would have not been possible without them.

TABLE OF CONTENTS

LIST OF FIGURES	6
LIST OF TABLES	7
ABSTRACT	8
ZUSAMMENFASSUNG	11
1 INTRODUCTION	14
1.1 MHC-restricted and non-MHC-restricted T cells.....	15
1.2 CD1d.....	17
1.2.1 CD1 family	17
1.2.2 Expression of CD1d	18
1.2.3 CD1d function: lipid antigen presenting molecule	19
1.3 CD1d-restricted T cells.....	21
1.4 Recognition of α -Gal-CD1d by semi-invariant TCRs.....	22
1.5 iNKT cell development	23
1.6 iNKT cell function.....	24
1.7 iNKT cells in the rat	25
2 MATERIALS AND METHODS	28
2.1 Materials	28
2.1.1 Chemical reagents	28
2.1.2 Media, buffers, solutions	30
2.1.3 Cell lines	32
2.1.4 Animals	33
2.1.5 Vectors	33
2.1.6 Oligonucleotides	35
2.1.7 Antibodies and secondary reagents	39
2.1.8 Enzymes and inhibitors	40
2.1.9 Commercially available kits and mixtures	40
2.1.10 Consumables	41
2.2 Methods	42
2.2.1 Routine molecular biology methods.....	42
2.2.2 Cloning	48

2.2.2.1 Cloning of <i>Mus musculus</i> CD1d2 and <i>Mus spretus</i> CD1d1 into pczCFG5 IEGN	48
2.2.2.2 Cloning of rat CD1d cDNA into pczCFG5 IZ.....	48
2.2.2.3 Cloning of rat β 2-microglobulin into the retroviral expression vector pczCFG5 IZ	48
2.2.2.4 Cloning of mouse CD1d into pXIg.....	48
2.2.2.5 Cloning of rat CD1d into pXIg	49
2.2.2.6 Cloning of rat β 2-microglobulin-CD1d fusion protein into the pFUSE-hIgG1-Fc2 vector	49
2.2.2.7 Cloning of rat CD1d into the pMT/BioHis-IA ^b α vector	50
2.2.2.8 Cloning of rat β 2-microglobulin-CD1d into the pcDNA3.1/V5 His A Bio vector	50
2.2.2.9 Cloning of rat β 2-microglobulin-CD1d into the pMT/BiP/His/Strep TagIII-IA ^b α vector .	50
2.2.2.10 Cloning of AV14-containing TCR α chains.....	51
2.2.3 Production and purification of CD1d oligomers	51
2.2.3.1 Mouse and rat CD1d-IgG dimers	51
2.2.3.2 Rat β 2-microglobulin CD1d human Fc dimers.....	51
2.2.3.3 Rat CD1d production in SC2 drosophila cells.....	52
2.2.3.4 Rat β 2-microglobulin-CD1d production in 293T human cells.....	52
2.2.3.5 Rat β 2-microglobulin-CD1d linked to a streptag production by SC2 drosophila cells	53
2.2.3.6 Protein G affinity chromatography	53
2.2.3.7 Photometric determination of protein concentration.....	53
2.2.3.8 Coomassie Blue staining	54
2.2.3.9 Specific biotinylation	54
2.2.3.10 Lipid loading into CD1d molecules	54
2.2.3.11 Oligomerization of rat β 2-microglobulin-CD1d linked to a streptag	54
2.2.4 Immunoprecipitation.....	55
2.2.5 Western blot analysis	55
2.2.5.1 Binding capacities of anti-CD1d mAbs under reducing and non-reducing conditions	55
2.2.5.2 Binding of 233 and 35 mAbs to mouse and rat CD1d.....	56
2.2.5.3 Western blot of proteins derived from rat tissues.....	56
2.2.6 CD1d Sandwich ELISA	56
2.2.7 Routine cell culture methods	57
2.2.7.1 Cell culture.....	57
2.2.7.2 Freezing and thawing	57
2.2.7.3 Preparation of primary single cell suspensions.....	58
2.2.7.3.1 Single cell suspension from thymus and spleen	58
2.2.7.3.2 Intrahepatic lymphocytes preparation.....	58

2.2.7.3.3 Isolation of peripheral blood cells.....	59
2.2.7.3.4 Isolation of peripheral mononuclear blood cells	59
2.2.8 Primary cell cultures	60
2.2.8.1 Stimulation assays and analysis of cytokine release	60
2.2.8.2 Seven-days intrahepatic lymphocytes cultures	60
2.2.8.3 Rat IL-4 ELISPOT assay.....	60
2.2.9 Transfection of 293T cells	60
2.2.10 Retroviral transduction	62
2.2.11 Immunofluorescence and flow cytometry	62
2.2.12 Statistical analysis	63
3 RESULTS	64
3.1 Further characterization of rat CD1d specific mAbs.....	64
3.1.1 Determination of V (D) J gene segment usage	64
3.1.2 mAb reactivity in immunoprecipitation and Western blot analyses.....	65
3.1.3 Epitope mapping	67
3.1.4 CD1d ELISA	70
3.2 Analysis of CD1d expression using mAbs 233 and 35	71
3.2.1 CD1d in different inbred rat strains.....	72
3.2.1.1 Identification of two rat CD1d alleles	72
3.2.1.2 Analysis of CD1d expression among different rat strains	73
3.2.1.3 CD1d expression in hematopoietic cells: Direct comparison between rat and mouse	73
3.2.1.4 CD4 expression by rat MZ B cells	78
3.2.1.5 CD1d expression in rat and mouse non-lymphatic organs	78
3.3 Analysis of CD1d-restricted immune response with the 233 and 35 mAbs.....	81
3.4 Rat iNKT cell identification	82
3.4.1 Production of CD1d oligomers	84
3.4.1.1 Mouse and rat CD1d-IgG dimers	84
3.4.1.2 Rat β 2m-CD1d-hFc dimers.....	84
3.4.1.3 Rat CD1d constructs for streptavidin based multimerization.....	85
3.4.1.4 Rat β 2m-CD1d-streptag	86
3.4.1.5 Efficient loading of CD1d with α -Gal	86
3.4.2 Binding of diverse CD1d oligomers to rat semi-invariant TCR.....	87
3.4.3 Binding of mouse and rat CD1d dimers to iNKT cells of either species.....	88

3.4.4 Phenotype of rat iNKT cells	90
3.5 iNKT cell frequencies in various rat strains	91
3.5.1 iNKT cells in F344 and LEW rats	92
3.5.2 Expression of AV14-AJ18 rearrangements in F344 and LEW rats	95
3.6 Analysis of AV14 gene family in the rat	97
3.6.1 Analysis of AV14 TCR α chains in F344 rats	101
3.6.2 AV14 and AJ18 gene segment usage in F344 and LEW rats	102
3.7 α -Gal responsiveness in the rat	108
3.7.1 Cytokine release in <i>ex vivo</i> cultures: Comparison of 5 different inbred rat strains	108
3.7.2 Analysis of F344 x LEW F1 generation	113
3.7.3 Analysis of C57BL/6	113
3.7.4 iNKT cell expansion in F344 but not in LEW and C57BL/6 IHL-cultures	114
3.8 Analysis of NKR-P1 and TCR expression in different rat strains	117
3.8.1 Analysis of NKR-P1 expression among T and non-T cells	118
3.8.2 CD4 and CD8 distribution among NKR-P1 ⁺ TCR ⁺ cells	120
3.8.3 BV chain usage among NKR-P1 ⁺ TCR ⁺ cells	121
3.8.4 CD4 and CD8 distribution among BV8 or BV16 expressing NKR-P1 ⁺ T cells	123
4 DISCUSSION	125
4.1 Further characterization of CD1d monoclonal antibodies	125
4.2 CD1d in the hematopoietic system	128
4.4 Rat CD1d as antigen presenting molecule	132
4.5 CD4 expression by MZ B cells	132
4.6 Production of rat CD1d oligomers	133
4.7 Species specificity of α -Gal-CD1d recognition by mouse and rat iNKT cells ...	134
4.8 Distribution and phenotype of rat iNKT cells	138
4.8.1 NKR-P1 expression	141
4.8.2 CD4 and CD8 distribution	143
4.8.3 BV usage	144
4.8.4 Activation markers	145
4.9 AV14 gene segment usage in the rat	146
4.10 α -Gal responsiveness in the rat	148
4.11 NKR-P1 ⁺ T cells	151
REFERENCES	154

ABBREVIATIONS	174
CURRICULUM VITAE	176
AFFIDAVIT	180

LIST OF FIGURES

Figure 1 Immunoprecipitation of biotinylated surface proteins with 233, 35, 58 or isotype control antibodies	66
Figure 2 Western blot analyses with 233, 35 and 58 mAbs	66
Figure 3 Epitope mapping of anti-CD1d mAbs	69
Figure 4 CD1d ELISA	71
Figure 5 Nucleotide and amino acid sequences of the two rat CD1d alleles identified in this study	72
Figure 6 CD1d cell surface expression in different inbred rat strains	73
Figure 7 Comparison of CD1d expression by rat and mouse primary cells	74
Figure 8 Comparison of CD1d expression by rat and mouse thymocytes	74
Figure 9 CD1d expression by B and T cells analyzed by multicolor flow cytometry	75
Figure 10 Relative CD1d expression by CD4 and CD8 positive T cells analyzed by multicolor flow cytometry	76
Figure 11 CD1d and CD4 expression by MZ B cells, dendritic cells and macrophages from the spleen ..	77
Figure 12 CD1d distribution in non-lymphatic tissues	80
Figure 13 Effects of mAbs 233 and 35 on CD1d antigen presentation to iNKT cells	81
Figure 14 CD1d recombinant proteins	83
Figure 15 Efficient glycolipid loading of CD1d dimers	87
Figure 16 Reactivity of CD1d oligomers from different species against rat semi-invariant TCR	88
Figure 17 Interspecies cross-reactivity of mouse and rat CD1d-IgG dimers	89
Figure 18 Phenotype of rat iNKT cells	91
Figure 19 iNKT cell frequencies in F344 and LEW rats	94
Figure 20 β -actin, iTCR α , AV14 TCR α and BV8 TCR β mRNA expression by F344 and LEW thymocytes, splenocytes and IHLs	96
Figure 21 Relative quantification of iTCR α mRNA among total TCR α chain mRNA	97
Figure 22 Nomenclature of rat AV14 gene segments	100
Figure 23 AV14 gene segments	101
Figure 24 Cloned AV14 TCR α chains	101
Figure 25 AJ gene segment usage by AV14-comprising TCR α chains	105
Figure 26 Analysis of nucleotides contained in the junctional regions of AV14-AJ18 TCR α chains ...	106
Figure 27 AV14 gene segments usage by AV14 and AV14-AJ18-containing TCR α chains	107
Figure 28 IL-4 and IFN- γ release by splenocytes and IHLs	111
Figure 29 IL-4 ELISPOT analyses of primary splenocytes and IHLs cultures of five different inbred rat strains	112
Figure 30 IL-4 release by splenocytes and IHLs <i>ex vivo</i> cultures of F344 and LEW F1 generation ...	113
Figure 31 Cytokine production in <i>ex vivo</i> cultures of splenocytes and IHLs from C57BL/6 mice	113
Figure 32 Primary F344, LEW and C57BL/6 IHLs cultures	115
Figure 33 After culture in the presence of α -Gal iNKT cells are expanded when primary IHLs are derived from F344 but not from LEW rats	116
Figure 34 BV usage and CD4/CD8 β distribution among cultured iNKT cells	117
Figure 35 iNKT cells are a very small population compared to NKR-P1 ⁺ T cells	118
Figure 36 NKR-P1 and TCR expression by thymocytes, splenocytes and intrahepatic lymphocytes in five different inbred rat strains	119
Figure 37 CD4 and CD8 β expression by NKR-P1 positive and negative F344 T cells	121
Figure 38 BV usage by NKR-P1 positive and negative F344 T cells	122
Figure 39 Amino acid sequences of human, mouse and rat CD1d, variable domains of invariant TCR α chains and various β chains	137

LIST OF TABLES

Table 1 Antibodies used in FACS stainings or Westernblot	39
Table 2 Secondary antibodies used in FACS stainings or Westernblot analyses	40
Table 3 Reagents used for the detection of biotin/Strep-tag conjugated antibodies or molecules	40
Table 4 Primers used in RT-PCR analyses of AV14- and AV14-AJ18-containing TCRs	44
Table 5 Gene segment usage of the heavy and light chains of the five studied hybridomas	65
Table 6 TCR ⁻ cells expressing various levels of NKR-P1 in the thymus, spleen and IHLs of five different inbred rat strains	120
Table 7 CD4 and CD8 β distribution among NKR-P1 positive and negative T cells	121
Table 8 R78 ⁺ and HIS42 ⁺ cells among NKR-P1 positive and negative T cells	122
Table 9 Frequencies of R78 ⁺ or HIS42 ⁺ cells among the indicated T cell subsets in the spleen (Spl) or liver (IHLs)	123
Table 10 CD4 and CD8 β distribution in R78 ⁺ or HIS42 ⁺ NKR-P1 positive and negative T cells	124

ABSTRACT

iNKT cells are a population of T cells with unique characteristics. In contrast to most $\alpha\beta$ T cells which recognize peptides presented by highly polymorphic MHC molecules, iNKT cells are reactive to glycolipids presented by CD1d, a non-polymorphic MHC-I like molecule. Moreover, whereas MHC-restricted $\alpha\beta$ T cells bear highly variable receptors (TCRs) formed after somatic recombination of the V(D)J gene segments, the TCR of iNKT cells is formed by an invariant α chain, which always contains the same gene segments: AV14 and AJ18; and a β chain of limited BV gene usage: BV8S2, BV7 or BV2, in the mouse. This invariant α chain is the reason for which these cells are named “i” and the NK part of their name refers to the expression of receptors typical of natural killer (NK) cells. iNKT cells recognize glycolipids of endogenous and microbial origin. After activation they secrete large amounts of very different cytokines such as IFN- γ and IL-4 and thus influence immune responses and pathological conditions. One of the most potent iNKT cell agonists, recognized by the semi-invariant TCR, is the synthetic glycolipid α -Galactosylceramide (α -Gal). iNKT cells can be visualized using CD1d-multimeric complexes loaded with α -Gal and flow cytometry, since this reagent has enough avidity to stain these cells. Interestingly, mouse iNKT cells can be stained with human α -Gal-loaded CD1d oligomers and human iNKT cells can also be visualized with mouse α -Gal-loaded CD1d oligomers, indicating a high degree of conservation of the recognition of α -Gal presented by CD1d through evolution.

Previous studies showed that rats have the genes necessary to build semi-invariant TCRs: They have a CD1d homologue; one or two BV8S2 homologues and interestingly, up to ten AV14 gene segments, which are highly conserved when compared to the mouse genes. Importantly, it has been shown at least for two of these AV14 gene segments that they can produce invariant TCR α chains which, when co-expressed with BV8-containing β chains, react to α -Gal presented by rat CD1d. Furthermore, *ex vivo* stimulation of primary splenocytes with α -Gal results in the secretion of IL-4 and IFN- γ . Surprisingly, rat semi-invariant TCRs do not recognize α -Gal presented by mouse CD1d and accordingly, mouse α -Gal-loaded CD1d tetramers failed to stain a discrete population of rat iNKT cells. Taking all together, despite that strong evidence suggested that iNKT cells are present in the rat, the direct identification of such population and the analysis of CD1d-restricted immune responses were still pending for this species. Hence the work presented in this doctoral thesis was aimed to

identify iNKT cells, to analyze their phenotype and also to study the distribution and function of CD1d in the rat. For these purposes, we produced essential reagents which were still lacking such as rat specific anti-CD1d monoclonal antibodies and rat CD1d oligomers.

Importantly, two of three anti-rat CD1d monoclonal antibodies (all of them generated in our laboratory before this thesis was initiated) also recognized mouse CD1d and therefore allowed a direct comparison of CD1d expression between rat and mouse. Whereas CD1d distribution in the hematopoietic system was found to be extremely similar between these two species; in non-lymphatic tissues important differences were observed. Interestingly, CD1d protein was detected at not yet described sites such as the rat exocrine pancreas and rat and mouse Paneth cells. These monoclonal antibodies did not only allowed the analysis of CD1d expression, but also the first demonstration of the function of rat CD1d as an antigen presenting molecule, since cytokine release in response to α -Gal was blocked when they were added to *ex vivo* cultures of rat primary cells.

Staining of primary rat iNKT cells (possible now with the newly generated rat CD1d oligomers) revealed interesting similarities with human iNKT cells. First, we observed that rat iNKT cells are only a minority among all NKR-P1A/B positive T cells. Human iNKT cells constitute also a very small proportion of NKR-P1A (CD161) expressing T cells, whereas in mice inbred strains which express NKR-P1C (NK1.1), most of NKR-P1C expressing T cells are iNKT cells. Second, the majority of rat iNKT cells are either CD4 or DN and only a small proportion expresses CD8 β . These findings are similar to humans and different to mice which lack CD8⁺ iNKT cells. Third, analysis of various inbred rat strains demonstrated different iNKT cell frequencies which correlated with cytokine secretion after α -Gal stimulation of primary cells. In comparison to mice, iNKT cell numbers are markedly reduced in rats. In F344 rats, inbred rat strain which released the highest cytokine amounts after α -Gal stimulation, approximately 0.25% and 0.1% of total liver and spleen lymphocytes, respectively, are iNKT cells. In contrast, in LEW rats iNKT cells were practically absent and neither IL-4 nor IFN- γ were detected after stimulation of primary cells with α -Gal. Once more, these frequencies are very close to those observed in humans. Last, as reported for human peripheral blood cells, rat iNKT cells could be easily expanded *in vitro* by adding α -Gal to cultures of intrahepatic lymphocytes, whereas the expansion of mouse iNKT cells was not possible using the same protocol.

The presence of a multimember AV14 gene segment family in the rat is an intriguing characteristic. These AV14 gene segments are extremely homologous except in the CDR2 α region. Based on the amino acid sequence of this region they have been divided into two different types: Type I and II. A specific tissue distribution of the different types was proposed in the first study where the presence of several AV14 gene segments was described. We also analyzed the AV14 gene segment usage in F344 and LEW inbred rat strains. In F344 rats we found no preferential usage of either AV14 gene segment type in the spleen and the liver but type II AV14 gene segments appeared more frequently in the thymus. In contrast, LEW rats show a preferential usage of type I AV14 gene segments in all three compartments analyzed: Thymus, spleen and liver.

Taken all together, the usage of newly generated reagents allowed to gain novel insights into CD1d expression in the rat and in the mouse and to directly identify rat iNKT cells for the first time. The phenotypic and functional analysis of rat iNKT cells revealed numerous similarities with human iNKT cells. These are of special interest, since rats serve to investigate several pathological conditions including models for autoimmune diseases. The possibility now to analyze iNKT cells and CD1d-restricted T cell responses in the rat might help to understand the pathogenesis of such diseases. In addition, the uncomplicated *in vitro* expansion and culture of rat iNKT cells should facilitate the analysis of the immunomodulatory capacities of these cells.

ZUSAMMENFASSUNG

iNKT Zellen sind eine Population von T Zellen mit einigen Besonderheiten. Anders als die meisten $\alpha\beta$ T Zellen, deren T Zell Rezeptoren (TZRs) für von hochpolymorphen MHC Molekülen präsentierte Peptide spezifisch sind, erkennen iNKT Zellen Glycolipide die von CD1d, einem nicht polymorphen MHC-I artigen Moleküle, präsentiert werden. Während MHC-restringierte $\alpha\beta$ T Zellen sehr unterschiedliche TZRs haben, die nach somatischer Rekombination der V(D)J Gensegmente generiert werden, besteht der TZR der iNKT Zellen aus einer invarianten α Kette und einer β Kette mit einem limitierten BV Gen Repertoire (BV8S2, BV7 und BV2 in Maus). Die invariante α Kette, auf die das i im Namen der iNKT Zellen verweist, enthält in der Maus immer AV14 und AJ18 kodierte V-Regionen. Das NK in ihrem Namen verweist darauf, dass sie häufig NK-Zell typische Oberflächenmoleküle exprimieren. iNKT Zellen erkennen Glycolipide endogenen und mikrobiellen Ursprungs und sezernieren nach Aktivierung große Mengen verschiedener Zytokine wie zum Beispiel IL-4 und IFN- γ . Auf diese Weise beeinflussen sie Immunantwort und pathologische Zustände. Eine der potentesten iNKT-Zell-TZR Agonisten ist das α -Galactosylceramid (α -Gal) und α -Gal beladene CD1d-Multimere ermöglichen es iNKT Zellen zu färben und mittels Durchflusszytometrie sichtbar zu machen. Die hohe Konservierung der iNKT TZR-CD1d Interaktion ermöglicht es sogar, Maus iNKT Zellen mittels α -Gal beladenen humanen CD1d-Multimere zu färben.

Vorhergehende Studien zeigten, dass Ratten die notwendigen Gene für die Generierung der semi-invarianten TZR haben: Sie besitzen ein CD1d Homolog, ein oder zwei BV8S2 Homologe und bis zu zehn AV14 Gensegmente, die im Vergleich zu den Maus-AV14 Genen hoch konserviert sind. Mehrere dieser AV14 Gensegmenten wurden mit AJ18 zusammen rearrangiert gefunden und für mindestens zwei dieser invarianten α Ketten wurde gezeigt, dass sie zusammen mit BV8 enthaltenden β Ketten TZR bilden, die von CD1d präsentierte α -Gal erkennen. Weiterhin wurde gezeigt, dass primäre Ratten- Milzzellen und intrahepatische Lymphozyten nach Kultur mit α -Gal IL-4 und IFN- γ sezernieren. Auf Grund dieser Befunde und der starken Konservierung der CD1d Gene und der Gene, die die semi-invarianten TZR kodieren, überrascht es, dass keine definierte Zellpopulation von intrahepatischen Rattenlymphozyten mittels α -Gal beladenen Maus CD1d-Tetrameren gefärbt wurde. Zusammengefasst kann gesagt werden, dass die direkte Identifizierung der Zellen und die Analyse der CD1d-

restringierten Immunantworten in der Ratte noch ausstand, obwohl es starke Hinweise für die Existenz der iNKT Zellen in dieser Art gab. Infolgedessen sind die Ziele dieser Arbeit: die Identifizierung der Ratten iNKT Zellen, die Analyse ihres Phänotyps und die Untersuchung der CD1d-restringierten Immunantworten. Um diese Ziele zu erreichen, wurden noch fehlende essentielle Reagenzien hergestellt, wie die ersten Ratten-CD1d spezifischen monoklonalen Antikörper und Ratten CD1d Oligomere.

Zwei der drei charakterisierten monoklonalen Antikörpern erkennen sowohl Ratten CD1d als auch Maus CD1d. Dies ermöglichte den direkten Vergleich der CD1d Expression zwischen beiden Spezies (diese Antikörper wurden in unserem Labor vor dem Anfang dieser Doktorarbeit hergestellt). Während die CD1d Verteilung im hämatopoetischen System beider Arten äußerst ähnlich ist, wurden in nicht lymphatischen Geweben sehr starke Unterschiede gefunden. Interessanterweise wurde das CD1d Protein auch an noch nicht beschriebenen Stellen wie im exokrinen Pankreas der Ratte und in Paneth Zellen von Maus und Ratte beobachtet. Die monoklonalen Antikörper erlaubten nicht nur die Analyse der CD1d Verteilung, sondern auch den Beweis der Funktion von CD1d als Antigen präsentierendes Molekül, weil die Zugabe der Antikörper zu *ex vivo* Kulturen von primären Zellen die Sekretion von Zytokinen bei der Stimulation mit α -Gal hemmt.

Färbungen von primären Ratten iNKT Zellen, jetzt möglich durch die neu generierte Ratten CD1d-Dimere, zeigten interessante Gemeinsamkeiten mit humanen iNKT Zellen. Es wurde erstens beobachtet, dass Ratten iNKT Zellen nur eine Minderheit unter allen NKR-P1A/B positiven T Zellen sind. Dies ähnelt den humanen iNKT Zellen, die ebenfalls auch nur ein sehr kleinen Teil der NKR-P1A (CD161) exprimierenden T Zellen stellen, während in Mausstämmen, die NKR-P1C (NK1.1) exprimieren, die Mehrheit der NKR-P1C positiven T Zellen iNKT Zellen sind. Zweitens sind die meisten Ratten iNKT Zellen CD4 positiv oder doppelt negativ während nur ein kleiner Anteil CD8 β exprimiert. Diese Befunde gleichen denen mit humanen iNKTs und unterscheiden sich von Maus iNKTs, die immer CD8 β negativ sind. Drittens zeigt die Analyse von verschiedenen Rattenstämmen, ähnlich wie beim Menschen, 10-100 fach geringere Frequenzen von iNKT Zellen als in der Maus. In F344 Ratten sind etwa 0.25% aller Lymphozyten in der Leber und etwa 0.1% aller Milzzellen iNKT Zellen. Wobei dies der Rattenstamm ist, der die größte Mengen an Zytokinen nach α -Gal Stimulation produziert. In LEW Ratten, die keine Zytokine nach α -Gal Stimulation produzierten, konnten iNKT Zellen praktisch nicht gefärbt werden. Schließlich konnten,

wie bei humanen peripherischen Blutzellen beobachtet, Ratten iNKT Zellen durch alleinige Zugabe von α -Gal *in vitro* expandiert werden, während dies mit Maus iNKT Zellen nicht möglich war.

Eine faszinierende bislang nur in der Ratte gemachte Beobachtung ist die Existenz einer AV14 Multigenfamilie, deren Mitglieder bis auf die CDR2 kodierende Region hochhomolog sind. Basiert auf der Aminosäuresequenz dieser Region wurde diese Familie in zwei Gruppen aufgeteilt: Typ I und II. Die erste Studie, in der diese zwei verschiedenen Typen beschrieben wurden, schlug eine spezifische Gewebsverteilung von AV14 positiven TCR vor. Wir haben ebenfalls die Benutzung dieser AV14 Gene in F344 und LEW Inzuchtrattenstämmen analysiert und gefunden, dass es in F344 Leber und Milz keine Präferenz für einen bestimmten AV14 Typ gibt. Jedoch wurde der Typ II häufiger in F344 Thymus gefunden. Im Vergleich zeigen LEW Ratten eine bevorzugte Benutzung des Typ I in allen analysierten Geweben (Thymus, Milz und Leber).

Zusammengefasst kann gesagt werden, dass diese Studie mit Hilfe neu generierter Reaganzien neue Erkenntnisse zur CD1d Expression in Ratte und Maus gewonnen wurden und erstmals eine direkte phänotypische und funktionelle Analyse von iNKT Zellen der Ratte durchgeführt wurde. Es wurden eine Reihe von Gemeinsamkeiten zwischen iNKT Zellen von Ratte und Mensch gefunden. Diese sind vor allem deshalb von Interesse, da das Versuchstier Ratte für eine Reihe von Autoimmunkrankheiten und andere pathologische Zustände als Modellorganismus dient. Es ist zu erwarten, dass weitere Untersuchungen von CD1d-restringierten Zellen der Ratte neue Einsichten in die Genese dieser Krankheiten ermöglicht. Darüberhinaus sollte die in der Ratte beobachtete einfach durchzuführende *in vitro* Kultur und Expansion von iNKT Zellen eine Analyse ihrer immunmodulatorischen Eigenschaften deutlich erleichtern.

1 INTRODUCTION

The immune system protects an organism from infections via many different mechanisms. Immune responses have typically been divided into two types: innate and adaptive, based on the need of a previous exposure to the microorganism and the time required to elicit a response. Innate immune responses are very fast and are generally triggered after recognition of typical structures shared by many microorganisms such as cell-wall components like lipopolysaccharide. In contrast, adaptive immunity needs a certain time to develop and has an exquisite capacity to distinguish between very similar microbes and molecules. One additional characteristic of adaptive immune responses is the development of memory responses, which imply a much more rapid and efficient response in the subsequent occasions in which the organism encounters the same infectious agent.

Both, innate and adaptive immune responses have cellular and soluble components. Typical cells of the innate immune system are natural killer cells, which after sensing various alterations of the host cells elicit strong cytolytic signals which “kill” them and phagocytes such as macrophages and neutrophils, which ingest and eliminate pathogens. The exquisite specificity of the adaptive immune responses is achieved with receptors and soluble molecules (antibodies) of enormous variability encoded by DNA sequences which are not present in the germline DNA but which are produced after somatic recombination. Basically, there are two different cell types capable of generating such non-germline encoded molecules: B and T cells, which differ considerably in their modes of action. B cells produce antibodies which are secreted forms of their surface receptors. Once secreted, antibodies recognize structures of the pathogens (antigens) and after binding can neutralize the infectivity of the microbes or target (opsonize) them for elimination by various mechanisms. Immunity mediated by antibodies is known as humoral immunity. In contrast, the responses elicited by T cells are regarded as cellular immunity. T cells eliminate or help to eliminate pathogens such as virus which survive and proliferate inside the host cells.

The division between innate and adaptive immunity has also helped to study the complex immune system. Nonetheless, the same cells, molecules and mechanisms very often have functions in both responses. One example are natural killer (NK) cells, which are a main component of the innate immune system but also exert effector functions in adaptive immune responses such as in antibody-dependent cell-mediated cytotoxicity.

Moreover, some cells which by definition belong to the adaptive branch because they express non-germline encoded receptors, such as iNKT cells or B1-B cells may have innate-like modes of action as described later in more detail.

1.1 MHC-restricted and non-MHC-restricted T cells

The antigen receptors of T cells are formed by two chains. Based on the molecules which form these T cell receptors (TCR) there are two types of T cells: $\alpha\beta$ T cells, which bear a TCR formed by an α and a β chain, and $\gamma\delta$ T cells, which bear a TCR formed by a γ and a δ chain. The enormous variability of these receptors is achieved after somatic recombination of various gene segments: variable (V), diversity (D) and joint (J), which encode the domains which will contact the antigen, namely, the variable domains. These variable domains of the α and γ chains are formed by VJ rearrangements and of β and δ by VDJ. The potential variability of these receptors is enormous since there are multiple copies of each gene segment which encode different amino acid sequences and in addition, non-germline encoded nucleotides are introduced during somatic recombination in the junctional regions of these rearranged genes. The most different amino acid residues of the different gene segments are localized in specific regions named complementarity-determining region (CDR). There are three CDRs in each TCR chain: CDRs 1 and 2 are encoded by the V gene segment and the CDR3 is the result of VJ or VDJ recombination.

In contrast to B cells whose receptors can directly recognize antigens, $\alpha\beta$ T cells recognize antigens which have previously been processed and which are presented by specialized molecules called antigen presenting molecules. Since TCRs are products of non-germline encoded DNA sequences, T cells bearing newly generated TCRs have to be selected in such a way that they will recognize self-antigen presenting molecules (positive selection and restriction) but will not react against self-derived molecules (negative selection). Although the mechanisms behind are not as well understood as for T cells, B cells also undergo negative selection.

The restriction elements of T cells can be encoded or not in the major histocompatibility complex (MHC) and depending on which is their restriction element T cells can be further subdivided. These different subtypes also have very different functions which are reflected in very different phenotypes. The first division that can be made is between MHC-restricted and non-MHC-restricted T cells, meaning T cells which are restricted by an element which is encoded in the MHC (MHC-restricted) or which is not (non-

MHC-restricted). The first antigen presenting molecules which were identified are classical major complex histocompatibility (MHC) molecules (Zinkernagel and Doherty, 1974), but in the last two decades, other molecules capable of presenting antigens such as CD1, HLA-E (H2-Qa1 in the mouse), or MR1 have also been reported (Rodgers and Cook, 2005).

Classical MHC molecules present peptides to T cells. There are two different types of these classical MHC molecules: class I and class II (henceforth referred simply as MHC-I and MHC-II). In addition, there are several molecules of each class which are in general encoded by highly polymorphic genes. These molecules are codominantly expressed, resulting in a very high variety of molecules expressed at the cell surface which present many different peptides. MHC-I molecules present cytoplasm-derived peptides to CD8⁺ T cells, which mainly exert cytolytic functions and are therefore commonly referred as cytotoxic T lymphocytes (CTLs). In contrast, MHC-II present peptides derived from extracellular compartments which enter the endocytic-lysosomal route to CD4⁺ T cells. CD4⁺ T cells are also known as T helper (Th) cells, because they “help” other cells to elicit their effector functions by releasing soluble products or by direct interaction of their cell-surface molecules with cell-surface molecules on the antigen presenting cell. One example among many of this help is the IFN- γ secreted by Th cells which stimulates macrophages to eliminate ingested pathogens. CD4⁺ T cells as well as CD8⁺ T cells can be further subdivided into more subsets depending on the products they release and the effector functions they have.

There are other $\alpha\beta$ T cells which are restricted to other MHC molecules (non-classical) encoded in the MHC such as HLA-E in humans and H2-M3 in mice. These MHC-molecules are regarded as non-classical MHC molecules and present peptides of very particular sources, such as signal peptides from MHC-I molecules (Rodgers and Cook, 2005). Interestingly, HLA-E is also recognized by CD94/NKG2 receptors and is involved in regulating NK-cell-mediated cytotoxicity (Braud et al., 1998).

Under the definition of non-MHC-restricted T cells falls any T cell which is not restricted to antigen presenting molecules encoded in the major histocompatibility complex and therefore this group is enormously heterogeneous, containing $\gamma\delta$ T cells, MR1-restricted mucosal-associated invariant T cells (MAIT cells) and CD1-restricted T cells. Interestingly, despite heterogeneity of this group these T lymphocytes share some important characteristics which can be regarded as typical of innate responses: i) in contrast to MHC-restricted T cells, which as result from somatic recombination and

positive and negative selection the TCR repertoires are expected to contain $\sim 2 \times 10^6$ and $\sim 2 \times 10^7$ different specificities in mice and humans, respectively (Arstila et al., 1999; Casrouge et al., 2000), non-MHC-restricted T cells bear invariant or semi-invariant TCRs formed by particular gene segments and often also invariant joining regions, making these receptors similar to pattern recognition receptors. ii) non-MHC-restricted T cells are activated very rapidly within hours after first antigen encounter, in contrast to MHC-restricted T cells which first undergo clonal expansion, a process which takes days and iii) these cells home to particular tissues, which are the first line of defense against pathogens such as the skin and the intestinal mucosa.

1.2 CD1d

1.2.1 CD1 family

Similar to MHC-I, CD1 molecules are glycoproteins expressed at the cell surface, which are non-covalently associated with $\beta 2$ -microglobulin and possess an antigen binding groove formed by two of their three extracellular domains: $\alpha 1$ and $\alpha 2$. Despite these structural similarities with MHC class I molecules, they considerably differ in other aspects (Brigl and Brenner, 2004; Kasmar et al., 2009; Silk et al., 2008): i) CD1d molecules are rather non-polymorphic whereas classical MHC class I molecules are highly polymorphic, ii) CD1d proteins bind and present antigens containing a lipid or other hydrophobic moieties while MHC class I molecules accommodate and present peptides, iii) so far, CD1 genes have only been identified in mammals and chicken, while MHC class I genes are present in all jawed vertebrates and iv) whereas MHC-I molecules are rather similar to each other with respect to function and expression, CD1 genes and molecules differ remarkably between each other and between species in number, expression pattern, type of presented antigens and mode of antigen loading.

In humans, the CD1 gene family is composed of five members (*CD1A*, *-B*, *-C*, *-D* and *-E*) which are subdivided into two groups based on the amino acid sequence similarity of the $\alpha 1$ and $\alpha 2$ domains of the encoded proteins (Calabi et al., 1989). *CD1a*, *-b*, and *-c* belong to group 1; *CD1d* is the only member of group 2 and *CD1e* cannot clearly be assigned to either group. In contrast, mice and rats possess only representatives of group 2: mice have two *CD1d* orthologues (*CD1d1* and *CD1d2*) (Bradbury et al., 1988) and rats have one (Ichimiya et al., 1994; Kasmar et al., 2009; Katabami et al., 1998). During the past ten years, the role of CD1 proteins, except for *CD1e*, as molecules presenting

lipid antigens to T cells has been well established (Brigl and Brenner, 2004; de la Salle et al., 2005; Kasmar et al., 2009; Silk et al., 2008).

1.2.2 Expression of CD1d

CD1d is expressed in the hematopoietic system but also in non-lymphatic tissues such as the liver. Interestingly, its distribution varies between different species (Brigl and Brenner, 2004). In humans its expression in the hematopoietic system is more restricted than in mice. Monocytes and circulating B cells express low levels of CD1d at the cell surface, whereas among resting mature T cells CD1d is hardly detectable at the cell surface although it seems to be intracellularly-stored after stimulation with phytohemagglutinin (PHA) (Exley et al., 2000; Salamone et al., 2001). Nonetheless, the low levels of CD1d detected on monocytes seem to be sufficient to present α -galactosylceramide (α -Gal) and promote proliferation of a T cell line (Spada et al., 2000). In contrast to mature T cells, human cortical thymocytes express high levels of CD1d (Exley et al., 2000). In the mouse hematopoietic system CD1d1 is constitutively expressed although surface expression levels vary among different cell types: Dendritic cells, macrophages and marginal zone (MZ) B cells are the cells with highest levels, followed by B cells and cortical thymocytes and subsequently, by mature T cells (Brossay et al., 1997; Park et al., 1998; Roark et al., 1998). Of the two CD1d genes present in mice, CD1d2 is only expressed on thymocytes and is of limited functionality with respect to antigen presentation and T cell selection (Chen et al., 1999). Notably, in C57BL/6 mice a frame shift mutation prevents CD1d2 surface expression (Park et al., 1998). Thus the functional orthologue is CD1d1.

In humans, CD1d expression outside the hematopoietic system has been detected in parenchymal cells, vascular smooth muscle cells and epithelial cells in organs such as the liver, kidney and gut (Canchis et al., 1993). Moreover, it also has been detected in Schwann cells of the peripheral nervous system (Im et al., 2006) and in the skin (Bonish et al., 2000). Interestingly, CD1d levels are increased under some pathological conditions such as psoriasis and atherosclerosis (Bonish et al., 2000; Melian et al., 1999). In mice, the expression in non-lymphatic organs such as liver and lung has also been reported (Bradbury et al., 1988; Brossay et al., 1997; Mosser et al., 1991). However, in other tissues like the intestine, the precise localization of CD1d molecules is still a matter of debate (Brigl and Brenner, 2004). In spite of this, a recent study by Blumberg and colleagues has demonstrated the importance of CD1d expression for gut

function since pathogenic and non-pathogenic bacterial intestinal colonization of CD1d-deficient mice was increased in comparison to wild type mice (Nieuwenhuis et al., 2009). Paneth cells, in which CD1d mRNA has been detected by *in situ* hybridization (Lacasse and Martin, 1992), play a crucial role in controlling intestinal homeostasis. Localized at the bottom of the crypts of Lieberkühn, these specialized cells control the microbiota content by secreting antimicrobial peptides (defensins) into the intestinal lumen. Interestingly, Blumberg and colleagues also showed that in CD1d knockout mice, compared to wild type mice, the morphology and content of the secretory granules of Paneth cells were altered, and more importantly, that degranulation of these cells was defective.

The actual knowledge about rat CD1d expression is based on experiments using reverse transcription-polymerase chain reaction (RT-PCR), *in situ* hybridization or polyclonal antiserum. These studies found CD1d to be widely distributed within and outside the hematopoietic system and, as in mice, high levels of CD1d mRNA were detected in Paneth cells (Ichimiya et al., 1994; Kasai et al., 1997). In two additional studies mAbs originally generated against mouse CD1d have been reported to cross-react with rat CD1d. In the first study, the rat IgMs 1H1 and 3C11 (Bleicher et al., 1990) were shown to bind a CD1d-like molecule which was detected in the liver but not in the thymus (Burke et al., 1994). In the second study, reactivity of mAb 3H3 with rat thymocytes and splenocytes was reported but not further investigated (Mandal et al., 1998). Hence, prior to our study, appropriate monoclonal antibodies for the analysis of CD1d expression and function in this species were still missing.

1.2.3 CD1d function: lipid antigen presenting molecule

As mentioned, CD1d function is to present lipids to T cells. CD1d-restricted T cells often, but not always, express receptors shared with natural killer (NK) cells and are therefore named NKT cells (Godfrey et al., 2004). As described in more detail in the introduction section 1.3, NKT cells are divided into type I and II depending on the genes used for the generation of the TCR α chain and the reactivity of the TCR to α -Gal. In this study and also in most of the publications what is commonly referred as α -galactosylceramide (α -Gal) is actually a synthetic analogue (termed KRN7000) of the natural α -galactosylceramide isolated from the marine sponge *Agelas mauritanus* in a screening of natural anticancer medicines (Morita et al., 1995). α -Gal is the first glycolipid antigen described to be presented by CD1d and is recognized by NKT cells

with an invariant TCR α chain rearrangement (type I NKT cells or iNKT cells, introduction section 1.3) (Kawano et al., 1997). Due to its marine origin, it is difficult to assign a physiological role for α -Gal. Nonetheless, its very potent capacity to activate iNKT cells makes α -Gal an indispensable tool to study and to “exploit” this T cell population. Moreover, the peculiar α -linkage of the sugar (most mammalian ceramide glycosphingolipids contain sugars in the β -anomeric form) has helped to identify other antigens presented by CD1d and numerous synthetic analogues, recently reviewed by Venkataswamy and Porcelli (Venkataswamy and Porcelli, 2010).

Since α -Gal was found, other lipid antigens from endogenous and microbial origin have been identified to be presented by CD1d and recognized by iNKT cells. Glycolipid antigens have been found in pathogen microorganisms such as α -glucuronosylceramide (GSL-1) from the ubiquitous bacterium *Sphingomonas* (Kinjo et al., 2005; Mattner et al., 2005) and diacylglycerols containing an α -linked galactose (BbGI-II) from *Borrelia burgdorferi*, which is a Gram negative species causative of Lyme disease. Furthermore lipids derived from protozoa pathogens which activate mouse iNKT cells have also been reported: Lipophosphoglycan (LPG or LD1S) from *Leishmania donovani* and a phosphatidylinositol (EhPIa) from *Entamoeba histolytica* (Amprey et al., 2004; Lotter et al., 2009).

Although the identity of endogenous lipids which are presented by CD1d and recognized by NKT cells remains largely unresolved, several functional and biochemical analyses have provided essential information. The recognition of endogenous antigens was evident with the finding that NKT cells are autoreactive when cultured *in vitro* with antigen presenting cells expressing CD1d without the addition of any exogenous antigen (Bendelac et al., 1995; Exley et al., 1997). The deficiency to stimulate iNKT cells of a cell line with a mutant β -glucosylceramide synthase indicated that the endogenous NKT cell ligands might include lysosomal glycosphingolipids (Stanic et al., 2003). Moreover, the fact that mice deficient for β -hexosaminidase B (enzyme which processes isoglobotetrahexosylceramide (iGb4) into isoglobotrihexosylceramide (iGb3)) have a severely impaired iNKT cell development together with the finding that purified and synthetic iGb3 can stimulate human and mouse iNKT cells (Zhou et al., 2004b), lead to the hypothesis that iGb3 is a major selecting ligand of iNKT cells *in vivo* (Zhou et al., 2004b). Nonetheless, later reports showed that alterations in other enzymes distinct from β -hexosaminidase B which cause accumulation of lysosomal glycosphingolipids also result in defective iNKT cell

development (Gadola et al., 2006b) and more importantly, that iNKT cell numbers are normal in mice lacking iGb3 synthase (Porubsky et al., 2007). Thus, although iGb3 is an endogenous ligand for iNKT cells, it is probably not the most important selecting lipid. Nonetheless and although the exact molecular structures are not known yet, three studies have clearly shown that after stimulation with TLR agonists or during infection the lipids bound to CD1d are altered, and strongly activate iNKT cells (Darmoise et al., 2010; Paget et al., 2007; Salio et al., 2007). This illustrates how the antigen presenting cells can sense the presence of pathogens and can “alert” the immune system also by presenting endogenous glycolipids to iNKT cells. Moreover, sulfatides are other endogenous lipids which have been shown to activate a distinct CD1d-restricted T cell population (type II NKT cells) (Jahng et al., 2004; Roy et al., 2008).

Taken all together, it is clear that CD1d functions as an antigen presenting molecule specialized in presenting lipids to CD1d-restricted T cells. Nonetheless, an additional function for CD1d distinct from that of antigen presenting molecule appears also possible since Nieuwenhuis and colleagues recently found intrinsic defects in the granular content and morphology of Paneth cells in CD1d-deficient mice (Introduction section 1.2.2 and (Nieuwenhuis et al., 2009)).

1.3 CD1d-restricted T cells

As previously mentioned, CD1d-restricted T cells have been named NKT cells due to the expression of receptors typically found in NK cells (Godfrey et al., 2004). Also as previously alluded, these cells can be categorized into two groups depending on the gene segments used to form their TCR and their reactivity to α -Gal. Type I NKT cells, also designated as invariant NKT cells (iNKT cells) or $V\alpha 14$ NKT cells, express an invariant TCR α chain characterized by AV14-AJ18 ($V\alpha 14$ -J $\alpha 18$) rearrangements in mice and by the homologous AV24-AJ18 rearrangements in humans (TRAV10-TRAJ18 and TRAV11-TRAJ18 according to the IGMT nomenclature for human and mice, respectively). Apart from the invariant α chain, the β chains of iNKT cells also show a limited BV ($V\beta$) repertoire with highly variable CDR3 β regions. In humans, most iNKT cells bear a BV11 (TRBV10 based on the IGMT gene nomenclature) comprising β chain and in mice more than 80% of these cells have BV8S2, BV7 or BV2 β chains (TRBV13, TRBV29 and TRBV1, based on IGMT nomenclature, respectively) (Benlagha et al., 2000; Lee et al., 2002a; Matsuda et al., 2000).

Neither all iNKT cells express receptors typical of NK cells such as NK1.1 (NKR-P1C) in mice or CD161 (NKR-P1A) in humans nor all NK1.1⁺/CD161⁺ T cells are iNKT cells, therefore unequivocal identification of iNKT cells should be carried out with α -Gal-loaded CD1d oligomers, which are reagents that exploit the specificity and high affinity of the semi-invariant TCR- α -Gal-CD1d interactions (Godfrey et al., 2004; Gumperz et al., 2002; Hammond et al., 2001; Matsuda et al., 2000).

The type II category includes all CD1d-restricted T cells which do not express the canonical α chain. Although the specificities of this diverse group remain largely unclear, as already pointed out, it has been demonstrated that some cells react to endogenous sulfatides and, similarly as iNKT cells, they can be identified with sulfatide-loaded CD1d tetramers (Behar and Cardell, 2000; Cardell et al., 1995; Jahng et al., 2004). A recent study has shown that these sulfatide-reactive T cells have an oligoclonal TCR repertoire with a predominant use of AV3/AV1-AJ7/AJ9 and BV8S1/BV3S1-BJ2S7 gene segments (Arrenberg et al., 2010).

1.4 Recognition of α -Gal-CD1d by semi-invariant TCRs

Crystal structures of human and mouse iTCR- α -Gal-CD1d complexes have provided a clear insight into the structural basis of the AV14 and AJ18 requirement to form the invariant TCR α chain (Borg et al., 2007; Pellicci et al., 2009). The recognition mode of α -Gal-CD1d by the semi-invariant TCR is very different from how other TCRs recognize peptide-MHC complexes. First, in contrast to MHC class I-peptide-TCR interactions, where α and β chains contribute more or less to the same extent, adopting a diagonal footprint with respect to the axis of the antigen binding groove of the MHC molecule; in the recognition of α -Gal-CD1d complexes by the semi-invariant TCR, the α chain makes many more contacts than the β chain and the foot print over α -Gal-CD1d is parallel to the antigen binding groove. Second, the docking mode of the TCR when it is bound to peptide-MHC complexes is perpendicular to the plane drawn by the α 1 and α 2 helices of the MHC molecule but the semi-invariant TCR adopts a very acute docking mode lying only above the F' pocket when it binds to α -Gal-CD1d and third, whereas all CDRs of both α and β chains make important interactions in the recognition of peptides presented by MHC molecules, there are big differences in the contributions of the CDRs of the semi-invariant TCR. The CDR3 loop of the α chain of the semi-invariant TCR, mainly formed by AJ18, spreads broadly over the α -Gal/CD1d complex making contacts with the protruding galactose head of α -Gal and the α 1 and α 2 helices

of CD1d. In contrast, the CDR1 α loop makes a few contacts only with α -Gal and the CDR2 α makes no evident interactions with CD1d or α -Gal. In the structures resolved to date with human BV11 and mouse BV8S2 and BV7 TCRs, the only contributions of the β chain are made with the CDR2 β loop which makes contacts with CD1d but not with the antigen. In addition to these crystallographic analyses, mutagenesis studies carried out by our and other laboratories have also demonstrated the important role of the CDR2 β region in α -Gal-CD1d recognition by the semi-invariant TCR (Borg et al., 2007; Mallevaey et al., 2009; Pellicci et al., 2009; Pyz et al., 2006; Scott-Browne et al., 2007; Wun et al., 2008).

1.5 iNKT cell development

iNKT cells as well as MHC-restricted T cells develop in the thymus from the same precursors, namely double positive (CD4⁺ and CD8⁺) thymocytes. The most important selecting factor driving iNKT cell development is the generation of the semi-invariant CD1d-restricted TCR. Thus mice lacking the AJ18 gene segment or CD1d lack iNKT cells (Cui et al., 1997; Mendiratta et al., 1997). Moreover, although V (D in the β chain) J gene segments are randomly recombined, the size of the excised DNA is limited and therefore, it is necessary to undergo multiple excisions in order to recombine distal gene segments such as AV14 and AJ18 (Guo et al., 2002). To be able to go through multiple excisions, thymocytes must have a prolonged lifespan. Consequently, mice which lack factors involved in prolonging survival such as ROR- γ t and BCL-X_L have reduced iNKT cell frequencies (Bezbradica et al., 2005; Egawa et al., 2005). After recombination and expression at the cell surface of the semi-invariant TCR, iNKT cells are positively selected but, in contrast to MHC-restricted T cells which are selected by cortical thymic epithelial cells (cTECs), iNKT cells are selected by cortical DP thymocytes (Bendelac, 1995). These homotypic interactions result in a distinct cell programming in comparison to MHC-restricted T cells since the costimulatory signals provided by thymocytes differ considerably from those provided by cTECs (Godfrey et al., 2010). In particular, it has been shown as iNKT cell development is dependent on signaling via SLAM molecules (Griewank et al., 2007; Jordan et al., 2007). SLAM proteins are cell surface receptors which signal through the SLAM adaptor protein (SAP). Mice lacking SAP or SLAM1 and SLAM6, which are the SLAM family members expressed by thymocytes, lack iNKT cells but have normal MHC-restricted T cells numbers (Chung et al., 2005; Griewank et al., 2007; Nichols et al., 2005; Pasquier

et al., 2005). Although demonstration of negative selection is a complicated task, the impaired iNKT cell development in the presence of α -Gal or of CD1d-overexpressing dendritic cells (Chun et al., 2003; Pellicci et al., 2003) suggests that iNKT cells also might undergo apoptosis if during development their semi-invariant TCR recognizes ligands with a very high affinity.

After positive and probably negative selection, iNKT cells undergo several maturation steps, which can be distinguished by differently-expressed cell surface molecules (Godfrey et al., 2010). Many factors are involved in this maturation process and have been extensively reviewed elsewhere (Godfrey and Berzins, 2007; Godfrey et al., 2010; Matsuda and Gapin, 2005). Several of them are also important for MHC-restricted T cell maturation. A lot of efforts have been made to identify a master regulator specific of the iNKT cell lineage. In two recent studies it has been shown that the transcription factor PLZF is expressed by iNKT cells but not by T cells restricted by classical MHC molecules (Kovalovsky et al., 2008; Savage et al., 2008). Although PLZF is also expressed by a subset of $\gamma\delta$ T cells and by human, but not mouse, MAIT cells, at least PLZF is limited to non-conventional T lymphocytes (non-classical MHC-restricted T cells). Accordingly, mice deficient for PLZF have much lower numbers of iNKT cells, and those iNKT cells which reach maturation, do not have the characteristic activated phenotype of normal iNKT cells. Once iNKT cells have matured, they home to tissues different from those where MHC-restricted T cells migrate and some of them stay in the thymus. iNKT cells are especially abundant in the liver (in mouse inbred strains such as C57BL/6 constitute a 30% of all intrahepatic lymphocytes) and whereas they are present at considerable amounts in the spleen (1% of total lymphocytes), they are hardly detectable in lymph nodes (Hammond et al., 2001; Matsuda et al., 2000).

1.6 iNKT cell function

During the last ten years, many studies have shown the *in vivo* role of iNKT cells at the interface between innate and adaptive immune responses. As mentioned, iNKT cells display an activated phenotype and respond very rapidly by secreting large amounts of cytokines within a few hours after activation. iNKT activation can occur in different ways referred as direct and indirect activation pathways (Brigl and Brenner, 2010). In the direct activation pathway iNKT cells are activated by the recognition of exogenous microbial lipid antigens such as BbGI-II or GSL-1 by their semi-invariant TCR (Introduction section 1.2.3). In contrast, in the indirect pathway in order to secrete large

amounts of cytokines, iNKT cells need two stimulatory signals: One is the recognition of endogenous ligands with their semi-invariant TCR and the other one is the binding of stimulatory cytokines released by the antigen presenting cells (such as IL-12 or type I IFNs) (Paget et al., 2007; Salio et al., 2007). Furthermore, two studies have demonstrated that iNKT cells release IFN- γ in response to recombinant innate cytokines such as IL-12 and IL-18 independently of TCR stimulation (Hou et al., 2003; Leite-De-Moraes et al., 1999).

Activation of iNKT cells often results in the activation or maturation of the antigen presenting cell (DC or B cells). This activation feedback is mainly dependent on cytokines released by iNKT cells and on CD40 ligation (Hermans et al., 2003; Lantz and Bendelac, 1994). In such a way, iNKT cell adjuvant activity enhances B and T cell responses (Cerundolo et al., 2009; Fujii et al., 2010). Additionally, also a cytolytic potential of iNKT cells has been shown, although this is probably not one of their main effector functions (Smyth et al., 2002).

The outcomes after iNKT cell activation are diverse: On the one hand they can enhance immune responses such as anti-tumor T cell activity but on the other hand, they are also able to inhibit the immune system resulting in an amelioration of autoimmune diseases (Bendelac et al., 2007; Godfrey and Kronenberg, 2004). How iNKT cells manage to exert these contradictory and most of the times beneficial roles for the host is being intensively investigated (Godfrey et al., 2010).

1.7 iNKT cells in the rat

Rats have the genes necessary for the generation and selection of semi-invariant TCRs: First, as mentioned in the introduction section 1.2.1, they have one CD1d gene which is highly homologous to its mouse counterpart (Katabami et al., 1998); second, they have several AV14 homologues which have been shown to rearrange with AJ18 (Matsuura et al., 2000) and third, they have two homologues of the mouse BV8S2 gene segment: BV8S2 and BV8S4 (Asmuss et al., 1996).

The presence of several AV14 gene segments in the rat (Kinebuchi and Matsuura, 2004; Matsuura et al., 2000; Pyz et al., 2006) is intriguing since humans contain one single AV14 gene segment and mice one or two (Koseki et al., 1991; Lefranc, 2001). These AV14 gene segments are highly similar except in the CDR2 α region, where two very different amino acid sequences are found. Based on the amino acid sequence of this region, these AV14 genes have been divided into two groups: Type I and type II

(Kinebuchi and Matsuura, 2004; Matsuura et al., 2000). Interestingly, the studies carried out by Matsuura and colleagues suggested a specific tissue distribution of these two different types: Invariant TCR α chains using type I AV14 gene segments were slightly more abundant among hepatic lymphocytes whereas in the spleen, type II invariant TCR α chains were expressed more frequently (Matsuura et al., 2000).

Up to date, two different *Tcrb* (loci encoding TCR β chains) haplotypes have been described in the rat which contain different alleles of each BV8S2 and BV8S4 gene segments. In the *Tcrb*^a haplotype, present in DA and F344 inbred rat strains, both gene segments encode functional BV8 polypeptides, in contrast, in inbred rat strains containing a *Tcrb*^l haplotype such LEW, BN and PVG, BV8S4 is predicted to be non-functional due to the deletion of one nucleotide which results in a frame shift. BV8S2^a and BV8S4^a differ in six amino acids located in the CDR2 and CDR4 regions. In contrast, the predicted amino acid sequences of the ^a and ^l BV8S2 alleles differ in three residues localized outside of the CDR regions (Asmuss et al., 1996). The mAb R78, often used in this study, binds to BV8S4^a but not to BV8S2^a, whereas in inbred rat strains of the ^l haplotype, it binds to BV8S2^l (Asmuss et al., 1996; Torres-Nagel et al., 1993). In addition, other BV8 family members have been described in rats such as BV8S3 (detected by the mAb B73 (Torres-Nagel et al., 1993)) and BV8S1 (Hashim et al., 1991; Smith et al., 1991). The predicted amino acid sequences of these BV8 gene segments differ considerably from BV8S2 and BV8S4, especially the CDR2 of BV8S3 (Asmuss et al., 1996).

E. Pyz et al. demonstrated that these gene segments can produce semi-invariant TCRs which are reactive to α -Gal presented by rat CD1d and that rat primary cells respond to α -Gal stimulation by secreting IFN- γ and IL-4. Nonetheless, despite these functional and genetic data, all attempts carried out to identify iNKT cells in the rat had been based on the one hand, on co-staining of NKR-P1 receptors on T cells detected by the mAbs 3.2.3 or 10/78 (which detect two NKR-P1 isoforms: A and B (Li et al., 2003)) together with mAbs specific for TCR β chains formed by certain BV gene segments (Knudsen et al., 1997; Li et al., 2003; Matsuura et al., 2000; Pyz et al., 2006; Ru and Peijie, 2009); and on the other hand on the usage of mouse α -Gal-loaded CD1d oligomers (Pyz et al., 2006). First, although it can be expected that rat iNKT cells are contained among NKR-P1⁺ T cells (as in mice and humans), it is possible that not all these cells bear the semi-invariant TCR and second, surprisingly, mouse α -Gal-loaded CD1d oligomers failed to identify a discrete rat iNKT cell population despite the high homology between rat and

mouse CD1d molecules. Since E. Pyz et al. also showed that cell lines bearing rat semi-invariant TCRs did not respond to α -Gal presented by mouse CD1d, the failure of the identification of a reliable rat iNKT cell population with mouse CD1d oligomers could be explained by the lack of binding of mouse CD1d by rat iNKT cells (Pyz et al., 2006). Taken all together, although strong evidence suggested that rats have iNKT cells the direct identification and phenotypical characterization of this particular T cell population in the rat was still pending. Therefore, the principal aims of this doctoral thesis were first, to develop appropriate reagents which allow the direct staining of rat iNKT cells and second, the analysis of these cells among different inbred rat strains.

2 MATERIALS AND METHODS

2.1 Materials

2.1.1 Chemical reagents

Agar-agar	Applichem (Darmstadt, Germany)
Acetic acid	Applichem (Darmstadt, Germany)
α -Gal (α -Galactosylceramide)	Alexis Biochemicals, Enzo Lifesciences (New York, USA)
Agarose	Roth (Karlsruhe, Germany)
Ammonium chloride	Roth (Karlsruhe, Germany)
Ampicillin	Gibco BLR (Eggenstein, Germany)
APS	Roth (Karlsruhe, Germany)
β -mercaptoethanol	Gibco BLR (Eggenstein, Germany)
Boric acid	Roth (Karlsruhe, Germany)
Bromophenol blue	Sigma (St. Louis, USA)
BSA	Roth (Karlsruhe, Germany)
Calcium Chloride	Roth (Karlsruhe, Germany)
Concanavalin A	ICN (Meckenheim, Germany)
Coomassie R250	Sigma (St. Louis, USA)
Diethylamine	Sigma (St. Louis, USA)
DMSO (Dimethyl sulfoxide)	Applichem (Darmstadt, Germany)
DMP	Pierce (Rocford, USA)
dNTP Set	Peqlab Biotechnologie (Erlangen, Germany)
EDTA	Applichem (Darmstadt, Germany)
Ethanol	Applichem (Darmstadt, Germany)
Ethidium bromide	Roth (Karlsruhe, Germany)
FCS	Sigma (St. Louis, USA)
Ficoll-Paque	GE Healthcare (Uppsala, Sweden)
Formaldehyde	Roth (Karlsruhe, Germany)
Formamide	Roth (Karlsruhe, Germany)
G418 (Geneticin solution)	Biochrom (Berlin, Germany)
Glycerol	Applichem (Darmstadt, Germany)
Glycine	Roth (Karlsruhe, Germany)

HEPES for cell culture	Applichem (Darmstadt, Germany)
Hydrogen peroxide 35%	Applichem (Darmstadt, Germany)
Isopropanol	Applichem (Darmstadt, Germany)
LB (Broth Base medium)	Applichem (Darmstadt, Germany)
Luminol	Applichem (Darmstadt, Germany)
Magnesium Chloride	Roth (Karlsruhe, Germany)
MEM (Non-essential amino acids)	Gibco BLR (Eggenstein, Germany)
Non fat dried milk powder	Applichem (Darmstadt, Germany)
NONIDET P-40	Sigma (St. Louis, USA)
p-Coumaric Acid	Merck (Darmstadt, Germany)
Penicillin	Grünenthal (Aachen, Germany)
Percoll	GE Healthcare (Uppsala, Sweden)
Acrylamide	Applichem (Darmstadt, Germany)
Polybrene (Hexadimthrinbromide)	Sigma (Deisenhofen, Germany)
Protein A Sepharose Fast Flow	GE Healthcare (Uppsala, Sweden)
Protein G Sepharose 4 Fast Flow	GE Healthcare (Uppsala, Sweden)
SDS (Sodium dodecyl sulphate)	Sigma (Deisenhofen, Germany)
Sodium Azide	Merck (Darmstadt, Germany)
Sodium Chloride	Roth (Karlsruhe, Germany)
Sodium Butyrate	Sigma (Deisenhofen, Germany)
Sodium Hydroxide	Applichem (Darmstadt, Germany)
Streptomycin	Riemser (Greifswald, Germany)
Sulfo-NHS-LC-Biotin	Pierce (Rocford, USA)
TEMED	Roth (Karlsruhe, Germany)
Tris	Applichem (Darmstadt, Germany)
TRITON X-100	Sigma (St Louis, USA)
Trypan blue	Sigma (Deisenhofen, Germany)
Tween 20	Sigma (Deisenhofen, Germany)
Zeocin	Invivogen (Toulouse, France)

2.1.2 Media, buffers, solutions

- Culture medias of eukaryotic cells
 - DMEM⁻: DMEM with Glucose and L-Glutamine (Gibco Invitrogen, Darmstadt, Germany)), supplemented with 10% FCS and antibiotics (Penicillin and Streptomycin).
 - DMEM⁺: DMEM + GlutaMAXTM-I (with Glucose and 25mM HEPES, Gibco Invitrogen, Darmstadt, Germany)) supplemented with 10% FCS and antibiotics (Penicillin and Streptomycin).
 - RPMI⁺: RPMI 1640 with L-Glutamine (Gibco Invitrogen, Darmstadt, Germany) supplemented with 10 % of SC (supplement complete)
 - RPMI⁺⁺: RPMI⁺ supplemented additionally with 5% FCS and 25 mM HEPES (pH 7.5)
 - ISF-1 media (Biochrom, Berlin, Germany) supplemented with antibiotics (Penicillin and Streptomycin).
 - SFM4MAb media supplemented with antibiotics (Penicillin and Streptomycin) (Fisher Scientific, Schwerte, Germany).
 - Freezing media (40% RPMI 1640, 50% FCS and 10% DMSO).
- SC-supplement (50 ml of SC per 500 ml of RPMI-): 500 ml heat-deactivated FCS, 100 ml Na pyruvate 100 mM, 100 ml non-essential amino acids, 100 ml Penicillin-Streptomycin (10000U/ml) and 5 ml β -Mercaptoethanol 50 mM.
- ATV: 0.05% Trypsin, 0.02% EDTA in PBS.
- BSS (Hanks balanced salt solution): to prepare BSS 125 ml of BSS I was mixed with 125 ml of BSS II add filled with water to 1 L.
 - BSS I: 50 g Glucose, 3 g KH_2PO_4 , 11.9 g NaH_2PO_4 , 0.4 g Phenylred and water to 5 L.
 - BSS II: 9.25 g CaCl_2 , 20 g KCl , 320 g NaCl , 10 g MgCl_2 , 10 g MgSO_4 and water to 5 L.
- BSS/BSA: BSS supplemented with 0.2% of BSA.
- 2xHBS: 50 mM HEPES pH 7.05 (different pHs were prepared and tested), 10 mM KCl , 12 mM Glucose, 280 mM NaCl and 1.5 mM NaH_2PO_4 .
- PBS (Phosphate buffered saline): 4 mM KH_2PO_4 , 16 mM Na_2HPO_4 and 115 mM NaCl with a pH of 7.3.
- FACS buffer: PBS with 0.1% BSA and 0.05% NaN_3 .

- TAC (Tris-Ammoniumchlorid) buffer: 20 mM Tris pH 7.2 and 0.82% NH₄Cl.
- LB-medium: 20 g LB and water to 1 L, autoclaved and stored at 4°C
- Low salt LB media: 10 g Tryptone, 5 g NaCl and 5 g Yeast Extract
- Bio-Rad Protein Assay, Bio-Rad (Munich, Germany)
- Coating buffer: 8.4 g NaHCO₃, 3.56 g Na₂CO₃ in 1 L H₂O, pH 9.5
- ECL-solutions (self made)
 - Solution I: 2.5 mM Luminol, 400 µM p-coumaric acid in 0.1 M Tris pH 8.5 (1% DMSO, dissolvent of Luminol and p-coumaric acid)
 - Solution II: 5.4 mM H₂O₂ in 0.1 M Tris pH 8.5 (prepared the same day in which it is used)

Equal volumes of solutions I and II were mixed and added to the blotted membrane.
- ECL solution, if not self-made was purchased from GE Healthcare (Uppsala, Sweden).
- BD™ ELISPOT AEC Substrate Set (BD Biosciences Pharmingen; San Diego, USA)
- BD OptEIA™ TMB Substrate Reagent Set (BD Biosciences Pharmingen; San Diego, USA)
- 10xTBE (Agarose electrophoresis buffer): 890 mM Tris, 890 mM Boric Acid and 20 mM EDTA
- 5xTGS (SDS-PAGE buffer): 15.1 g Tris, 94 g Glycine, 50 ml 10% SDS and water to 1 L.
- SDS-PAGE gel staining solution: 12.5% isopropanol, 10% acetic acid 0.25% Coomassie Brilliant Blue R250.
- SDS-PAGE gel destain solution: 12.5% isopropanol and 10% acetic acid
- Stripping buffer: 62 mM Tris, 2% SDS and 100 µM Tris HCl pH 6.7
- Buffers for semi-dry protein transfer into a PVDF membrane:
 - Anode Buffer I: 0.3 M Tris, pH 10.4, 10% methanol
 - Anode Buffer II: 25 mM Tris, pH 10.4, 10% methanol
 - Cathode Buffer: 25 mM Tris, 40 mM glycine, 10% methanol, pH 9.4
- IP loading buffer: 2% SDS, 62.5 mM Tris pH 6.8, 10% glycerol, 770 mM β-mercaptoethanol and 0.04% bromophenol blue

- IP Lysis buffer: 50 mM Tris, pH 7.4, 150 mM NaCl, 0.25% Na-deoxycholate, 1 mM EDTA, 1% NP40 and protease inhibitors.
- WB reducing loading buffer is the same as the IP loading buffer but 4x concentrated.
- WB non-reducing loading is the same as the WB reducing loading buffer but without β -mercaptoethanol.

2.1.3 Cell lines

<i>293T</i>	Highly transfectable derivative of the 293 cell line into which the temperature sensitive gene for SV40 T-antigen was inserted (ATCC# CRL-11268).
<i>58C (BW58)</i>	Do-11.10.7 hybridoma derived AKR/J mouse $\alpha\beta$ TCR-negative cell lymphoma; ATCC#TIB-233. Kindly provided by Dr. Palmer (Basel Institute, Switzerland).
<i>BW58 r/mCD28</i>	BW58 cells transduced with r/mCD28 (Luhder et al., 2003).
<i>BW58 rAV14S6 + CDR2+4</i>	BW58 cells transduced with r/mCD28 and a rat semi-invariant TCR generated by E. Pyz and described elsewhere (Pyz et al., 2006). The TCR α chain contains the AV14S6 gene segment (previously named AV14S1).
<i>J558L</i>	J558L is a spontaneous heavy chain-loss-variant myeloma cell line obtained from the J558 cell line (Oi et al., 1983).
<i>P80rCD1d</i>	P815 mouse (DBA/2) cell mastocytoma (ATCC# TIB-64) transduced with rat CD80 and CD1d generated by E. Pyz (Pyz et al., 2006).
<i>Raji rCD1d</i>	Raji human Burkitt's lymphoma cell line (ATCC# CCL-86) transduced with rat CD1d (Pyz et al., 2006).
<i>Raji mCD1d</i>	Raji human Burkitt's lymphoma (ATCC #CCL-86) transduced with mouse CD1d (Pyz et al., 2006).
<i>SC2</i>	<i>Drosophila melanogaster</i> cells.

2.1.4 Animals

Animals were used at 6 – 16 weeks of age. C57BL/6J, BALB/c, C57BL/6, CD1d^{-/-} and BALB/c CD1d^{-/-} mice, as well as LEW/Crl and F344/Crl rats were bred in the animal facilities of the Institute for Virology and Immunobiology Virology and Immunobiology, University of Würzburg, Würzburg, Germany. Breeding pairs for CD1d^{-/-} mice, previously bred on a BALB/c background were a kind gift of Heidrun Moll, Institute for Infection Biology, Würzburg University. C57BL/6 CD1d^{-/-} (Mendiratta et al., 1997) were kindly provided by Manfred Lutz, Institute for Virology and Immunobiology, University of Würzburg, Würzburg, Germany. BN/SsNOlaHsd, DA/OlaHsd, PVG/OlaHsd, BUF/SimRijHsd, AGUS/OlaHsd, AUG/OlaHsd and WF/NHsd rats were purchased from Harlan laboratories. BH/Ztm rats and CBA/N mice were provided by Kurt Wonigeit, Medical School Hannover, Hannover, Germany.

2.1.5 Vectors

- pczVSV-G* Encodes the *env* protein from Vesicular Stomatitis Virus (Pietschmann et al., 1999).
- pHIT 60* pHIT60-CMV-MLV-*gag-pol*-SV40ori; containing *gag* and *pol* from Moloney Murine Leukemia Virus (MoMLV) under the control of human Cytomegalovirus (CMV) promoter (Soneoka et al., 1995).
- pczCFG5 IZ* Retroviral vector for the MuLV driven constitutive expression of a gene of interest and through IRES mediated expression the protein which confers Zeocin resistance. This vector was kindly provided by I. Berberich, Institute for Virology and Immunobiology, University of Würzburg, Würzburg, Germany.
- pczCFG5 IEGN* Retroviral vector for the MuLV driven constitutive expression of a gene of interest and through IRES mediated expression the EGFP-Neo fusion protein which serves as reporter and confers neomycin resistance (Knodel et al., 1999). This vector was kindly provided by I. Berberich, Institute for Virology and Immunobiology, University of Würzburg, Würzburg, Germany.

- pXIg* Vector containing MluI and XhoI unique restriction sites. The vector encodes the signal sequence of the IgG1 heavy chain 5' of the MluI site and the IgG1 heavy chain starting from the intact variable domain after the XhoI restriction site (Dal Porto et al., 1993). This plasmid was derived from the pSN-RCCR2, a plasmid which contains the gene encoding an IgG1 heavy chain specific for the hapten NP (Hebell et al., 1991).
- pFUSE-hIgG1-Fc2* Commercially available vector containing the IL-2 signal sequence and the CH2 and CH3 domains and the hinge region of the human IgG1. Invivogen, San Diego, USA.
- pMT/BioHis-IA^bα* Vector containing the metallothionein promoter, necessary for expression of proteins in the Drosophila cells, the BiP signal sequence, a mouse MHC-II α chain, the specific biotinylation site (Schatz, 1993) recognized by the BirA enzyme and a polyhistidine tag (Schiemann, 2005). This vector was kindly provided by D. Busch, Institute of Medical Microbiology, Dept. of Medicine, Technical University Munich.
- pcDNA3.1/V5HiABio* Vector containing the CMV promoter, a multiple cloning site and encoding the specific biotinylation site recognized by the BirA enzyme and Polyhistidine tag. This vector was kindly provided by I. Müller, Dept. of General Paediatrics, Hematology and Oncology, University Children's Hospital, Tübingen.
- pMT/BiP/His/StrepTagIII-IA^bα* Vector containing the metallothionein promoter, necessary for expression of proteins in the Drosophila cells and DNA sequences encoding the BiP signal sequence, a mouse MHC-II α chain, a thrombin cleavage site, an acidic leucine zipper domain and after the Kpn2I restriction site the Strep-Tag III amino acid sequence (Neudorfer et al., 2007). This vector was kindly provided by D. Busch, Institute of Medical Microbiology, Dept. of Medicine, Technical University Munich.

2.1.6 Oligonucleotides

The orientation of all oligonucleotides is 5' to 3'. Restriction sites contained in the oligonucleotides appear underlined. All oligonucleotides were synthesized by MWG-Biotech AG (Ebersberg, Germany) or Sigma (Taufkirchen, Germany).

- Primers used for the amplification and direct sequencing of rat CD1d genomic DNA sequences:

gCD1d fo 77: CAAGGGGAGTTGGCTTTGTA

gCD1d re 78: GTGGAGAACCAGGGTGAAAA

- Primers used for IgG heavy chain and kappa light chain RT-PCR and direct sequencing. These oligonucleotides were adapted from Wang et al. (Wang et al., 2000):

MH2_82: SARGTNMAGCTGSAGSAGTCWGG

IgGrev 2_101: CAGACTGCAGGAGAGCTGG

Mk_84: GAY ATT GTG MTS ACM CAR WCT MCA

Igk rev 1_103: CACTTGACATTGATGTCTTTGG

Igk rev 2_104: TTTGCTGTCCTGATCAGTCC

- Primers used for RT-PCR of rat β -actin. The forward and reverse primers are complementary to the exon 4 and 5, respectively (designed by R. Rudolf):

RNBetaActFwd17: CACCACCACAGCTGAGAGG

RNBetaActRev18: AGACAGCACTGTGTTGGCATAG

- Primers used for RT-PCR and sequencing of AV14-containing TCR α mRNAs:

rVa14lead gDNA f (50): CTTCTGCAGAAAAACCATGGGGAAG

rJa18lead gDNA r(51): AGGTGTGACAGTCAGCTGAGTTCC

rCa_seq2nd_118: AGTCGGTGAACAGGCAGAGGG

rAV14int_124: CCTTCAATGCAATTACACTGTG

- Primers used for RT-PCR of BV8-containing TCR β mRNAs:

rVb8_seq_fow_122: TGGGCTCCAGGTTCCCTTCTTAGTG

rVb8_seq_rev_123: GCCAAGCACACGAGGGTAGC

- Oligonucleotides used for real time PCR:
 - rVa14_Bendef 79: CTAAGCACAGCACCCCTGCACA
 - rJ281_Bende 80: CAGGTGTGACAGTCAGCTGAGTTC
 - rt_rCaE1_fo 71: AAGCTTCAGCTGCAAAGACG
 - rt_rCaE3_re 72: GATTCGGAGTCCCATGACTG

- Primers used for cloning of *Mus musculus* CD1d2 and *Mus spretus* CD1d1 into pczCFG5 IEGN retroviral expression vector:
 - mCD1d_fo EcoRI: GGGGAGAATTCCGGCGCTATGCGGTACCTACC
 - msCD1d_BamHIrev_113: GCATGGATCCTCACCGGATGTCTTGATAG

- Primers used for cloning of rat CD1d into pczCFG5 IZ retroviral expression vector:
 - rCD1d_EcoRI_f62: CTTCGAATTCGACCGCCGGCACTATGCTGT
 - rCD1d_BamHI_r63: GTTGGGATCCCTCACATGATGTCTTGATAGG

- Primers used for rat β 2-microglobulin cloning into pczCFG5 IZ retroviral expression vector:
 - MfeI b2 fow P3: TGCCAATTGGCCGCCACCATGGCTCGCTCGGTGACC
 - rb2m BamHI re P2: TGAGGATCCTTACATGTCTCGGTCCCAGG

- Primers used for cloning mouse CD1d and rat CD1d into the pXIg vector were based in the work of MacDonald and colleagues (Schumann et al., 2003):
 - mCD1d-MD-MluI-F:
 - GTCCACGCGTCGCAGCAAAAGAATTACACCTTCCGC
 - mCD1d-MD-XhoI-Rev:
 - GTCACTCGAGCCAGTAGAGGATGATATCCTGTC
 - rCD1d-MD-MluI-F: GTCCACGCGTCGCAGCAGAATTACACCTTCCGC
 - rCD1d-MD-XhoI-R: GTCACTCGAGCCAGTAGAGGATGATGTCCTGCC

- Primers used for cloning of rat CD1d into the pFUSE-hIgG1-Fc2 vector:
 - rCD1dEcoRI Fc2_88: CTCAGAATTCGGTCCAGCAGAATTACACCTTC
 - rCD1dBamHI Fc_86: CTACGGATCCCCAGTAGAGGATGATGTC

- Primers used for cloning of rat β 2-microglobulin and the glycine-serine polylinker into the rat CD1d-pFUSE-hIgG1-Fc2:
 - rb2 MunI fo_105: CCCCAATTGTCAGAAAACTCCCCAAATTCAAG

rb2m MunI rev_106:

CCCCAATTGCTTCCACTTCCACTTCCACTTCCACTTCCACTTCCCATGT
CTCGGTCCCAGGTG

- Primers used for cloning of rat CD1d into pMT/BioHis-IA^b α vector once the Kpn2I restriction site had been inserted:

Ok CD1d SacII For: AATTGGCCGCGGGTCCAGCAGAATTACACCT
CD1d Kpn2I Rev: AGTAATTCCGGACCAGTAGAGGATGATGTC

- Primers used for the insertion of the Kpn2I site into the pMT/BioHis-IA^b α vector:

Kpn2I Forward:
GGAAAAGGAACTGGCTCAGTTCCGGACTTAATGACATTTTCGAGG
Kpn2I Reverse:
CCTCGAAAATGTCATTAAGTTCCGGACTGAGCCAGTTCCT

- Primers used for cloning of rat β 2-microglobulin-CD1d into the pcDNA3.1/V5 His A Bio vector (Methods section 2.2.2.8):

IL2ko EcoRV_111: TAGAGATATCGAAGGAGGGCCACCATGTA
rCD1drev XhoI_112/3: TACACTCGAGCCAGTAGAGGATGATGTCCT

- Primers used for cloning of rat β 2-microglobulin-CD1d into the pMT/BiP/His-IA^b α StrepTag III vector (Methods section 2.2.2.9):

rb2mSacII_114: TGCACCGCGGACAGAAAACCTCCCAAATTCAAG
CD1d Kpn2I Rev: AGTAATTCCGGACCAGTAGAGGATGATGTC

- Primers used for cloning of AV14-containing TCR α chains into the retroviral expression vector (designed by E. Pyz):

rVa14EcoRI-Fow: GGGCTAGAATTCTGCAGAAAAACCATGGGGAAG
Ca end BamH1 antisense:
ATGCGGATCCTCAACTGGACCACAGCCTTAGCGTCATGAG
TTTCC

- Primers used for sequencing of pczCFG5 IZ and pczCFG5 IEGN vectors:

PSI: CACGTGAAGGCTGCCGACC
IRE II seq: TGGAAAATAACATATAGA

- Primers used for sequencing of pXIg/CD1d-pXIg vectors (designed by E. Pyz and I. Müller):
 - pX/Ig fow: CAG GTC CAA CTG CAC GCG
 - N4 (fow): TGGGTGATGTGGATGCGGGGT
 - r/mCD1-alpha1-Re: GTCTTCTTTAGGTGACATCATTTTGAC
 - pX/Ig rev: GAC CTG GCT CAC CTC GAG

- Primers used for sequencing of pFUSE-hIgG1-Fc2 vectors:
 - pFUSE Fc fow_90: TTGCTCAACTCTACGTCTTTG
 - pFUSE Fc rev_91: GGTGTCCTTGGGTTTTGG

- Primers used for sequencing of pMT/BiP/BioHis vectors:
 - MT Forward: CATCTCAGTGCAACTAAA
 - BGH Reverse: TAGAAGGCACAGTCGAGG

- Primers used for sequencing of rat pcDNA3.1/V5 His A Bio vector:
 - pcDNA3 fo_107: GAGCTCTCTGGCTAACTAGAG
 - pcDNA3 rev_108: GGCAAACAACAGATGGCTGG

- Primers used for sequencing of pMT/BiP/His/StrepTagIII vectors:
 - OpIE2 Forward_59: CGCAACGATCTGGTAAACAC
 - OpIE2 Reverse_60: GACAATACAACTAAGATTTAGTCAG
 - rCD1d seq_61: GCAGATACTCCTGAACGACA

2.1.7 Antibodies and secondary reagents

• Primary antibodies

Antigen	Clone	Conjugation	Isotype	Purchased from
m TCR β	H57-597	APCy or FITC	hamster IgG2, λ 1	BD Pharmingen
m CD4	RM4-5	APCy or PE-Cy5	rat IgG2a, κ	BD Pharmingen
m CD21 (CR2/CR1)	7G6	FITC	rat IgG2b, κ	BD Pharmingen
m CD23 (Fc ϵ RII)	B3B4	PE	rat IgG2a, κ	BD Pharmingen
m CD19	1D3	APCy	rat IgG2a, κ	BD Pharmingen
m CD8	53-6.7	APCy	rat IgG2a, κ	BD Pharmingen
m NK1.1	PK136	FITC or PE	mouse IgG2a, κ	BD Pharmingen
r TCR β	R73	FITC, PE or bio	mouse IgG1, κ	BD Pharmingen
r CD4	OX-35	PE, PE-Cy5 or APCy	mouse IgG2a, κ	BD Pharmingen
r CD4	OX-38	PE	mouse IgG2a, κ	BD Pharmingen
r CD8 β	341	bio	mouse IgG1, κ	BD Pharmingen
r CD8 α	OX-8	PerCP	mouse IgG1, κ	BD Pharmingen
r dendritic cell marker	OX-62	unconjugated	mouse IgG1, κ	BD Pharmingen
r CD11b/c	OX-42	PE	mouse IgG2a, κ	BD Pharmingen
r CD45RA	OX-33	FITC or bio	mouse IgG1, κ	BD Pharmingen
r MZ B cell marker	HIS57	bio	mouse IgG1, κ	BD Pharmingen
r IgM	G53-238	FITC	mouse IgG1, κ	BD Pharmingen
r IgD	MARD-3	bio	mouse IgG1	AbD Serotec
r BV8 TCR β	R78	bio or unconjugated		BD Pharmingen or purified in our laboratory
r BV16 TCR β	HIS42	unconjugated	mouse IgG1, κ	Hybridoma supernatant
r NKR-P1A/B	10/78	bio or PE	mouse IgG1, κ	BD Pharmingen
m CD1d	1B1	PE	rat IgG2b, κ	BD Pharmingen
h CD1d	CD1d42	PE		Kind of gift of Ekkehard Kämpgen, Dermatology Dept. University of Erlangen.
r/m CD1d	233 (WTH-1)	bio, FITC or unconjugated	mouse IgG2a, κ	purified and conjugated in our laboratory
r/m CD1d	35 (WTH-2)	bio, FITC or unconjugated	purified and conjugated in our laboratory	purified and conjugated in our laboratory
r CD1d	58	bio, FITC or unconjugated	purified and conjugated in our laboratory	purified and conjugated in our laboratory
ERK2			C-14, sc-154, polyclonal rabbit antiserum	Santa Cruz Biotechnology

Table 1. Antibodies used in FACS stainings or Westernblot. Abbreviations: m, mouse; r, rat and h, human.

- **Secondary antibodies**

Antigen	Antibody	Conjugation	Purchased from
Mouse IgG (H+L)	Donkey F(ab') ₂ fragment with minimal cross-reaction to rat and other species serum proteins	FITC or PE	Jackson Immunoresearch Laboratories
Human IgG, Fc _γ Fragment Specific	Goat AffiniPure F(ab') ₂ fragment with minimal cross-reaction to bovine, mouse and rabbit serum proteins	PE	Jackson Immunoresearch Laboratories
Mouse IgG1	Rabbit serum	unconjugated	ICN Biochemicals
Mouse	Goat secondary antibody	HRP	Santa Cruz Biotechnology
Rabbit	Goat secondary antibody	HRP	Santa Cruz Biotechnology

Table 2. Secondary antibodies used in FACS stainings or Westernblot analyses.

- **Secondary Reagents**

Reagent	Binds to	Conjugation	Purchased from
Streptavidin	Biotin	HRP	BD Pharmingen
Streptavidin	Biotin	APCy, PE or PE-Cy5	BD Pharmingen
Strep-Tactin [®]	Strep-tag	PE	IBA (Göttingen, Germany)

Table 3. Reagents used for the detection of biotin/Strep-tag conjugated antibodies or molecules.

2.1.8 Enzymes and inhibitors

T4-DNA-Ligase	Fermentas (St.Leon-Rot, Germany)
Pfu-DNA Polymerase	Finnzymes (Espoo, Finland)
Restriction Enzymes: BamHI, EcoRI, EcoRV, MfeI (MunI), MluI, XhoI, Cfr42I (SacII), Kpn2I (BspEI) and PvuI	Fermentas (St.Leon-Rot, Germany)
Trypsin	BD Biosciences Pharmingen (San Diego, USA)
Biotin-protein ligase BIRA500	Avidity (Colorado, USA)
Complete Mini	Roche (Mannheim, Germany)

2.1.9 Commercially available kits and mixtures

Big Dye 3.1	AB applied biosystems (California, USA)
ELISA kits: rat IFN-γ and IL-4 and IL-10; mouse IFN-γ and IL-4	BD Biosciences
GeneJET Plasmid Miniprep Kit	Fermentas (St.Leon-Rot, Germany)
JET quick DNA clean Up Spin Kit	Genomed (Löhne, Germany)

MESA GREEN qPCR MasterMix	Eurogentec (Seraign, Belgium)
Midi and Maxi JETSTAR Kits	Genomed (Löhne, Germany)
Mini Elute Gel Extraction Kit	Qiagen (Hilden, Germany)
Mouse monoclonal antibody isotyping test kit	AbD Serotec (Kidlington, UK)
PCR Master Mix containing Taq-DNA	Fermentas (St.Leon-Rot, Germany)
QIAamp DNA Mini Kit	Qiagen (Hilden, Germany)
QuikChange II Site-Directed Mutagenesis Kit	Qiagen (Hilden, Germany)
Rat IL-4 ELISPOT Set	BD Biosciences Pharmingen (San Diego, USA)
RNAeasy Mini Kit	Qiagen (Hilden, Germany)
QIAshredder	Qiagen (Hilden, Germany)

2.1.10 Consumables

6 well flat bottom culture plates	Greiner Bio-One (Germany)
12 well flat bottom culture plates	Greiner Bio-One (Germany)
24 well flat bottom culture plates	Greiner Bio-One (Germany)
48 well flat bottom culture plates	Greiner Bio-One (Germany)
96 well U bottom culture plates	Greiner Bio-One (Germany)
6 cm tissue culture dish	Greiner Bio-One (Germany)
50 ml cell culture flask	Greiner Bio-One (Germany)
5, 15 and 25 ml single use pipettes	Greiner Bio-One (Germany)
1.5 ml Eppendorf centrifuge tube	Eppendorf (Eppendorf, Germany)
15 ml centrifuge tube 50 ml centrifuge tube	Greiner Bio-One (Germany)
Cuvette	Bio-Rad (Munich, Germany)
10 µl tips	Molecular Bioproducts (USA)
200 µl yellow tips	Roth (Karlsruhe, Germany)
1000 µl blue tips	Roth (Karlsruhe, Germany)
2 ml and 5ml single-use syringe	BD Biosciences Pharmingen (San Diego, USA)
60 ml single-use syringe	Dispomed (Gelnhausen, Germany)
Cell strainer 70 µm	BD Biosciences Pharmingen (USA)
Needles (of different sizes) for single use	Dispomed (Gelnhausen, Germany)
Polystyrene half area 96 well plates	Corning Incorporated (New York, USA)
Absorbent paper for Western-Blot	Schleicher & Schuell (Dassel, Germany)

Poly-Prep Columns	Bio-Rad (Munich, Germany)
Roti-PVDF membrane for Western-Blot	Roth (Karlsruhe, Germany)

2.2 Methods

2.2.1 Routine molecular biology methods

- **Spectrophotometric determination of RNA and DNA amounts**

Quantification of RNA and DNA was performed at wavelengths of 260 and 280 nm using the Ultrospec 2000 spectrophotometer (Pharmacia Biotech) following the instructions provided by the manufacturer.

- **Genomic DNA isolation**

Genomic DNA from thymocytes or ears was purified using the QIAamp DNA Mini Kit from Qiagen following the instructions provided by the manufacturer.

- **RNA isolation**

RNA isolation was carried out with the RNeasy Mini Kit following the instructions of the manufacturer and using QIAshredder to disrupt the cells. $4\text{-}5 \times 10^6$ and $1\text{-}2 \times 10^6$ cells were used to isolate RNA from primary cells (thymocytes, splenocytes and IHLs prepared as described in the methods section 2.2.7.3) and from hybridomas, respectively.

- **cDNA synthesis**

cDNA synthesis was carried out using the First Strand cDNA Synthesis Kit from Fermentas. 500 ng RNA and oligo(dT)₁₈ primers were used for cDNA synthesis. cDNA was generally directly used as template for PCR except in real time PCR where cDNA was cleaned using the DNA Clean and ConcentratorTM-5 Kit and eluted in water.

- **Polymerase chain reactions (PCRs)**

Various PCR protocols were followed depending on the aim of the experiment:

- **Amplification of IgG heavy and light chain cDNA from the hybridomas 232, 233, 244, 35 and 58**

To assess the V(D)J gene segment usage of Ig genes of anti-CD1d mAb secreting hybridomas, heavy and light chain mRNAs were amplified by RT-PCR. After purification from agarose gels PCR products were directly sequenced.

PCR mixture (50 µl) contained:

2.5 µl cDNA

5 µl primer mix (10µM)

17.5 µl H₂O

25 µl PCR Master Mix 2x containing *Taq* DNA polymerase, MgCl₂, and dNTPs

The primer pairs used for the amplification of the heavy and light chains were *MH2_82/IgGrev 2_101* and *Mk_84/Igk rev 2_104*, respectively. Forward degenerate primers were slightly modified from (Wang et al., 2000).

PCR was carried out in an Eppendorf Mastercycler thermocycler as follows:

1 min at 94 °C

1 min at 45 °C

2 min at 72 °C

Repeated 30 times

Sequencing of the heavy chain was carried out with the *IgGrev 2_101* primer and of the light chains with the *Igk rev 1_103* and *Igk rev 2_104* primers.

- **1.5.2 Analysis of rat CD1d alleles by PCR amplification of genomic DNA**

Genomic DNA from 10 different inbred rat strains (see animals) containing the exons 1 to 3 and the respective introns was amplified by PCR and directly sequenced after purification on agarose gels.

The PCR mixture contained:

500 ng of genomic DNA as template

2.5 µl primer mix (10µM)

10 µl 5x HB buffer (containing 7.5 mM MgCl₂)

1 µl dNTPs (10mM)

0.5 µl Phusion DNA polymerase

H₂O until a final volume of 50 µl was obtained

The primers used for PCR amplification and also direct sequencing were *gCD1d fo 77* and *gCD1d re 78*.

The PCR program repeated 30 times was:

10 sec at 98 °C
30 sec at 60 °C
45 sec at 72 °C

- **RT-PCR and direct sequencing of AV14- and BV8-containing TCRs**

In order to assess the presence of AV14⁺ TCR α and BV8⁺ TCR β chains, AV14-AJ18 rearrangements and β -actin transcripts among thymocytes, splenocytes and IHLs RT-PCR was performed as follows:

PCR Mixture (20 μ l) contained:

1 μ l cDNA template
1 μ l primer mix (10 μ M)
8 μ l H₂O
10 μ l PCR Master Mix 2x containing *Taq* DNA polymerase, MgCl₂, and dNTPs

The primer pairs used were:

Amplified product	Primers
β -actin	<i>RNBetaActFwd17</i> and <i>RNBetaActRev18</i>
AV14-AJ18 (Fig. 20)	<i>rVa14lead gDNA f(50)</i> and <i>rJa18lead gDNA r(51)</i>
AV14-AC (Fig. 20)	<i>rVa14lead gDNA f(50)</i> and <i>rCa_seq2nd_118</i>
BV8-BC	<i>rVb8_seq_fow_122</i> and <i>rVb8_seq_rev_123</i>

Table 4. Primers used in RT-PCR analyses of AV14- and AV14-AJ18-containing TCRs.

The program followed in the Eppendorf Mastercycler, repeated 28 and 35 times for β -actin and for the other PCR products, respectively, was:

10 sec at 98 °C
30 sec at 66 °C
30 sec at 72 °C

13 μ l of PCR products were mixed with 3 μ l of 6 \times loading buffer and were loaded onto 1% agarose gels containing 1 μ g/ml ethidium bromide. After electrophoresis DNA amounts were visualized and imaged using a UV transilluminator (Intas UV System) equipped with a camera.

In order to assess AV14 and AJ gene segment usage in AV14 and AV14-AJ18 comprising TCRs by direct sequencing, the primers used were the same as in the RT-PCR described above (Table 4) but the PCR mixture differed.

PCR mixture (50 μ l):

1-3.5 μ l cDNA template
2.5 μ l primer mix (10 μ M)

10 µl 5x HB buffer (containing 7.5 mM MgCl₂)
1 µl dNTPs (10mM)
0.5 µl Phusion DNA polymerase
32.5-35 µl H₂O

The program followed in the Mastercycler (Eppendorf) and repeated 35-40 times was:

10 sec at 98 °C
30 sec at 66 °C
30 sec at 72 °C

After purification on agarose gels, the PCR products were directly sequenced using the same forward and reverse primers as in the RT-PCR and the *rAV14int_124* primer.

– **Insert preparation by PCR.**

Inserts for cloning were generated by PCR with primers containing the desired modifications such as restriction sites or the nucleotide sequences needed for the creation of fusion proteins.

The PCR mixture generally contained:

2-3 µl of cDNA or 50 ng of cloned template
2.5 µl primer mix (10µM)
10 µl 5x HB buffer (containing 7.5 mM MgCl₂)
1 µl dNTPs (10mM)
0.5 µl Phusion DNA polymerase
and H₂O until a final volume of 50 µl

The program followed in the thermocycler and repeated 25 to 35 times depending on the nature of the template was:

10 sec at 98 °C
30 sec at 66 °C
30 sec at 72 °C

• **Real time PCR**

Real time PCR was conducted running triplicates. The PCR mixture (25 µl) contained:

1 µl cDNA (previously cleaned with the DNA Clean and ConcentratorTM-5 Kit)
1 µl primers (7.5 µM AC primer mix or 2.5 µM iTCR primer mix)
10.5 µl H₂O
12.5 µl 2x MESA GREEN including: dNTPs, Meteor *Taq* DNA polymerase, MgCl₂ 8 mM, SYBR Green I and stabilizers.

The primer-pairs used were *rVa14_Bendef 79/rJ281_Bende 80* and *rt_rCaE1_fo 71/rt_rCaE3_re 72* for amplification of AV14-AJ18 rearrangements (iTCR) and the constant region of the TCR α chain (AC), respectively (Fig. 21).

The protocol followed in the thermocycler iCycler (Bio-Rad) was:

Cycle 1 (1 repetition): 5 minutes at 95 °C

Cycle 2 (40 repetitions): 15 sec at 95 °C, 20 sec at 65 °C and 40 sec at 72 °C. Data collection

Cycle 3 (1 repetition): 1 minute at 95 °C

Cycle 4 (1 repetition): 1 minute at 52 °C

Cycle 5 (86 repetitions): 10 sec at 52 °C and then increase set point temperature after repetition 2 by 0.5 °C. Data collection.

Cycle 6 (1 repetition): Hold at 15 °C.

- **Sequencing**

Amplification of DNA was carried out in a 5 μ l mixture containing:

3 μ l template DNA (750 ng if the amplified template was contained in an expression vector)

0.5 μ l sequencing primer (10 μ M)

0.5 μ l sequencing buffer

1 μ l Big Dye terminator v3.1 containing DNA polymerase and fluorescently-labelled ddNTPs

25 amplification cycles were performed in the thermocycler:

30 sec 96 °C

15 sec 50 °C

4 min 60 °C

Sequences were analyzed in an ABI sequencer.

- **Preparation and ligation of inserts and vectors**

Inserts and vectors were prepared by digestion with restriction enzymes. The digestion was performed following the manufacturer's indications. Purification of digested DNA was carried out on agarose gels. After purification small aliquots of vector and insert were loaded on an agarose gel and electrophoresis was performed in order to assess purity and relative quantity of each component. Ligation was carried out at a 3:1 insert:vector ratio with DNA T4 ligase following the manufacturer's instructions.

- **DNA purification from agarose gels**

After electrophoresis, the fragment of the agarose gel containing the desired DNA was cut out from the gel and DNA was extracted with two different kits depending on whether the purified DNA was going to be sequenced or not. The Mini Elute Gel Extraction Kit (Qiagen) was used to purify PCR products which were subsequently sequenced and the JET quick DNA clean Up Spin Kit (Genomed) was used to purify vectors and inserts after digestion.

- **Transformation**

1-10 μ l of the ligation product were added to 50 or 100 μ l of competent cells contained in a 1.5 ml plastic tube and incubated for 5 minutes on ice. Subsequently the tubes were placed for 90 seconds in a water bath preheated at 42 °C and the tubes were returned to ice where they were incubated for 2 minutes. After the addition of 150 μ l of LB-SOC media, the bacteria were incubated for 1 hour with agitation at 37 °C. Then the bacteria were spread on 1 or 2 agar plates containing selecting antibiotics and were incubated over night at 37 °C.

- **Bacteria cultures**

Most of the vectors used in this study contained ampicillin resistance. Thus, cultures in agar plates and LB media were carried out with in the presence of 100 μ g/ml ampicillin, unless the cultured bacteria contained pFUSE-hIgG1vectors, in which case, 50 μ g/ml Zeocin were added to low-salt LB-agar plates and liquid cultures.

- **Mini, midi and maxi preparations of DNA vectors**

Different volumes of bacteria cultures, depending on the type of desired DNA amounts were incubated overnight at 37°C with rotation (180 rpm): 5 ml for mini- 50 ml for midi- and 250 ml for maxi-preparations. All the DNA-preparations were carried out with commercial kits following the indications of the manufacturer. The kits used were: GeneJET Plasmid Miniprep Kit (Fermentas), and Midi and Maxi JETSTAR Kits (Genomed). After purification of midi- and maxi-preparations, DNA concentration measured by spectrophotometry (Methods section 2.2.1) and generally, an aliquot (250 ng) was digested analyzed by electrophoresis to assess the quality of the DNA sample.

2.2.2 Cloning

2.2.2.1 Cloning of *Mus musculus* CD1d2 and *Mus spretus* CD1d1 into pczCFG5 IEGN

Mus musculus CD1d2 and *Mus spretus* CD1d1 cDNA sequences were cloned into the EcoRI and BamHI sites of pczCFG5 IEGN. Vectors containing the CD1d cDNA sequences amplified by PCR to use as inserts, were kindly provided by Wang, C.R and are described elsewhere (Chen et al., 1999; Zimmer et al., 2009). PCR was performed using the *mCD1d_fo EcoRI* and *msCD1d_BamHIrev_113* primers in order to introduce the EcoRI and BamHI restriction sites at the 5' and 3' ends of the CD1d cDNA sequences.

2.2.2.2 Cloning of rat CD1d cDNA into pczCFG5 IZ

CD1d cDNA sequences derived from LEW, DA, BN and PVG thymocytes were cloned into the EcoRI and BamHI sites of pczCFG5 IZ after PCR amplification of thymus-derived cDNA with the primers: *rCD1d_EcoRI_f62* and *rCD1d_BamHI_r63* and subsequent double digestion.

2.2.2.3 Cloning of rat β 2-microglobulin into the retroviral expression vector pczCFG5 IZ (Carried out by P. Neuhöfer)

Rat β 2-microglobulin was amplified from LEW splenocytes cDNA by PCR using the *MfeI b2_fow P3* and *rb2m BamHI re P2* primers, with which the restriction sites MfeI and BamHI were introduced at the 5' and 3' ends of β 2-microglobulin, respectively. After double digestion with MfeI and BamHI, the resulting product was inserted into the EcoRI and BamHI restriction sites of the retroviral expression vector pczCFG5 IZ. The sequence of the cloned β 2-microglobulin was identical to the sequence published in the GenBank under the accession number NM_012512.

2.2.2.4 Cloning of mouse CD1d into pXIg (Carried out by E. Pyz and I. Müller)

As previously described by others (Schumann et al., 2003), the α 1- α 3 domains of mouse CD1d cDNA were cloned into MluI and XhoI restriction sites of the pXIg vector. For this purpose, the insert was prepared by introducing MluI and XhoI restriction sites by PCR using mouse CD1d cDNA cloned into pczCFG5 IZ (Pyz et al., 2006) as template and the *mCD1d-MD-MluI-Fow* and *mCD1d-MD-XhoI-Rev* primers. To assure the

correct sequence of the mouse CD1d-IgG1 fusion molecule, sequencing was carried out with the primers: *pX/Ig fow, N4 (fow)*, *r/mCD1-alpha1-Re* and *pX/Ig rev*.

2.2.2.5 Cloning of rat CD1d into pXIg (Carried out by E. Pyz and I. Müller).

As mouse CD1d, the cDNA encoding the α 1- α 3 domains of rat CD1d was cloned into the MluI and XhoI restriction sites of the pXIg vector. By PCR, CD1d cDNA was amplified from rat CD1d cloned into pczCFG5 IEGZ (Pyz et al., 2006) and restriction sites were introduced. *rCD1d-MD-MluI-F* and *rCD1d-MD-XhoI-R* are the primers which were used. The signal sequence of CD1d was not included, because the pXIg vector contains the signal sequence of the IgG1 heavy chain. In order to prove the correct insertion of rat CD1d into the pXIg vector, *pX/Ig fow, N4 (fow)* and *pX/Ig rev* primers were used for sequencing.

2.2.2.6 Cloning of rat β 2-microglobulin-CD1d fusion protein into the pFUSE-hIgG1-Fc2 vector

First of all, rat CD1d was cloned into the pFUSE-hIgG1-Fc2 plasmid, creating a fusion protein with the rat CD1d extracellular domains (α 1- α 3) inserted between the IL-2 signal sequence and the human IgG1 Fc portion. The CD1d insert was produced by PCR from previously cloned rat CD1d cDNA (Pyz et al., 2006) using the primers *rCD1dEcoRI Fc2_88* and *rCD1dBamHI Fc_86*. The PCR product contained the EcoRI and BamHI restriction sites, and after double digestion it was inserted into the EcoRI and BglIII sites of the pFUSE-hIgG1-Fc2 vector. Subsequently, rat β 2-microglobulin was attached to this fusion protein-construct. To this end, rat β 2-microglobulin cDNA was amplified from a retroviral expression vector (see methods section 2.2.2.3) using *rb2 MunI fo_105* and *rb2m MunI rev_106* primers, which did not amplify the rat β 2-microglobulin signal sequence. These primers allowed not only to insert the MunI restriction site at both, 5' and 3' ends of the β 2-microglobulin cDNA, but also to include a glycine-serine linker at the 3' end. The resulting product was digested with MunI and inserted into the EcoRI site of the previously cloned rat CD1d pFUSE-hIgG1-Fc2 plasmid. Sequencing was carried out with the *pFUSE Fc fow_90* and *pFUSE Fc rev_91* primers to assure that the final fusion protein consists of the IL-2 signal sequence, rat β 2-microglobulin linked to rat CD1d by a glycine-serine linker and, at the 3' end of CD1d, the human IgG1Fc portion.

2.2.2.7 Cloning of rat CD1d into the pMT/BioHis-IA^b α vector

In the first place, in order to allow the insertion of rat CD1d between the BiP signal sequence and the biotinylation site contained in the pMT/BioHis-IA^b α vector produced by M. Schiemann, Institute of Medical Microbiology, Dept. of Medicine, Technical University Munich (Schiemann, 2005), the Kpn2I restriction site was included before the specific biotinylation sequence by site directed mutagenesis with the QuikChange II Site Directed Mutagenesis Kit. The primers used were *Kpn2I Forward* and *Kpn2I Reverse*. This vector contains a metallothionein promoter and a BiP signal sequence which are necessary for protein production in SC2 cells. After addition of the Kpn2I restriction site, the insert (an MHC II α chain) was excised by double digestion with SacII and Kpn2I and replaced by the extracellular domains of rat CD1d. The rat CD1d insert was prepared by PCR using rat CD1d cDNA (Pyz et al., 2006) as template and the *Ok CD1d SacII For* and *CD1d Kpn2I Rev* primers, followed by double digestion with the SacII and Kpn2I restriction enzymes. Sequencing of the final plasmid was carried out with the *MT Forward* and *BGH Reverse* primers.

2.2.2.8 Cloning of rat β 2-microglobulin-CD1d into the pcDNA3.1/V5 His A Bio vector

The fusion protein containing the IL-2 signal sequence, rat β 2-microglobulin and rat CD1d (see methods section 2.2.2.6), previously constructed for the production of the human Fc dimers, was amplified by PCR with the *IL2ko EcoRV_111* and *rCD1drev XhoI_112/3* primers. After double digestion it was inserted into the EcoRV and XhoI sites of the pcDNA3.1/V5 His A Bio vector 5' to the biotinylation sequence and the polyhistidine tag. Sequencing of the final construct was carried out with the *pcDNA3 fo_107* and *pcDNA3 rev_108* primers.

2.2.2.9 Cloning of rat β 2-microglobulin-CD1d into the pMT/BiP/His/Strep TagIII-IA^b α vector

To produce the rat CD1d strep-tag fusion construct, the cDNA encoding the rat β 2m-CD1d fusion protein (described in the methods section 2.2.2.6), was cloned into the pMT/BiP/His-IA^b α StrepTag III. This vector contains the BiP signal sequence necessary for secretion in SC2 cells. Therefore, the rat β 2-microglobulin CD1d construct was cloned into the SacII and Kpn2I restriction sites without the IL-2 signal sequence. The vector was linearized by double digestion with SacII and Kpn2I and the insert (a mouse

MHC class II α chain) was replaced by the rat β 2m-CD1d construct. The SacII and Kpn2I restriction sites in the rat β 2m-CD1d insert were introduced by PCR amplification using the *rb2mSacII_114* and *CD1d Kpn2I Rev* primers. Sequencing of the final construct was carried out with the *MT Forward priming site* and *rCD1d seq_61* primers to assure that it contained the BiP signal sequence, rat β 2-microglobulin fused to CD1d by a glycine-serine linker and the strep-tag.

2.2.2.10 Cloning of AV14-containing TCR α chains

AV14-containing TCR α chain cDNAs were cloned into the EcoRI and BamHI of the retroviral expression vector pczCFG5 IZ after RT-PCR amplification of splenocytes or intrahepatic lymphocytes-derived RNA using the primers *rVal14EcoRI-Fow* and *Ca end BamHI antisense*.

2.2.3 Production and purification of CD1d oligomers

2.2.3.1 Mouse and rat CD1d-IgG dimers

Plasmids encoding CD1d-IgG proteins were transfected by electroporation (after linearization with PvuI) into the endogenously λ light chain expressing J558L murine plasmocytoma cell line, as previously described (Schneck, 2000). After G-418 selection and single cell cloning, screening of clones secreting high CD1d-Ig levels was carried out with the CD1d Sandwich ELISA described in the methods section 2.2.6. Subsequently, J558L cells producing rat CD1d-IgG dimers were retrovirally transduced with rat β 2-microglobulin. Dimers were purified from large-scale serum-free cultures (ISF-1 media) by protein G affinity chromatography (Methods section 2.2.3.6). Protein purity of the different eluted fractions was monitored by SDS-PAGE and Coomassie Blue R250 staining (Fig. 14). Fractions containing CD1d dimers were collected and concentrated using Centriprep YM-30 columns or Vivaspin 6 (50.000 MWCO) at the same time as the elution buffer was exchanged for PBS. Final protein concentration was determined by photometry.

2.2.3.2 Rat β 2-microglobulin CD1d human Fc dimers

293T cells were transfected using calcium chloride, selected with Zeocin, and cloned by limiting dilution. Clones were screened for protein secretion by CD1d Sandwich ELISA (see methods section 2.2.6) and the clone expressing the highest levels of rat β 2-microglobulin CD1d human Fc (rat β 2m-CD1d-hFc) dimers was expanded with serum

containing media (DMEM). Prior to protein purification, culture media was exchanged by serum free media (ISF-1) and 48 hours later, the supernatant was harvested. Protein was purified by protein G affinity chromatography (Methods section 2.2.3.6). Purity of the different eluted fractions was controlled by SDS-PAGE followed by Coomassie Blue R250 staining (Fig. 14). As described for the mouse CD1d-IgG dimers, the fractions containing the rat β 2m-CD1d-hFc dimers were collected, concentrated and the elution buffer was exchanged for PBS using a Centrprep YM-30 column. Since other proteins were present in the preparation (Fig. 14), only half of the protein concentration obtained by photometry was considered to be rat β 2m-CD1d-hFc dimers.

2.2.3.3 Rat CD1d production in SC2 drosophila cells

Rat CD1d fused to a specific biotinylation sequence followed by a polyhistidine tag (rat CD1d-biotag) was constructed as described in the methods section 2.2.2.7. Plasmid transfection into SC2 cells, selection and isolation of CD1d producing clones, protein purification and biotinylation was performed by M. Schiemann, Institute of Medical Microbiology, Dept. of Medicine, Technical University Munich as previously described by A. Bendelac and colleagues (Benlagha et al., 2000). Protein purity was monitored by SDS-PAGE and Coomassie Blue R250 staining (Fig. 14).

2.2.3.4 Rat β 2-microglobulin-CD1d production in 293T human cells

293T cells were transfected with the vector described in the methods section 2.2.9 using calcium chloride and selected with G-418. After single cell cloning, the clone producing the highest amounts of soluble rat CD1d protein, identified by analyzing the supernatants using CD1d Sandwich ELISA (Methods section 2.2.6), was expanded with serum containing media (DMEM). 72 hours prior harvesting, media was exchanged by serum free media (HyQ). S. Saremba, Julius von Sachs Institute, Dept. of Biology, University of Würzburg, purified the CD1d soluble protein by Ni-NTA chromatography. Protein purity was assessed by SDS-PAGE and Coomassie Blue R250 staining (Fig. 14). Concentration was determined by photometry, taking in consideration the molar absorptivity of the final rat β 2m-CD1d fusion protein.

2.2.3.5 Rat β 2-microglobulin-CD1d linked to a streptag production by SC2 drosophila cells

Transfection with the plasmid encoding the fusion protein described in the methods section 2.2.2.9 into SC2 drosophila cells, selection of the clones producing CD1d and protein purification using the strep-tag was carried out by M. Schiemann, Institute of Medical Microbiology, Dept. of Medicine, Technical University Munich. Protein purity was assessed by SDS-PAGE and Coomassie Blue R250 staining (Fig. 14).

2.2.3.6 Protein G affinity chromatography

1 ml of Protein G sepharose 4 Fast Flow stored with PBS containing 0.9% of sodium azide at 4 °C was placed in a Poly-Prep 9 cm column and washed firstly with 5 ml of 50 mM diethylamine (pH 11) at 1 ml/min and secondly with 10 ml PBS. The supernatant of 1.5 l of J558L cultures (in serum free media) was loaded at 1ml/min. The column was washed with 10 ml of PBS and with 5 ml of PBS containing 1M NaCl. Elution was carried out with 5 ml 50 mM diethylamine (pH 11) and protein was collected in 1.5 ml plastic tubes containing Tris buffer (2M at pH 6.0, 300 μ l Tris for 5 ml eluted proteins). After elution, the column was washed with 20 ml of PBS and further purifications were carried out until the concentration of the dimers contained in the supernatant had dropt at least to one fifth of the initial concentration (monitored by CD1d Sandwich ELISA, methods section 2.2.6).

2.2.3.7 Photometric determination of protein concentration

Monoclonal antibody and dimer concentrations were measured by photometry using the Ultrospec 2000 spectrophotometer and calculated using the formula $A_{280} * 1.46 - A_{260} * 0.74 = c$ (mg/ml), where A is absorbance and c is concentration. The concentration of monomeric rat β 2m-CD1d-biotag (Methods section 2.2.3.4) was measured considering the molar absorptivity of the final fusion protein with the formula: $c = A_{280} / \epsilon L$, where L is 1 cm; A the absorbance at 280 nm and ϵ the molar absorption coefficient which can be calculated with the formula: $\epsilon = (nW * 5500) + (nY * 1490) + (nC * 125)$, where n is the number of each amino acid residue and the stated values are the amino acid molar absorptivities at 280 nm (W, tryptophan; Y, tyrosine and C, cysteine).

2.2.3.8 Coomassie Blue staining

After proteins were separated by SDS-PAGE and stacking gel was removed, polyacrylamide gels were submerged for 4 to 16 hours in Coomassie Blue staining solution. Subsequently, several incubations were carried out with destainig solution until the polyacrylamide gel appeared transparent and proteins could be visualized stained in blue.

2.2.3.9 Specific biotinylation

Specific biotinylation of the soluble CD1d-purified protein (150 μg) from 293T cells supernatants (Methods section 2.2.3.4) was carried out with BirA (3 μg) enzyme during 2 hours and 45 minutes at 30 °C and in a final volume of 279.5 μl , conditions which are recommended by the manufacturer. Specific biotinylation was assessed by incubating the biotinylated samples during 2 hours at room temperature in Polystyrene 96 well plates which had been pre-coated overnight with 50 μl of unconjugated 233 mAb diluted in coating buffer (100 ng/ml). After 5 washing steps with PBS containing 0.05% Tween, SA-HRP was added, incubated 1 hour at room temperature. Plates were washed 5 more times (30 sec to 1 min incubations) and substrate solution was added for 30 minutes. Reaction was stopped by addition of 25 μl of 2M H_2SO_4 solution and plates were read at 450 nm in the Vmax Kinetic Microplate Reader (Molecular Devices).

2.2.3.10 Lipid loading into CD1d molecules

α -Gal and β -Gal loading into CD1d recombinant proteins (rat and mouse CD1d-IgG dimers, rat β 2m-CD1d-hFc dimers and of rat β 2m-CD1d-streptag) was carried out at 37 °C during 24 hours in the presence of 0.05% TRITON X-100. Rat and mouse CD1d-IgG dimers were loaded with 40x molar excess of α -Gal or β -Gal at a final concentration of 250 $\mu\text{g}/\text{ml}$. The rat β 2m-CD1d-hFc dimers were also loaded with a 40x molar excess of α -Gal or β -Gal but at a final concentration of 138 $\mu\text{g}/\text{ml}$. Rat β 2m-CD1d-streptag monomers were loaded with 20x molar excess of α -Gal or β -Gal at a final concentration of 100 $\mu\text{g}/\text{ml}$.

2.2.3.11 Oligomerization of rat β 2-microglobulin-CD1d linked to a streptag

Rat β 2m-CD1d-streptag monomers loaded with α -Gal or β -Gal as described in the methods section 2.2.3.10, and thus containing 0.05% TRITON X-100, were incubated with Strep-Tactin-PE for 45 min on ice. For each microgram of rat β 2-m-CD1d-streptag

monomers, 5 μ l Strep-Tactin-PE were added in a final volume of 50 μ l achieved with the addition of FACS buffer.

2.2.4 Immunoprecipitation

Thymocytes and transduced cell lines were biotinylated with 2 mg/ml Sulfo-NHS-LC-Biotin in PBS for 15 min on a rotating platform at 4 °C and washed twice with RPMI (supplemented as for cultures) followed by two additional washing steps with BSS/BSA. After biotinylation, 10^6 transductants or 5×10^7 thymocytes were lysed in 1 ml of IP lysis buffer for 30 min on ice. Nuclei were removed by centrifugation immediately after lysis. Subsequently, the lysate was pre-absorbed one hour on Protein A Sepharose at 4 °C. For specific immunoprecipitation, Protein A Sepharose beads were pre-coated with rabbit anti-mouse IgG before the addition of monoclonal antibodies. Then, the matrices were covalently linked as previously described (Schneider et al., 1982). Pre-absorbed lysates were incubated overnight with specific immunomatrices. Precipitates were then washed four times with IP lysis buffer and were resuspended in IP loading buffer and boiled for 5 min before loading onto SDS-PAGE. The molecular weight marker used, PageRuler™ Prestained Protein Ladder, was purchased from Fermentas. After SDS-PAGE and blotting, membranes were incubated with streptavidin-HRP diluted 1:10000 in PBS containing 0.1% Tween during two hours at room temperature. After four washing steps with PBS containing 0.1% Tween detection was carried out using commercially available ECL reagents.

2.2.5 Western blot analysis

2.2.5.1 Binding capacities of anti-CD1d mAbs under reducing and non-reducing conditions

In order to assess the binding capacities of the 233, 35 and 58 mAbs under reducing and non-reducing conditions, 250 μ l of whole cell lysate-proteins from P80 cells transduced with rat CD1d (2×10^7 P80rCD1d cells were lysed in 1 ml of lysis buffer) were mixed with reducing and non-reducing WB loading buffer and were separated by SDS-PAGE. In this case the stacking gel was casted with a comb containing one large sample well and one reference well. Proteins were transferred to a Roti-polyvinylidene difluoride membrane. Protein-free sites of the membranes were blocked with PBS containing 0.1% BSA and 5% non-fat dried milk was carried out during one hour at room temperature. After washing five times with PBS containing 0.1% Tween, membranes were placed

into a multiscreen apparatus which allowed the incubation of the membranes with at least 20 different antibodies solutions (specific antibodies and final concentrations are specified in the legend of Fig. 2). After overnight incubation at 4 °C with the different antibody solutions, the membranes were washed and bound antibody was detected with a secondary HRP-conjugated Goat anti-mouse secondary antibody diluted in PBS containing 0.1% of Tween and 2.5% of non-fat dried milk during one hour at room temperature. After four washing steps with PBS containing 0.1% Tween, detection was carried out with commercially available ECL reagents.

2.2.5.2 Binding of 233 and 35 mAbs to mouse and rat CD1d

For the analysis of cell lines expressing rat and mouse CD1d, whole cell lysates (2×10^7 cells in 1 ml WB lysis buffer) were mixed with WB non-reducing loading buffer and 18 μ l were separated by 10% SDS-PAGE. The molecular weight marker used, PageRuler™ Prestained Protein Ladder, was purchased from Fermentas. Proteins were transferred to a Roti-polyvinylidene difluoride membrane. For CD1d detection, 233 and 35 mAbs were used at a final concentration of 0.75 μ g/ml. Protein loading control anti-ERK2 rabbit polyclonal antibody was used at a final concentration of 2 μ g/ml. Primary antibodies were detected with HRP-conjugated goat anti-mouse antibody. All antibodies were diluted in PBS, 0.1% Tween and 2.5% non-fat dried milk. Films were developed by chemiluminescence using self-made or commercially available ECL reagents.

2.2.5.3 Western blot of proteins derived from rat tissues

Protein preparation from rat tissues was performed by disrupting the tissues with a rotor-stator homogenizer directly into WB lysis buffer supplemented with protease inhibitors. After protein concentrations had been determined by using the Bio-Rad protein assay, 20 μ g of protein were mixed with WB non-reducing loading buffer, boiled, and separated by 10% SDS-PAGE. For detection of CD1d, only the 233 mAb was used. The protocol followed was the same as described in the previous section including the anti-ERK loading control (Methods section 2.2.5.2).

2.2.6 CD1d Sandwich ELISA

A CD1d Sandwich ELISA was established with the 233 and 35 mAbs and carried out in Polystyrene 96 well plates. Proteins derived from rat CD1d transduced P80 cells (complete cell lysate, 2×10^6 cells /ml) were used as standard.

- Coating was carried out overnight with the unconjugated 233 mAb diluted in coating buffer at a final concentration of 100 ng/ml (50 µl).
- Plates were washed five times with PBS-T (0.05% Tween) (200 µl).
- Non-specific binding sites were blocked with PBS containing 10% FCS (100 µl) 1 hour at room temperature.
- Plates were washed five times with PBS-T (0.05% Tween) (200 µl).
- Samples (50 µl) were incubated for two hours at room temperature.
- Plates were washed five times with PBS-T (0.05% Tween) (200 µl).
- Biotinylated 35 mAb (50 µl) diluted in PBS containing 10% FCS, at a final concentration of 176 ng/ml, was incubated for one hour at room temperature.
- Plates were washed five times with PBS-T (0.05% Tween) (200 µl), with 1 min to 30 sec soaks.
- Substrate solution (50 µl) was added and incubated from 10 to 30 min depending on the velocity of the reaction
- 25 µl stop solution (2M H₂SO₄) was added to each well.

Plates were read at 450 nm within 30 minutes of stopping reaction in the Vmax Kinetic Microplate Reader (Molecular Devices).

2.2.7 Routine cell culture methods

2.2.7.1 Cell culture

Cells were cultured in sterile conditions at 37 °C with 5% CO₂ and H₂O-saturated atmosphere. Unless otherwise indicated, cell lines were cultured with RPMI 1640 supplemented with 5% FCS, 1 mM sodium pyruvate, 2.05 mM glutamine, 0.1 mM nonessential amino acids, 5 mM β-mercaptoethanol and Penicillin-Streptomycin 100 U/ml. J558L cells and primary cells, unless otherwise specified, were cultured with RPMI 1640 supplemented additionally with 10 mM HEPES and 10% FCS. 293T cells were cultured with DMEM containing pyruvate supplemented with 10% FCS and Penicillin-Streptomycin 100 U/ml. For adherent cells ATV was used to detach cells from the plates.

2.2.7.2 Freezing and thawing

Cell lines were cryopreserved at -140 °C. For this purpose cells were harvested and resuspended in 1 ml of freezing media. Before transferring them to -140 °C, cells were

frozen at -70 °C. When cells were again cultured, vials were thawed at room temperature and immediately washed with complete media twice. After washing, the pelleted cells were resuspended in fresh media and incubated at 37 °C.

2.2.7.3 Preparation of primary single cell suspensions

Animals were sacrificed by asphyxia with CO₂. When PBCs were analyzed, heart puncture was firstly performed and heparin was added to the collected blood in order to avoid coagulation. After dissection, organs were removed and kept in BSS/BSA at 4°C until tissue disruption.

2.2.7.3.1 Single cell suspension from thymus and spleen

Organs were homogenized by passing them through a metal mesh, cells were transferred to a 15 ml tube in 14 ml BSS/BSA and were let stand for 10 min to allow that tissue debris settle at the bottom of the tube. Supernatant containing the cells was transferred to a fresh 15 ml tube and centrifuged at 1600 rpm for 5 min at 4 °C. Then, always in spleen preparations and if desired in thymus preparations, erythrocytes were lysed by incubating the cell pellet with 3 ml TAC buffer for 10 minutes at room temperature. Subsequently, 10 ml of BSS/BSA were added and cells were centrifuged at 1600 rpm for 5 min at 4 °C. Cells were washed one additional time with BSS/SBA, resuspended into BSS/BSA or complete media and counted.

2.2.7.3.2 Intrahepatic lymphocytes preparation

Mouse and rat intrahepatic lymphocytes were isolated as previously described by E. Pyz et al. (Pyz, 2004; Pyz et al., 2006) with slight modifications. 100% Percoll was prepared with 90 ml Percoll and 10 ml 10x PBS. Different concentrations of Percoll were prepared with this 100% Percoll and RPMI 1640 containing 5% FCS. Percoll solutions were used at room temperature to avoid gradient perturbations.

- After excision of any other organ which also was going to be analyzed, heart puncture was performed in order to reduce the blood flowing in the animal.
- Blood was flushed of the liver by perfusing it with BSS/BSA (100 to 180 ml in rats and 10 ml in mice) through the portal vein with a syringe until the liver became pale.
- Once all the blood had been eliminated from the liver, this organ was removed and placed in a 10 cm dish containing BSS/BSA and kept at 4 °C until homogenization.

- Liver was cut into small pieces and homogenized in a Glass/Teflon Potter Elvehjem homogenizer.
- Liver homogenate was then passed through a stainless steel mesh adding BSS/BSA up to a final volume of 50 ml and cells were transferred into a 50 ml tube, in case of rats and into a 15 ml tube in case of mice.
- Cell suspension was centrifuged at 1600 rpm at 4°C.
- Pellet containing cells was resuspended into 40% Percoll (28 ml with rat livers and 7 ml with mouse livers) and layered over of 80% Percoll (12 and 4 ml, with rat and mouse livers, respectively).
- Centrifugation was carried out at 2500 g (rcf) with no brake for 20 minutes at room temperature.
- The supernatant containing liver tissue was aspirated to facilitate the collection of the lymphocytes from the interface. Some erythrocytes appeared at the bottom of the tube.
- Lymphocytes were harvested from the interface (12 ml for rats and 2 ml for mice approximately), transferred to a fresh 50 ml tube and washed with 35 ml BSS/BSA (10 min 1600 rpm at 4 °C).
- Pellet was washed an additional time with BSS/BSA
- Cells were resuspended in 5 or 10 ml BSS/BSA or complete RPMI media and filtered through a 70 µm mesh.
- Cells were counted and kept on ice until further use.

2.2.7.3.3 Isolation of peripheral blood cells

Heparin treated blood was isolated by heart puncture and transferred to a 15 ml plastic tube. After washing 2 ml of blood with 50 ml BSS/BSA by centrifuging at 1600 rpm for 10 minutes, erythrocytes were lysed by 3 to 4 incubations with 10 ml TAC buffer. After each lysis-incubation, cells were washed by adding 40 ml BSS/BSA directly to the cells contained in TAC buffer and centrifugation for 10 min at 1600 rpm. After lysis of erythrocytes, the pelleted cells were resuspended into BSS/BSA or complete RPMI 1640 media and counted.

2.2.7.3.4 Isolation of peripheral mononuclear blood cells

2-4 ml blood were collected by heart puncture and treated with heparin and diluted with an equal volume of phosphate buffered saline (PBS). Blood samples were carefully

layered over 3 ml of Ficoll-Hypaque in a 15 ml tube and centrifuged at 400 rcf for 30 minutes at 20 °C with no brake. The PBMCs at the interface were aspirated with a Pasteur pipette and washed twice with BSS/BSA. The PBMCs were finally resuspended in 1 ml of RPMI medium or BSS/BSA and counted.

2.2.8 Primary cell cultures

2.2.8.1 Stimulation assays and analysis of cytokine release

Primary cells harvested as described in the methods section 2.2.7.3 were cultured for 24 hours in 96 well plates (U bottom) with different stimuli: α -Gal, β -Gal, ConA or only media. The final concentrations of these stimuli in each experiment are specified in the legends of the figures. Cell numbers added to each well were 2×10^6 thymocytes, 2×10^6 splenocytes and 5×10^5 IHLs, unless otherwise indicated in the figure legends. In CD1d-blocking experiments, purified antibodies or isotype-specific controls were added to the culture at a final concentration of 3.6 μ g/ml. After harvesting the supernatants cytokine production was quantified using commercial ELISA kits from BD Biosciences (rat and mouse IFN- γ and IL-4).

2.2.8.2 Seven-days intrahepatic lymphocytes cultures

10^6 intrahepatic lymphocytes were incubated for seven days with 1ml RPMI⁺⁺ per well in 48-well plates with α -Gal (20 ng/ml), β -Gal (20 ng/ml), ConA (3 μ g/ml), or only media.

2.2.8.3 Rat IL-4 ELISPOT assay

Rat IL-4 ELISPOT assay from BD Biosciences was carried out following the manufacturer's instructions using 250.000 IHLs, 10^6 splenocytes or 1.5×10^6 thymocytes per ELISPOT well. In CD1d-blocking experiments, purified antibodies or isotype-specific controls were added to the culture at a final concentration of 3.6 and 7.2 μ g/ml in splenocytes and IHLs cultures, respectively. The substrate used was BDTM AEC Reagent. Spots were automatically enumerated and analyzed using the CTL-ImmunoSpot S5 Versa analyzer ELISPOT reader and ImmunoSpot 4.0 Software (CTL).

2.2.9 Transfection of 293T cells

Calcium chloride transfection of 293T cells was carried out with two different purposes: First, to produce retrovirus for transduction of a gene of interest into other cells as

previously described by Soneoka et al. (Soneoka et al., 1995) or second, to obtain 293T cells which produced and secreted CD1d recombinant proteins. The same protocol was used for both aims, only the plasmids which were transfected were different. 293T cells were cultured in DMEM⁺ (containing HEPES) except during the transfection step.

- Day 1

1.5*10⁶ 293T cells were plated into a 6 cm tissue culture dish with 5 ml DMEM⁺.

DNA was precipitated with 500 µl iso-propanol in a 1.5 ml tube at maximum speed (13.000 rpm) precipitation. Once iso-propanol had been discarded, DNA was sterilized by adding 500 µl of ethanol (70%) and inverting the tube several times. After 30 min centrifugation at maximum speed for 30 minutes at 4°C, ethanol was discarded and the tubes were dried in the laminar flow hood to maintain sterile conditions. Once all ethanol had been evaporated, DNA was resuspended into 100 µl of sterile H₂O and was kept at 4 °C, if used the next day or at -20°C if used at a later time point.

The total amount of DNA transfected in each culture dish was 15 µg. For production of retrovirus; 5 µg of pHIT 60, 5 µg of pVSV and 5 µg of the retroviral expression vector containing the gene of interest were precipitated together. For CD1d-recombinant protein expression; 15 µg of the desired vector (see methods sections 2.2.2.6 and 2.2.2.8) were precipitated.

- Day 2: Transfections

After aspiration of the media in which the 293T cells had been cultured, 4 ml of fresh DMEM without HEPES were gently added. Culture dishes were incubated one hour at 37°C, 5% CO₂, in order to equilibrate the pH of the media.

The transfection mixture was prepared as follows: 338 µl of sterile H₂O and 62 µl of CaCl₂ 2M were added to the 100 µl of H₂O containing the DNA previously prepared, obtaining a final volume of 500 µl. Then, 500 µl of 2X HBS were pipetted into a fresh sterile 1.5 ml tube and the mixture of DNA and CaCl₂ was added to the 2x HBS while “bubbling” with a Pasteur pipette and a pipette helper. The mixture was incubated for 15-20 minutes at room temperature and added drop wise to the culture plates. Dishes were carefully shaken in order to distribute the precipitate evenly. Dishes were incubated 6 to 8 hours at 37°C, 5% CO₂. Subsequently media

was aspirated and replaced by 5 ml of fresh DMEM⁺. Cells were incubated overnight at 37 °C with 5% CO₂.

- Day 3 (only carried out if the aim of the transfection was the production of retrovirus)

Media was replaced with 5 ml D-MEM⁺ containing 10 mM Na-Butyrate and cells were incubated for six to seven hours at 37 °C with 5% CO₂. Subsequently Na-Butyrate containing media was aspirated and replaced with 5 ml of fresh DMEM⁺ media and cells were incubated overnight at 37 °C with 5% CO₂.

2.2.10 Retroviral transduction

At day four of the transfection procedure, target cell lines were transduced with the supernatant derived from the transfected 293T cells (containing the retroviral particles). The viral supernatant was aspirated with a syringe and passed through a 0.45 µm filter. 10⁵ target cells were infected with 3 ml of viral supernatant containing 4 µg/ml Polybrene. Infection was carried out for 30 minutes at 37 °C in the cell culture incubator, 3 hours centrifuging at 2000 rcf at 37 °C and 30 further minutes again at 37 °C in the cell culture incubator. Finally, viral supernatant was exchanged by fresh culture media (for example, RPMI 1640).

2.2.11 Immunofluorescence and flow cytometry

Flow cytometry was carried out using a FACSCalibur (BD Biosciences) and data were analyzed with CellQuest (BD Biosciences) or FlowJo software (Tree Star).

For the analysis of rat and mouse primary cells, 1-2*10⁶ cells were diluted in 100 µl FACS buffer. When mouse primary cells were stained, unspecific binding to Fc receptor was blocked using the 2.4G2 mAb. Combinations of antibodies and/or CD1d oligomers used in each staining are specified in the figure legends. When mouse-derived unconjugated antibodies or CD1d-IgG dimers were used in multicolor stainings, samples were first incubated only with the unconjugated reagent, washed, and bound antibody was detected by incubation with a FITC or PE labeled donkey F(ab')₂ fragment anti-mouse IgG (H+L) with minimal crossreaction to rat and other species serum proteins. After a further washing step, unspecific binding to the donkey anti-mouse reagent during

subsequent stainings was blocked by adding substantial amounts of serum mouse IgG for 15 min.

Staining of BW cells expressing a rat semi-invariant TCR (rAV14S6 + CDR2+4, (Pyz et al., 2006)) with various CD1d oligomers was carried out as specified in the legend of the figures 15 and 16.

2.2.12 Statistical analysis

Statistical differences between various cell populations were analyzed by conducting two-tailed paired Student's t test: see results section 3.8. All analyses were performed with the statistical software GraphPad Prism.

3 RESULTS

3.1 Further characterization of rat CD1d specific mAbs

The lack of monoclonal antibodies had impaired the study of CD1d and its function in the rat. Therefore, five different hybridomas: 232, 233, 244, 35 and 58, which secreted anti-rat CD1d mAbs had previously been generated in our laboratory (Pyz, 2004) and were further characterized in this thesis. All the antibodies bound to rat CD1d on primary thymocytes or transduced cell lines. Importantly, the mAbs 232, 233 and 35 recognized mouse CD1d1 on transduced cells or thymocytes with the same efficacy as rat CD1d while, mAbs 244 and 58 only showed such cross-reactivity for mouse CD1d1 expressed by transduced cells but not for CD1d1 positive primary mouse cells.

Titration and cross-competition flow cytometric analyses using primary as well as CD1d-transduced cells revealed indistinguishable binding properties of 232 and 233 on the one hand, and of 244 and 58 mAbs on the other hand. The antibody with the highest avidity for CD1d was 35, followed by 232 or 233 and by 58 or 244. Moreover, the mAbs 35 and 232 or 233 do not cross-compete while 58 and 244 partially compete with 35 and with 233 or 232.

Part of the results presented in this doctoral thesis obtained with two of these monoclonal antibodies (233 and 35) has already been reported by us in a recent publication (Monzon-Casanova et al., 2010). In this published work the 233 and 35 mAbs were renamed as WTH-1 and WTH-2, respectively, in order to give to the mAbs a more distinctive name than only numbers.

3.1.1 Determination of V (D) J gene segment usage

In order to analyze which V-(D)-J gene segments form the variable regions of the heavy and light chains of each hybridoma, both chains were amplified by RT-PCR and sequenced. RT-PCR was carried out according to (Wang et al., 2000) but using slightly modified degenerate forward primers. The isotype of all mAbs was IgG2a, κ , therefore the same primers were used for PCR amplification of all heavy chains. Sequencing of the heavy chain was successful for all the hybridomas, whereas it was only possible to sequence the light chain of 244, 35 and 58. Identification of which V-(D)-J segments were used was accomplished using IMGT/V-QUEST at the international ImMunoGeneTics information system (Brochet et al., 2008). This and the direct comparison between the sequences obtained for the chains of the different hybridomas

revealed on the one hand, identical heavy chains of the 232 and 233 hybridomas and on the other hand, that also the 244 and 58 heavy and light chains were the same. In contrast, the variable regions of the heavy and light chains of the hybridoma 35 are distinct from all the other mAbs (Table 5).

Hybridoma	Heavy chain	Light chain
232	IGHV12-1-1*01	no PCR product was obtained
	IGHJ4*01	
	IGHD1-14*01 in reading frame 2	
233	IGHV12-1-1*01	no PCR product was obtained
	IGHJ4*01	
	IGHD1-14*01 in reading frame 2	
244	IGHV3S1*01	IGKV6-25*01 IGKJ2*01
	IGHJ3*01	
	various IGHD	
35	IGHV1-77*01	IGKV19-93*01 IGKJ2*01
	IGHJ4*01	
	IGHD1-1*01 in reading frame 3	
58	IGHV3S1*01	IGKV6-25*01 IGKJ2*01
	IGHJ3*01	
	various IGHD	

Table 5. Gene segment usage of the heavy and light chains of the five studied hybridomas. Identification of the gene segments was carried out using the V-QUEST integrated alignment tool under the IMGT information system (http://imgt.cines.fr/IMGT_vquest/share/textes/imgtvquest.html)

3.1.2 mAb reactivity in immunoprecipitation and Western blot analyses

Immunoprecipitation and Western blot experiments were performed in order to further confirm CD1d specificity of the mAbs, as well as to study their reactivities under denaturing conditions. As shown in figure 1 the three mAbs (233, 35 and 58) precipitated two chains from primary rat thymocytes as well as from rat CD1d transduced cells. Under reducing conditions the apparent molecular size of the heavy chain was between 50 and 60 kDa, corresponding to the heavily glycosylated CD1d and the light chain run at the expected weight of β 2-microglobulin (12 kDa). Precipitation by 58 mAb was less efficient than by 35 or 233. Furthermore, the ratio of precipitated β 2-microglobulin to CD1d heavy chain was lower than for the other two mAbs. Densitometric analysis of material precipitated from primary rat cells revealed ratios of 0.15, 0.65 and 0.63 for 58, 35 and 233, respectively. The equivalent ratios for rat CD1d transductants were: 0.07, 0.62, and 0.87.

233 and 35 precipitated the corresponding heavy and light chains from mouse thymocytes and from mouse CD1d1-transduced cells, while mAb 58 precipitated only very weakly the heavy chain from lysates of mouse CD1d transductants but not from mouse primary thymocytes (Fig. 1). These results are also in line with the data obtained

by flow cytometry. The apparent molecular weight after SDS-PAGE of the precipitated proteins was the same regardless of the species origin or the cell source.

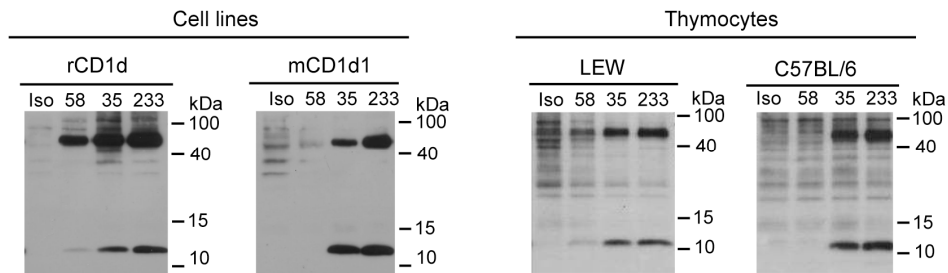


Figure 1. Immunoprecipitation of biotinylated surface proteins with 233, 35, 58 or isotype control antibodies. Immunoprecipitated material was size separated under reducing conditions on a 15% SDS-PAGE, blotted to a membrane and detected by addition of streptavidin-HRP. The two blots on the left show precipitates from rat (r) CD1d or mouse (m) CD1d1 transductants. The blots on the right show precipitates derived from thymocytes.

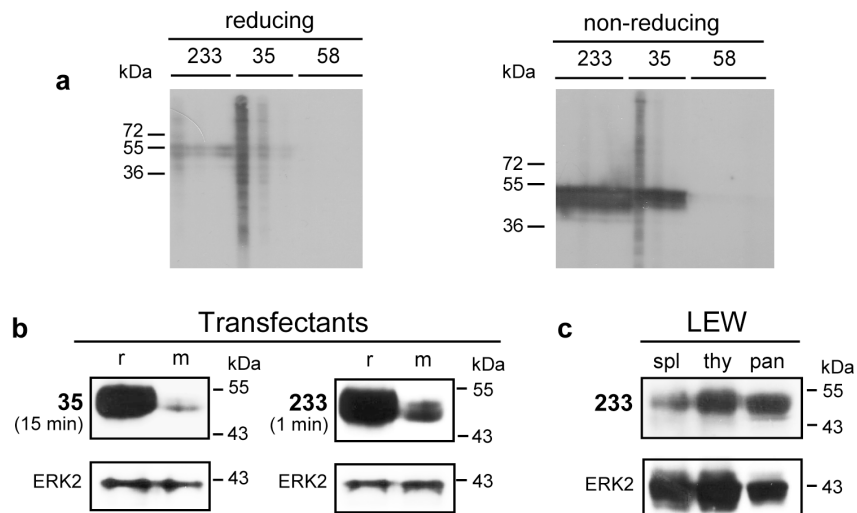


Figure 2. Western blot analyses with 233, 35 and 58 mAbs. *a* Proteins derived from rat CD1d-transduced P80 cells were separated by SDS-PAGE on 15 and 10% polyacrylamide gels, for reducing and non-reducing conditions, respectively, and blotted to a membrane. Detection of CD1d was carried out with decreasing concentrations of the antibodies in a multiscreen apparatus. The final concentrations used were: 17.28, 3.45 and 0.69 $\mu\text{g/ml}$ for 233 mAb; 24.48, 4.89 and 0.979 $\mu\text{g/ml}$ for 35 mAb and 6, 1.2 and 0.240 $\mu\text{g/ml}$ for the mAb 54. *b* Western blot analysis of proteins derived from rat CD1d (r) or mouse CD1d1 (m) transduced cells. Proteins were separated on a 10% polyacrylamide gel under non-reducing conditions and blotted to a membrane. CD1d was detected with the 233 or 35 mAbs. Film exposure duration for the CD1d blots is indicated under the names of the mAb. After CD1d detection, the blots were stripped and re-probed with a polyclonal anti-ERK2 antibody as protein loading control (lower blots). *c* Western blot analysis of proteins derived from LEW tissues: spleen (spl), thymus (thy) and pancreas (pan). SDS-PAGE and blotting conditions were the same as in *b*.

Western blot analysis of protein extracts derived from rat CD1d transductants after SDS-PAGE run under reducing and non-reducing conditions revealed the loss of the reactivity of the 58 mAb in immunoblots but the conservation of 233 and 35 and

mapped their bound epitopes to the heavy chain of CD1d. A remarkable contrast to the flow cytometry data was the better binding of 233 mAb in comparison to 35 in both, reducing and non-reducing conditions (Fig. 2 *a, b* and data not shown). Moreover, and also in contrast to the results observed by flow cytometry, in immunoblots both mAbs bound mouse CD1d much less efficiently than rat CD1d (Fig. 2 *b*), since both, rat and mouse CD1d transduced cell lines are expected to express very similar levels of cell surface CD1d due to the nearly identical expression of the reporter gene EGFP observed by flow cytometry (Fig. 3 *b*).

The 233 mAb was also used to analyze rat CD1d in protein extracts derived from rat thymus, spleen and pancreas. Pancreas was included in the study because outstanding levels of CD1d had been detected in immunohistological analyses carried out in collaboration with Prof. Steiniger, Institute of Anatomy and Cell Biology, Philipps-University of Marburg, Marburg, (Fig. 12). As shown in figure 2 *c*, CD1d was detected in all three tissues, being the pancreas the organ with the highest levels of CD1d (Ratios between CD1d and ERK2 signals obtained by densitometric evaluation of the films were: spleen, 0.8 ; thymus, 1.2 and pancreas, 1.7). Interestingly, CD1d isolated from pancreatic lysates had a slightly higher mobility in SDS-PAGE than CD1d from thymus or spleen protein extracts.

3.1.3 Epitope mapping

Cross-competiton experiments had demonstrated that the 233 and 35 mAbs recognize non-overlapping epitopes on rat CD1d (rCD1d) and mouse CD1d1 (mCD1d1). In order to define more precisely the binding sites of these mAbs, firstly, Raji cells were also transduced with mouse CD1d2 (mCD1d2) and CD1d1 from *Mus spretus* (sCD1d) and were tested for mAb reactivity by flow cytometry. Figure 3 *a* shows the high conservation of the predicted amino acidic sequences of these different CD1d molecules. The observed loss of 233 mAb binding to sCD1d and the massive reduction in its reactivity to mCD1d2 (Fig. 3 *c*) facilitated the mapping of its epitope since only three amino acidic residues were unique for sCD1d when compared to rCD1d and mCD1d1: alanine (A), isoleucine (I) and threonine (T) at positions 93, 118 and 162, respectively. The residue at position 118 is located in the antigen-binding groove (side chains are depicted in gray in Fig. 3 *c*) and is probably not accessible to the mAb 233 in contrast to position 93 at the border of the α 1-helix and position 162 which lies in the α 2 helix on the top of the molecule (red and green spheres, respectively, in Fig. 3 *c*). To

test whether any of these last two residues was responsible for the lack of reactivity of the 233 mAb against sCD1d, the aspartic acid at position 93 and the methionine 162 of mCD1d1 were exchanged by their sCD1d counterparts: Alanine and threonine, and named as: mCD1d1D93A and mCD1d1M162T (Fig. 3). In addition, chimeras of mouse and human CD1d were generated, expressed in Raji cells and analyzed by flow cytometry (Fig. 3 *b*). The generation of these cells lines, performed by Stefanie Schweigle in the course of her diploma thesis and described in our published work (Monzon-Casanova et al., 2010), allowed the mapping of the aspartic acid at positions 92 and 93 of rat CD1d and mouse CD1d1, respectively, as part of the 233 epitope, because cells expressing mCD1d1D93A were not stained by this mAb. The arrow in figure 3 *a* points out the position where the regions of mouse CD1d1 and human CD1d were exchanged. The structure models shown in figure 3 illustrate with green and gray ribbon diagrams, which parts of the $\alpha 1$ and $\alpha 2$ domains of the chimeric CD1d molecules correspond to one or the other species. These chimeras confirmed the results obtained with the mCD1d1 mutants and the 233 mAb and in addition, restricted the $\alpha 1$ domain and the 23 following amino acids of the $\alpha 2$ domain as crucial for formation of the 35 epitope, since the 35 mAb did not stain the h/mCD1d chimera.

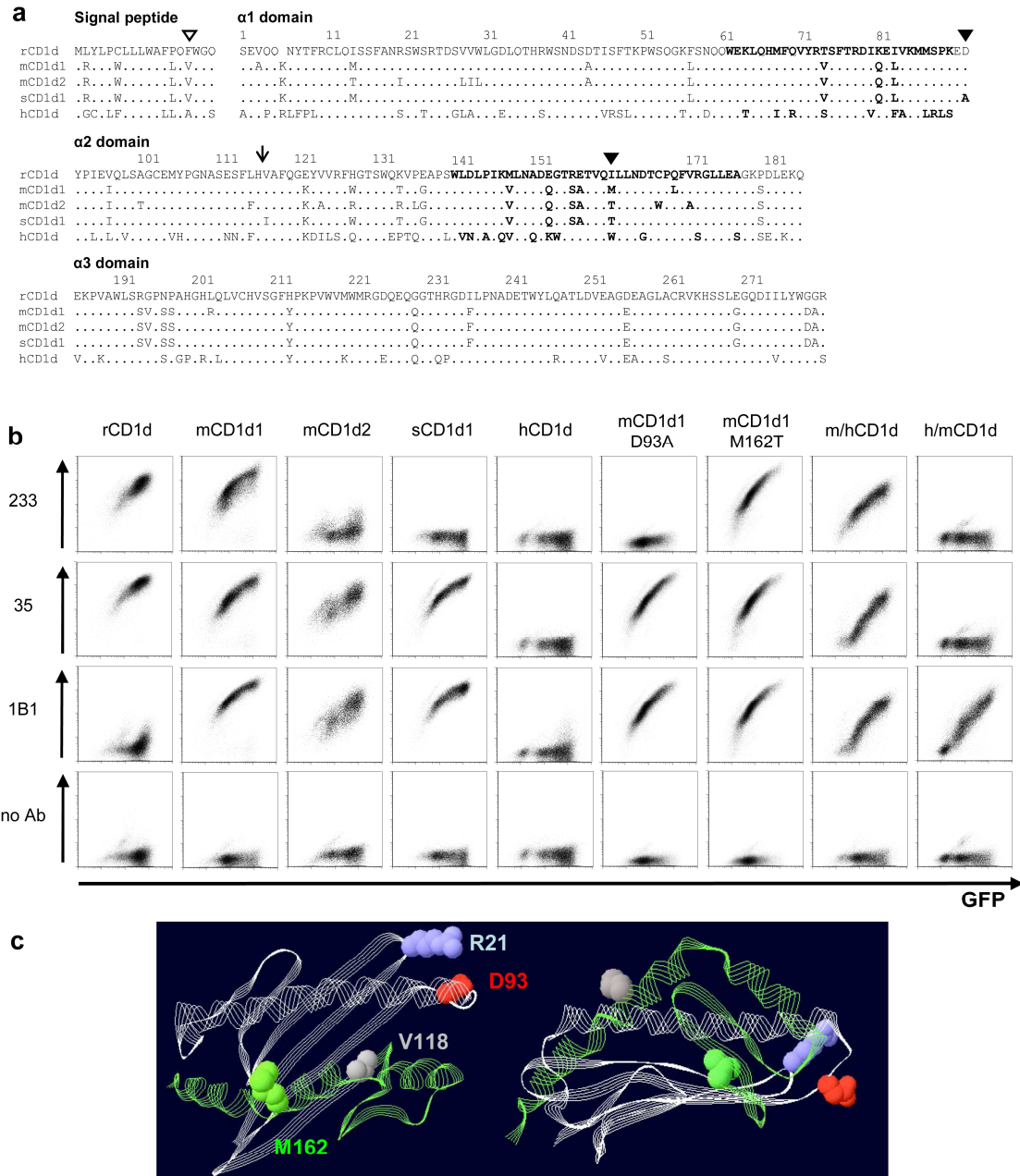


Figure 3. Epitope mapping of anti-CD1d mAbs. *a* Alignment of amino acid sequences of the extracellular domains of the CD1d molecules used in this study. α -helical regions are illustrated in bold. The open triangle points out the localization of rat CD1d allelism. Mutations in mouse CD1d1 are highlighted with closed triangles. The arrow indicates where mouse/human chimeras were joined. Numbers show rat CD1d amino acid positions. Accession numbers for the amino acid sequences can be found in GenBank: rCD1d (*Rattus norvegicus* CD1d), BAA82323; mCD1d1 (*Mus musculus* CD1d1), NP_031665; sCD1d1 (*Mus spretus* CD1d1), ACM45455; hCD1d1 (*Homo sapiens* CD1d), NP_001757. The mCD1d2 (*Mus musculus* CD1d2) amino acidic sequence differs in one amino acid in the signal peptide (tryptophan, position -13) from the sequence published under the accession number: P11610. *b* Binding capacity of mAbs to different CD1d molecules. Raji cells were transduced with CD1d molecules using a retroviral expression system. Bicistronic EGFP in the CD1d expression vectors served as reporter gene. Cells were stained with unconjugated 233 or 35 mAbs followed by PE-labeled donkey anti-mouse IgG or PE-labeled 1B1 mAb and were analyzed by flow cytometry. All primary antibodies were used at a final concentration of 250 ng/ml. *c* Localization of relevant amino acids in the CD1d tertiary structure. The model depicts part of the co-crystal of the PBS25 glycolipid and mouse CD1d (PDB: 3GMP) and it was visualized using PDB Swiss Viewer Deep View v4.0 (Guex and Peitsch, 1997) (<http://www.expasy.org/spdbv/>). The α 1 and α 2 domains are shown. Gray and green ribbon diagrams highlight the regions constituting the N- and C-terminal parts, respectively, of the chimeric molecules. Discussed amino acids are depicted as spheres: aspartic acid (D) 93 in red, methionine (M) 162 in green, valine (V) 118 in gray and arginine (R) 21 in blue.

3.1.4 CD1d ELISA

The lack of competition between mAbs 233 and 35 permitted the establishment of a CD1d Sandwich ELISA, which allows the detection of CD1d in fluid samples as cell or tissue protein extracts, serum or recombinant CD1d molecules purified or in culture supernatants. Standardization of the ELISA was carried out with soluble rat β 2m-CD1d-biotag recombinant proteins purified as described in the results section 3.4.1.3 (Fig. 4 *a*). The detection levels reached 0.5 to 1 ng of CD1d per ml. The rat β 2m-CD1d-biotag recombinant protein was used to determine the amounts of rat CD1d contained in the cell-lysate from P80 cells transduced with rat CD1d, which was then further used as standard in all CD1d Sandwich ELISAs (Fig. 4 *a*). Figure 4 *b* shows the amounts of CD1d detected in protein extracts derived from thymus, spleen and pancreas of LEW rats. In line with immunohistochemistry and Western blot analyses, CD1d levels are increased in pancreas compared to spleen, whereas with this technique no big differences were observed between thymus and pancreas. The presence of CD1d in the serum derived from various rat strains was also addressed by ELISA. Analysis of single samples from the following inbred rat strains led to the subsequent results: F344: 2.5 ± 0.18 , BN: 10.01 ± 0.46 , DA: 7.3 ± 0.56 , LEW: 3.6 ± 0.3 and PVG 14.5 ± 8.3 ng/ml \pm SD for duplicate samples.

Similar to Western blot analyses, the reactivity of the 233 and 35 mAbs in ELISA against mouse CD1d1 was lower than for rat CD1d (Fig. 2 *b* and 4 *c*). The signal given by mouse CD1d-IgG dimers was 2 to 3 fold lower than rat CD1d-IgG dimers.

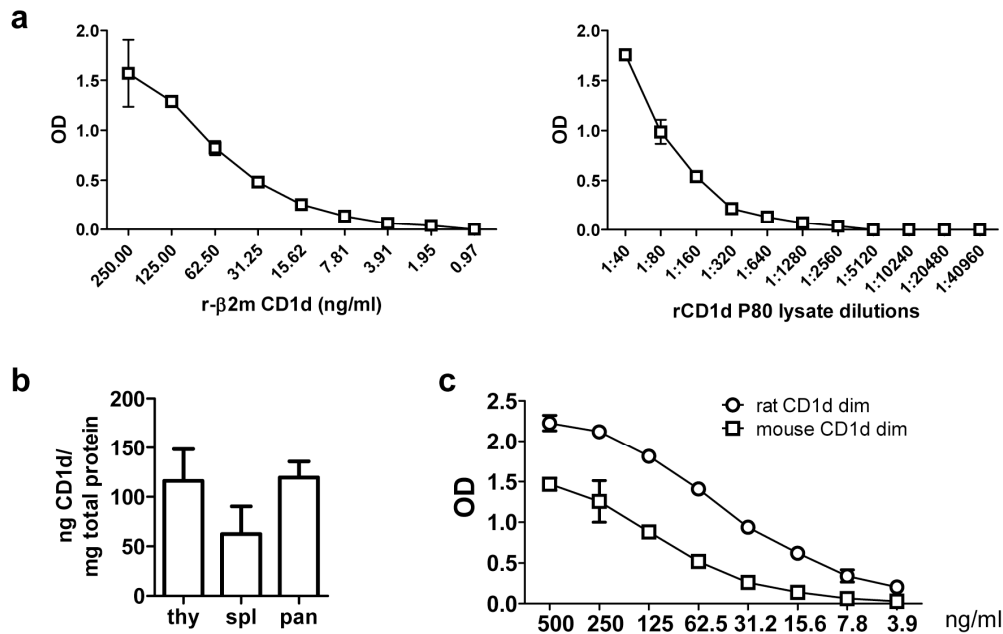


Figure 4. CD1d ELISA. *a* Standardization of rat CD1d-transduced P80 cell lysate with soluble recombinant rat β2m-CD1d-biotag purified protein. Shown are the optical density values obtained in 1:2 dilutions of the analyzed samples. Shown is the mean value of duplicated samples. *b* CD1d quantification in LEW protein extracts derived from thymus (thy), spleen (spl) and pancreas (pan). Shown are the mean values obtained from three rats independently analyzed +SD. *c* Optical density (OD) obtained after analysis of the same amounts of rat CD1d-IgG or mouse CD1d-IgG dimers (X axis). The mean value obtained for duplicated samples ±SD is shown.

3.2 Analysis of CD1d expression using mAbs 233 and 35

Up to date, a detailed analysis of CD1d protein expression in the rat has been hampered by the lack of suitable mAbs. The widely used and commercially available mouse CD1d specific mAb, 1B1, does not recognize rat CD1d (figure 3) and although in two additional publications mAbs originally generated against mouse CD1d were reported to cross-react with rat CD1d, the investigation of rat CD1d in these studies was rather limited. In the first case, the rat IgMs 1H1 and 3C11 (Bleicher et al., 1990) were shown to bind a CD1d-like molecule, which was detected in rat liver but not in thymus (Burke et al., 1994) and in the second case, reactivity of the mAb 3H3 with rat thymocytes and splenocytes was reported but not further investigated (Mandal et al., 1998). Therefore, the following data obtained with 233 and 35 mAbs provide the first detailed analysis on CD1d expression in the rat and the unique possibility of direct comparison of rat and mouse.

3.2.1 CD1d in different inbred rat strains

3.2.1.1 Identification of two rat CD1d alleles

Two allelic variants of rat CD1d protein coding sequence have been reported and defined by an alanine to valine substitution at position 101 of the mature polypeptide sequence, which is located in the antigen binding groove. The alanine 101 allele was reported for F344, BN and five other rat strains, whereas the valine should be present in LEW, Wistar, TO, WKAH and W (Katabami et al., 1998). This reported allelism could be of special significance since position 101 is localized in the antigen binding groove and consequently could influence the orientation of α -Gal and/or other lipids contained in this pocket. Therefore, we analyzed the sequences encoding CD1d in the inbred rat strains tested here for α -Gal responsiveness (and of five additional strains (BUF, BH, AGUS, AUG and WF) by amplifying genomic DNA by PCR and subsequent sequencing of the region covering the exons one to three. Furthermore, the complete coding region of CD1d was cloned from splenocytes cDNA derived from BN, LEW, PVG and DA. CD1d cDNA from F344 rats had previously been cloned by E. Pyz (Pyz et al., 2006). These analyses confirmed the sequence of F344 inbred rats published by Katabami et al. (Katabami et al., 1998), but the proposed valine substitution could neither be confirmed in LEW nor was it found in any other strain tested by us. In contrast, we found a single nucleotide substitution in the signal peptide replacing the phenylalanine at position -4 of the F344 allele by a valine (Fig. 5). The CD1d sequences obtained (except for F344 rats) were identical to the BN-derived rat genomic sequence. Interestingly, the valine at position -4 is also encoded in both mouse CD1d genes (Fig. 3 a).

```
F344 atgctgtacctaccgtgctgttgctgtgggcattcccacagttctggggacaa
      M L Y L P C L L L W A F P Q F W G Q
LEW  atgctgtacctaccgtgctgttgctgtgggcattcccacaggtctggggacaa
      M L Y L P C L L L W A F P Q V W G Q
```

Figure 5. Nucleotide and amino acid sequences of the two rat CD1d alleles identified in this study. Since the only difference among the complete CD1d coding sequence was found in the signal peptide, only this part is shown. The substitution resulting in the phenylalanine to valine change is highlighted in bold. The F344 allele was only found in F344 inbred rats, whereas the LEW allele, apart from LEW inbred rats was also found in BN, LEW, PVG, DA, BUF, BH, AGUS, AUG and WF inbred rats

3.2.1.2 Analysis of CD1d expression among different rat strains

In order to investigate whether the phenylalanine to valine substitution in the signal peptide affected CD1d surface expression; thymocytes, splenocytes, intrahepatic lymphocytes and PBMCs from the five inbred rat strains tested for α -Gal responsiveness in this study (F344, BN, DA, LEW and PVG, results section 3.7.1) were stained with the 233 mAb and analyzed by flow cytometry (Fig. 6). Thymocytes, splenocytes and PBMCs showed no strain-specific differences in CD1d expression. Based on FCS/SCC characteristics the negative/low population, which appears in DA PBMCs, are contaminating erythrocytes. Only among IHLs some differences could be observed: In DA and PVG inbred rat strains there are more cells expressing high CD1d levels. CD1d expression by different cell types of the thymus and spleen is described in more detail in the following section of the results.

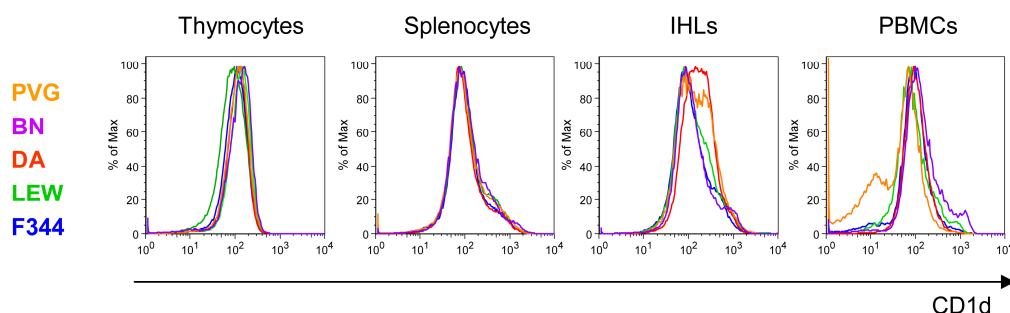


Figure 6. CD1d cell surface expression in different inbred rat strains. CD1d cell surface expression was analyzed by flow cytometry using the biotinylated 233 mAb visualized with SA-APCy in various primary cells: thymocytes, splenocytes, intrahepatic lymphocytes (IHLs) and peripheral blood mononuclear cells (PBMCs) derived from PVG, BN, DA, LEW and F344 inbred rat strains. One experiment is shown for each compartment and each strain except for LEW thymocytes, where two independent experiments are shown: light and dark green.

3.2.1.3 CD1d expression in hematopoietic cells: Direct comparison between rat and mouse

The 233 and 35 mAbs allowed us to directly compare CD1d surface expression on mouse and rat hematopoietic cells by immunofluorescence flow cytometry. The results obtained with the two mAbs were nearly the same, therefore, only stainings performed with the 35 mAb are shown. In the analysis, LEW rats and C57BL/6 mice were used. The staining intensity was very similar for both species and between thymocytes and most splenocytes (Fig. 7). The only striking difference was the higher proportion of CD1d high cells in rat, which, as shown later, can be accounted to MZ B cells (Roark et al., 1998). This is consistent with the very broad marginal zone and large number of

these cells found in rats (Kroese et al., 1990; Kumararatne et al., 1981; Steiniger et al., 2006).

Co-staining of CD1d and TCR in thymocytes revealed that in rats, as in mice (Park et al., 1998), TCR low cells, which are double positive thymocytes, express higher levels of CD1d than TCR high cells, which are single positive thymocytes (Fig. 8).

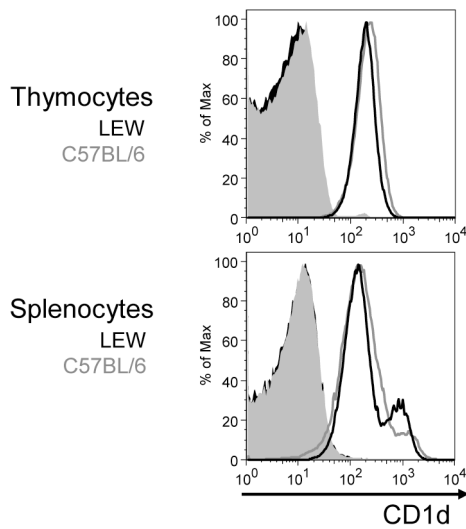


Figure 7. Comparison of CD1d expression by rat and mouse primary cells. Representative data from one out of three experiments are shown. Staining of total thymocytes or splenocytes with biotinylated 35 or isotype control antibodies and SA-PE. Gray and black lines correspond to C57BL/6 and LEW cells, respectively. Filled histograms are control stainings.

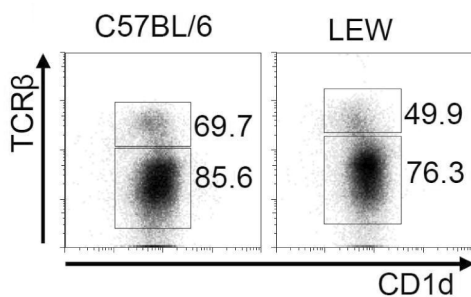


Figure 8. Comparison of CD1d expression by rat and mouse thymocytes. Representative data from one out of three experiments are shown. Co-expression of CD1d and TCR on thymocytes was analyzed by two-color flow cytometry. CD1d was stained using the unconjugated 35 mAb and PE-labeled donkey anti-mouse IgG. For staining of mouse and rat TCRs, H57-597-APCy and R73-bio + SA-APCy were used, respectively. Numbers indicate the geometric mean fluorescence intensity of CD1d expression in the gated populations.

CD1d expression by mouse T and B cells of the spleen and lymph nodes has been extensively studied (Brossay et al., 1997; Makowska et al., 1999; Park et al., 1998; Roark et al., 1998). CD1d surface expression was found to be lower on T cells than on B cells and among T cells, was higher on CD4 T cells than on CD8 T cells. Using the 35 and 233 antibodies we reproduced the findings obtained in mice, and observed that rat B cells also express higher CD1d levels than T cells (Fig. 9). Nonetheless, in rats the pattern of CD1d distribution among T cell subpopulations is different than in mice. Rat CD1d levels on CD4 T cells are not higher than those on CD8 T cells, as it was demonstrated by different staining and gating strategies (Fig. 10).

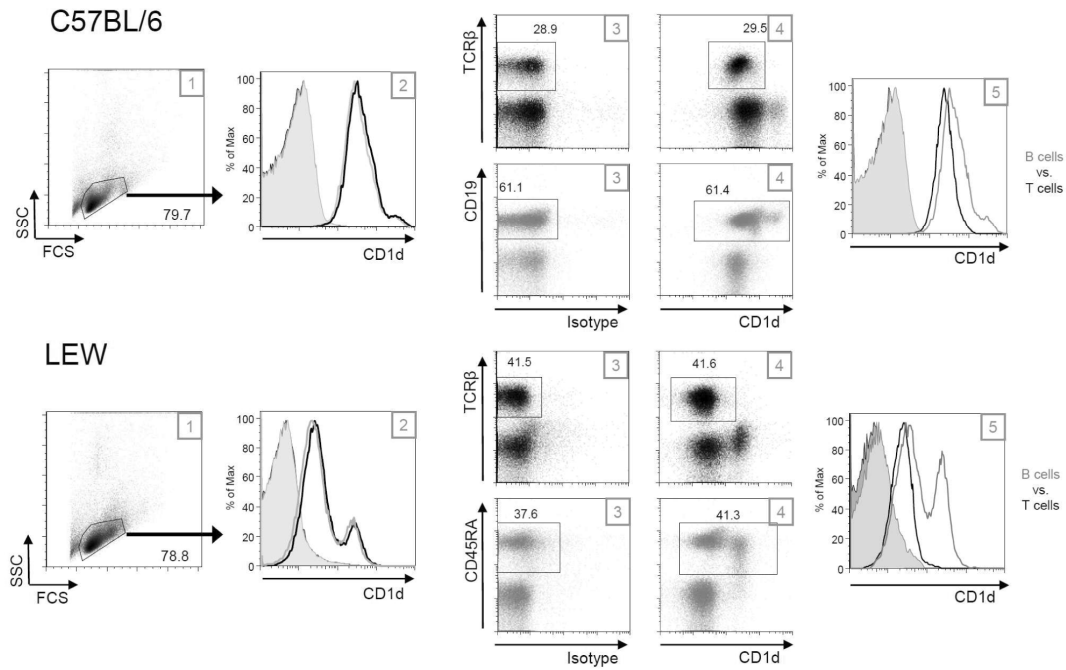


Figure 9. CD1d expression by B and T cells analyzed by multicolor flow cytometry. T and B cells were identified using antibodies visualized with APCy in order to avoid unspecific signal due to fluorescence spectral overlap in the PE channel, which was used for CD1d expression detection. Therefore, CD1d was analyzed on separate multicolor experiments with same CD1d staining intensity (Number 2 histograms: gray and black lines correspond to B and T cell stainings, respectively). Number 1 dot plots show gates on total splenocytes which were further analyzed. For CD1d detection in C57BL/6 mice, biotinylated 35 mAb followed by SA-PE was used. In rats, CD1d was detected with unconjugated 35 mAb followed by PE-labeled donkey anti-mouse IgG secondary antibody. Number 4 dot plots indicate co-expression of CD1d and T or B cell markers. Number 3 dot plots represent isotype control stainings for anti-CD1d mAbs. Gray and black dot plots correspond to B and T cell stainings, respectively. In mouse, B cells were stained with anti-CD19 (1D3-APCy) mAb and T cells with anti-TCR β chain mAb (H57-597-APCy). In rat, B cells were defined as CD45RA (OX-33-biotin + SA-APCy) positive cells and for the identification of T cells, anti-TCR β chain (R73-biotin + SA-APCy) antibody was used. Boxes indicate gated cells shown in number 5 histograms and numbers inside the plots correspond to the percentage of gated cells. Data shown is one representative experiment out of three.

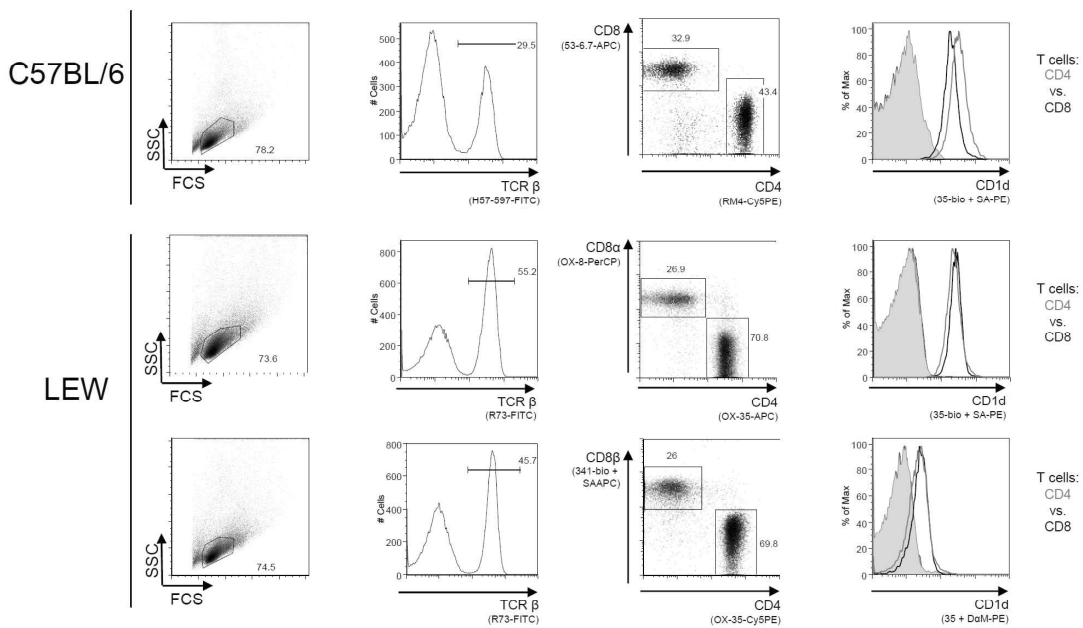


Figure 10. Relative CD1d expression by CD4 and CD8 positive T cells analyzed by multicolor flow cytometry. Dot plots on the left show the gated splenocytes which were studied. CD4 and CD8 positive T cell gating strategies are illustrated with the histograms and dot plots of the columns in the middle. Two different antibody combinations were used to stain LEW cells: one with biotinylated 35 visualized with SA-PE (upper row) and other with unconjugated 35 mAb detected with PE-labeled donkey anti-mouse IgG (DaM-PE, lower row). Numbers in the plots indicate percentages of gated cells. The antibodies used for each staining appear in the axes of the figures. Fluorescence 2 geometric MFI of CD4- and CD8-gated T cells in stainings where instead of the anti-CD1d mAb, an isotype control Ab was used were: in the staining of C57BL/6 cells, 5.98 and 4.58 in CD4- and CD8-gated cells, respectively; in the upper LEW staining: 10.2 and 10.6 for CD4 and CD8 T cells, respectively, and in the lower rat staining: 5.32 for CD4, and 5.09 for CD8 positive T cells. In the histograms on the right, gray and black lines correspond to CD4 and CD8 positive T cells respectively. Filled histograms are control stainings.

In the mouse, in addition to MZ B cells also antigen presenting cells show very high CD1d levels (Roark et al., 1998). Analysis of mouse MZ B cells (CD21^{high}/CD23^{low}) with the mAbs reported here confirmed their high CD1d expression levels (Fig. 11). Rat MZ B cells defined either by combinations of the B cell marker CD45RA (OX-33) and the MZ B marker HIS57 or by gating on IgM^{high}/IgD^{low} cells (Fig. 11) (Kroese et al., 1990) are CD1d high as well.

CD1d expression on rat dendritic cells (OX-62⁺) and macrophages (CD11b/c⁺) was also analyzed and compared to that of MZ B cells, identified as HIS57⁺ in this case. The stainings of figures 11 b and c show that, similar to what has been reported for mouse antigen presenting cells, CD1d levels on rat dendritic cells and macrophages are as high as those of MZ B cells.

Last, we also analyzed CD1d expression on natural killer cells from the spleen which were defined as NK1.1 or NKR-P1 positive TCR negative cells in mice and rats, respectively. In C57BL/6 mice, NK1.1 positive cells express lower CD1d levels

compared to the rest of splenocytes, whereas in rats NKR-P1 positive cells and T cells express CD1d at similar levels (data not shown).

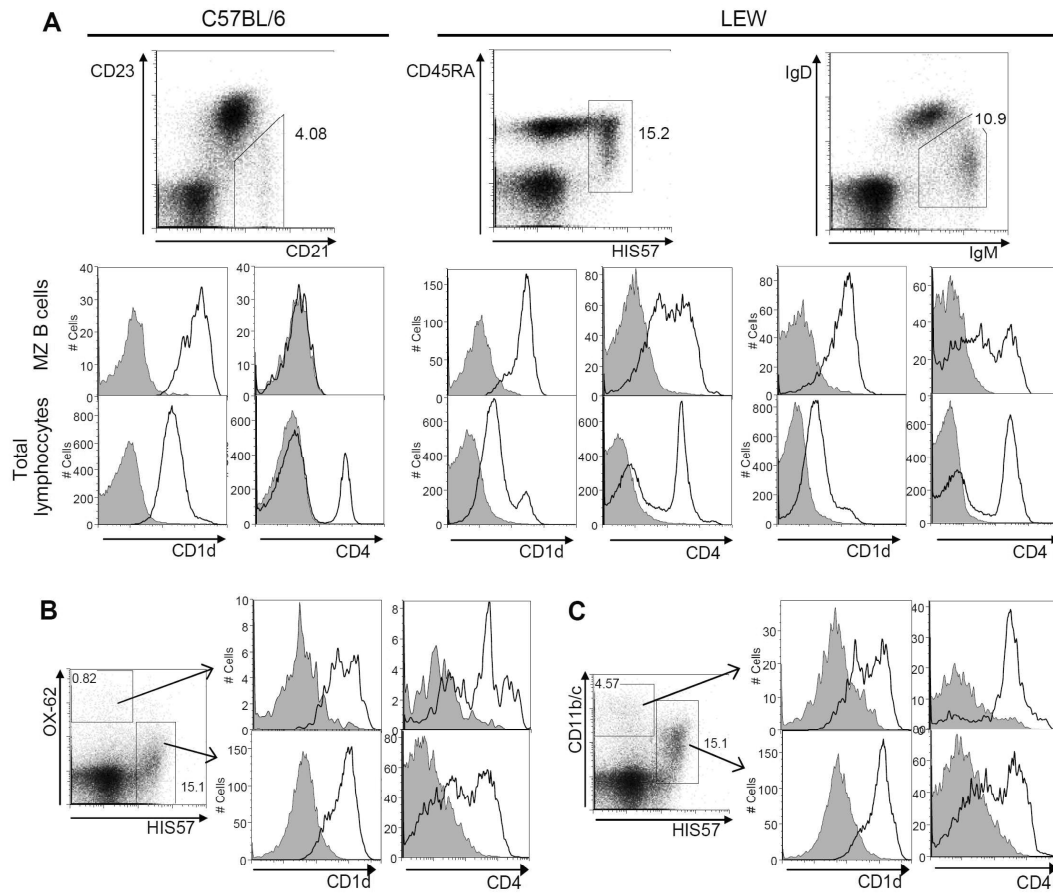


Figure 11. CD1d and CD4 expression by MZ B cells, dendritic cells and macrophages from the spleen. One representative experiment out of three is shown. Dot plots illustrate the followed gating strategies and numbers in them indicate the percentage of gated cells. Histograms show CD1d and CD4 expression levels. (A) MZ B cells analysis. In C57BL/6 mice, CD1d was stained with biotinylated 35 mAb + SA-Cy5-PE and CD4 with RM4-APCy. In LEW, CD1d was detected with unconjugated 35 mAb followed by PE-labeled secondary antibody and CD4 with OX-35 labeled with PE-Cy5 unless otherwise indicated. Upper row histograms show gated MZ B cells, whereas, lower row histograms show total lymphocytes. MZ B cells in C57BL/6 mice were identified by gating on CD21 hi (7G6-FITC) and CD23 low/negative (B3B4-PE) cells. In LEW rats, MZ B cells were stained with two different marker combinations: CD45RA (OX-33-FITC) / HIS57-biotin + SA-APCy and IgM (G53-238-FITC)/IgD (MARD-3-biotin + SA-APCy), respectively. Analysis of CD1d and CD4 in MZ B cells defined as HIS57- and CD45RA positive cells was carried out with one single multicolor experiment. Expression of CD1d and CD4 in MZ B cells defined as IgD-low and IgM-high cells was determined in separated multicolor experiments as both, the anti-CD1d and the anti-CD4 mAbs were visualized with the PE fluorochrome (CD1d: 35 mAb + PE-secondary Ab, CD4: OX-35-PE). (B) CD1d and CD4 expression by LEW dendritic cells (OX-62 detected with anti-mouse IgG PE secondary antibody) and MZ B cells (HIS57-biotin and SA-APCy). CD1d was detected with 35-FITC mAb and CD4 with OX-35-PE-Cy5. (C) CD1d and CD4 expression by LEW macrophages – defined as CD11b/c+ cells (OX-42-PE) – and MZ B cells (HIS57-biotin + SA-APCy). CD1d was stained with unconjugated 35 mAb followed by FITC-labeled anti-mouse IgG Ab. For CD4 detection, OX-35-PE-Cy5 antibody was used.

3.2.1.4 CD4 expression by rat MZ B cells

Surprisingly, while analyses of CD1d among different cell populations in the spleen were carried out, it was observed that MZ B also expressed CD4 and nearly half of them as much as other splenocytes (e.g. CD4 T cells) (Fig. 11). These findings were confirmed with a different anti-CD4 mAb (OX-38) and in another inbred rat strain (F344) (data not shown). The multicolor stainings of MZ B cells and antigen presenting cells also demonstrate that the expression of CD4 by rat MZ B cells was not the result of some CD4 positive macrophages or dendritic cells included in the gate of MZ B cells. Moreover, immunohistochemical analysis carried out in the laboratory of Prof. Steiniger, Institute of Anatomy and Cell Biology, Philipps-University of Marburg, Marburg, with another anti-CD4 mAb (W3/24) also showed that CD4 expression in the white pulp was not only restricted to the T cell area and to some dendritic cells but also to the marginal zone of the spleen (data not shown).

3.2.1.5 CD1d expression in rat and mouse non-lymphatic organs

In collaboration with Prof. Steiniger, Institute of Anatomy and Cell Biology, Philipps-University of Marburg, Marburg, CD1d was analyzed outside the hematopoietic system by immunohistochemistry. Figure 12 shows stainings with the 233 mAb of LEW heart, liver, pancreas and small intestine.

In rat liver, all hepatocytes are stained and their reactivity increases in direction to the central vein of the lobule (Fig. 12 *a*). Sinusoidal endothelia express higher CD1d levels than hepatocytes and the most strongly stained cells may correspond to Kupffer cells or stellate cells scattered among the hepatocytes. However, these cells are difficult to diagnose due to the strong staining of the sinusoidal endothelia. In the heart (Fig. 12 *b*), 233 stains the interior and surface of cardiomyocytes and the intercalated discs are also clearly visible. Capillary endothelia between the muscle cells and, in addition, the endocardium are also CD1d positive.

When CD1d expression was addressed in the rat ileum, the distribution pattern turned out to be as diverse as the cellular components of this organ (Fig. 12 *c*). Enterocytes are clearly detected by the 233 mAb with crypt cells staining more strongly than cells covering the villi. Enteroendocrine cells are most probably also positive, but this is difficult to distinguish. Remarkably, Paneth cells at the base of the crypts show very strong staining intensity. Beneath the epithelium many different cells lodge in the lamina propria, such as lymphocytes, myeloid cells, smooth muscle cells, fibroblasts

and endothelial cells forming capillaries and lymphatic vessels. A large number of these cells are also positive. Smooth muscle cells forming the gut wall are almost CD1d negative, but there are some elongated CD1d positive cells in the lamina muscularis mucosae and in the circular layer of the tunica muscularis, some of which may be endothelia.

Staining of the rat pancreas (Fig. 12 *f*) with 233 and 35 revealed massive CD1d expression in the apical granules of exocrine acinar cells, being detected even at extremely high dilution (1:100.000). Interacinar capillary endothelial cells and/or intercalated duct epithelia also express CD1d. The epithelium in larger interlobular ducts and the endothelium in arteries and veins are CD1d positive as well. mAb 35 tends to produce a somewhat reduced staining reaction in these cells compared to mAb 233 (data not shown). Interestingly, in many islets of Langerhans central endocrine cells stain with variable intensity, while the peripherally situated glucagon-containing islet cells appear almost non-reactive. Whether nerve fibers are CD1d positive is difficult to recognize, because endothelia and certain connective tissue cells surrounding larger vessels react with mAb 233. The strong CD1d expression in the rat pancreas was verified by ELISA and Western Blot analyses (figures 2 *c* and 4 *b*).

Because reactivity of the 233 and 35 mAbs against mouse CD1d in histochemistry is not as high as against rat CD1d, immunohistology of mouse ileum and pancreas was performed using the more sensitive tyramide amplification procedure including organs from CD1d^{-/-} mice as negative controls (Fig. 12 *d, e, g* and *h* and data not shown for 35 mAb). This analysis revealed a considerable species-specific difference of CD1d expression intensity and, at least with respect to the pancreas, also of expression pattern among mouse and rat. In mouse ileum the expression of CD1d is reduced in comparison to rats. The reduction is especially evident in parenchymal cells such as epithelia. It is less pronounced in the lamina propria and in the muscle layers, where the staining pattern corresponds to that of rats (Fig. 12 *c-e*). Even with the tyramide amplification technique, enterocytes of the ileum do not react with any of the antibodies. A subpopulation of Paneth cell apical granules is, however, reliably visualized in the small intestine. It is not clear whether the apical cell membrane of Paneth cells is also slightly stained. In addition, enteroendocrine cells in the epithelial layer of the ileum are CD1d positive. These cells are especially numerous in the crypts. In contrast to rats, in mouse pancreas the highest CD1d levels are found in the epithelium of larger ducts and in interacinar capillary endothelia, while the exocrine granules of acinar cells appear very

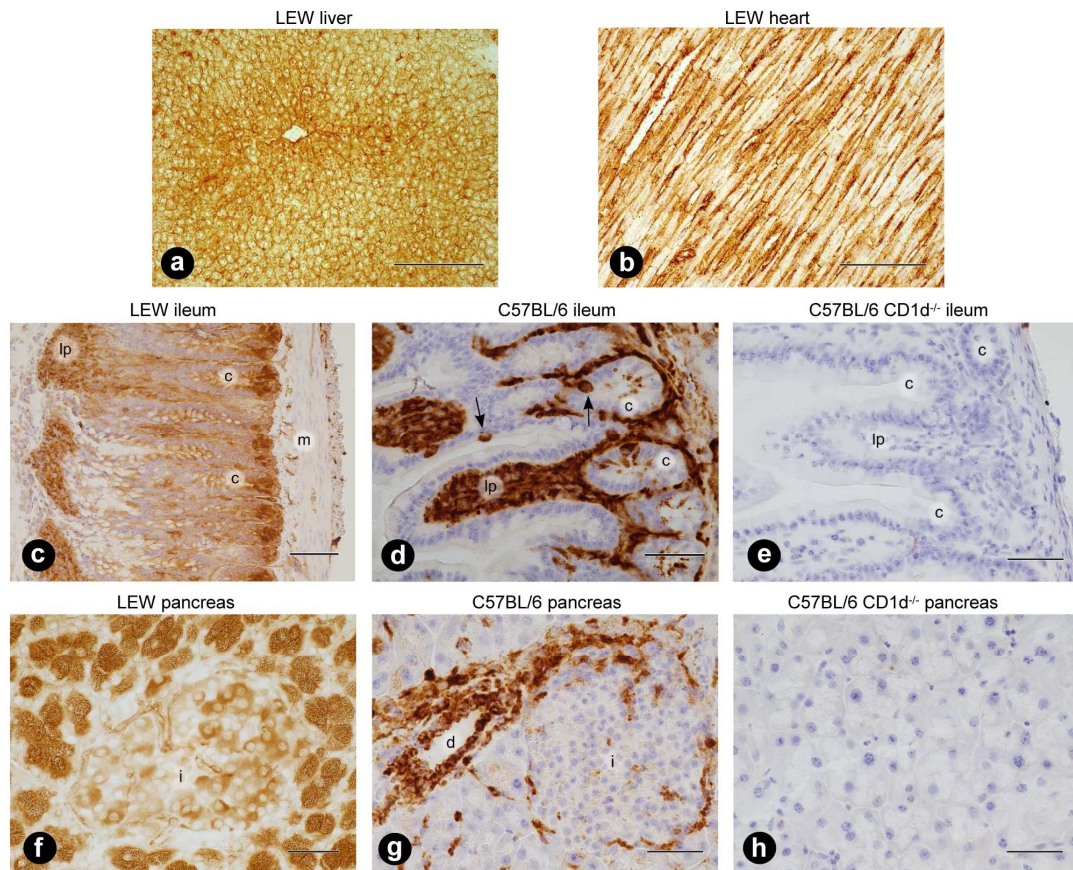


Figure 12. CD1d distribution in non-lymphatic tissues. Experiments performed by Prof. Steininger, Phillips-University of Marburg. ABC technique with unconjugated mAb 233 was applied unless otherwise stated. (a) LEW liver. Bar = 250 μ m. (b) LEW heart. Hemalum counterstain was included. Bar = 250 μ m. (c) LEW ileum. The epithelium at the tips of the villi (left rim of picture) is not preserved. Analysis was carried out with biotinylated 233 and hemalum counterstain. Bar = 100 μ m. (d) C57BL/6 ileum. Arrows indicate CD1d positive enteroendocrine cells in the epithelium. Biotin-conjugated primary antibody, tyramide-amplified ABC technique and hemalum counterstain were used. Bar = 50 μ m. (e) C57BL/6 CD1d^{-/-} ileum. Biotin-conjugated primary antibody, tyramide-amplified ABC technique and hemalum counterstain were applied. Bar = 50 μ m. (f) LEW pancreas. Biotinylated 233 was used. Bar = 50 μ m. (g) C57BL/6 pancreas. Biotin-conjugated primary antibody and tyramide-amplified ABC technique were used. Hemalum counterstain was included as well. Bar = 50 μ m. (h) C57BL/6 CD1d^{-/-} pancreas. Biotin-conjugated primary antibody and tyramide-amplified ABC technique were applied and hemalum counterstain was also carried out. Bar = 50 μ m. Abbreviations used: c, crypts; lp, lamina propria; m, smooth muscle cells of the gut wall; i, islet of Langerhans and d, interlobular duct.

faintly stained and are only prominent in few single cells in spite of tyramide amplification (Fig. 12 *f-h*). Whether epithelial cells of the intercalated ducts are also positive cannot be clearly distinguished. Moreover, endocrine islet cells appear only very faintly stained and the endothelium in arteries and veins does not react at all, although vessel-associated nerve fibers appear positive. With the exception of some epithelial cells in larger ducts, mAb 35 is nearly unreactive with the pancreas. To address the question whether in contrast to C57BL/6 mice, CD1d expression in the pancreas of other strains is comparable to that observed in rats due to the expression of CD1d2, we also studied BALB/c and CBA/N mice with both mAbs and found that this

is not the case because very similar results were obtained for the pancreas of all analyzed mouse strains (data not shown).

3.3 Analysis of CD1d-restricted immune response with the 233 and 35 mAbs

Upon stimulation with the potent antigen α -Gal, iNKT cells secrete Th1 and Th2 cytokines very rapidly being the only lymphocytes described to date that can secrete large amounts of IL-4 within few hours after primary antigen contact. CD1d restriction of α -Gal responsiveness has been extensively demonstrated by the use of CD1d-deficient mice and the use of monoclonal antibodies. However in the rat, although an α -Gal response of intrahepatic lymphocytes and splenocytes has been previously been shown by E. Pyz et al. (Pyz et al., 2006), direct demonstration of the role of CD1d as an antigen presenting molecule had not been shown yet. Thus, in order to investigate whether the 233 and 35 mAbs interfere with the presentation of α -Gal by CD1d to primary iNKT cells, C57BL/6 and F344 splenocytes were cultured with α -Gal in the presence or absence of the anti-CD1d mAbs. After 24 hours of culture, supernatants were harvested and IL-4 and IFN- γ amounts were measured by ELISA. As controls, cells were also incubated with β -Gal, ConA or culture medium only. As it is shown in figure 13, regardless of the species origin, addition of the antibodies blocked cytokine release. A toxic or unspecific effect of the antibodies could be ruled out as they did not inhibit cytokine production after ConA stimulation and the isotype control did not affect α -Gal-dependent cytokine release (figure 13).

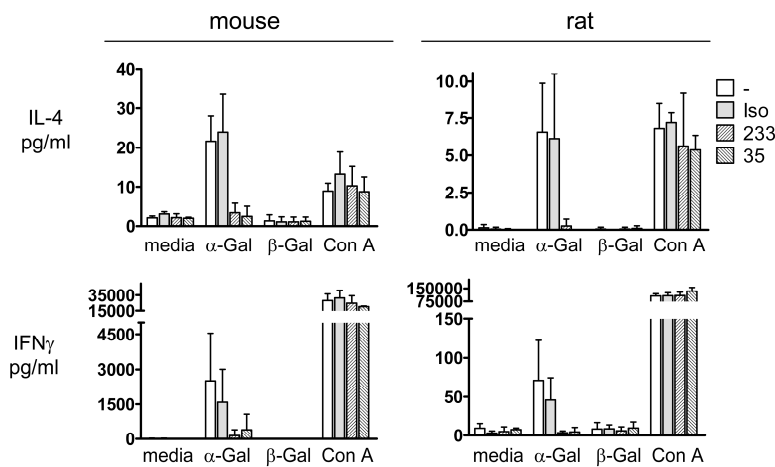


Figure 13. Effects of mAbs 233 and 35 on CD1d antigen presentation to iNKT cells. IL-4 and IFN- γ production was analyzed by measuring cytokine release into the culture supernatant by ELISA after 24 hours. 10^7 splenocytes per ml from C57BL/6 mice or F344 rats were cultured with various stimuli: α -Gal (10 ng/ml), β -Gal (10 ng/ml) or ConA (3 μ g/ml) or media alone, in the presence or absence of 233, 35 or isotype control antibodies (with a final saturating concentration of 3,6 μ g/ml). Bars

show mean values + SD of cytokine concentrations obtained in three independent experiments.

3.4 Rat iNKT cell identification

TCRs bind to peptides loaded on MHC molecules or to glycolipids loaded on CD1d with rather low affinity, resulting in complexes which have a very fast on-off dissociation rate (Matsui et al., 1994). For this reason it is not possible to visualize antigen-specific T cells with soluble monomeric peptide-MHC complexes, but they can be stained and analyzed by flow cytometry using multimerized complexes which have a much higher avidity for the TCR (Altman et al., 1996). In the same way, iNKT cells can also be identified with α -Gal-loaded CD1d oligomers. As mentioned in the introduction, this enables to distinguish these cells from other T cells expressing NK receptors and from other CD1d-restricted T cells, which do not bear the semi-invariant TCR reactive to α -Gal (Godfrey et al., 2004).

Cross-species recognition of α -Gal presented by CD1d has been described (Benlagha et al., 2000; Karadimitris et al., 2001; Matsuda et al., 2000; Schumann et al., 2003). An example of this cross-reactivity are mice and humans: The human semi-invariant TCRs recognize α -Gal presented by mouse CD1d and vice versa, mouse T cells with semi-invariant TCRs recognize α -Gal presented by human CD1d. Nonetheless, despite that iNKT cells can be stained with CD1d oligomers from the other species, the affinity with which the semi-invariant TCR of one species recognizes CD1d from the other species is lower than when both molecules are from the same species (Schumann et al., 2003). Moreover, this cross-species reactivity is not universally conserved, being lost or impaired between closer species than mouse and human. One example is the loss of reactivity of human semi-invariant TCR against α -Gal-loaded tree shrew (*Tupaia belangeri*) CD1d (Zhang et al., 2009). Another example is that of mouse and rat. As it was described by E. Pyz et al. in our laboratory, whereas the mouse semi-invariant TCR recognizes α -Gal-loaded rat CD1d almost to the same extent as it recognizes mouse α -Gal presented by the syngenic CD1d, the rat semi-invariant TCR response to α -Gal presented by mouse CD1d is severely impaired (Pyz et al., 2006). Furthermore, staining of rat IHLs with mouse α -Gal-loaded CD1d tetramers did not lead to the clear identification of a tetramer positive cell population, despite the reactivity of rat primary cells to α -Gal. Based on this data, the most simple explanation for the impossibility to reliably detect rat iNKT cells using α -Gal mouse CD1d tetramers is a poor binding of semi-invariant rat TCR to α -Gal/mouse CD1d complexes although it still might be possible that the numbers of iNKT cells in the rat are below the detection limit of flow cytometry. To address these questions, rat CD1d oligomers were produced. Different

strategies were followed, since each of them has advantages or disadvantages over the others (Fig. 14). First, divalent oligomers were produced with CD1d-IgG fusion proteins. Second, to avoid the difficulties which can result from using mouse IgG1 comprising molecules to stain primary cells from rats and mice, dimers were also produced with CD1d human IgG Fc fusion proteins and third, three different approaches were taken to produce tetramers, in order to generate a reagent with higher avidity than that of dimers. In two of the three strategies, directly targeted biotinylation of the soluble CD1d molecules was required for tetramerization. In the other one, a strep-tag which can be directly bound without biotinylation to a modified streptavidin (Strep-Tactin) was used.

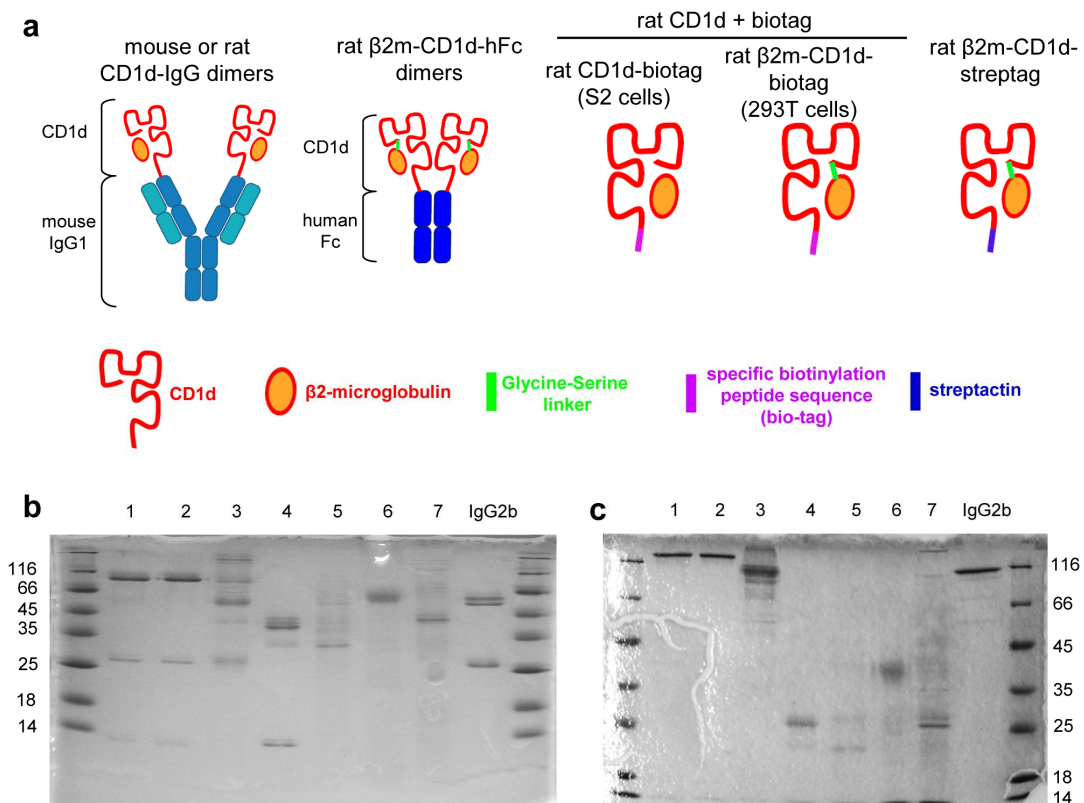


Figure 14. CD1d recombinant proteins. *a* Illustration of the different produced CD1d recombinant proteins. *b* Purified CD1d recombinant proteins analyzed by SDS-PAGE (15%) under reducing conditions. Proteins were stained with Coomassie Blue R250. Different amounts of each recombinant protein were loaded. Protein concentrations were calculated after photometric analysis as described in the methods section 2.2.3.7. 1: mouse CD1d-IgG dimers (2 μ g); 2: rat CD1d-IgG dimers (2 μ g); 3: rat β 2m-CD1d-hFc dimers (4 μ g); 4: biotinylated mouse CD1d, kindly provided by M. Schiemann (2 μ g); 5: biotinylated rat CD1d-biotag produced in S2 cells (2,6 μ g); 6: rat β 2m-CD1d-biotag produced in 293T cells (10 μ g) and 7: rat β 2m-CD1d-streptag (10 μ g). Commercially purchased mouse IgG2b (2 μ g) was loaded as control. The real amount of CD1d recombinant protein in lanes 6 and 7 is about 5 times less than the calculated one after photometric analysis. *c* Purified CD1d recombinant proteins analyzed by SDS-PAGE (10%) under non-reducing conditions. Lanes are the same as in *b*. The used molecular weight marker was pepGOLD Protein Marker (Peqlab).

3.4.1 Production of CD1d oligomers

3.4.1.1 Mouse and rat CD1d-IgG dimers

Dimer production of MHC-I, -II, as well as mouse and human CD1d molecules using IgG antibodies as platform for the creation of divalent molecules has previously been described (Dal Porto et al., 1993; Greten et al., 1998; Hamad et al., 1998; Lebowitz et al., 1999; Schumann et al., 2003). In order to produce mouse and rat CD1d dimers in this way, fusion proteins containing the $\alpha 1$ - $\alpha 3$ domains of CD1d and the mouse IgG1 heavy chain were created as previously described by cloning rat or mouse CD1d cDNAs into the pXIg vector and expressing the recombinant proteins into the J558L murine plasmocytoma cell line (Dal Porto et al., 1993; Schumann et al., 2003). The J558L cells producing rat CD1d-IgG dimers were additionally transduced with rat $\beta 2$ -microglobulin. In the figure 14, the different subunits which form the mouse or rat CD1d-IgG recombinant proteins can be appreciated when analyzed under reducing conditions: the CD1d-IgG1 heavy fusion protein of about 100 kDa, the λ light chain of 27 kDa and the $\beta 2$ -microglobulin at approximately 12 kDa.

E. Pyz and I. Müller generated the plasmids encoding CD1d-IgG1 fusion proteins and did the first transfections into J558L cells. Cloning of rat $\beta 2$ -microglobulin into the retroviral expression vector pczCFG5 IZ was carried out by P. Neuhöfer.

3.4.1.2 Rat $\beta 2$ m-CD1d-hFc dimers

Rat CD1d extracellular domains ($\alpha 1$ - $\alpha 3$) were fused to the human IgG1 Fc region encoded in the pFUSE-hIgG1-Fc2 vector. As previously described for human CD1d molecules (Li et al., 2008), the N-terminus of the $\alpha 1$ domain of CD1d of this fusion molecule was then connected to rat $\beta 2$ m by a glycine-serine linker. This assures constant binding of rat CD1d to rat $\beta 2$ -microglobulin and not to $\beta 2$ -microglobulin of the dimer producing human 293T cells or of the fetal calf serum present in the culture medium. The final fusion construct was abbreviated as: $\beta 2$ m-CD1d-hFc. The recombinant dimer should be formed by two identical rat $\beta 2$ -microglobulin CD1d human IgG1 Fc fusion heavy chains with a molecular weight about 90-95 kDa. Western blot analysis using the biotinylated 233 mAb demonstrated that among all the bands which appeared in the purified extracts, the band running at approximately 95 kDa under reducing conditions was the rat $\beta 2$ m-CD1d-hFc fusion protein (Fig. 14, and data not shown for the Western blot). Most likely, the bands observed at 55 and 25 kDa are heavy and light Ig chains since they were also detected by the HRP-conjugated

secondary polyclonal anti-mouse Ig antibody used in the Western blot (data not shown). These Ig chains are probably traces comprised in the serum containing media, which remained in the cultures after having exchanged it by serum free media and which also bound to the protein G.

3.4.1.3 Rat CD1d constructs for streptavidin based multimerization

Two different approaches were taken in order to produce rat CD1d monomers containing a specific peptide sequence (bio-tag) recognized by the enzyme BirA, which adds one single biotin molecule to the lysine contained in such amino acidic sequence (Schatz, 1993). The first approach was originally designed for production of mouse CD1d in the *Drosophila* derived cell line SC2 (Benlagha et al., 2000) and it was carried out in collaboration with M. Schiemann and D. Busch, Institute of Medical Microbiology, Dept. of Medicine, Technical University Munich. The second approach was conceived to produce rat CD1d in the mammal cell line 293T.

Production of rat CD1d fused to bio- and polyhistidine-tags in insect cells was performed as described in Materials and Methods (Methods section 2.2.3.3). Soluble biotinylated mouse CD1d was loaded onto the gel as control (line 4). The lane of the mouse CD1d comprises three clear bands: Two prominent bands appear at 38 and 12 kDa and are likely mouse CD1d and β 2-microglobulin, respectively. Another band with a more reduced intensity appears at 33 kDa and is probably the BirA enzyme used for biotinylation, since that is exactly its molecular weight (Schatz, 1993). In contrast, in the lane where rat CD1d (line 5) was loaded, no prominent bands appear at 38 or at 12 kDa, but one at 33 kDa.

For production of rat CD1d in the mammal cell line 293T (second strategy) rat β 2-microglobulin was attached to CD1d by a glycine-serine linker, as described above for the human Fc dimers, resulting in a fusion protein formed by rat β 2-microglobulin, rat CD1d extracellular domains, bio- and polyhistidine-tags. In figure 14 *b* and *c* it can be appreciated as this fusion protein is highly glycosylated in the 293T cells, appearing as a broad band of approximately 60 kDa under reducing conditions and of about 50-55 kDa under non-reducing conditions. Unfortunately, specific biotinylation of rat CD1d tested as described in the methods section 2.2.3.9 was not efficient.

These recombinant proteins were not further used to produce rat CD1d oligomers due to the reported inconveniences: Not enough protein amounts and inefficient biotinylation.

3.4.1.4 Rat β 2m-CD1d-streptag

In order to avoid problems of inefficient biotinylation and in addition, to produce a reagent whose oligomerization can be reversed (Knabel et al., 2002), also in collaboration with M. Schiemann and D. Busch, a rat CD1d soluble molecule containing a strep-tag and a polyhistidine-tag was produced in the SC2 fly cell line. This soluble CD1d molecule also contained the rat β 2-microglobulin fused by a glycine-serine linker. SDS-PAGE and Coomassie Blue R250 staining shows the purified protein as a sharp band running at the expected molecular weight of non N-glycosylated CD1d and β 2-microglobulin, approximately 43 and 36 kDa under reducing and non-reducing conditions, respectively (Fig. 14).

3.4.1.5 Efficient loading of CD1d with α -Gal

Loading of glycolipids with long fatty acid chains as α -Gal into CD1d *in vivo* is facilitated by proteins belonging to the saposine family, GM2 activator proteins, and Niemann-Pick type C1 and C2 proteins (Sagiv et al., 2006; Schrantz et al., 2007; Yuan et al., 2007; Zhou et al., 2004a), which contribute to the solubilisation and transport of these glycolipids from hydrophobic membranes or micelles to the antigen binding groove of CD1d. Such biological conditions can be simulated *in vitro* for example by adding recombinant saposine B or detergent (TRITON X-100 at a final concentration of 0.05%) to the CD1d/lipid mixtures (Im et al., 2009). As shown in figure 15, only when α -Gal loading was carried out in the presence of 0.05% of TRITON X-100 staining of rat semi-invariant TCR transductants with the dimers correlated with the TCR levels and all cells could be visualized. In contrast, without TRITON X-100 not all cells bound to the dimers. Moreover, the binding of the dimers did not correlate directly with the TCR levels expressed at the cell surface of the transductants. Thus, proper loading of α -Gal into rat CD1d was only achieved when TRITON X-100 was also added to the lipid/CD1d mixture. Nonetheless it is very important to take into account the detrimental effects that the use of detergents can cause to living cells. Indeed, after staining with dimers containing TRITON X-100 the size of BWs cells was smaller. These damaging effects were even more pronounced with primary cells which were lysed to a substantial proportion if the final concentration of TRITON X-100 reached 0.0063% and/or the incubation times were longer than one hour during the staining with the dimers (data not shown). For these reasons stainings were usually carried out during

one hour at room temperature and at a final concentration of 0.0037% TRITON X-100, conditions which most of the cells resisted.

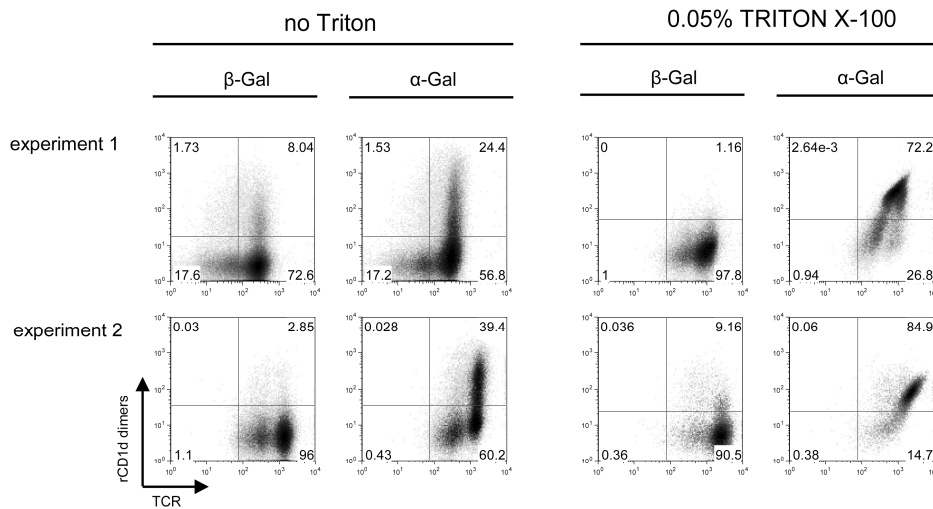


Figure 15. Efficient glycolipid loading of CD1d dimers. BW r/mCD28 rAV14S6 + CDR2+4 cells were stained with dimers loaded with either α -Gal or β -Gal in the presence or absence of 0.05% TRITON X-100 detergent. Dimers were visualized with D α M-PE, and TCR levels were analyzed with R73-bio + SA-APC. Two independent experiments are shown. Numbers in the density plots correspond to the percentages of cells in each quadrant.

3.4.2 Binding of diverse CD1d oligomers to rat semi-invariant TCR

At first, the capability of the newly generated rat CD1d oligomers to bind to rat semi-invariant TCRs was tested with transductants expressing a rat semi-invariant TCR (AV14S6^FAJ18 α chain and BV8 β chain) (Pyz et al., 2006). In this experiment, the newly generated rat CD1d oligomers were compared to mouse and human CD1d oligomers (figure 16). β -Gal-loaded controls were included to assess unspecific binding. As previously shown by E. Pyz, these cells were stained by α -Gal-loaded mouse CD1d tetramers to some extent. Similarly, α -Gal-loaded mouse CD1d-IgG dimers also stained this cell line very weakly. α -Gal-loaded human CD1d tetramers did not bind to the transductants. Importantly, staining of these cells with α -Gal-loaded rat CD1d-IgG dimers was much better than with mouse CD1d-IgG dimers. α -Gal-loaded rat CD1d human Fc dimers also bound this rat semi invariant TCR, although not as efficiently as rat CD1d-IgG dimers. Unfortunately, and even though oligomerization was carried out in one single experiment, the differences observed between α -Gal- and β -Gal-loaded rat CD1d streptamer stainings were very modest. Moreover, this reagent gave a very high unspecific signal shown by the β -Gal-loaded control staining. This unspecific binding was independent from TCR recognition since it also appeared when untransduced BWs were stained (data not shown).

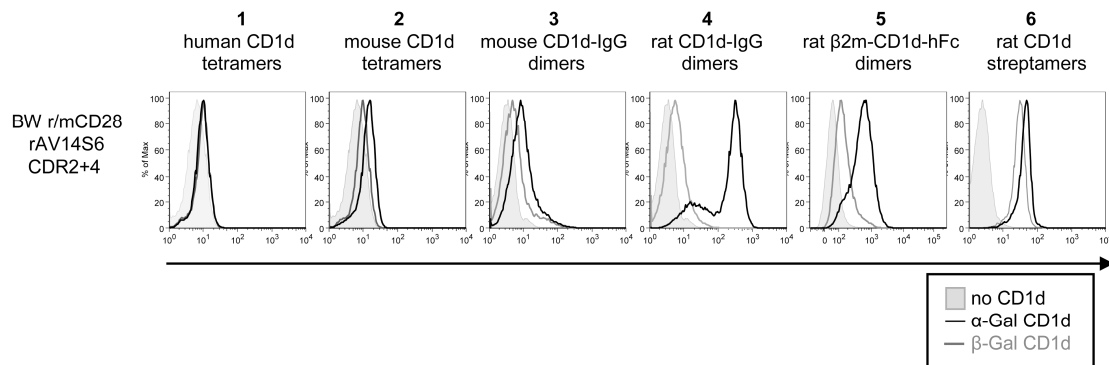


Figure 16. Reactivity of CD1d oligomers from different species against rat semi-invariant TCR. BW r/mCD28 rAV14S6 + CDR2+4 transductants were stained with various α -Gal- or β -Gal-loaded CD1d oligomers. 1 *Human CD1d tetramers*: 10^5 cells were stained for 40 min at room temperature with 0.025 μ g of α -Gal- or β -Gal-loaded human CD1d-PE tetramers (black and gray lines, respectively) in a final volume of 50 μ l of FACS buffer. Filled histograms correspond to unstained BW cells. 2 *Mouse CD1d tetramers*: Staining of BW transductants with mouse CD1d-PE tetramers was carried out as with human CD1d tetramers. Human and mouse CD1d tetramers were kindly provided by S. A. Porcelli. 3 *Mouse CD1d-IgG dimers*: 2×10^5 cells were stained with 2 μ g of α -Gal- or β -Gal-loaded mouse CD1d-IgG dimers during 1 hour at room temperature in a final volume of 100 μ l, where the final concentration of TRITON X-100 was 0.0037%. After washing, dimers were detected with D α M-PE. Filled histograms show BW cells which were stained with D α M-PE in the absence of CD1d-IgG dimers. 4 *Rat CD1d-IgG dimers*: Staining of BW transductants with rat CD1d-IgG dimers was carried out as with mouse CD1d-IgG dimers. 5 *Rat β 2m-CD1d-hFc dimers*: 2×10^5 cells were stained with 2 μ g of α -Gal- or β -Gal-loaded rat β 2m-CD1d-hFc dimers for one hour at room temperature in a final volume of 100 μ l, where the concentration of TRITON X-100 was 0.0063%. Rat β 2m-CD1d-hFc dimers were detected, after washing, with PE labeled goat F(ab')₂ anti-human IgG Fc fragment. Filled histograms represent non-stained cells. 6 *Rat CD1d streptamers*: 10^5 cells were stained with rat CD1d streptamers (50 μ l containing 1 μ g α -Gal- or β -Gal-loaded rat β 2m-CD1d-streptag + 0.75 μ g Strep-Tactin-PE, which had previously been pre-incubated for 45 min at 4°C in a final volume of 50 μ l). The final concentration of TRITON X-100 was 0.01%. Filled histograms represent non-stained BW cells.

3.4.3 Binding of mouse and rat CD1d dimers to iNKT cells of either species

From all rat CD1d oligomers produced and tested, rat CD1d-IgG dimers were chosen to analyze rat primary cells, firstly, because they were the best reagent to stain a cell line expressing a rat semi invariant TCR (Fig. 16) and secondly, because the production of mouse CD1d-IgG dimers had also been established in our laboratory, allowing a direct comparison of rat and mouse primary cells with the same CD1d reagent from each species.

The following results were obtained when mouse (C57BL/6) and rat (F344) intrahepatic lymphocytes were stained with rat and mouse CD1d-IgG dimers (Fig. 17): i) mouse CD1d-IgG α -Gal-loaded dimers stained mouse iNKT cells, which as previously reported were the major proportion of T cells in the liver (45%) (Hammond et al., 2001). ii) α -Gal-loaded rat CD1d-IgG dimers, stained also mouse iNKT cells, although the proportion of iNKT cells stained by rat the rat oligomers (29% of the intrahepatic T cells) was smaller than the proportion stained by mouse CD1d dimers (45%). iii) Rat

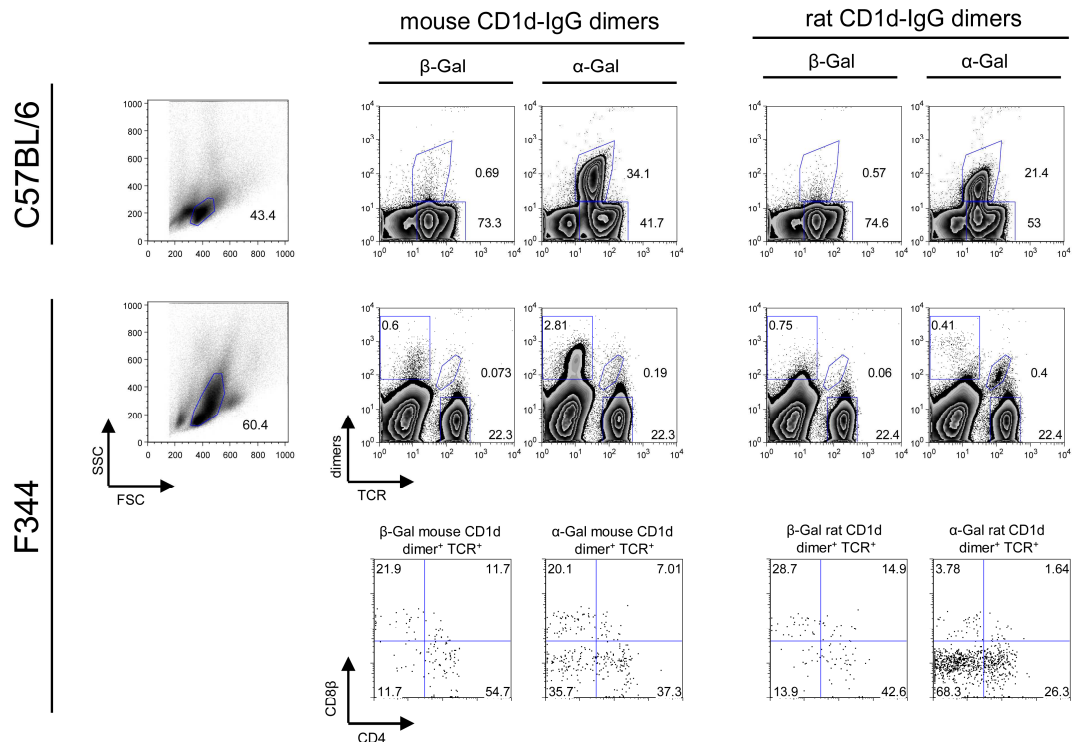


Figure 17. Interspecies cross-reactivity of mouse and rat CD1d-IgG dimers. C57BL/6 and F344 intrahepatic lymphocytes were stained with rat and mouse CD1d-IgG dimers loaded with either α -Gal or β -Gal. Dimers were detected with DaM-PE. To assure specific dimer staining of T cells, mouse and rat T cells were identified with H57-597 or R73 FITC-labeled mAbs, respectively. FCS/SSC dot plots depict the gated populations among total isolated cells, which are shown in the dimers/TCR plots. In mouse IHLs stainings, B cells, defined as CD19-positive cells stained with the 1D3-APCy mAb, were excluded and are not shown in the dimers/TCR plots. In rat cells, CD8 β (341-bio + SA-APCy) and CD4 (OX-35-Cy5PE) expression was also analyzed. CD4/CD8 plots show F344 IHLs-gated cells which were double positive for the different dimers and TCR. Numbers in the plots indicate the percentages of gated cells.

iNKT cells could be identified with rat CD1d-IgG α -Gal-loaded dimers, revealing that compared to mouse, iNKT cell numbers in the rat are a much lower: only a 1.4% (± 0.37 , SD) of all rat intrahepatic T cells are iNKT cells. Moreover, in line with CD4 and CD8 expression by mouse and human iNKT cells (Bendelac et al., 2007) these α -Gal-loaded rat CD1d-IgG dimer positive T cells are mostly CD4 or DN cells, and only a very small proportion expresses CD8 β (4.58% ± 1.43). In contrast, the few T cells which are included in the gate of rat CD1d-IgG β -Gal-loaded positive cells have a completely different CD4/CD8 distribution: Many of them CD8 β and double positive and very few DN. In a single experiment binding of mouse CD1d-IgG α -Gal-loaded dimers to rat iNKT cells was also tested. In this experiment the proportion of TCR positive cells stained by the CD1d-IgG α -Gal-loaded dimers was less than half of that stained by rat dimers, while the number of cells stained by the β -Gal-loaded control was slightly higher. Nevertheless, much of this staining was probably specific for iNKT cells given

the increased number of DN cells in this population. However, the lower staining efficacy and the rather high degree of staining of non-T cells underscore that mouse CD1d-IgG dimers are not suitable for the analysis of rat primary iNKT cells. A point which is underlined by results obtained with cultured iNKT cells later in this section (Results 3.7.4).

3.4.4 Phenotype of rat iNKT cells

Once rat iNKT cells could be identified by flow cytometry its phenotype was analyzed. First, based on their FCS and SCC properties, iNKT cells were relatively big and fairly granular (Fig. 18 *a*). These properties allowed the reduction of the gate set on total lymphocytes in such a way that unspecific staining was reduced while the proportion of iNKT cells among the gated cells was increased (Fig. 18 *a*). Second, approximately the half of F344 iNKT cells bear a TCR β chain which contains the BV8S4 gene segment, whereas among the other intrahepatic T cells only a $6.5 \pm 0.5\%$ have this particular BV gene segment (Fig. 18 *b*). Third, almost all α -Gal-loaded rat CD1d-IgG dimer positive T cells expressed NKR-P1A/B receptors detected by the mAb 10/78, hereafter referred simply as NKR-P1. Nonetheless, from all T cells expressing NKR-P1 only a very small proportion were iNKT cells (5%, Fig. 18 *c*) and fourth, as shown in the previous section of the results, most of rat iNKT cells were CD4 or DN (Fig. 17).

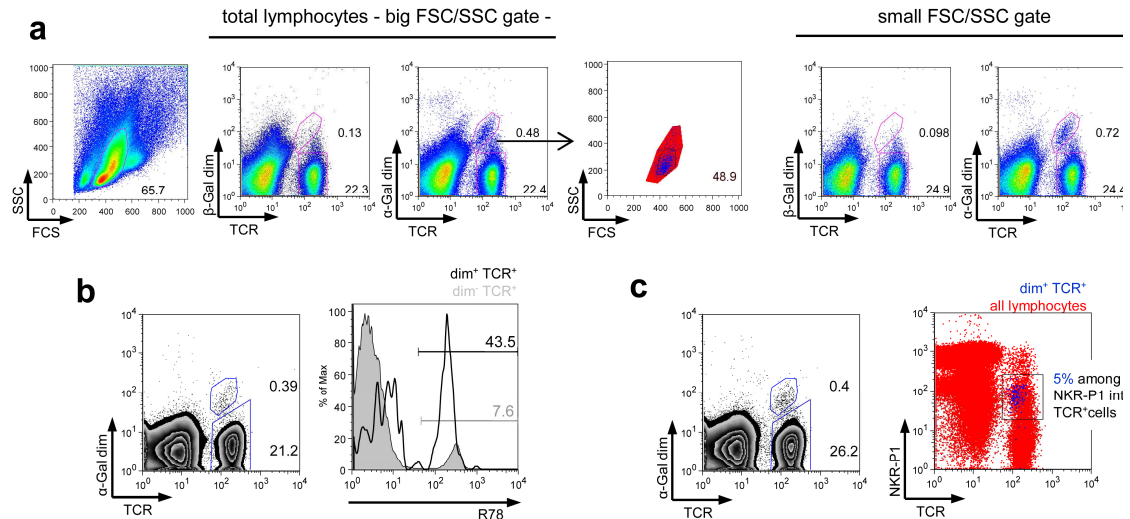


Figure 18. Phenotype of rat iNKT cells. F344 intrahepatic lymphocytes were stained with rat CD1d-IgG dimers loaded with either α -Gal or β -Gal, which were detected with DaM-PE. To assure specific dimer staining of T cells, after blocking of free binding sites of DaM-PE with mouse IgG, anti-TCR mAb (R73-FITC) was included in the analysis. *a* Size and granularity of iNKT cells. To determine the size and granularity of rat iNKT cells compared to other intrahepatic lymphocytes first, dimer and TCR co-staining was analyzed among all lymphocytes. The FCS/SSC plot on the left, illustrates how total lymphocytes were gated. Subsequently, iNKT cells (in blue), defined as shown in the plot in the center of the figure (α -Gal-loaded rat CD1d-IgG dimer⁺ TCR⁺), were superimposed to the gate of all lymphocytes (red). In such a way a new gate was defined where iNKT are mostly localized (black gate in the overlay of iNKT cells and total lymphocytes). As expected, the proportion of iNKT cells increased among the cells contained in this narrower gate (dimers/TCR plots on the right). *b* BV8S4 usage by F344 iNKT cells compared to $\alpha\beta$ T cells. Multicolor flow cytometry allowed to assess the proportion of BV8S4⁺ cells among iNKT cells (α -Gal-loaded rat CD1d-IgG dimer⁺ and TCR⁺ cells) by including the biotinylated R78 mAb (visualized with SA-APCy) in the staining. The dimer/TCR plot illustrates which cells were analyzed for their BV8S4 usage. In the histogram overlay the percentages of R78⁺ among iNKT cells (black) or $\alpha\beta$ T cells (gray) are shown. *c* NKR-P1 expression. Similar to *b*, NKR-P1 (10/78-Bio + SA-APCy) analysis was included into the iNKT cell staining. The NKR-P1/TCR dot plot shows total lymphocytes in red (gated as shown in *a*, big FCS/SSC gate) and iNKT cells in blue (α -Gal-loaded rat CD1d-IgG dimer⁺ TCR⁺ cells, density blot shown in *a*). In the experiment shown, iNKT cells constitute a 5% of NKR-P1 intermediate TCR⁺ lymphocytes (black gate).

3.5 iNKT cell frequencies in various rat strains

In human and mouse iNKT cell numbers are under strict genetic control, as shown by very similar frequencies in genetically identical individuals but varying up to 100 fold among different genetic backgrounds (Lee et al., 2002b). These differences are also well illustrated in studies where different mouse strains were investigated (Hammond et al., 2001; Rymarchyk et al., 2008). Therefore, apart from the direct identification of iNKT cells in the rat, the analysis of iNKT cell frequencies and function among different rat strains was one of the aims of this study. Prior results from E. Pyz investigating α -Gal responsiveness in F344 and LEW rats, showed that whereas F344 splenocytes secreted cytokines in an antigen-dose dependent manner, cytokine release by LEW splenocytes was absent (IL-4) or very low (IFN- γ) even at high concentrations of α -Gal. Based on

these findings both strains were chosen as representative of α -Gal responder and non-responder inbred rat strains and were tested for the presence of iNKT cells.

3.5.1 iNKT cells in F344 and LEW rats

Using rat CD1d-IgG α -Gal-loaded dimers, iNKT cell frequencies were analyzed in different compartments of F344 and LEW rats. The particular CD4/CD8 distribution of these cells helps to identify false positive cells when the frequencies of cells stained with the dimers are very low. Therefore, CD4 and CD8 β expression was also addressed (Fig. 19).

As shown in a previous section (Results 3.4.3) iNKT cell frequencies in F344 rats are, when calculated as proportion of hepatic T cells, 10 fold lower than that of C57BL/6 mice and at least 50 fold lower when the frequencies among total hepatic lymphocytes were compared. Nonetheless, the distribution of these cells in liver, spleen and blood correlate with the data obtained in mice: rat iNKT cell numbers were also much higher in the liver than in the spleen and than in the blood: 3.5, 0.4 and 0.05% of the T cells which were included in the electronically-set gate as shown in figure 18 (Fig. 19, FSC-SCC dot plots). This gate contained only big-sized lymphocytes and it was necessary to reduce unspecific staining. However, this gate does not include the small-sized lymphocytes and therefore the frequencies which are shown in the dot plots are not representative for all lymphocytes. Among F344 IHLs the mean values of the frequencies of iNKT cells among total intrahepatic lymphocytes and among total T cells analyzed in four animals are 0.25 (± 0.1 SD) and 1.4 (± 0.37 SD), respectively. Importantly, although sometimes only very few iNKT cells were stained with the α -Gal-loaded CD1d-IgG dimers (for example in the blood where 1 only of 2300 cells was stained, Fig. 19), the constantly reduced numbers positive for β -Gal-loaded CD1d-IgG dimers, and the nearly absolute lack of DN cells among cells stained with β -Gal-loaded CD1d-IgG dimers indicate a large specific staining of iNKTs.

In agreement with the functional data obtained by E. Pyz, iNKT cell numbers were much more reduced in LEW compared to F344. Indeed, whereas iNKT cells appear as a clearly distinct population among F344 intrahepatic lymphocytes, the results obtained with LEW rats were close to the detection limit.

iNKT cell development has been extensively studied in the mouse. In this species iNKT cells are selected in the thymus by DP thymocytes, after AV14-AJ18 rearrangements. In the early stages of its development iNKT cells express CD4, which will be lost later on.

This loss of CD4 already occurs in the thymus (Bendelac et al., 2007; Godfrey et al., 2010). Therefore, it was surprising when no differences were observed between the frequencies of α -Gal- or β -Gal-loaded CD1d-IgG dimer positive cells in thymocytes from both strains (Fig. 19) and when no more DN cells were found among the cells stained with α -Gal CD1d-IgG dimers. To which extent the observed increased proportion of CD4 single positive among α -Gal-loaded CD1d-IgG positive cells compared to β -Gal-loaded CD1d-IgG positive cells in F344 but not in LEW thymocytes relates to iNKT cells remains to be elucidated.

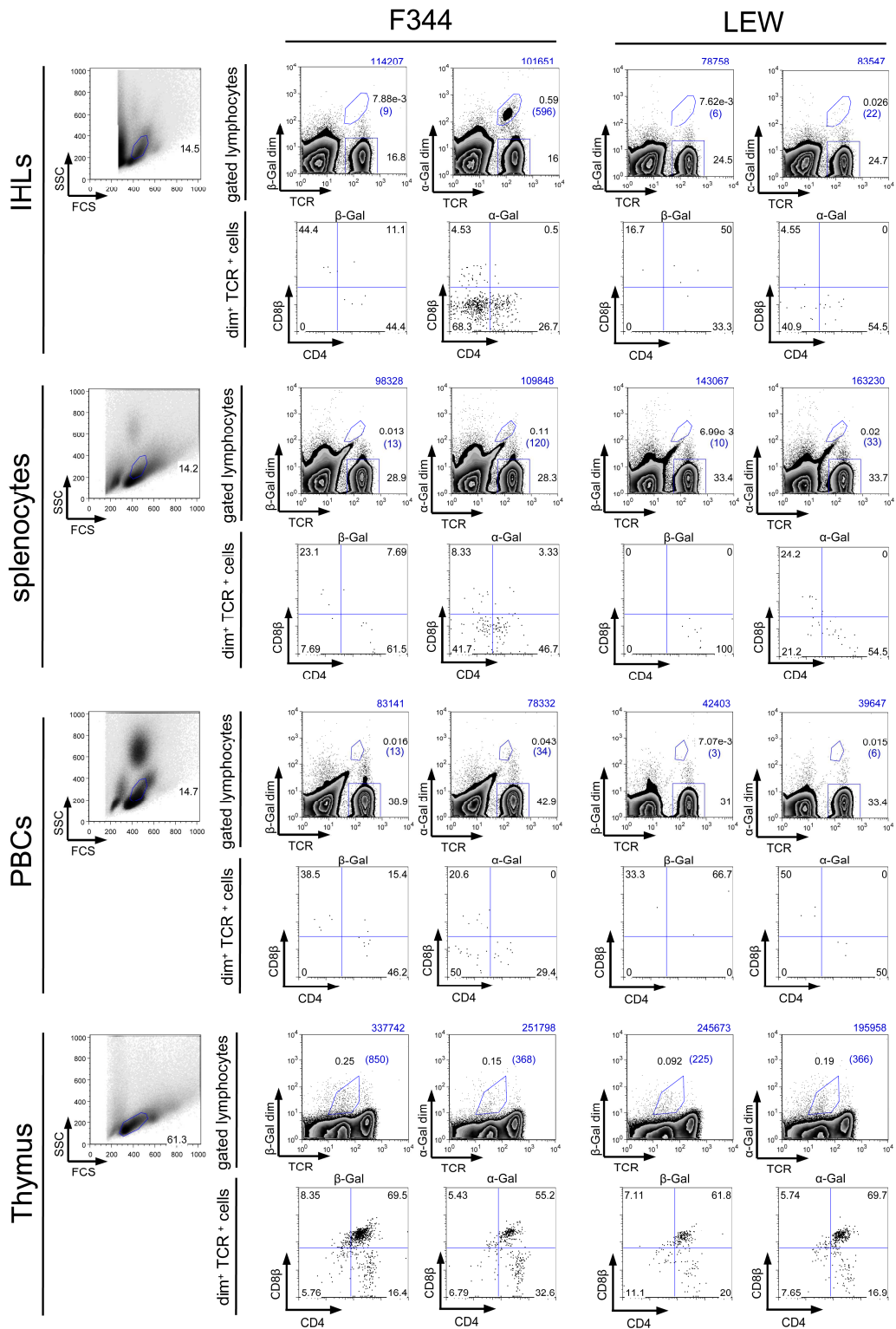


Figure 19. iNKT cell frequencies in F344 and LEW rats. Frequencies of iNKT cells were analyzed among intrahepatic lymphocytes (IHLS), splenocytes, peripheral blood cells (PBCs) and thymocytes by flow cytometry after having stained the cells with either α -Gal- or β -Gal-loaded rat CD1d-IgG dimers (visualized with DaM-PE) and anti-TCR β (R73-FITC), anti-CD4 (OX-35-CyPE) and anti-CD8 β (341-bio + SA-APC) mAbs. Based on the size and granularity of iNKT cells (FIG phenotype *a*), the FCS/SSC plots on the left depict which cells are shown in the dimer/TCR plots. CD4/CD8 plots show either α -Gal- or β -Gal-loaded rat CD1d-IgG dimer⁺ TCR⁺ gated cells. Numbers in black indicate the percentages of gated cells in each plot. Numbers in blue above each plot correspond to the total events which are shown. Blue numbers with brackets in the plots indicate the total events of the dimer⁺ TCR⁺ gated cells.

3.5.2 Expression of AV14-AJ18 rearrangements in F344 and LEW rats

The fact that iNKT cells express an invariant TCR α chain formed by rearranged AV14-AJ18 gene segments can be exploited to detect iNKT cells by amplifying such invariant α chains by PCR. Such rearrangements were analyzed in F344 and LEW thymocytes, splenocytes and IHLs by RT-PCR using AV14 and AJ18 primers. All AV14-containing TCR α chains were amplified as well with AV14 and AC primers (Fig. 20). Figure 20 *a* depicts the positions of these primers. Moreover, TCR β chains containing BV8 gene segments and β -actin were also analyzed as controls of a specific product expressed by T cells and of the general quality of the cDNA, respectively.

In line with iNKT cell frequencies detected by flow cytometry using rat CD1d dimers, the highest signal intensity of AV14-AJ18 products was obtained with F344 IHLs-derived mRNA and it was followed by spleen and thymus. The signal of AV14-AC products was also higher in F344 IHLs than splenocytes and thymocytes. In LEW, signals for BV8-BC and β -actin controls were the same or even higher than for F344 but AV14-AJ18 rearrangements were hardly detected regardless of the tissue origin. Moreover, intensity of AV14-AC PCR products was also lower than in F344.

As mentioned in the introduction, LEW rats have one functional BV8S2 like gene segment (BV8S2¹) and F344 rats have two (BV8S2^a and BV8S4^a) (Asmuss et al., 1996). The forward primer used to amplify TCR β chains bind to both, BV8S2 and BV8S4 genes.

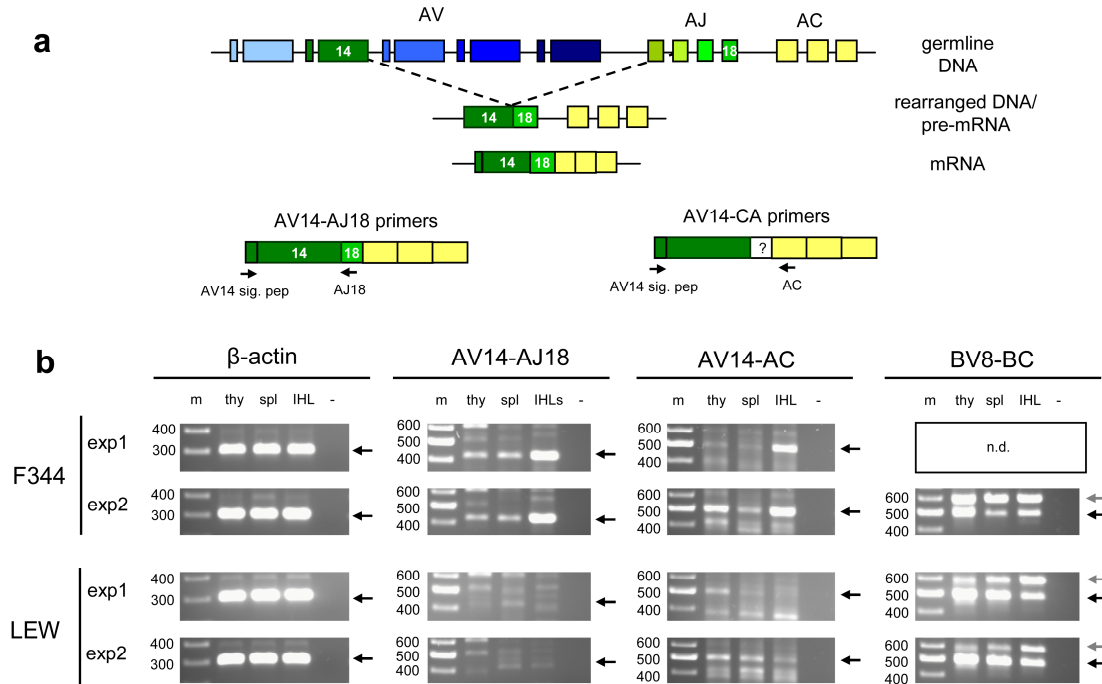


Figure 20. β-actin, iTCRα, AV14 TCRα and BV8 TCRβ mRNA expression by F344 and LEW thymocytes, splenocytes and IHLs. *a* Schematic representation of the position of the primers used to amplify iTCRα (AV14-AJ18) or AV14-containing TCRα (AV14-CA) chain mRNA by RT-PCR. *b* iTCRα (AV14-AJ18), AV14 TCRα (AV14-CA), BV8 TCRβ (BV8-BC) and β-actin mRNA expression was analyzed by RT-PCR in two independent experiments: exp1 and exp2, respectively. The products obtained after PCR amplification using cDNA derived from F344 or LEW thymocytes (thy), splenocytes (spl) and intrahepatic lymphocytes (IHLs) are shown. - lanes are water controls. Numbers indicate the size of the bands of the DNA marker (m). Black arrows point out the expected size of each RT-PCR product: β-actin: 300 bp; AV14-AJ18: 420 bp; AV14-AC: 500 bp; BV8-BC: 484 bp. Gray arrows in the BV8-BC products indicate the expected size of amplified DNA containing the intron between the signal peptide and the variable gene segment: 582 bp. n.d. non determined.

A real time PCR was also established to detect iTCRα chains. In addition of being a more quantitative approach, it also allowed the confirmation of the results obtained by RT-PCR, because the primers used in each PCR lay in different regions (Fig. 20 *a* and 21 *a*). Relative quantification of iTCRα mRNA among the different tissues of F344 and LEW rats was based in the delta delta cycle threshold method ($\Delta\Delta C_t$), but interpretation of the results is rather limited since efficiencies for iTCRα (iTCR) and total TCRα (AC) PCR products were not determined, final concentrations of each primer pair were different (iTCR 100 nM and AC 300 nM) and serial dilutions of the cDNA were not routinely included. Moreover, for the detection of the iTCRα chain one primer had to anneal to AV14 and the other to AJ18. However, since the size of the PCR product should not be bigger than 300 bp for detection with SYBR Green, the forward primer had to anneal to the exon encoding the variable region (Fig. 21*a*). Therefore it was not possible to discriminate between amplicons of genomic or complementary DNA as it was

possible when the forward primer anneals to the exon encoding the signal peptide (Fig. 20). For all these reasons, instead of only showing the relative values obtained after $\Delta\Delta Ct$ calculations (Fig. 21 *c* and *d*), all Ct values obtained for iTCR and AC products are shown (Fig. 21 *b*). Despite the mentioned limitations, it is clear that the ratio of iTCR α to total TCR α mRNA is much higher in IHLs than in other compartments of F344 rats or in any of the tissues analyzed in LEW.

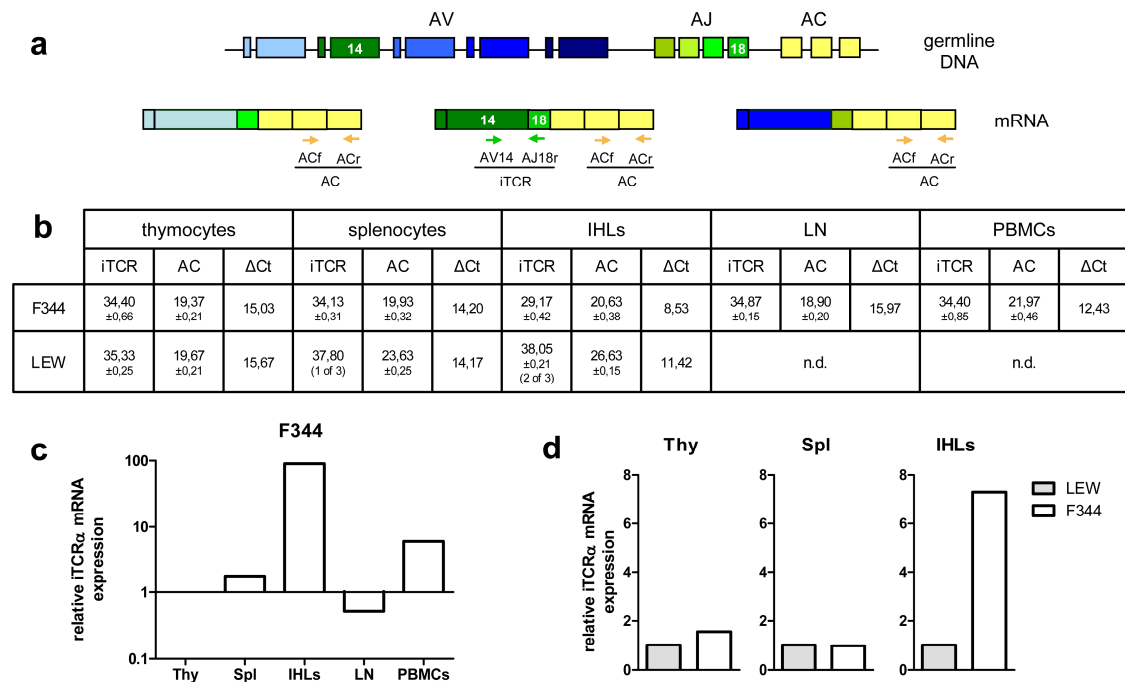


Figure 21. Relative quantification of iTCR α mRNA among total TCR α chain mRNA. *a* Schematic representation of the position of the primers used to analyze iTCR (AV14-AJ18) mRNA expression among total TCR α (AC) chain mRNA by real time PCR. *b* Mean values of the cycle thresholds obtained for iTCR α and total TCR α mRNA in triplicate samples \pm SD and ΔCt calculation, except for LEW iTCR in splenocytes and IHLs, where only in 1 of 3 and 2 of 3 replicated samples, respectively, a PCR product appeared. Relative iTCR α mRNA expression was analyzed in different F344 and LEW compartments: thymocytes (Thy), splenocytes (Spl), intrahepatic lymphocytes (IHLs), lymph nodes (LN) and peripheral blood mononuclear cells (PBMCs). n.d. non determined. *c* Relative iTCR α mRNA expression in F344 rats calculated by the $\Delta\Delta Ct$ method. In order to allow such a graphical representation, the relative iTCR α mRNA expression in the thymus was set as 1. The $\Delta\Delta Ct$ values were obtained from the results shown in *c*. *d* Relative iTCR α expression among F344 and LEW thymocytes (Thy), splenocytes (spl) and intrahepatic lymphocytes (IHLs) calculated by the $\Delta\Delta Ct$ method from the values shown in *c*. LEW relative iTCR α mRNA expression. Values were set as 1.

3.6 Analysis of AV14 gene family in the rat

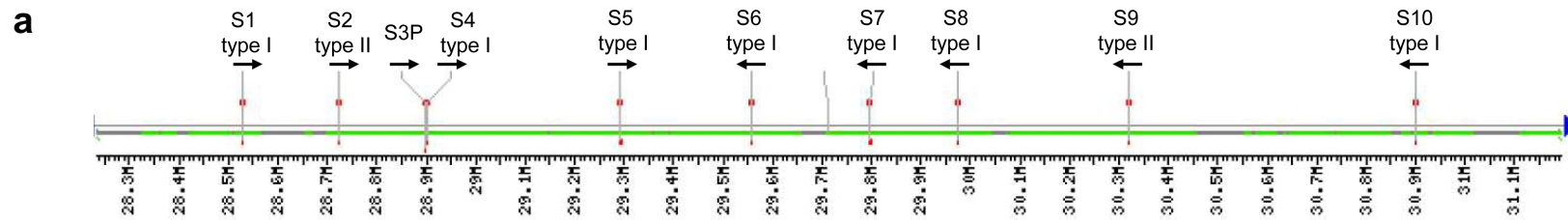
The size of the AV14 gene family varies considerably between species: Humans possess one AV14 gene whereas mice one or two and rats up to ten (Kinebuchi and Matsuura, 2004; Koseki et al., 1991; Lefranc, 2001; Matsuura et al., 2000; Pyz et al., 2006). In a previous report based on an obsolete supercontig sequence (NW_042969), it was reported that BN rats have ten AV14 gene segments, which based on their

localization in this contig were designated as TRAV11-1 to TRAV11-10 (Kinebuchi and Matsuura, 2004). The designation of AV14 as AV11 is based on the IMGT nomenclature. This nomenclature is maintained in this study to distinguish them from the actual BN genomic sequence (NW_047454.2, April 15th, 2005). All these gene segments were expected to be functional and some of them (i. e. TRAV11-5 and -6, as well as, TRAV11-2 and -8) had identical sequences. Blasting of these ten AV14s (TRAV11-1 to -10) with the most recent NCBI release (NW_047454.2) reveals a change in the order of the AV14 gene segments (Fig. 22). In the actual version, all the gene segments have unique sequences expected to encode different polypeptides (Fig. 23 *a*). Consequently, two segments were absent in the former report: AV14S1 and AV14S3 (Fig. 22). AV14S3 is expected to produce a non-functional TCR α chain due to the deletion of two nucleotides resulting in a reading frame shift and a premature stop codon (Fig. 23 *a*).

Currently, there are no mAbs which recognize and/or distinguish the predicted products of these AV14 gene segments (shown in Fig. 23 *a*) therefore analysis of expression of a specific AV14 is restricted to the mRNA level. In F344 rats five different AV14 gene segments and one pseudogene have been identified by cloning AV14 comprising TCRs from cDNA and genomic DNA, respectively (Matsuura et al., 2000; Pyz et al., 2006). In this study we propose a new nomenclature for some of these F344 AV14 gene segments based on their homology degree with BN AV14 gene segments in order to simplify the comparisons between these two species (Fig. 22). All the F344 AV14 gene segments are found in the BN rat genome with 100% homology for the exon encoding the mature polypeptide, except the pseudogene AV14S4P^F which shows only 98% homology compared to AV14S4^B. Consequently, its predicted amino acid sequence is not present in BN (Fig. 22 and 23). In the exons encoding the signal peptide, some of the F344 gene segments have a nucleotide substitution when compared to BN, which would encode a glutamine (Q, F344 allele) at position 4 instead of a histidine (H, BN allele) (Fig. 24).

AV14 gene segments from F344 rats have been divided into two different types based on their CDR2 sequence similarity: AV14S6^F, AV14S7^F, AV14S8^F and the pseudogene AV14S4P^F belong to type I and AV14S2^F is the only type II representative (Matsuura et al., 2000). Among all BN AV14 gene segments only 2 belong to the type II (AV14S2^B and AV14S9^B, figure 22 and 23 *a* and *b*). Interestingly, in the work published by Matsuura et al. a specific tissue distribution of these types was proposed: Type II

bearing rearrangements were more frequent in the spleen, whereas type I containing invariant TCRs were slightly more abundant in the liver (Matsuura et al., 2000).



b

CDR2 Type	BN actual genome		BN obsolete sequence NW_042969		F344 AV14 gene segments identified up to date			
	Gene Name	Positions at NW_047454.2	Gene Name (Kinebuchi et al. 2004)	Homology	New gene name	Previous gene name	Homology with BN genome	Reference
I	AV14S1	390863-391393						
II	AV14S2 ^B	583401-583932	<i>TRAV11-10</i>	99%	AV14S2 ^F	<i>AV14S3</i>	98% s.p. 100% v.	(Matsuura et al., 2000) and this study
(I)	AV14S3P ^B	759841-760370						
I	AV14S4 ^B	762278-762809	<i>TRAV11-3</i>	100%	AV14S4 ^F	<i>AV14S4</i>	98% s.p. 98% v.	(Matsuura et al., 2000)
I	AV14S5 ^B	1154998-1155529	<i>TRAV11-7</i>	100%	AV14S5 ^F		98% s.p. 100% v.	Identified in this study
I	AV14S6 ^B	1418612-1419143	<i>TRAV11-1</i>	100%	AV14S6 ^F	<i>AV14S1</i>	100% s.p. 100% v.	(Matsuura et al., 2000)
I	AV14S7 ^B	1659363-1659894	<i>TRAV11-5</i> <i>TRAV11-6</i>	100% 100%	AV14S7 ^F	<i>AV14S2</i>	100% s.p. 100% v.	(Matsuura et al., 2000)
I	AV14S8 ^B	1834544-1835071	<i>TRAV11-2</i> <i>TRAV11-8</i>	100% 100%	AV14S8 ^F	<i>AV14S8</i>	100% s.p. 100% v.	(Pyz et al., 2006) and this study
II	AV14S9 ^B	2181139-2181670	<i>TRAV11-4</i>	100%				
I	AV14S10 ^B	2760694-2761225	<i>TRAV11-9</i>	100%				

Figure 22. Nomenclature of rat AV14 gene segments. According to their position in the most actual version of the rat genome at the NCBI (NW_047454.2, April 15th, 2005) (a), we have named the AV14 gene segments of the BN inbred rat strain according to their position in the rat genome (b). In the table are also listed the AV14 gene segments reported by Kinebuchi and colleagues in 2004, based in the obsolete supercontig sequence and all AV14 gene segments reported up to date for F344 inbred rat strains with their new nomenclature based in their homology to the BN AV14 gene segments.

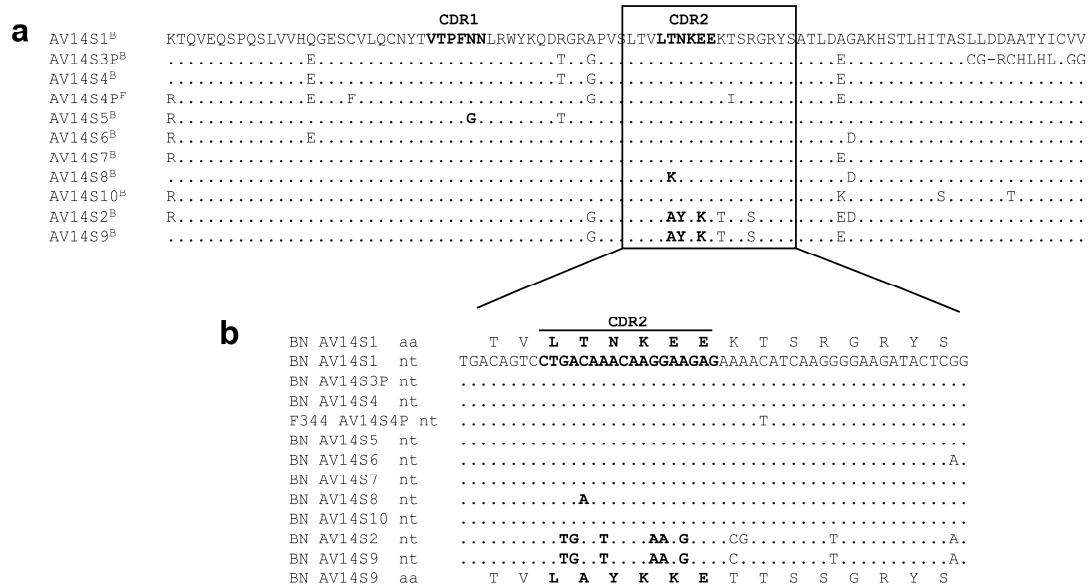


Figure 23. AV14 gene segments. *a* Alignment of the predicted amino acidic sequence of all VA14 gene segments. The only F344 gene segment identified to date which is different (without considering the signal peptide exon) from those of BN rats, is AV14S4P^F (Accession Nr. AB036697.1) therefore it is the only F344 derived sequence included in this alignment. CDR regions are illustrated with bold letters. The box indicates the peptide region containing the CDR2 whose nucleotide sequences are shown in *b*. *b* Nucleotide sequence (nt) of regions encoding the CDR2 region. Above and below the alignment, the amino acidic (aa) sequences of representative type I (BN AV14S1) and type II AV14 (BN AV14S9) gene segments are shown. The CDR2 region is highlighted in bold.

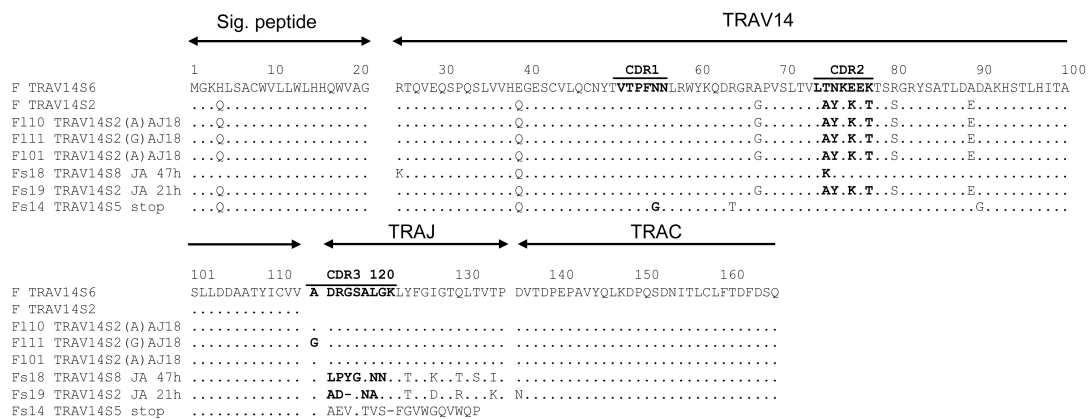


Figure 24. Cloned AV14 TCR α chains. The predicted amino acid sequences of various AV14-containing TCR α chains which were cloned after amplification by PCR using F344 splenocytes (Fs) or intrahepatic lymphocytes (F1) derived cDNA as template are shown. The obtained clones are compared to a previously described type I iTCR α chain (AV14S6^F (previously named AV14S1, Pyz E. et al., 2006)) and to a type II AV14 gene segment AV14S2^F (previous AV14S3, Matsuura, H. et al. 2000)). Dots indicate same amino acid residue as the first sequence. CDR regions are highlighted with bold letters.

3.6.1 Analysis of AV14 TCR α chains in F344 rats

At first, in order to analyze AV14 and AJ gene segment usage in F344 rats as in the previous study of Matsuura et al. (Matsuura et al., 2000), AV14-containing TCRs from F344 IHLs or splenocytes derived cDNA were cloned (Methods section 2.2.2.10). Three

clones selected randomly from each tissue were sequenced. Their predicted amino acid sequences are shown in Fig. 24.

All the clones isolated from IHLs contained the AJ18 gene segment. In two of them, the amino acid encoded in the junction region was an alanine whereas in the other one was a glycine. In contrast, none of the splenocytes derived AV14 TCRs comprises the AJ18 segment. Instead, based on sequence similarity with mouse AJ gene segments, the Fs18 and Fs19 clones encode the AJ47 and AJ21 rat homologues, respectively. The Fs14 also used a different AJ segment (the rat homologue of the mouse AJ38) but a stop codon appears in the cDNA resulting in a non-functional TCR α chain. In the BN genome, identical sequences were found for all these rat AJ genes.

All clones generated from IHLs cDNA used the type II AV14 gene segment AV14S2. On the contrary, TCR α chains isolated from the spleen contained different AV14 gene segments: One was again AV14S2, but the other two were AV14S8 (type II), previously identified by E. Pyz (Pyz et al., 2006), and AV14S5 (type I) which had not yet been described for F344 (Fig. 22).

3.6.2 AV14 and AJ18 gene segment usage in F344 and LEW rats

In order to study the usage of AV14 and AJ gene segments in the thymus, the spleen and the liver of F344 and LEW rats, the products obtained in the RT-PCR experiments: AV14-AJ18 and AV14-AC (Fig. 20) were directly sequenced. This approach does not provide information about single TCR α chains but it gives a relative quantification of which are the gene segments used in each compartment of each strain. On the one hand, sequences of the AV14-AJ18 products show which AV14 gene segments are exclusively rearranged with AJ18. On the other hand, sequences from AV14-AC products indicate the AV14 gene segments used, in principle, by any AV14-positive TCR and in addition also reveal which AJ gene segments are contained in these AV14 positive TCRs.

Sequencing of the AV14-AC products from F344 and LEW thymocytes, splenocytes and IHLs in the AV14 forward direction, showed an AJ18 dominance only among F344 IHLs (Fig. 25). In the product obtained from F344 splenocytes, AJ18 is not the only AJ gene segment comprised among AV14 TCRs but still AJ18 nucleotides stand out in such a way that parts of this gene segment can be read. In contrast, in AV14-AC products from F344 thymocytes or from any of the analyzed compartments of LEW

inbred rats, AJ18 is neither preferentially used by the AV14 TCRs nor a unique reading frame was identified (Fig. 25).

Sequencing was also carried out in the 3' to 5' direction using AC binding primers. These sequences confirmed the results of the forward sequences: only where the AJ18 gene segment stood out in one unique reading frame a complete reverse sequence was achieved i.e. F344 IHLs, which reached the AV14 gene segment. On the contrary, in the organs where no AJ18 was legible, the readable sequence ended as soon as the AJ segment started and a mixture of many sequences appeared (F344 thymus) or a sequence with no homology to any AJ gene segment was found (LEW thymus and spleen, analyzed by blasting the sequences to the rat genome and GeneBank at the NCBI). The intermediate situation is perfectly illustrated by F344 spleen sequences: the AJ18 gene segment can still be detected and parts of the AV14 as well, but other AJ segments interfere with AJ18 (Fig. 25).

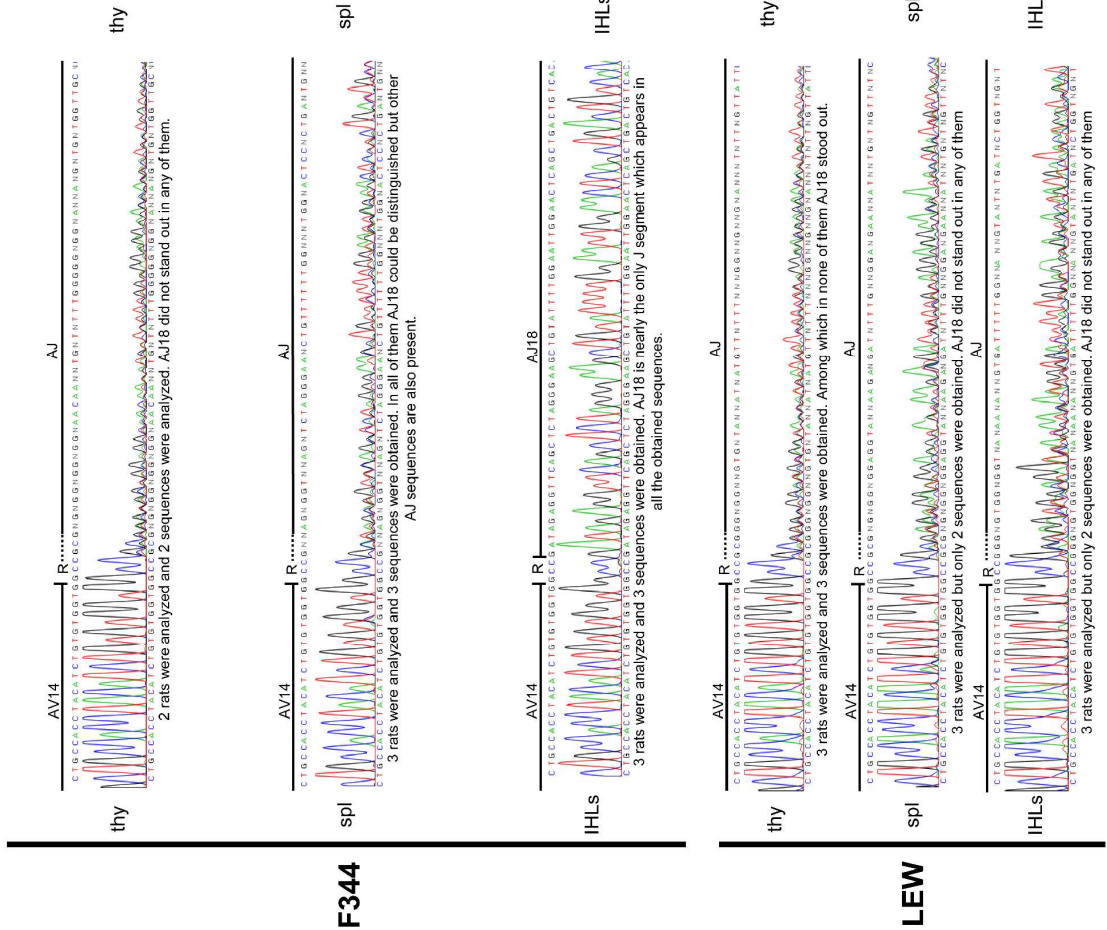
In line with the conserved CDR3 region of mouse and human iTCR α chains, whose joining region contains three nucleotides encoding a single amino acid, (Koseki et al., 1991; Lantz and Bendelac, 1994), the joining region of the AV14 TCRs (AV14-AC products) of F344 IHLs, most of which contained the AJ18 segment, also contains a three-nucleotide stretch encoding alanine (GCx, where x is any nucleotide) and glycine (GGx) are detected (Fig. 25) – being even more evident in the reverse sequence – whereas all AV14 gene segments of the BN genome bear GCC at these positions. Alanine and glycine are also the joining amino acids described for cloned iTCR α chains by Matsuura et al. (Matsuura et al., 2000).

Among TCRs formed by AV14 and AJ18 gene segments in F344 splenocytes and IHLs, the same three-nucleotide joining region containing various nucleotides encoding alanine or glycine was consistently found (Fig. 26). In contrast, among F344 thymocytes the AV14-AJ18 transition contained junctional regions of various sizes resulting in different reading frames and illustrated by the appearance of various nucleotides at the same positions of the AJ18 gene segment (Fig. 26) although the intensity of the AV14-AJ18 RT-PCR products was approximately the same as in splenocytes (Fig. 20). In LEW rats the analysis of such AV14-AJ18 products was not always possible due to the very low amount of amplified material which, as described above, may reflect the small numbers or absence of iNKT cells in this strain (Fig. 19 and 20). Indeed, from three analyzed animals no IHL-derived sequence could be obtained; in the spleen, two sequences were achieved, but AJ18 was legible only in one

of them, indicating that not all AV14AJ18-rearranged TCRs contained the same reading frame; and at last, in thymocytes in one single case a sequence was obtained whose VJ transitions differed in size.

Fig. 27 *a* illustrates how we evaluated the usage of AV14 gene segments. A type I to II ranking was established depending on which dideoxynucleotides and with which intensity appeared in the CDR2 region. In such a way, I >>> II was assigned when only nucleotides were observed which correspond to type I CDR2s and I ~ II when nucleotides of both types were detected with the same intensity. In order to exclude sequencing artifacts reverse sequencing was generally carried out. The table in Fig. 27 *b* summarizes all the data obtained. Three different rats were analyzed (except for F344 thymus) but sequencing often failed in the cases where the obtained RT-PCR product was difficult to detect (Fig. 20 and 27 *b*). First of all, there were no differences on the types of AV14 gene segments used by invariant TCRs (AV14-AJ18) and AV14 positive TCRs with various AJ segments. Second, in the periphery of F344 rats (spleen and IHLs) both types of AV14 gene segments seem to be equally used. Third, in the thymus however, a preference towards type II can be appreciated and fourth, LEW TCRs in contrast show a general bias to type I AV14 gene segments in all the tissues.

AV14-AC products: forward sequencing



AV14-AC products: reverse sequencing

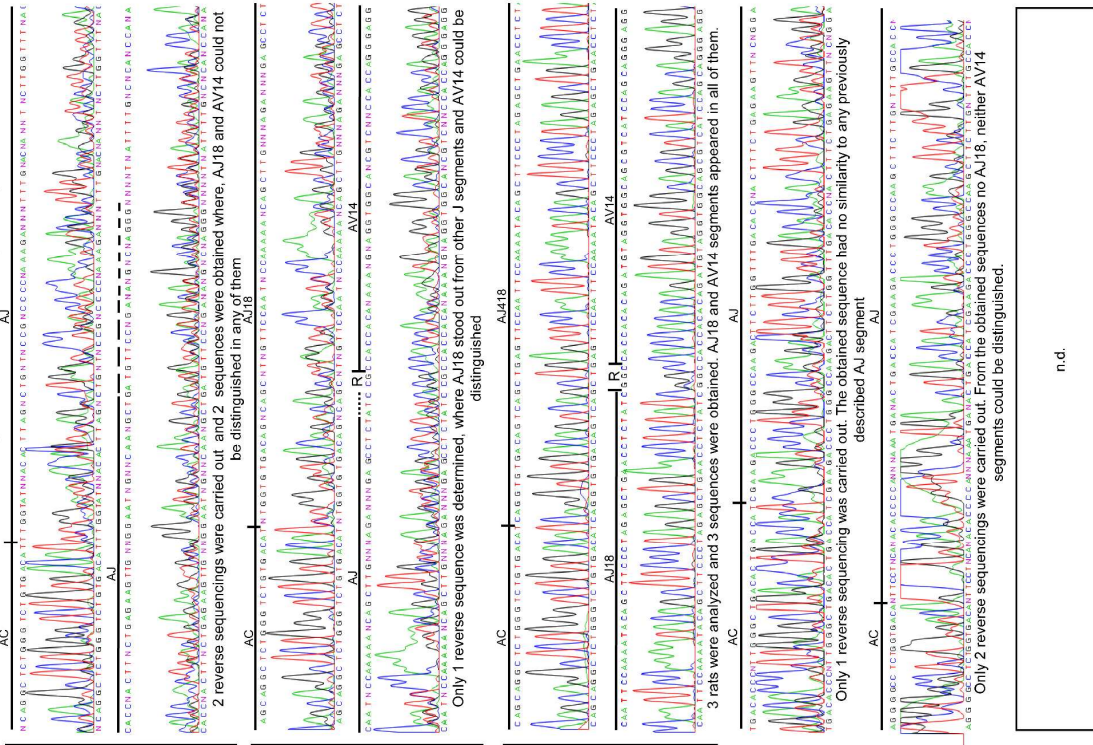


Figure 25. AJ gene segment usage by AV14-comprising TCR α chains. AJ gene segment usage by AV14-containing TCR α chains was analyzed in F344 and LEW thymocytes (thy), splenocytes (spl) or IHLs derived mRNA by RT-PCR and subsequent sequencing of the obtained AV14-AC products (as in Fig. 20). RT-PCR products were sequenced in both, forward and reverse directions. When possible, a representative example is shown. Below each example, it is specified how many rats were analyzed, how many sequencings were carried out and how many legible sequences were obtained. R: junctional region. n.d.: non determined.

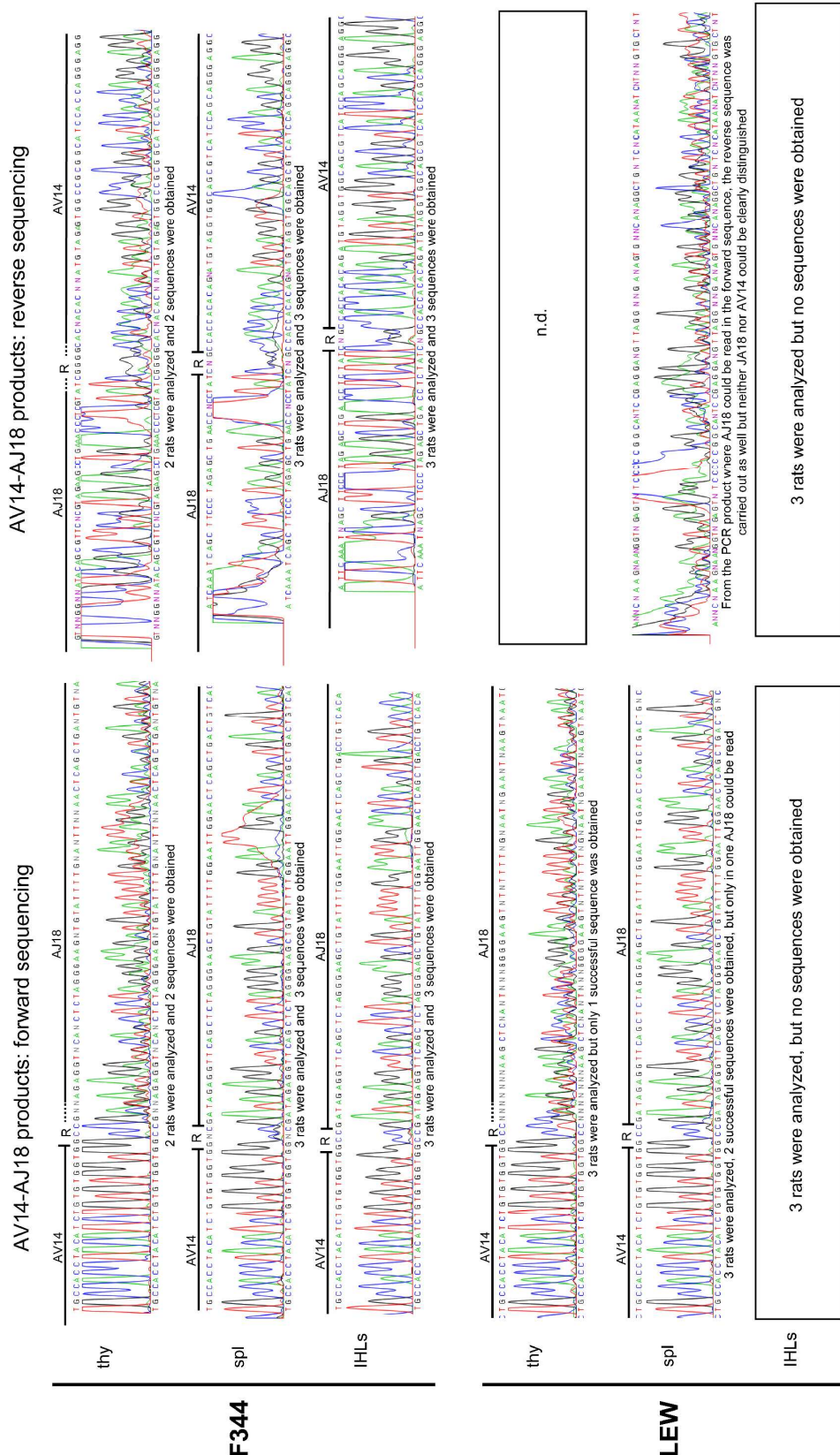


Figure 26. Analysis of nucleotides contained in the junctional regions of AV14-AJ18 TCR α chains. TCR α chains containing AV14 and AJ18 gene segments were analyzed in F344 and LEW thymocytes (thy), splenocytes (spl) or IHLs derived mRNA by RT-PCR and subsequent sequencing of the obtained products (as in Fig. 20). RT-PCR products were sequenced in both forward and reverse directions. When possible, a representative example is shown. Below the representative example, how many rats were analyzed, as well as how many sequences were carried out and how many legible sequences were obtained is specified. R: junctional region. n.d.: non determined.

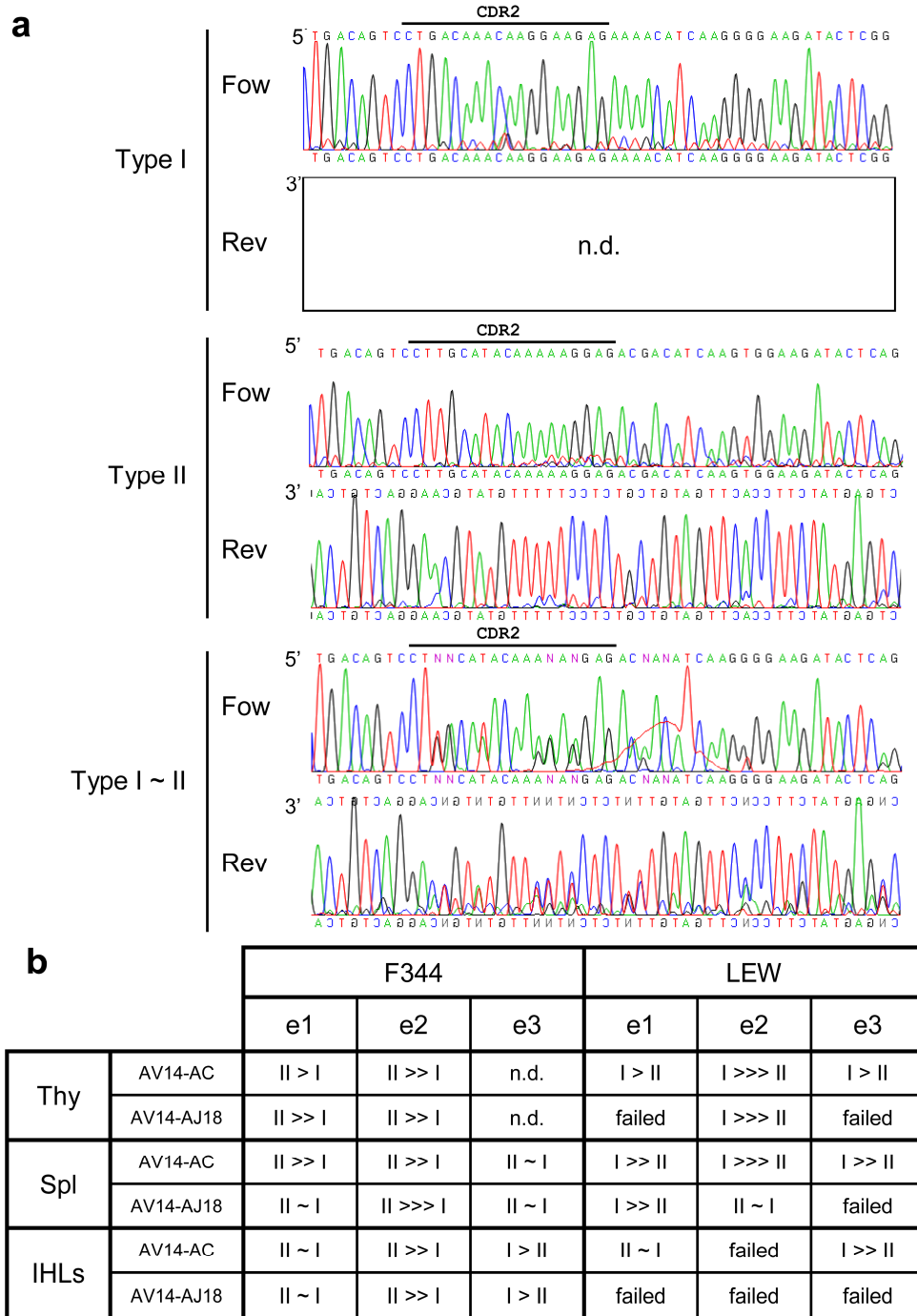


Figure 27. AV14 gene segments usage by AV14 and AV14-AJ18-containing TCR α chains. *a* Illustration of the relative quantification of the AV14 usage. AV14-AJ18 as well as AV14-AC RT-PCR products (Fig. 20) were sequenced to analyze the usage of the different AV14 segments by invariant and AV14-containing TCR α chains. Three representative examples are shown where the usage of either type I and type II or both (type I ~ II) AV14 genes predominated. RT-PCR products were generally sequenced in both, forward (Fow) and reverse (Rev), directions demonstrating that when in one particular position more than one nucleotide was detected the reason behind was not a sequencing artifact. *b* AV14 gene segment usage by invariant and AV14-containing TCR α chains of F344 and LEW thymocytes (Thy), splenocytes (Spl) and intrahepatic lymphocytes (IHLs) obtained in three independent experiments (e 1 to 3). Abundance of one or the other AV14 gene types in each particular case, when a successful sequence was obtained, was summarized with > symbols. The examples shown in *a* for type I and type II would correspond to I>>>II and II>>>I, respectively, whereas I~II was used when the signals observed were nearly equal for both AV14 types. “Failed” appears when sequencing of RT-PCR products failed.

3.7 α -Gal responsiveness in the rat

KRN7000 is a synthetic analogue of α -Galactosylceramide (α -Gal), a compound isolated from the marine sponge *Agelas mauritiauns*. Due to its origin, KRN7000 is usually referred simply as α -Gal and, as mentioned in the introduction, is the first glycolipid antigen described to be presented by CD1d and to be recognized by the semi-invariant TCR of iNKT cells (Kawano et al., 1997). α -Gal is still one of the most potent iNKT cell agonists described up to date (Venkataswamy and Porcelli, 2010). Therefore, it was used in this study to analyze iNKT cell presence among different rat strains.

3.7.1 Cytokine release in *ex vivo* cultures: Comparison of 5 different inbred rat strains

As mentioned before, a particular characteristic of iNKT cells is the very fast secretion of various cytokines. We used this property as test system for the occurrence of functional iNKT cells in 5 different inbred rat strains including F344 and LEW. Primary cultures of IHLs and splenocytes in presence or absence of α -Gal were carried out and IL-4 and IFN- γ released into the supernatants were measured after 24 hours by ELISA. In order to demonstrate that the cytokine release was due to the presentation of α -Gal by CD1d, cultures with mAb 233 were included in the assay. In addition to cultures with medium only, β -Gal was also used as negative control. Furthermore, to assess the general capacity of the cultured cells to secrete IL-4 or IFN- γ , ConA was also added to the cultures (Fig. 28).

Splenocytes and IHLs derived from F344 rats secreted IL-4 and IFN- γ in an α -Gal dose- and CD1d-dependent manner. Considering the different cell densities of splenocyte- and IHL-cultures, 10^7 and $2.5 \cdot 10^6$ cells/ml, respectively, cytokine release by IHLs was much higher than by splenocytes, as expected from the different frequencies of iNKT cells detected in these organs (Results section 3.5.1). Remarkably, the IL-4 amounts secreted by splenocytes after α -Gal stimulation were approximately the same as after ConA stimulation.

In cultures of BN- and DA-derived cells, IL-4 secretion also appeared in an α -Gal dose-dependent manner and was inhibited by the anti-CD1d mAb 233, although ConA induced IL-4 production by DA cells was also partially inhibited when the mAb was added to the culture. LEW and PVG splenocytes completely lacked an α -Gal-induced IL-4 production despite the presence of cells with IL-4 secreting potential demonstrated by ConA stimulation. IL-4 production by PVG IHLs seemed to be largely α -Gal-

independent and partially inhibited by 233. Apparently, this mAb also inhibited IL-4 release by PVG IHLs after ConA stimulation.

An α -Gal-induced and CD1d-specific IFN- γ production can be clearly stated for IHL and splenocytes of F344 rats while the results for BN rats were less clear. The other inbred rat strains showed only a varying spontaneous IFN- γ production, which may have obscured an α -Gal-specific response. For all these strains spontaneous IFN- γ secretion by IHLs was at least as high as the maximum of the α -Gal-induced production by F344 IHL. The spontaneous IFN- γ release by PVG IHLs was even higher than after ConA stimulation of all the other inbred strains, except DA where it was at least as high.

Despite the strict attachment to experimental protocols, results varied considerably as indicated by the high standard deviations obtained in five independent experiments, in the case of cells without addition of the 233 mAb (Figure 28).

Cytokine release by thymocytes was also addressed at least for one rat of each strain with the same conditions as indicated above. An α -Gal response was never observed even at high cell density cultures (2×10^7 cells/ml), where after ConA stimulation at least some IL-4 production (1-10 pg/ml) was detected.

Even in F344, which is the inbred rat strain in which the highest α -Gal responsiveness was observed, iNKT cell frequencies are very low (Results section 3.5.1). Thus single-cell based techniques, which facilitate the detection of low frequencies of cytokine producing cells, were also used and IL-4 secretion after α -Gal stimulation of splenocytes and IHLs (10^6 and 2.5×10^5 cells per well, respectively) was analyzed by ELISPOT (Fig. 29). In addition to the detection of the number of IL-4 producing cells, ELISPOT results also allow the analysis of the relative levels of IL-4 secretion by determining the size of the spots. The intensity and size of the spots vary depending on the settings used to read the plate and on the duration of the incubation with the substrate reagent in the experimental procedure. Hence, the wells and the quantification of the spots according to their size are shown only for one representative experiment of each strain. The general variability between experiments is illustrated by the high SD of the total spot numbers obtained in two or more independent experiments. Moreover, the non standardized sensitivity of the method, surely contributes to this variability.

With the IL-4 ELISPOT, basically, the same α -Gal responsiveness pattern was observed as in the ELISA experiments with the exception of DA rats. A comparable size of the spots after ConA and α -Gal-induced activation was only found in F344. In this strain

the number of large spots (above -1.6 and -1.8 Log mm² for spleen and IHLs, respectively) was even higher after α -Gal than after ConA stimulation. Importantly, the 233 mAb inhibited the formation of these large spots in α -Gal but not ConA cultures. In the experiment shown 270 and 117 big-sized spots (above -2.2 Log mm²) were found among α -Gal-stimulated IHLs and splenocytes, respectively. Emphasizing the importance of the size of the spots, the total number of the spots was higher in splenocytes but not in IHLs cultures after α -Gal stimulation compared to β -Gal or medium only. Thus the graphics showing only the number of the spots but not the size are not sufficient to interpret the results in these assays (Fig. 29).

A response such as that of F344 rats was not observed among any of the other inbred rat strains. Only cell cultures from BN rats showed an increase above the background (obtained with β -Gal or only media) in the number of relatively-big spots after α -Gal stimulation which disappeared when the 233 mAb was added. In contrast, in LEW and PVG cultures, the spots obtained after α -Gal stimulation were not more abundant or bigger than the spots observed in cultures where β -Gal or no antigen was added. Nonetheless ConA-stimulated splenocytes cultures contained a considerable amount of IL-4 secreting cells. Among IHLs, a high number of cells producing IL-4 was observed in a non-specific manner.

In DA-derived ELISPOT assays, in contrast to the results obtained by ELISA, the number of IL-4-secreting cells and sizes of the spots after α -Gal stimulation were not higher than in β -Gal or only media cultures. Moreover, IL-4 secretion of IHLs was in one case even reduced when the cells were incubated with α -Gal compared to β -Gal or only media (Fig. 29), while in another experiment the response of all three culture conditions was similar (not shown). In BN cultures the number of cells producing small amounts of IL-4 appearing in ConA stimulations was reduced when the 233 mAb was added. This mAb also inhibited the ConA response of DA splenocytes.

Thymocytes (1.5×10^6 cells / well) derived from F344 and LEW rats were also analyzed in ELISPOT assays. IL-4 secreting cells were completely absent in α -Gal stimulations. Nonetheless a very low but constant number of spots were observed in both strains after ConA stimulation: 4 and 13 in F344 and 12 and 8 in LEW thymocytes. The secretion of IL-4 by these cells was not inhibited by the 233 mAb (data not shown).

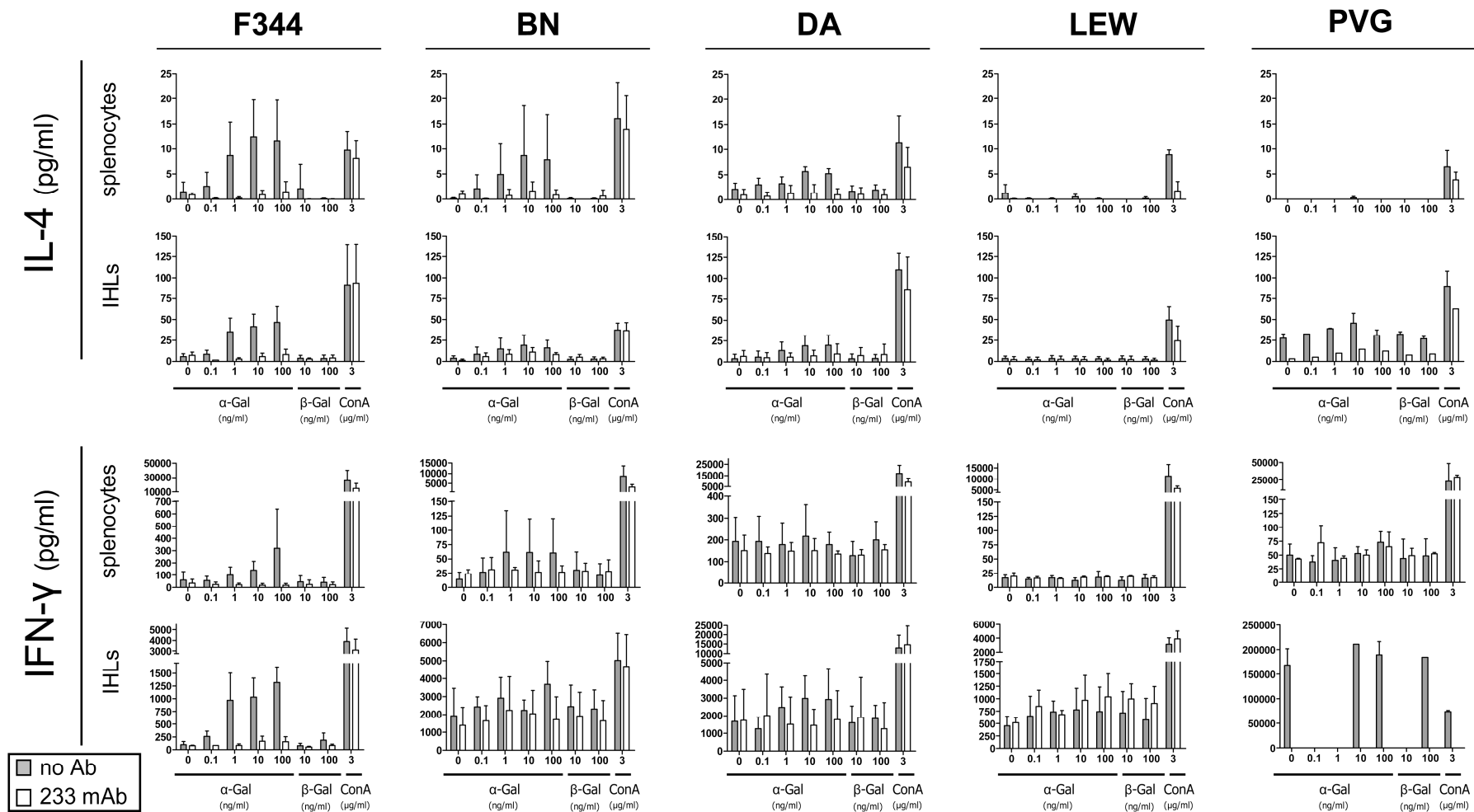


Figure 28. IL-4 and IFN- γ release by splenocytes and IHLs. 2×10^6 splenocytes or 5×10^5 IHLs from five different inbred rat strains were cultured in 96 well plates with α -Gal, β -Gal or ConA at the indicated final concentrations for 24 hours (gray bars). Moreover, also the 233 mAb was added to each culture condition (white bars). IL-4 and IFN- γ release into the supernatant was analyzed by ELISA. The mean values obtained in three independent experiments + SD, except for PVG rats where only two experiments were performed, are shown. Duplicates were carried out when sufficient cells were isolated. The 233 mAb was included in two of three experiments.

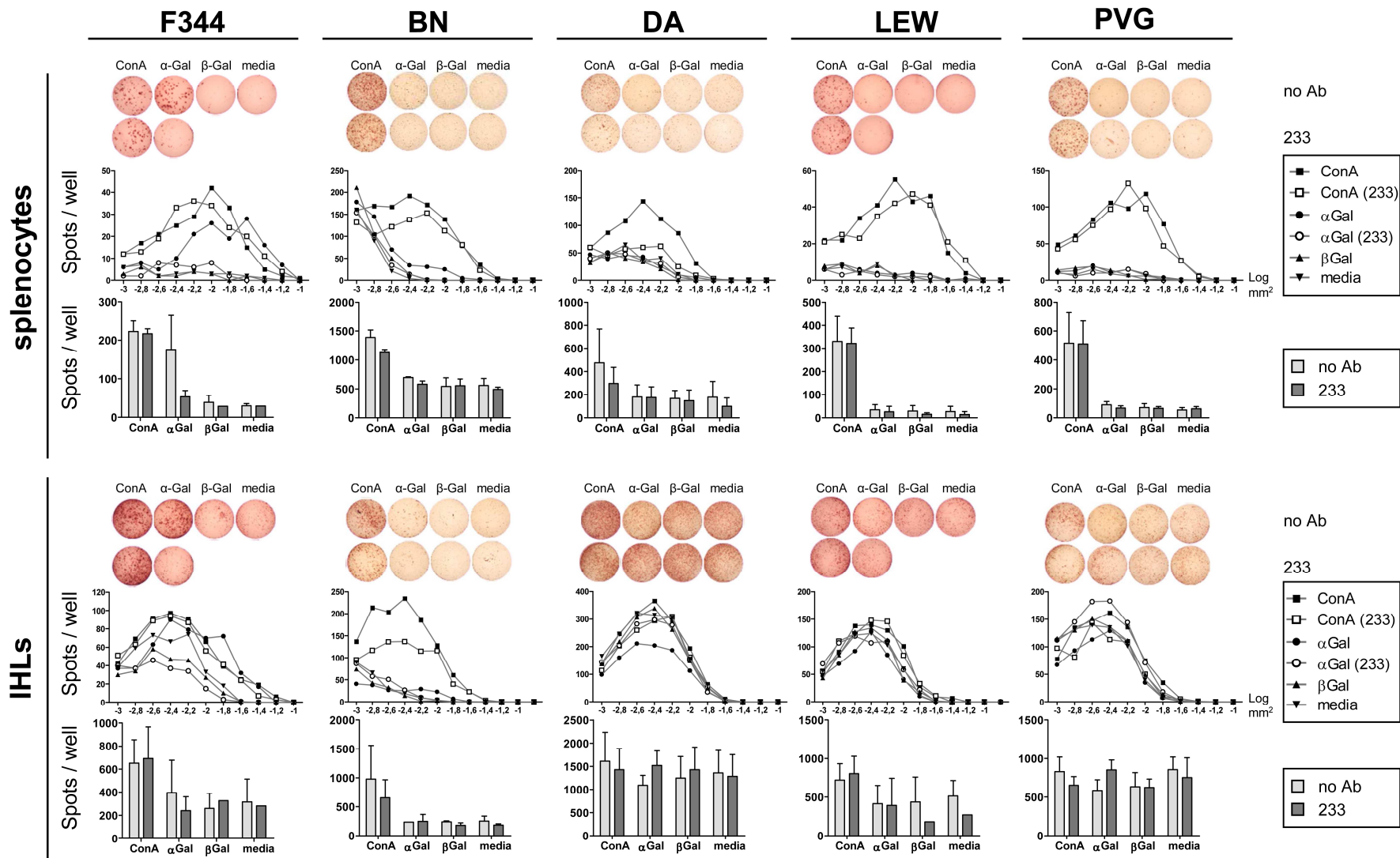


Figure 29. IL-4 ELISPOT analyses of primary splenocytes and IHLs cultures of five different inbred rat strains. 10^6 splenocytes or 2.5×10^5 IHLs from five different rat strains were cultured for 24 hours with α -Gal (10 ng/ml), β -Gal (10 ng/ml), ConA (3 μ g/ml) or only media in the presence or absence of the 233 mAb. The wells of one single experiment for each tissue and each rat strain are shown. The first row of graphs shows the number of counted spots according to their size (X axis Log mm²) in one single experiment. In addition, the mean values + SD of the total spots detected in at least two independent experiments are shown in the second graph-row (bar graphs). The number of conducted experiments is two for BN, DA and PVG; three for F344; three for LEW IHLs and five for LEW splenocytes.

3.7.2 Analysis of F344 x LEW F1 generation

Analysis of supernatants harvested from cultures of primary splenocytes and IHLs derived from F1 generations between F344 and LEW rats (2 male rats from F344xLEW, and 1 male rat from LEWxF344) revealed an α -Gal dose-dependent release of IL-4 which was CD1d-restricted (Fig. 30). A codominant, no sex-linked inheritance of the alleles controlling iNKT cell frequencies and cytokine release after α -Gal stimulations is expected because cytokine amounts were approximately half of those observed in F344 cultures and because there was no difference between the two F1 generations, regardless of the strain origin of the Y chromosome.

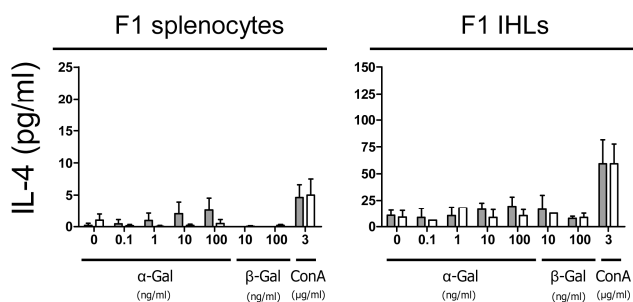


Figure 30. IL-4 release by splenocytes and IHLs *ex vivo* cultures of F344 and LEW F1 generation. 2×10^6 splenocytes or 5×10^5 IHLs were cultured in 96 well plates with α -Gal, β -Gal or ConA at the indicated final concentrations for 24 hours and IL-4 release into the supernatant was analyzed by ELISA (gray bars). Moreover, the 233 mAb was also added into each culture condition (white bars). The mean values obtained in three independent experiments + SD are shown. Duplicates were carried out when sufficient cells were isolated.

3.7.3 Analysis of C57BL/6

In order to compare rat α -Gal responsiveness to mouse, similar cultures with C57BL/6 splenocytes and IHLs (10^7 and 5×10^5 cells/ml, respectively) were carried out. Figure 31 shows that C57BL/6 derived primary cells produce much more cytokine amounts after α -Gal stimulation than rat primary cells. Having in consideration that five times less C57BL/6 IHLs than rat IHLs were used, α -Gal-dependent cytokine release by mouse IHLs is about 50 fold higher than that of F344 IHLs. C57BL/6 splenocytes produce also much more IFN- γ than F344 splenocytes.

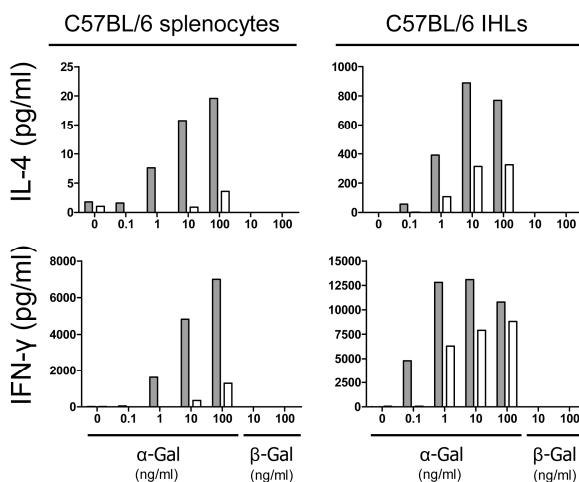


Figure 31. Cytokine production in *ex vivo* cultures of splenocytes and IHLs from C57BL/6 mice. 2×10^6 splenocytes or 10^5 IHLs were cultured in 96 well plates with α -Gal, β -Gal or ConA at the indicated final concentrations for 24 hours. IL-4 and IFN- γ release into the supernatant was analyzed by ELISA (gray bars). Moreover, the 233 was also added into each culture condition (white bars). The values obtained in one single experiment are shown.

3.7.4 iNKT cell expansion in F344 but not in LEW and C57BL/6 IHL-cultures

IHLs derived from F344 and LEW rats or from C57BL/6 mice were cultured with different stimuli (ConA, α -Gal, β -Gal or no stimulus) for 7 days. After this time, apart from ConA cultures, a clear population of large, granular cells appeared exclusively in F344-derived IHLs incubated with α -Gal (Fig. 32). These cells express NKR-P1 and low TCR levels in contrast to the small-sized T cells that are also present in these cultures and in the cultures with β -Gal or without stimulus. Cultures with 3 μ g / ml ConA were used as positive control for activated T cells.

NKR-P1⁺ and TCR-low cells are stained with α -Gal-loaded rat CD1d-IgG dimers, as shown in figure 33, but not by α -Gal-loaded mouse CD1d-IgG dimers. As illustrated in the histogram of Fig. 33, most of the cells are stained by α -Gal-loaded rat CD1d-IgG dimers, although the staining intensity of many cells is not very high. Therefore, in contrast to primary cells (Results section 3.4.4), TCR and NKR-P1 are suitable markers for the identification of rat iNKT cells in rat IHLs cultures.

About 50 percent of F344-cultured iNKT cells express the BV8S4^a gene segment, whereas none of them expresses BV16 (Fig. 34). Moreover, most of them are CD4 and CD8 β negative in contrast to the T cells present among the gate of small-sized cells, whose CD4 and CD8 β distribution is the same as in primary T cells (Fig. 34 and 37).

The presence of iNKT cells after seven days of culture with α -Gal is due to an expansion because the initial number of iNKT cells added to the cultures was about 3000 cells per well (0.03 % of the total IHLs) and the number of living cells recovered at the end of the culture was 30000 to 300000 and about half of them were iNKT cells.

Although it is not shown, the AV14 gene segment usage of F344 expanded iNKT cells was also addressed in the same way as described in the results section 3.6.2. Interestingly, both types of AV14 gene segments were found after 7 days of culture with α -Gal.

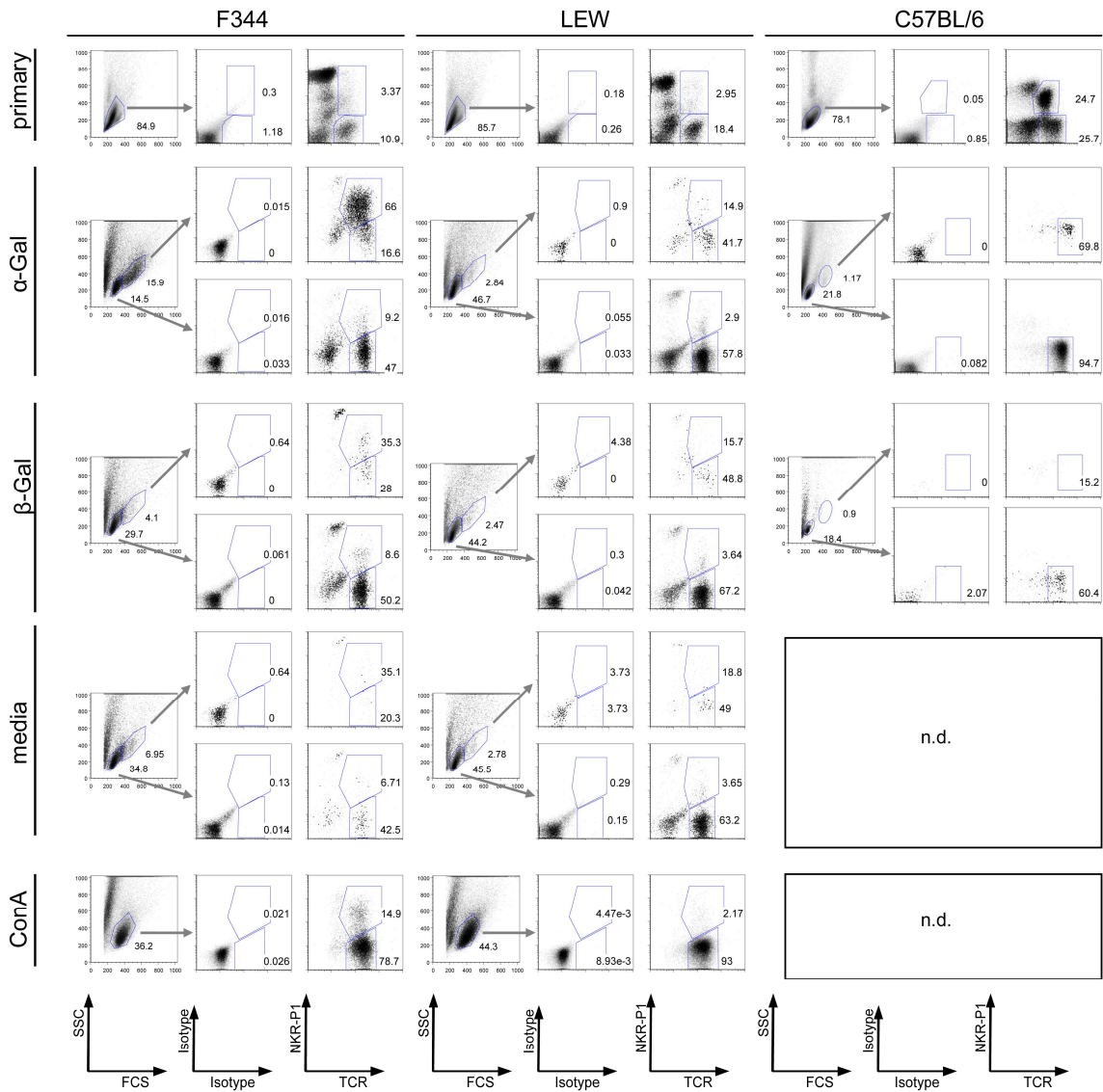


Figure 32. Primary F344, LEW and C57BL/6 IHLs cultures. IHLs derived from C57BL/6 mice, F344 or LEW rats were cultured for 7 days in the presence of α -Gal (20 ng/ml), β -Gal (20 ng/ml), ConA (3 μ g/ml) or only media and were analyzed by flow cytometry. Numbers indicate percentages of gated cells. FCS/SSC plots, show characteristics of the cultured cells and depict the gated cells for which TCR and NKR-P1 expression was analyzed. Gray arrows indicate gated cells shown in the subsequent TCR/NKR-P1 plots. Cells were stained with anti $\alpha\beta$ TCR (R73) visualized with $\Delta\alpha$ M-FITC and with anti NKR-P1 (10/78-PE). Isotype control stainings were included.

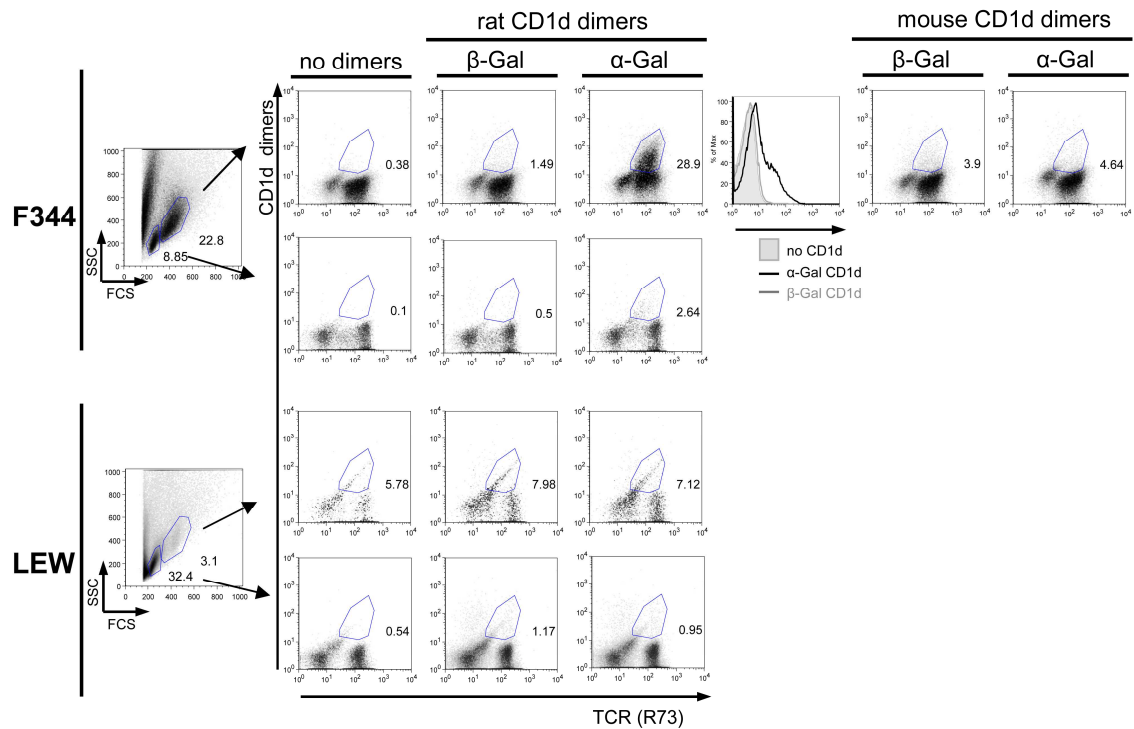


Figure 33. After culture in the presence of α -Gal iNKT cells are expanded when primary IHLs are derived from F344 but not from LEW rats. After 7 days of culture with 20 ng/ml α -Gal, intrahepatic lymphocytes from F344 and LEW rats were analyzed by flow cytometry. Cells were stained with anti-TCR β mAb (R73-FITC) and α -Gal- or β -Gal-loaded rat CD1d-IgG dimers, which were visualized with D α M-PE. F344 cells were also stained with mouse CD1d-IgG dimers. In F344, but not in LEW cultures two different populations based on their FSC/SSC properties were clearly distinguished (FSC/SSC plots). Dimer and TCR stainings are shown separately in the density plots for each population, as it is pointed out by the arrows coming out of the FSC/SSC plots. The histogram on the upper right shows all the dimer stainings of the big-sized cells observed in the F344 cultures.

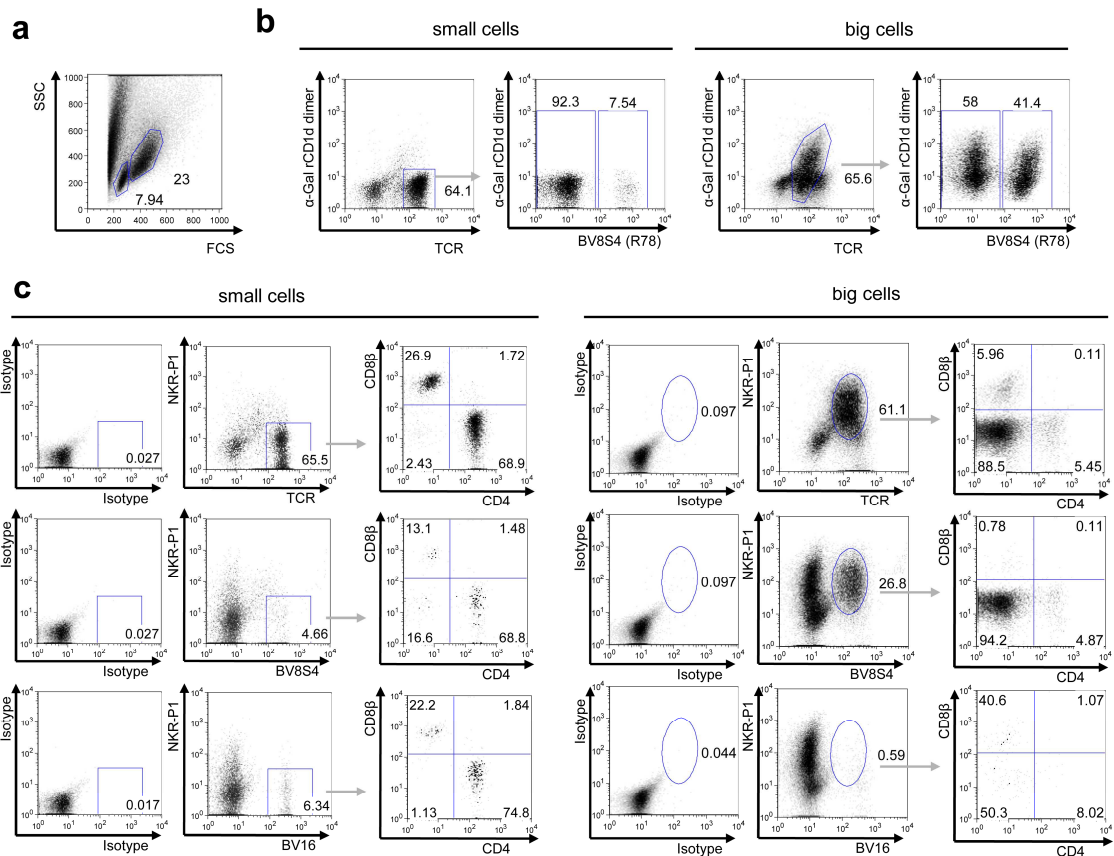


Figure 34. BV usage and CD4/CD8 β distribution among cultured iNKT cells. Cultured F344 iNKT cells were analyzed by flow cytometry. Numbers indicate percentages of gated cells depicted in the dot plots. Gray arrows indicate gated cells shown in the subsequent dimer/BV8 (*b*) or CD4/CD8 β (*c*) plots. *a* The FCS/SSC plot depicts the gating strategy followed to analyze BV usage by the two different cell populations - labeled as small and big cells - which appeared in 7 day α -Gal F344 IHLs cultures. *b* Analysis of BV8S4^a usage. Cultured cells were stained with α -Gal-loaded rat CD1d-IgG dimers (detected with DaM-PE) followed by anti-TCR β (R73-FITC) and biotinylated anti-BV8S4^a (R78, visualized with SA-APCy) mAbs. *c* Analysis of BV usage. Cells were stained with unconjugated antibodies against TCR β (R73), BV8S4^a (R78) or BV16 (HIS42) which were visualized with DaM-FITC and with anti-NKR-P1 (10/78-PE), anti-CD4 (OX-35-Cy5PE) and anti-CD8 β (341-bio + SA-APC) mAbs. Isotype control stainings were included.

3.8 Analysis of NKR-P1 and TCR expression in different rat strains

In the results section 3.4.4 it is shown as in contrast to some mouse strains (e. g. C57BL/6), where most of NK1.1⁺ T cells are iNKT cells (Hammond et al., 2001; Matsuda et al., 2000), in the rat only a minor part of all NKR-P1⁺ TCR⁺ cells are iNKT cells, what is similar to the situation found in humans. Indeed in F344, the strain with the strongest α -Gal-induced cytokine secretion and therefore the strain where the highest number of iNKT cells is expected, only 3% NKR-P1⁺ TCR⁺ splenocytes and 5 to 10% of NKR-P1⁺ TCR⁺ IHLs are iNKT cells (Fig. 35). From all the strains in which the response to α -Gal was investigated (Results section 3.7.1), iNKT cell frequencies were only addressed in F344 and LEW. This results section summarizes our analysis of

NKR-P1 expression as well as the frequencies of certain BV gene segments used by different T cell subsets. This analysis also served to gain more information about the cells added to the cultures described in the results section 3.7.

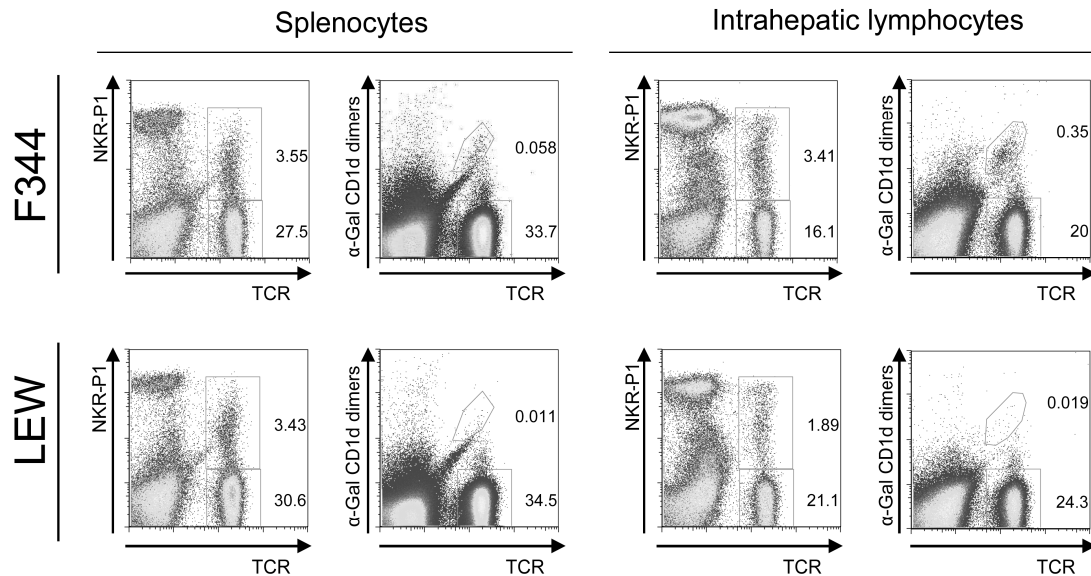


Figure 35. iNKT cells are a very small population compared to NKR-P1⁺ T cells. iNKT cells and NKR-P1 expressing T cells were analyzed by FACS among splenic and intrahepatic lymphocytes from F344 and LEW rats. iNKT cells were identified as α -Gal-loaded rat CD1d-IgG dimer⁺ TCR⁺ cells (control stainings are shown in Fig. 17). Dimer staining was revealed with D α M-PE. TCR was stained with the FITC conjugated mAb R73 and NKR-P1 was visualized with 10/78-PE labeled mAb.

3.8.1 Analysis of NKR-P1 expression among T and non-T cells

In line with the low numbers of iNKT cells among NKR-P1⁺ TCR⁺ cells in the rat, no correlation was found between the frequencies of T cells expressing NKR-P1 and the observed α -Gal response pattern (Fig. 36 and Fig. 28). These frequencies are very similar among all the strains, with the only exception of DA splenocytes. In general, the frequencies of NKR-P1 positive T cells in the liver are higher than in the spleen.

In contrast, the percentages of NKR-P1 expressing cells which are not T cells differ between these five inbred strains in the thymus and in the liver. Apart from NK cells, monocytes and some dendritic cells also express NKR-P1 at intermediate levels (Josien et al., 1997; Scriba et al., 1997). Among thymocytes, a small population expressing high levels of NKR-P1 was clearly detected in F344, DA and PVG rats. This population was much more reduced in BN and LEW (Fig. 36 and table 6). Within the isolated IHLs, F344, BN, DA and LEW have similar frequencies of cells expressing intermediate NKR-P1 levels but in PVG these cells are absent. Noteworthy, the numbers of cells expressing NKR-P1 at high levels vary between all the strains from almost 50% of all

IHLs in DA to 14% in BN rats. These differences reflect variations on the frequencies of the other cell types (Fig. 36 and table 6). Moreover, NKR-P1 expression by the cells with the highest levels also differs between the strains in the liver and in the spleen, being more reduced in BN and PVG compared to F344, LEW and DA (Fig. 36 and means of geometric MFI \pm SD in four to five independent experiments in spleen: BN: 871 \pm 203; PVG: 935 \pm 404; F344: 2087 \pm 230; DA: 1602 \pm 208 and LEW: 1926 \pm 203 and in IHLs: BN: 807 \pm 162; PVG: 542 \pm 208; F344: 1560 \pm 85; DA: 1208 \pm 415 and LEW: 1252 \pm 202).

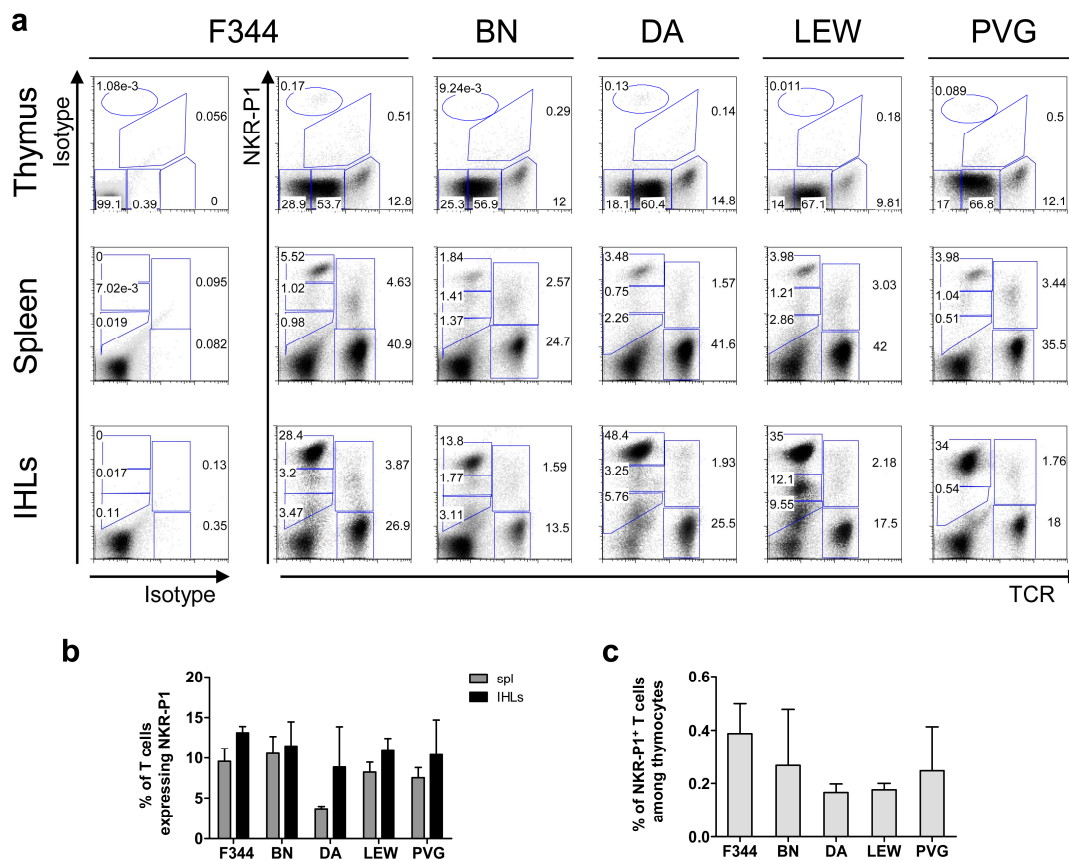


Figure 36. NKR-P1 and TCR expression by thymocytes, splenocytes and intrahepatic lymphocytes in five different inbred rat strains. *a* NKR-P1 (10/78-PE mAb) and TCR (unconjugated R73 mAb followed by D α M-FITC) expression was analyzed by FACS. Isotype controls were included, although they are only shown for F344 stainings. Different gates were set according to the various NKR-P1/TCR levels observed. Numbers indicate the percentages of the gated cells. *b* Percentages of $\alpha\beta$ T cells expressing NKR-P1 were obtained as illustrated in *a* by dividing the percentage of NKR-P1⁺ TCR⁺ cells among the total percentage of TCR⁺ cells. *c* Percentages of NKR-P1⁺ TCR⁺ thymocytes. In the bar graphs the means + SD of four to five independent experiments are shown. Unspecific stainings, determined as in *a* for F344 with isotype control antibodies, were subtracted.

	F344	BN	DA	LEW	PVG
Thymus	0.2516 ± 0.0994	0.0404 ± 0.0500	0,1220 ± 0,0277	0.0037 ± 0.0054	0.0667 ± 0.0191
Spleen	high 4.86 ± 0.60	1.92 ± 0.09	3.68 ± 0.46	3.41 ± 0.53	3.86 ± 0.77
	int 1.17 ± 0.24	1.56 ± 0.16	0.82 ± 0.19	1.00 ± 0.10	0.90 ± 0.07
	low 1.29 ± 0.33	1.28 ± 0.26	1.12 ± 0.51	2.21 ± 0.42	0.46 ± 0.1
IHLs	high 25.40 ± 2.19	14.72 ± 2.58	46.54 ± 8.12	27.26 ± 4.93	40.11 ± 5.01
	int 6.00 ± 2.58	3.84 ± 1.89	3.03 ± 1.05	6.56 ± 3.16	1.03 ± 0.43
	low 4.56 ± 1.26	5.25 ± 1.78	3.47 ± 1.39	5.77 ± 2.35	

Table 6. TCR⁺ cells expressing various levels of NKR-P1 in the thymus, spleen and IHLs of five different inbred rat strains. The means of the percentages obtained as illustrated in figure 36 *a* in four or five independent experiments ±SD are shown. Among splenic and intrahepatic lymphocytes of all the strains, except in PVG, three TCR⁺ populations with high, intermediate (int) and low NKR-P1 levels were observed. In PVG the intermediate and low NKR-P1⁺ populations could not be distinguished (Fig. 36 *a*); therefore, one gate containing intermediate and low NKR-P1 expressing cells was established.

3.8.2 CD4 and CD8 distribution among NKR-P1⁺ TCR⁺ cells

Rat iNKT cells are mostly CD4 or DN (Fig. 19). As previously described (Knudsen et al., 1997; Li et al., 2003; Matsuura et al., 2000; Pyz et al., 2006; Ru and Peijie, 2009), most NKR-P1⁺ TCR⁺ rat cells express CD8β in the spleen and in the liver of all the strains (Fig. 37 and Table 7). In F344, changes on the relative frequencies of CD4 and DN positive cells among NKR-P1⁺ TCR⁺ cells due to the presence of iNKT cells can only be expected within IHLs, where iNKT cells are about a 10% of all NKR-P1⁺ TCR⁺ cells, but not in splenocytes, where the frequency of iNKT cells is only 2% approximately of all NKR-P1⁺ TCR⁺ cells (Fig. 35). Indeed, more DN and less CD8β⁺ appear in F344 IHLs compared to splenocytes (Table 7). A significant increase of the DN NKR-P1⁺ TCR⁺ cells in IHLs compared to splenocytes was also found in BN and DA, the two other α-Gal responding inbred strains. Nevertheless, it remains to be shown whether this increase is due to augmented iNKT cell numbers. In fact in PVG rats, which did not show a clear response to α-Gal, the frequency of DN NKR-P1⁺ T cells in IHLs was also higher compared to splenocytes (although the differences are not statistically significant) (Table 7). CD4⁺ frequencies among NKR-P1⁺ TCR⁺ cells are not augmented in IHLs of any strain compared to splenocytes. Remarkably, the CD4/CD8 distribution in NKR-P1 negative T cells differs little (i. e. LEW CD8⁺ T cells and PVG CD4⁺ T cells) if at all between splenocytes and IHL from the same strain whereas the inter-strain differences can be high (Table 7).

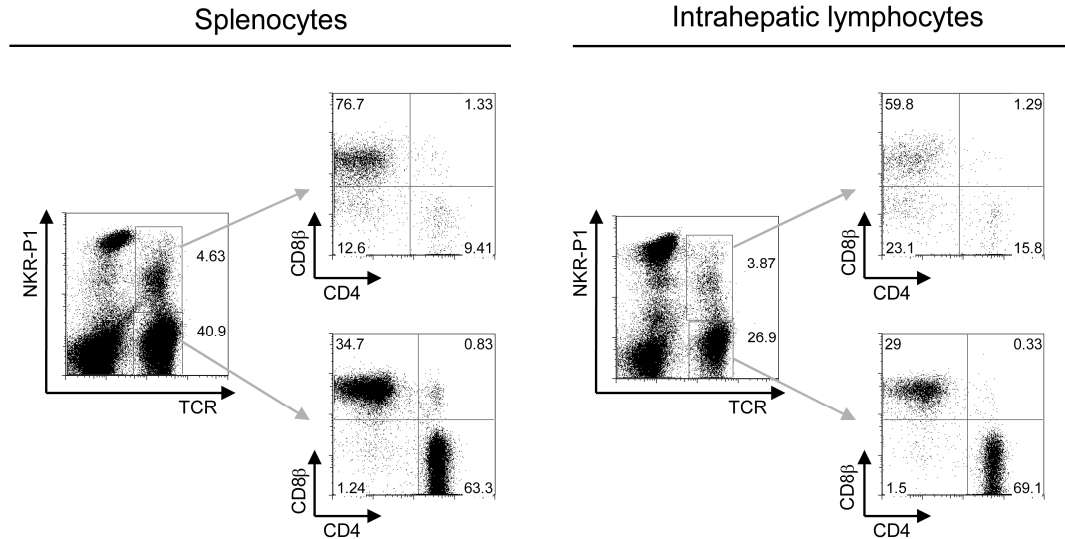


Figure 37. CD4 and CD8 β expression by NKR-P1 positive and negative F344 T cells. Lymphocytes from the spleen and the liver were analyzed by flow cytometry. CD4 (OX-35-Cy5PE) and CD8 β (341-bio + SA-APCy) expression by NKR-P1 (10/78-PE) positive or negative T cells (R73 and D α M-FITC) was analyzed by flow cytometry. Numbers inside the dot plots indicate the percentages of gated cells. Gray arrows indicate which T cell subpopulations are shown in the CD4/CD8 β plots.

		F344		BN		DA		LEW		PVG	
		Spl	IHLs	Spl	IHLs	Spl	IHLs	Spl	IHLs	Spl	IHLs
NKR-P1⁺	CD8β	71.9 ± 3.9	54.5 $\pm 4.9^{**}$	60.2 ± 3.8	51.3 ± 6.4	69.5 ± 5.8	65.8 ± 5.5	71.2 ± 7.4	68.1 ± 10.7	77.5 ± 2.1	63.3 $\pm 1.3^*$
	CD4	11.1 ± 2.5	13.5 ± 3.6	12.1 ± 3.4	15.0 ± 3.2	17.5 ± 6.7	12.6 ± 3.7	11.5 ± 5.4	12.3 ± 5.6	8.4 ± 3.0	16.4 ± 2.8
	DN	14.8 ± 2.1	30.7 $\pm 6.9^*$	26.4 ± 1.2	33.0 $\pm 5.0^*$	10.7 ± 2.8	20.3 $\pm 3.0^{**}$	15.1 ± 5.6	17.7 ± 5.6	12.0 ± 2.3	18.7 ± 2.5
NKR-P1⁻	CD8β	34.2 ± 2.3	31.7 ± 1.7	6.4 ± 0.8	6.0 ± 1.5	19.9 ± 1.3	20.9 ± 3.7	24.1 ± 0.5	22.0 $\pm 1.2^*$	13.7 ± 1.3	10.2 ± 2.5
	CD4	63.5 ± 2.0	65.8 ± 2.0	91.1 ± 0.6	91.8 ± 1.6	78.4 ± 1.2	77.1 ± 4.1	73.7 ± 0.9	75.3 ± 1.2	84.5 ± 1.6	88.2 $\pm 2.5^*$
	DN	1.3 ± 0.3	1.8 ± 0.5	1.8 ± 0.5	1.7 ± 0.5	1.3 ± 0.8	1.7 ± 0.6	1.7 ± 0.7	2.0 ± 1.0	1.3 ± 0.7	1.0 ± 0.5

Table 7. CD4 and CD8 β distribution among NKR-P1 positive and negative T cells. Percentages of CD4, CD8 β or DN cells among NKR-P1⁺ TCR⁺ or NKR-P1⁻ TCR⁺ cells were obtained after analysis of splenic (Spl) and intrahepatic (IHLs) lymphocytes as shown in figure 37 by flow cytometry. Numbers indicate the mean of three to five independent experiments \pm SD. Two-tailed paired t-test was conducted to determine significant differences in the distribution of the subpopulations in the spleen compared to the liver of each rat strain. P values * < 0.05 and ** < 0.005.

3.8.3 BV chain usage among NKR-P1⁺ TCR⁺ cells

Similar to mouse, rat iNKT cells show a bias in their BV gene segment usage, with 50% of iNKT cells being BV8S4 positive (Fig. 18). With this in mind, expression of BV8S2¹ and BV8S4^a (detected by the mAb R78 (Asmuss et al., 1996) and of BV16 (detected by the mAb HIS42 (Kampinga et al., 1989)) gene segments was analyzed among NKR-P1 positive and negative T cells in the liver and the spleen of the five studied rat inbred

strains (Fig. 38 and table 8). Only in F344 IHLs the frequency of BV8S4^{a+} cells is increased in NKR-P1A⁺ T cells compared to NKR-P1A⁻ T cells, being also the highest frequency found among all the tissues and strains.

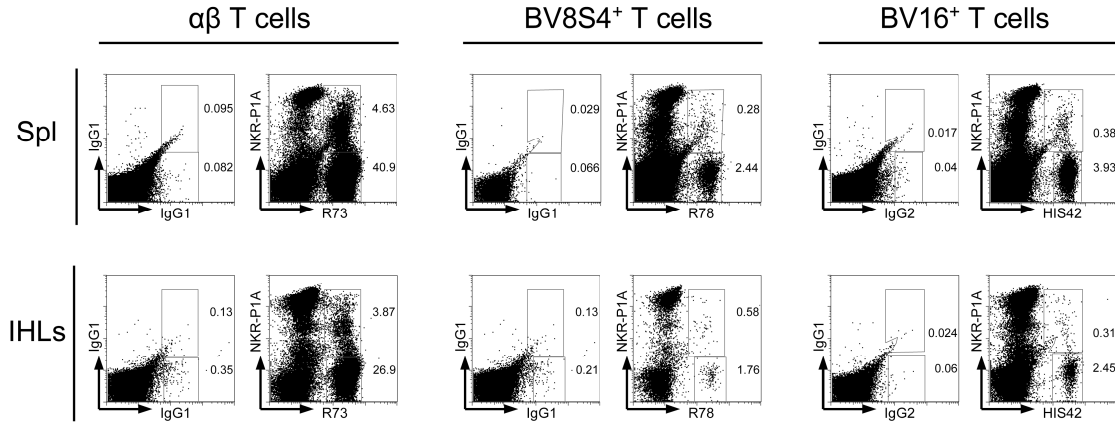


Figure 38. BV usage by NKR-P1 positive and negative F344 T cells. Lymphocytes from the spleen (Spl) and liver (IHLs) were analyzed by flow cytometry. All $\alpha\beta$ T cells were detected with the mAb R73, BV8S4^{a+} T cells were stained with the mAb R78 and BV16⁺ T cells were visualized with the mAb HIS42. The antibodies recognizing various TCRs were unconjugated and therefore were detected with D α M-FITC. NKR-P1 was analyzed with the PE labeled mAb 10/78. Isotype control stainings were included to determine unspecific binding of the antibodies. Numbers in the dot plots indicate the percentage of gated cells.

	F344 ^a		BN ^l		DA ^a		LEW ^l		PVG ^l	
	Spl	IHLs	Spl	IHLs	Spl	IHLs	Spl	IHLs	Spl	IHLs
R78⁺ among NKR-P1⁺ TCR⁺	6.0 ±1.3	13.2 ±2.8**	4.9 ±0.6	5.6 ±2.2	4.6 ±1.1**	7.0 ±1.1	4.6 ±0.5	4.9 ±1.8	4.3 ±0.7	8.4 ±4.4
HIS42⁺ among NKR-P1⁺ TCR⁺	8.0 ±0.6	6.6 ±3.7	6.4 ±1.0***	7.5 ±2.5	7.4 ±1.2	8.2 ±0.9	7.0 ±1.6*	7.9 ±1.5	10.5 ±1.0*	11.7 ±1.5
R78⁺ among NKR-P1⁻ TCR⁺	6.3 ±0.6	6.5 ±0.5	5.1 ±0.5	4.8 ±1.4	6.3 ±0.6	6.0 ±1.2	4.6 ±0.5	5.0 ±0.3	4.1 ±0.8	9.1 ±2.0
HIS42⁺ among NKR-P1⁻ TCR⁺	9.0 ±0.5	8.7 ±0.4	10.0 ±0.7	9.5 ±1.4	8.2 ±0.2	7.8 ±0.7	9.1 ±0.4	9.2 ±0.5	8.9 ±0.1	9.0 ±0.6

Table 8. R78⁺ and HIS42⁺ cells among NKR-P1 positive and negative T cells. The *Tcrb* haplotype of each inbred rat strain is indicated in their name. The mAb R78 stains BV8S4 TCR β chains of the haplotype a and BV8S2 TCR β chains of the haplotype l (Assmus et al., 1996). The mAb HIS42 detects BV16-containing TCR β chains. Splenic and intrahepatic lymphocytes from five different rat strains were analyzed by flow cytometry as shown in figure 38 for F344 rats. Numbers indicate the mean of the percentages obtained from three to five independent experiments \pm SD. Specific staining was determined after subtraction of the unspecific binding of the antibodies obtained with isotype control stainings as illustrated in figure 38. Two-tailed paired t-test was carried out to determine differences between NKR-P1⁺ T cells and NKR-P1⁻ T cells for their BV usage in each organ and each inbred rat strain. P values: * < 0.05, ** < 0.005 and *** < 0.0005

The majority of rat iNKT cells are CD4 or DN (Fig. 19), whereas conventional T cells express either CD4 or CD8 β . Therefore, the frequencies of BV8 or BV16 positive cells were also compared between NKR-P1⁺ and NKR-P1⁻ CD4 or CD8 β T cell subsets

(Table 9). Often, the frequency of BV8 positive cells among NKR-P1⁺ CD4 T cells was higher than among NKR-P1⁻ CD4 T cells. However, this increase is not restricted to subsets, tissues or strains where iNKT cells are expected to be found.

Moreover, also an increase of BV8 positive cells was found among NKR-P1⁺ CD8 β T cells compared to NKR-P1⁻ CD8 β T cells and the frequencies of T cells using the BV16 gene segment, which is not expected to be present in iNKT cells, were also higher in NKR-P1⁺ CD4 T cells than in NKR-P1⁻ CD4 T cells.

	F344 ^a		BN ^l		DA ^a		LEW ^l		PVG ^l	
	Spl	IHLs	Spl	IHLs	Spl	IHLs	Spl	IHLs	Spl	IHLs
R78⁺ among NKR-P1⁺ TCR⁺ CD8β⁺	4.9 $\pm 0.9^*$	6.0 $\pm 1.7^*$	3.1 ± 0.3	2.0 ± 0.7	3.3 ± 0.7	3.4 ± 0.8	3.5 ± 0.6	2.6 $\pm 0.9^*$	3.6 ± 0.3	3.2 $\pm 0.2^*$
R78⁺ among NKR-P1⁻ TCR⁺ CD8β⁺	3.8 ± 0.2	4.4 ± 0.6	4.3 ± 2.0	5.2 ± 4.7	3.4 ± 0.6	2.6 ± 0.5	3.9 ± 0.3	4.1 ± 0.1	3.2 ± 0.7	7.0 ± 0.7
R78⁺ among NKR-P1⁺ TCR⁺ CD4⁺	14.1 $\pm 4.7^*$	27.6 $\pm 12.2^*$	13.7 $\pm 2.7^{**}$	19.1 ± 13.2	8.4 ± 3.2	23.7 $\pm 5.6^{**}$	11.4 $\pm 3.0^*$	19.5 ± 11.2	11.2 $\pm 1.2^{**}$	15.2 ± 7.2
R78⁺ among NKR-P1⁻ TCR⁺ CD4⁺	7.4 ± 0.8	7.5 ± 0.9	4.9 ± 0.4	4.6 ± 1.2	7.1 ± 1.2	6.9 ± 1.6	4.8 ± 0.5	5.1 ± 0.2	4.1 ± 0.7	8.5 ± 2.1
HIS42⁺ among NKR-P1⁺ TCR⁺ CD8β⁺	7.6 ± 0.9	7.0 ± 2.7	4.9 $\pm 1.0^*$	4.6 $\pm 1.7^*$	6.8 ± 1.4	6.6 ± 1.4	6.3 ± 1.5	6.3 ± 1.6	9.7 ± 1.0	9.0 ± 0.8
HIS42⁺ among NKR-P1⁻ TCR⁺ CD8β⁺	7.2 ± 0.6	7.4 ± 0.4	6.5 ± 0.8	6.9 ± 1.7	7.4 ± 0.3	6.6 ± 0.8	7.2 ± 0.4	7.0 ± 0.9	9.5 ± 0.7	10.7 ± 0.7
HIS42⁺ among NKR-P1⁺ TCR⁺ CD4⁺	13.4 $\pm 1.2^{**}$	14.0 ± 7.7	13.6 ± 6.1	22.5 ± 12.1	11.6 ± 5.4	17.7 $\pm 5.0^*$	13.0 ± 7.9	15.7 ± 4.6	16.1 $\pm 1.9^{**}$	21.1 ± 9.2
HIS42⁺ among NKR-P1⁻ TCR⁺ CD4⁺	9.8 ± 0.5	9.2 ± 0.6	10.1 ± 0.8	9.7 ± 1.3	8.3 ± 0.2	8.0 ± 1.0	9.7 ± 0.5	9.8 ± 0.9	8.7 ± 0.2	8.9 ± 0.7
R78⁺ among NKR-P1⁺ TCR⁺ DN	5.5 ± 2.3	21.5 ± 4.4	4.5 ± 1.0	3.7 ± 2.4	4.8 ± 1.1	8.5 ± 5.0	4.2 ± 2.0	6.3 ± 5.4	3.5 ± 1.5	6.9 ± 3.9
HIS42⁺ among NKR-P1⁺ TCR⁺ DN	6.3 ± 1.9	4.2 ± 4.4	5.0 ± 1.0	5.4 ± 1.1	6.7 ± 2.6	7.4 ± 1.8	6.6 ± 2.9	9.1 ± 2.7	10.3 ± 1.8	10.5 ± 3.3

Table 9. Frequencies of R78⁺ or HIS42⁺ cells among the indicated T cell subsets in the spleen (Spl) or liver (IHLs). The *Tcrb* haplotype of each rat inbred strain is indicated in their name. The mAb R78 stain cells bearing BV8S4 β chains of the a haplotype and BV8S2 β chains of the l haplotype (Asmuss et al., 1996). Splenic or intrahepatic lymphocytes were analyzed by flow cytometry. Four-colour analysis and two independent probes were needed to obtain the frequencies of R78⁺ or HIS42⁺ cells among each T cell subset. In one probe, CD4 and CD8 β distribution among NKR-P1 positive and negative T cells was determined as shown in Fig 37. In the other probe, the frequencies of R78⁺ or HIS42⁺ NKR-P1 positive and negative T cells were calculated as illustrated in figure 38. Numbers shown are the means obtained in three to five independent experiments \pm SD. Variations in the frequencies of R78 and His42 positive cells between NKR-P1 positive and negative T cell subsets (CD4 and CD8 β) were analyzed conducting the two-tailed paired t-test. P values: * <0.05 , ** <0.005 and *** <0.0005 .

3.8.4 CD4 and CD8 distribution among BV8 or BV16 expressing NKR-P1⁺ T cells

CD4 and CD8 β expression by the BV8 and BV16 positive T cell subsets was also studied (Table 10). In F344 rats, BV8S4 iNKT cells constitute approximately 0.15% of all IHLs, while the percentage of BV8S4⁺ NKR-P1⁺ T cells among total IHLs is 0.44% ± 0.08 SD. In the spleen, only a 0.025% of all lymphocytes are expected to be BV8S4⁺

iNKT cells, whereas a 0.22% \pm 0.05 are BV8S4⁺ NKR-P1⁺ T cells. Having this in mind, if changes in the CD4/CD8 distribution of BV8S4⁺ NKR-P1⁺ T cells are due to the presence of iNKT cells, those should be more evident in IHLs than in splenocytes. In line with this hypothesis, the percentage of BV8S4⁺ NKR-P1⁺ T cells isolated from F344 livers which are DN is markedly increased compared to the percentage of DN cells among BV16⁺ NKR-P1⁺ T cells. In the spleen both CD4 and DN cells are slightly augmented (Table 10). Nonetheless, in all the other strains, regardless of whether they secreted cytokines in response to α -Gal *ex vivo* stimulation, also less CD8 β positive, and therefore more CD4 and/or DN, cells were found among NKR-P1⁺ T cells bearing BV8 than among BV16⁺ NKR-P1⁺ T cells.

		F344 ^a		BN ^l		DA ^a		LEW ^l		PVG ^l	
		Spl	IHLs	Spl	IHLs	Spl	IHLs	Spl	IHLs	Spl	IHLs
R78 ⁺ NKR-P1 ⁺	CD8 β	56.5 \pm 7.9*	22.4 \pm 6.8**	39.2 \pm 8.6	23.2 \pm 8.7*	52.3 \pm 13.2	32.0 \pm 6.7*	52.4 \pm 6.6*	35.8 \pm 3.1**	66.6 \pm 6.5	33.2 \pm 3.6**
	CD4	25.9 \pm 8.0	26.3 \pm 5.6	33.2 \pm 7.6	52.0 \pm 17.7	30.6 \pm 10.5	41.5 \pm 11.8	31.0 \pm 9.0	43.1 \pm 7.5**	21.3 \pm 4.5**	38.1 \pm 12.4
	DN	14.5 \pm 3.1	49.5 \pm 6.9***	24.3 \pm 3.6*	23.8 \pm 9.1	11.1 \pm 1.4	22.7 \pm 7.5	12.8 \pm 4.7	18.3 \pm 4.4	9.1 \pm 1.9	21.1 \pm 11.5
HIS42 ⁺ NKR-P1 ⁺	CD8 β	65.3 \pm 4.3	55.8 \pm 12	47.6 \pm 8.1	32.4 \pm 10.9	63.6 \pm 3.3	52.7 \pm 8.2	64.7 \pm 7.6	54.4 \pm 8.7	72.1 \pm 5.0	50.8 \pm 1.1
	CD4	18.4 \pm 2.4	27.6 \pm 8.6	27.6 \pm 6.1	40.8 \pm 10.4	23.8 \pm 4.0	26.2 \pm 8.7	18.2 \pm 6.0	22.6 \pm 4.4	13.0 \pm 5.4	29.3 \pm 7.1
	DN	12.5 \pm 1.6	14.0 \pm 4.7	22.2 \pm 2.3	24.6 \pm 7.5	9.5 \pm 3.2	18.0 \pm 3.0	13.2 \pm 2.1	20.1 \pm 6.1	11.9 \pm 2.4	17.5 \pm 5.3
R78 ⁺ NKR-P1 ⁻	CD8 β	20.8 \pm 2.8***	21.3 \pm 3.0*	5.2 \pm 1.0	6.3 \pm 4.9	10.6 \pm 1.0***	9.1 \pm 2.0***	20.3 \pm 0.7	17.6 \pm 1.5	10.6 \pm 1.2**	8.4 \pm 1.7
	CD4	74.6 \pm 3.0**	75.5 \pm 3.5	88.5 \pm 1.5*	88.5 \pm 5.7	86.6 \pm 0.6***	87.5 \pm 3.2**	76.3 \pm 1.5*	77.1 \pm 0.9	85.2 \pm 2.7	88.9 \pm 0.4
	DN	2.8 \pm 0.2	2.6 \pm 1.1	5.3 \pm 0.9*	4.5 \pm 1.0*	1.7 \pm 1.0	2.7 \pm 1.5	3.0 \pm 1.6*	4.8 \pm 2.4	3.4 \pm 2.2	1.8 \pm 0.8
HIS42 ⁺ NKR-P1 ⁻	CD8 β	27.7 \pm 2.9	27.0 \pm 2.6	4.2 \pm 0.6	4.3 \pm 1.1	18.1 \pm 1.6	17.6 \pm 2.6	19.1 \pm 0.9	16.8 \pm 2.5	14.6 \pm 1.2	12.0 \pm 3.3
	CD4	69.3 \pm 2.4	69.9 \pm 3.3	91.7 \pm 2.6	93.5 \pm 1.6	80.1 \pm 1.4	79.0 \pm 1.5	78.9 \pm 0.9	79.6 \pm 3.4	82.6 \pm 2.4	85.9 \pm 3.3
	DN	2.0 \pm 0.9	2.2 \pm 1.1	3.1 \pm 1.3	1.7 \pm 0.7	1.2 \pm 0.5	2.9 \pm 1.3	1.4 \pm 0.6	3.0 \pm 3.0	1.8 \pm 1.1	1.3 \pm 0.4

Table 10. CD4 and CD8 β distribution in R78⁺ or HIS42⁺ NKR-P1 positive and negative T cells. Splenic (Spl) and intrahepatic (IHLs) lymphocytes were analyzed by flow cytometry as shown in figure C but with R78 (anti-BV8S4^a and anti- BV8S2^l) or HIS42 (anti-BV16) unconjugated mAbs instead of R73. Shown are the means obtained in three to five independent experiments \pm SD. Changes in the CD4/CD8 β distribution between BV8 and BV16 T cell subsets were analyzed using the two-tailed paired t-test. P values: * $<$ 0.05, ** $<$ 0.005 and *** $<$ 0.0005.

4 DISCUSSION

4.1 Further characterization of CD1d monoclonal antibodies

Previous knowledge about rat CD1d expression was based on experiments using RT-PCR, in situ hybridization or polyclonal antiserum, but the analysis of rat CD1d protein with specific monoclonal antibodies was still pending (Ichimiya et al., 1994; Kasai et al., 1997). To this end, five hybridomas (232, 233, 244, 35 and 58) derived from CD1d^{-/-} mice immunized with rat CD1d transductants had been generated which produced such monoclonal antibodies (Pyz, 2004). These antibodies have been characterized in greater detail in this study.

The analysis of the variable regions of the IgG2a heavy and kappa light chains (when possible) revealed that on the one hand, the 232 and 233, and on the other hand, the 244 and 58 hybridomas secreted antibodies encoded by the same rearranged Ig genes. Since all hybridomas were generated in the same fusion and single cell cloning of the hybridomas was carried out, it seems likely that those with the same rearranged Ig genes arose from an expanded B-cell clone. Nonetheless, descentance from the same hybridoma cannot formerly be ruled out.

Unfortunately, although the 232 and 233 antibodies comprised kappa light chains, as demonstrated with the kit used to determine their isotype, no PCR product was obtained for the light chain of these hybridomas with the universal primers used to amplify the kappa light chains of the other hybridomas. These forward universal primers contained a mixture of sequences of the FR1 regions of the IGLKV gene segments most commonly used in the mouse based on the Kabat-Wu database book (Wang et al., 2000). Nonetheless, it is still possible that a sequence which anneals to the particular V gene segment comprised in the 232 and 233 light chains is not present among the degenerated primers, and that therefore, no PCR product was obtained.

As mentioned in the results section 1.1, in flow cytometry experiments the mAbs 233 and 35 recognized mouse CD1d1 on transduced cells or thymocytes with the same efficacy as rat CD1d while, the mAb 58 only showed such cross-reactivity for mouse CD1d-expressed by transduced cells but not for CD1d positive primary mouse cells. In accordance with their CD1d specificity, both 233 and 35 mAbs precipitated two chains of molecular weight corresponding to the heavily glycosylated mature CD1d molecule and the non-covalently bound β 2-microglobulin, respectively, from primary rat and

mouse thymocytes as well as from rat and mouse CD1d-transduced Raji cells. mAb 58, in line with the results obtained by flow cytometry, precipitated rat CD1d from transduced and primary cells but mouse CD1d1 only from transduced cells. The reduced ratio of precipitated β 2-microglobulin to CD1d heavy chain found for 58 compared to the other two mAbs, might reflect a preferential binding to a β 2m independent form of CD1d. Such β 2m-independent forms have been previously described in mouse and humans (Amano et al., 1998; Blumberg et al., 1991; Kim et al., 1999). However, another possibility is that the interaction of the 58 mAb with CD1d somehow displaces the bound β 2-microglobulin, resulting in the preferential precipitation of single CD1d heavy chains.

The different reactivity of the 58 mAb depending of which cell type expresses mouse CD1d is not yet understood. In contrast to 233 and 35 mAbs, the epitope recognized by mAb 58 was disrupted under denaturing conditions in Western blot experiments, indicating that this mAb is more sensitive to changes in the tertiary structure of CD1d than the other two mAbs. Thus, subtle differences in the tertiary structure between transduced and primary cells could be the cause of the distinct reactivity of mAb 58. The binding of the 233 and 35 mAbs to CD1d in Western blot demonstrated the localization of both epitopes to the heavy CD1d chain. Both mAbs bound much more efficiently to CD1d molecules which had been separated by SDS-PAGE under non-reducing compared to reducing conditions, probably reflecting the importance of the intramolecular disulfide bridges in the conservation of the epitopes. The slightly higher mobility of the CD1d heavy chain separated by SDS-PAGE under non-reducing compared to reducing conditions is probably a consequence of the more compact structure maintained by the intact intramolecular disulfide bridges. Both mAbs recognized only mature forms of the CD1d molecules, since no bands were observed where immature CD1d proteins are expected (as it has been shown for human CD1d at 37 or 30-35 kDa under reducing and non-reducing conditions, respectively (Kim et al., 1999)). To our knowledge this is the first demonstration of IgG mAbs binding to mouse or rat CD1d heavy chain in a Western blot.

Titration of the antibodies in flow cytometry experiments revealed that the avidity of mAb 35 was 3- to 5-fold higher than that of 233 and that both mAbs bound rat CD1d and mouse CD1d1 to the same extent (data not shown generated by S. Schweigle and L. Starick). This was in contrast to the results observed in Western blot (Fig. 2), immunohistology (not shown) and sometimes also immunoprecipitation where 233 was

superior to 35 and where binding to rat CD1d was more efficient than to mouse CD1d1. These findings suggest that the 233 epitope is more resistant to denaturation than the 35 epitope and also that denaturation affects more the epitopes recognized in mouse CD1d1 than in rat CD1d. Nonetheless, it remains to be investigated, whether these differential binding efficacies result from protein denaturation and/or effects of detergents or alcohols on CD1d-bound lipid-containing antigens.

Analysis of 233 and 35 mAb reactivities against various CD1d transductants allowed a partial mapping of the epitopes as discussed in the results section. The mAb 233 is likely to bind to an area above the β 2-microglobulin where the ends of the α 1 and α 2 helices meet, as demonstrated by the lack of binding of the mCD1dD93A mutant. Thus it was surprising that mCD1d2 staining by 233 was also severely impaired, since the aspartic acid at position 93 is conserved. This loss of the 233 epitope in mCD1d2 could be due to several unique substitutions but it is worth noting that the positively charged arginine at position 21 (indicated as blue spheres in Fig. 3), close to the negatively charged aspartic acid 93, is substituted by a hydrophobic isoleucine in mCD1d2. This substitution may either directly induce a conformational change of the aspartic acid at position 93 thereby disrupting the 233 epitope or directly affect the contact with the antibody. The epitope recognized by the 35 mAb could only be mapped to the α 1 domain and the first 26 amino acids of the α 2 domain of mouse CD1d1 because it is conserved in mouse-human CD1d chimeras but it is lost in human-mouse CD1d chimeras. The binding of 35 mAb to the mouse/human chimera was reduced compared to complete mCD1d1 molecule but this reduction was also observed with other mAbs (233 and 1B1, Fig. 3). These findings together with the fact that EGFP levels are very similar between the cell lines expressing these CD1d variants suggest that the lower binding of the 35 mAb to the m/h chimera is the result of a reduced cell-surface expression of the m/h chimera compared to the intact molecule rather than from a contribution to the 35 epitope of the non-conserved residues of the mouse CD1d1 C-terminal part. Nevertheless, the aspartic acid 93 can be excluded to be part of the 35 epitope since this mAb stained sCD1d- and mCD1d1D93A-transduced cells (Fig. 3).

233 and 35 binding to distinct non-overlapping epitopes allowed the establishment of a Sandwich ELISA which was routinely used to monitor concentrations of CD1d during preparation and purification of recombinant CD1d molecules. Similar to Western blot and immunohistochemistry analyses, the detection of mouse CD1d was less efficient than the detection of rat CD1d in this Sandwich ELISA. The samples analyzed with this

technique contained CD1d molecules which were either secreted forms of CD1d (e.g. CD1d-IgG dimers) or cell lysates where cell membranes had been disrupted by the use of detergents. The binding capacities of the antibodies may differ depending on whether the CD1d molecules have a soluble or a membrane-bound form. Thus it is possible that the recognition of mouse CD1d in such a soluble form by these mAbs is more affected compared to rat CD1d.

4.2 CD1d in the hematopoietic system

The 233 and 35 mAb allowed not only the analysis of CD1d protein expression in the rat but also the direct comparison to mouse, where CD1d expression in the hematopoietic system has been largely studied (Brossay et al., 1997; Park et al., 1998; Roark et al., 1998). Moreover, binding of both mAbs to different epitopes further validated results, e.g. determination of tissue distribution, where a cross-reactivity of both mAbs with an unknown tissue antigen would be most unlikely.

Among different inbred rat strains, CD1d expression levels at the cell surface of splenocytes, thymocytes and PBMCs were nearly the same, demonstrating that the two rat CD1d alleles identified in this study did not show different expression patterns at the cell surface. Only among IHLs from DA and PVG, more cells with elevated CD1d levels appeared compared to the other inbred rat strains. It remains to be determined whether this is due to an increase in the frequency of a particular cell type with high CD1d levels.

CD1d expression at the cell surface of hematopoietic cells is also remarkably similar between rat and mouse. The only notable difference between these species was found among CD4 and CD8 peripheral T cells. In the rat, both subsets express similar CD1d levels whereas in the mouse, CD4 T cells express higher CD1d levels than CD8 T cells. Nonetheless, the difference is rather small and a physiological role for CD1d on mature T cells still has to be described.

The nearly identical expression among thymocytes, where CD1d selects iNKT cells (Wei et al., 2005) is of special interest because their level of CD1d considerably affect NKT cell frequency and state of activation (Zimmer et al., 2006). Since CD1d levels are also practically the same between the rat and mouse in other cells for which a role for CD1d has been established in the mouse i. e. APCs, B cells and MZ B cells (Brigl and Brenner, 2004), no qualitative differences are expected between the CD1d-restricted

immune responses of these two species. If in contrast differences appear, those should not be intrinsic to variations in CD1d expression on hematopoietic cells.

Apart from being used to identify MZ B cells in the mouse, CD1d serves also as a marker to distinguish between other B cell subsets (Mizoguchi et al., 2002; Yanaba et al., 2008). With 233 and 35 mAbs we can investigate now whether these distinct B cell populations are also present in the rat with the same CD1d expression patterns.

4.3 CD1d in non-lymphatic tissues

Similar to previous studies using polyclonal antiserum, *in situ* hybridization and RT-PCR in the rat (Ichimiya et al., 1994; Kasai et al., 1997), CD1d protein was also found with the 233 and 35 mAbs in non-lymphatic organs as the liver, heart, intestine and pancreas. Here, in contrast to the hematopoietic system, CD1d distribution varies enormously between different cell types and in some cases also between mice and rats.

CD1d present at the cell surface of any cell may display endogenous or exogenous lipids. Endogenous lipids vary between different cells as well as between different activation states of the same cells, as shown for example by the production of charged β -linked glycosphingolipids (which will activate iNKT cells) by dendritic cells which sense danger signals through TLR-9 (Paget et al., 2007). Thus in a similar way, CD1d present in non-hematopoietic cells may warn the immune system of changes by presenting certain lipids which activate CD1d-restricted T cells.

CD1d protein was detected in the serum of different inbred rat strains by CD1d Sandwich ELISA. To assure the specificity of these measurements, further controls are necessary, as for example the analysis of serum of CD1d knockout mice. Assuming that the presence of CD1d in the serum is indeed specific, it would be interesting to learn about its source and whether it is soluble and/or it is contained in lipidic membranes of vesicles such as exosomes.

The vast expression of CD1d in rat exocrine cells in the pancreas and small intestine and its biological implications are intriguing, therefore these tissues were also analyzed in the mouse. Several studies addressing CD1d expression in the mouse small intestine with different mAbs have not lead to a general consensus about its cellular distribution (Brigl and Brenner, 2004). Terhorst and colleagues detected CD1d protein expression in epithelial cells such as enterocytes was with a rat IgM antibody (1H1); in contrast, Kronenberg et al. found these cells to be negative for the staining with the rat anti-mouse CD1d IgG mAb 1B1 (Bleicher et al., 1990; Brossay et al., 1997). In spite of

these opposite findings, a recent study by Blumberg and colleagues has demonstrated the importance of CD1d expression for gut function since intestinal colonization with pathogenic and non-pathogenic bacteria was increased in CD1d-deficient mice compared to wild type mice (Nieuwenhuis et al., 2009). An essential cell type in controlling intestinal homeostasis are Paneth cells, in which CD1d mRNA has been detected by *in situ* hybridization in mice and rats (Kasai et al., 1997; Lacasse and Martin, 1992). Localized at the bottom of the crypts of Lieberkühn, these specialized cells control the microbiota content by secreting antimicrobial peptides (defensins) to the intestinal lumen. Interestingly, Blumberg and colleagues also showed that in CD1d knockout mice, compared to wild type, the morphology and content of the secretory granules of the Paneth cells were altered, and more importantly, that the degranulation activity of these cells was defective (Nieuwenhuis et al., 2009).

Using the 233 and 35 mAbs we found that among the different types of epithelial cells in the mouse none of our antibodies stained CD1d in enterocytes, although detection of CD1d in other epithelial (e.g. enteroendocrine cells) and non-epithelial (e.g. cells of the lamina propria) cells was possible. Therefore, if there is any expression of CD1d by mouse enterocytes its level must be very low. Importantly however, the mAbs served to detect CD1d protein in mouse Paneth cells for the first time.

In contrast, in the rat ileum CD1d was broadly detected being expressed by most of the different cell types including all intestinal epithelial cell types; among which, the outstanding levels found in Paneth cells are remarkable. As mentioned above, CD1d expression in the rat ileum had previously been addressed using a polyclonal antiserum and *in situ* hybridization (Ichimiya et al., 1994; Kasai et al., 1997). In this study high levels of CD1d mRNA were found in Paneth cells as well, but the polyclonal antiserum failed to detect protein in this cell type.

The physiological function of CD1d in Paneth cells remains unclear, but there are several possible biological processes in which it might be involved. On the one hand, since it also has been shown that degranulation of Paneth cells could be triggered *in vivo* after injection of α -Gal and *in vitro* after stimulation with α -Gal and iNKT cells (Nieuwenhuis et al., 2009), it is tempting to speculate that CD1d on Paneth cells may present activating antigens to CD1d-restricted T cells, which in turn could trigger directly or indirectly the degranulation and secretion of antimicrobial peptides to the intestinal lumen by the antigen presenting Paneth cells.

On the other hand, a T cell-independent function of CD1d in the secretion process of this specialized cell type appears also possible. Two observations support the latter view: first, as mentioned before, CD1d-deficient Paneth cells show an altered content and morphology of their granules compared to wild type cells (Nieuwenhuis et al., 2009), indicating a contribution of CD1d to the formation of the exocrine granules of Paneth cells, and second, CD1d was mainly detected in apical granules (Fig. 12 *d*) but not in basolateral membranes where it would be more accessible to T cells. In addition, it has been shown that cross-linking of human CD1d with mAbs induce intracellular signals and provoke cytokine production (Colgan et al., 1999; Yue et al., 2005), implying that clustering of CD1d molecules either by reactive TCRs or by other yet unidentified molecules can result in intracellular signaling events.

The histological finding of an unexpected vast CD1d expression in rat pancreatic exocrine acinar cells is not only supported by Western blot and ELISA analyses of pancreatic extracts, but also by two independent proteomic analyses which also identified CD1d in rat pancreatic exocrine granules (Chen et al., 2006; Rindler et al., 2007). Surprisingly, such expression was not found in mouse pancreas. The slightly lower apparent molecular weight of the rat pancreatic CD1d compared to that from extracts of spleen or thymus could indicate a different processing during intracellular maturation e.g. proteolytic cleavage of membrane bound material or the generation of a truncated form. Since the staining observed in the acinar cells was localized to the mature exocrine granules, it is tempting to speculate about a soluble CD1d which might be secreted into the intestinal lumen together with other pancreatic products. A potential function of this soluble CD1d might be the sampling of microbial glycolipids in the intestinal lumen - helped by the low pH of the duodenum - and the transport to various cells of the intestine. Another option inspired by the human CD1e, which is cleaved resulting in a soluble form that facilitates glycolipid processing by α -mannosidase (Angenieux et al., 2000; de la Salle et al., 2005) and by other proteins secreted by the pancreas (e.g. lipase) could be the participation in intestinal lipid processing and absorption. Since CD1d was also found in some endocrine cells and in exocrine granules of rat parotid glands (Steiniger, Monzon-Casanova, Herrmann; data not shown), this repeated localization of CD1d in secretory granules might indicate, as mentioned before for Paneth cells, a role of CD1d in the exocytosis process of certain cell types.

A functional specialization of the different CD1 isoforms is indicated by their differential intracellular localization and specificity in antigen-binding, or as in the case of CD1e, by the identification of functions distinct from direct presentation of antigens to TCRs. Interestingly, although a substantial variability has been found between number and types of CD1 isoforms in different clades of placental mammals, complete CD1 deficiency has not been reported yet (Kasmar et al., 2009). This, not only supports the idea that CD1 molecules fulfill essential biological functions, but also implies that the function of CD1 isoforms may vary between species and that to some extent CD1 isoforms could substitute each other. In muridae CD1d is the only CD1 isoform. Therefore, one may speculate a need for “multitasking” of CD1d in these species. Such a requirement may explain the – in comparison to humans – less restricted intracellular distribution and tissue expression (Brigl and Brenner, 2004).

4.4 Rat CD1d as antigen presenting molecule

An α -Gal response of rat primary cells has previously been shown in our laboratory by E. Pyz and colleagues (Pyz et al., 2006). Here we have demonstrated the CD1d dependence of such a response, since the 233 and 35 monoclonal antibodies efficiently inhibited cytokine release after α -Gal activation of rat and mouse primary cells. These results are consistent with mapping the 233 epitope to the loop connecting the α 1 and α 2 domains of the CD1d at the side of the F' pocket, because it is this side of the CD1d molecule where in the three dimensional structure, the semi-invariant NKT TCR contacts α -Gal/CD1d complexes (Borg et al., 2007).

Now these mAbs provide also the tool to investigate *in vivo* CD1d-restricted responses in the rat, what in contrast to the mouse, cannot be done using CD1d-deficient animals. Furthermore, the antibodies enable the direct comparison of CD1d responses in the rat to the mouse and since they were generated in mice, are ideally suited for *in vivo* studies in this species as they will not provoke a response against xenogenic Ig.

4.5 CD4 expression by MZ B cells

A major surprise was the not yet described substantial CD4 expression on rat MZ B cells, which was shown to be specific using three different monoclonal antibodies which bind to two different domains of the CD4 molecule (van den Berg et al., 2001). It is retrospectively difficult to explain, why this observation has not been reported before.

The functional implications of this finding are unclear, but it is important to know that any experimental setting addressing CD4, e.g. in depletion studies with CD4 specific antibodies in the rat, can be expected to affect not only CD4 T cells and to some extent antigen presenting cells but MZ B cells as well. Since rats and humans are more similar to one another with respect to CD4, CD8 and MHC-II expression by immune cells than rats and mice (Broeren et al., 1995; Crocker et al., 1987; Kenny et al., 2004), it may be worthwhile to reinvestigate CD4 expression on human MZ B cells as well.

4.6 Production of rat CD1d oligomers

As mentioned in the results section 3.4, different approaches with different advantages, were taken to produce rat CD1d oligomers. From the three variants that were tested with a semi-invariant TCR-transduced cell line, rat CD1d-IgG dimers showed the best staining (Fig. 16). The weaker staining capacity of the rat β 2m-CD1d-hFc dimers compared to the rat CD1d-IgG dimers, apart from intrinsic differences of the protein preparation and α -Gal loading efficiency (see Methods 2.2.3.10 and Results 3.4.1.5), could be explained by a reduced avidity of this bivalent molecule resulting from a different orientation or less flexibility of the CD1d molecules when they are bound to the constant domain of the Fc portion compared to the variable domain of an intact antibody. A different conformation of the CD1d molecule induced by the covalently linked β 2-microglobulin, although it can not be excluded, seems unlikely since covalent linkage by glycine-serine polylinkers are commonly used to fuse protein subunits and have been used for the optimization of production of human CD1d tetramers (Li et al., 2008).

In principle, CD1d tetramers would be advantageous over CD1d-IgG dimers in so far that they should have a higher avidity for the semi-invariant TCR and that they lack the IgG molecule which can cause problems by Fc receptor binding and the use of secondary reagents when primary cells are stained. Nonetheless, the rat CD1d-IgG dimers were highly superior to the rat CD1d streptamers, since the latter gave a very high unspecific staining which was independent from TCR expression because untransduced BW cells were also stained. Additionally, these CD1d streptamers showed little differences between α -Gal- and β -Gal-loaded reagents. The most likely explanation for the small differences between α -Gal- and β -Gal-loaded streptamers is the inefficient multimerization of the reagent. Strep-Tag/Strep-Tactin based multimerization has been successfully used in the production MHC class I oligomers

(Knabel et al., 2002; Neudorfer et al., 2007), but to our knowledge, this is the first attempt with CD1d molecules. Antigen loading of CD1d, in contrast to that of MHC-I molecules, was carried out in the presence of DMSO and TRITON X-100, thus it might well be that solvents and detergents still present in the multimerization mixture affect the Strep-Tag/Strep-Tactin interactions.

4.7 Species specificity of α -Gal-CD1d recognition by mouse and rat iNKT cells

Functional data generated in our laboratory with transduced cell lines and primary antigen presenting cells by E. Pyz et al. showed that while mouse semi-invariant TCR bearing cells responded to α -Gal-presented by rat CD1d almost to the same extent as to α -Gal-presented by mouse CD1d, rat semi-invariant TCR reactivity to mouse CD1d- α -Gal was severely impaired compared to rat CD1d- α -Gal (Pyz et al., 2006). This species specificity of CD1d- α -Gal recognition by rat semi-invariant TCR was now confirmed by flow cytometry since the fluorescence intensity of these rat semi-invariant TCR (AV14S6^F + CDR2+4) transduced cells stained with rat α -Gal-loaded CD1d-IgG dimers was about 30-fold better than with mouse α -Gal-loaded CD1d-IgG dimers (Results section 3.4.2). Moreover, this cell line was not stained by human α -Gal CD1d tetramers at all.

Flow cytometry analysis of rat and mouse primary intrahepatic lymphocytes with these newly generated IgG dimers showed the same species specificity in CD1d/ α -Gal recognition: on the one hand, most mouse primary iNKTs, stained with mouse α -Gal-loaded CD1d-IgG dimers, were also stained with rat CD1d-IgG α -Gal-loaded dimers; on the other hand, among rat intrahepatic lymphocytes the small but distinct population detected with rat CD1d-IgG α -Gal-loaded dimers was not observed when mouse CD1d-IgG α -Gal-loaded dimers had been used (Fig. 17). These results were confirmed by staining *in vitro* expanded rat iNKT cells. This species specificity of α -Gal-CD1d recognition by iNKT cells of rats and mice was unexpected since human CD1d α -Gal-loaded oligomers stain mouse iNKT cells and vice versa, mouse CD1d α -Gal-loaded oligomers stain human iNKT cells (Benlagha et al., 2000; Matsuda et al., 2000) and also because the predicted amino acid sequences of all the genes (CD1d, AV14, AJ18 and BV8) necessary for the generation of such CD1d-restricted T cells are highly conserved between mice and rats (Fig. 39 and (Kinebuchi and Matsuura, 2004; Matsuura et al.,

2000; Pyz et al., 2006). Nonetheless, apart from the CDR2 α region of the invariant TCR α chain, which differs considerably but does not contribute to the recognition of α -Gal-CD1d with evident interactions (Borg et al., 2007; Pellicci et al., 2009), two amino acids, one in CD1d and the other one in AJ18, which are conserved between mouse and human and which make energetically important interactions and are not preserved in the rat (Fig. 39, (Borg et al., 2007; Pellicci et al., 2009)). Although these non-conserved residues are only two, one single amino acid substitution in tree shrew CD1d compared to human CD1d is enough to cause the loss of cross-reactivity between human semi-invariant TCR and tree shrew CD1d (human CD1d contains a lysine (K) at position 86 where the tree shrew CD1d contains a glutamine (Zhang et al., 2009)). Therefore these single substitutions in AJ18 or CD1d may be responsible for the described need of syngeneic CD1d as presenting element in the rat. More precisely, on the one hand, the human and mouse arginine (R) 103 present in the CDR3 α loop (encoded by the AJ18 gene segment) is substituted by a lysine (K) in the rat. R103 makes Van der Waal interactions with R at position 79. In addition, in the mouse BV8S2 (but not BV7) ternary complex, this R103 in the α chain contacts the glutamic acid (E) at position 83 of the mouse CD1d. On the other hand, in human and mouse CD1d a valine at position 147 and 150, respectively, is substituted by a methionine in the rat. This valine makes Van der Waal interactions with serine (S) 97 and leucine (L) 99, which are present in all three species (Fig. 39, (Borg et al., 2007; Pellicci et al., 2009)).

In F344 inbred rats approximately half of iNKT cells bear BV8S4⁺ TCRs. The detection of BV8S2 comprising TCRs using mAbs in this strain is not possible at the moment, but it would be interesting to learn whether the other half of iNKT cells use BV8S2 TCRs or TCR with other BV gene segments. Similarly, once demonstrated that the double negative and CD4 positive rat intrahepatic lymphocytes stained with mouse CD1d-IgG α -Gal dimers are indeed iNKT cells, it would be worth to address the V-D-J gene segments of their TCR β chains to see whether there is any particular bias in the BV usage.

No evident interactions between CDR3 β and α -Gal-CD1d appeared in the crystal structures (Borg et al., 2007; Pellicci et al., 2009), but they still play an important role as it has been recently described for mouse and humans: First in mouse, certain CDR3 β amino acid sequences allowed the usage of BV gene segments which are rarely found among the iNKT cell pool and, second in humans, the CDR3 β region controlled the affinity of the binding to CD1d independently of the presented ligand (Mallevaey et al.,

2009; Matulis et al., 2010). Thus it would be also interesting to analyze the CDR3 β regions and BV usage of mouse iNKT cells which are stained with rat CD1d-IgG α -Gal-loaded dimers to see whether there is any particular bias.

The different usage of AV14 gene segments by iNKT cells in the rat is later discussed in the discussion section 4.9.

a CD1d: α 1 domain

	1	11	21	31	41	51	61	71	81	91
hCD1d	AEV P QRL F PL R CL Q ISS F AN S SW T RT D GL A WL G EL Q TH S W S ND S DT V RS L K P W S Q T F S D Q W E T L Q H I F R V Y R S S F T R D V K E F A K M L R L S									
mCD1d1	S.A Q .K N Y T F.....M.....R.....S.....S V V...D...R...A . IS F T.....K L .N.....K...M . Q...V...I Q .L V ..M S P K E D									
rCD1d	S..Q..-N Y T FR.....S.....S V V...D...R...A . IS F T.....K . N.....K...M . Q...T...I...I V ..M S P K E D									
	1	10	20	30	40	50	60	70	80	90

α 2 domain

	92	102	112	122	132	142	152	162	172	182
hCD1d	Y P LE L Q V S A G E V H P G N A S N FF H V A F Q G K D I L S F Q G T S W E P T Q E A P L W V N L A I Q V L N Q D K W T R E T V Q W L L N G T C P Q F V S G L L E S G K S E L K K Q									
mCD1d1	..I.I.L.....M YE S .L.....Y V V R .W....Q T V P G..S .L D .P .K...A .Q G .S A...M...D...L...R...A...D .E ..									
rCD1d	..I.V.L.....M YE S .L.....E Y V V R.H...Q K V P ...S .L D .P .K M ..A .E G.....I...D...R...A...P D .E..									
	93	103	113	123	133	143	153	163	173	183

b TCR α chain:

				CDR1		CDR2				CDR3
		10	20	30	40	50	60	70	80	90 95 98 103
hAV24/AJ18	-N Q V E Q S P Q S L I I L E G K N C T L Q C N Y T V S P F S N L R W Y K Q D T G R G P V S L T I M T F S E N T K S N G R Y T A T L D A D T K Q S S L H I T A S Q L S D S A S Y I C V V/S/DRG S T L G R L Y F G R G T Q									
mAV14S1A2/AJ18	K TV V R Q .E..V.....S .T .D N H...F...K.L...V L V D Q K D K T.....S...K.A.H.T...T L .D.T.T.../A/...A...H.A...									
rAV14S6/AJ18	R TV V H..E S .V.....T .NR.A...V L .N K .E K T.R...S...A.H.T...L.D.A.T.../A/...A.K...I...									
	1	11	21	31	41	51	61	71	81	91 95 101

c TCR β chain:

				CDR1		CDR2		HV4/CDR4		CDR3
	1	11	21	31	41	51	61	71	81	91 101
hBV11BDJ2	E A D I Y Q T P R Y L V I G T G K K I T L E C S Q T M G H D K M Y W Y Q D P G M E L H L I H Y S Y G V N S T E K G D L S S E S T V S R I R T E H F L T L E S A R P S H T S Q Y L C A S S /E N I G T A Y E Q Y F G P G T R									
mBV8S2	..A V T.S..N K .A V ..G.V..S.N.. <u>NN.NN</u> ...R..T.H G .R... <u>AG</u> ...I P D G Y K A.. <u>PSQ.N</u> .S.I..L.T..Q..V.F...G/.G L G G P T									
rBV8S4T.K.....K.N.....M.....N.....V.N...V...N K ...F.T..S.S.....S									
rBV8S2	----- <u>DV</u>D..... <u>SQGD</u>									
	1	11	21	31	41	51	61	71	81	91

Figure 39. Amino acid sequences of human, mouse and rat CD1d, variable domains of invariant TCR α chains and various β chains. Alignments of mature amino acid sequences necessary or relevant for the development of iNKT cells. Dots represent same amino acid as the first amino acid sequence. Numbers above and below the sequences correspond to mature human and rat predicted amino acid sequences, respectively. *a* Predicted amino acid sequences of human CD1d (GBN: NM_001766), mouse CD1d1 (GBN: X13170) and rat CD1d (AB029486) α 1 and α 2 domains. Bold letters indicate α -helical regions. *b* Predicted amino acid sequence of human AV24/AJ18 (GBN protein: 2CDE_A, IGMT nomenclature TRAV11-TRAVJ18), mouse AV14S1A2/AJ18 (GBN: DQ340292) IGMT nomenclature TRAV11*02 and TRAJ18) and rat AV14S6^{F344}/AJ18 (GBN: DQ340293). CDRs are indicated with underlined letters. Numbers in bold and cursive are assigned as published for human and mouse invariant TCR α amino acid sequences (Wun et al., 2008) although the numbering of the arginine 103 should be 101. This numbering has been conserved to allow a direct comparison with the iTCR- α -Gal-CD1d crystal structures published to date (Borg et al., 2007; Pellicci et al., 2009). *c* Predicted amino acid sequence of human BV11 (GBN protein: 2CDE_B), mouse BV8S2 (GBN: DQ340294), rat BV8S4 (EMBL-Bank: X77995) and rat BV8S2 (EMBL-Bank: X98251.1) both from the a haplotype (Asmuss et al., 1996). CDRs are indicated with underlined letters.

4.8 Distribution and phenotype of rat iNKT cells

In mice iNKT cell frequencies are a stable phenotype under genetic control of at least two different recessive loci (Esteban et al., 2003; Rocha-Campos et al., 2006). In humans, iNKT cells numbers vary noticeably among different individuals but are also under strict genetic control since they are approximately the same between identical twins (Lee et al., 2002b). In this study we have analyzed iNKT cell frequencies in two different rat strains: F344 and LEW. In F344 rats iNKT cells were clearly detectable with α -Gal-loaded rat CD1d oligomers in the liver and the spleen. Similar to mice, the frequencies of iNKT cells found in the liver were higher than those in the spleen: 0.25 and 0.05% of total lymphocytes or 1.65 and 0.16% among $\alpha\beta$ T cells in the liver and the spleen, respectively. Nonetheless, these frequencies are much lower than in C57BL/6 or BALB/c mice, where 30 and 20% of the liver lymphocytes, respectively, are iNKT cells (Matsuda et al., 2000). Among F344 PBCs a very low number of cells were stained with α -Gal-loaded but not with β -Gal-loaded rat CD1d oligomers. Despite these low numbers, the fact that the cells stained with rat CD1d-IgG α -Gal-loaded dimers were mostly DN and CD4 positive supports the interpretation that these cells are indeed circulating iNKT cells. However, in order to exclude that the CD1d-IgG dimer positive cells were not other T cells which serendipitously contained a TCR reactive to α -Gal-CD1d complexes, these results should be confirmed at least for spleen and PBCs first, with further stainings in which more events are acquired and second, with other supporting methods as for example by sorting the stained cells and analyzing the TCR α chains by RT-PCR and sequencing.

In LEW rats, except in the liver, where very few cells were stained by the α -Gal-loaded rat CD1d-IgG dimers, no iNKT cells were detected in the spleen or in PBCs. Although the cells stained with α -Gal-loaded rat CD1d-IgG dimers in the liver were mostly DN and CD4 and did not appear with β -Gal-loaded dimers, further analyses are required to confirm that these are indeed iNKT cells.

In the thymus of both inbred rat strains, staining with α -Gal- or β -Gal-loaded rat CD1d-IgG dimers revealed no differences. Taken into consideration that in the thymus of C57BL/6 or BALB/c mice, the frequencies of iNKT cells are low: 0.7 and 1.5%, respectively (Matsuda et al., 2000) and that in the other organs in the rat the frequencies of iNKT cells were 10 to 100 fold lower than in the mouse, it is well possible that iNKT cells are below the detection limit with the staining protocol used in these analyses.

Taken all together, the numbers of iNKT cells observed among rats are strikingly lower than those of mice. In fact, LEW rats can, in principle, be considered as an iNKT cell deficient inbred rat strain. To find such low frequencies among rats was in part surprising because in all the “wild type” mouse inbred strains analyzed to date, no strain has been reported yet in which liver iNKT cells could not be stained with mouse CD1d oligomers, although some strains such as 129 and LG contained very low iNKT cell numbers (Rymarchyk et al., 2008).

Interestingly, the frequencies of iNKT cells in the rat resemble much more the frequencies observed in humans. In two independent studies where human livers were analyzed, the observed iNKT cell numbers varied from 0.03 to 0.3% among total intrahepatic lymphocytes in patients with end-stage viral-induced liver cirrhosis (Karadimitris et al., 2001) and were about 0.5% of all CD3⁺ T cells in healthy individuals (Kenna et al., 2003). In another study where human thymocytes were analyzed, the frequencies observed were much lower than those of mice: The mean value for 30 individuals was 0.0016%. Importantly, in this study a very high number of thymocytes (30×10^7) had to be acquired to detect a reliable population by flow cytometry analyses. Moreover, this study also showed that the iNKT cell frequencies observed in the thymus have limited correlation with the frequencies found in the periphery (Berzins et al., 2005). Although this is not surprising in humans because adult individuals were analyzed and the only peripheral “organ” studied was the blood, this phenomenon is also observed in mice maintained under specific pathogen-free conditions (Matsuda et al., 2000) and therefore, it could occur in the rat as well.

All the data obtained by flow cytometry with α -Gal-loaded CD1d-IgG dimers are supported by RT-PCR and sequencing experiments described in the results sections 3.5.2 and 3.6.2. Briefly, where a relative high number of iNKT cells were observed (i.e. F344 liver and spleen) the AJ18 gene segment was preferentially used among all the AV14-containing TCR α chains, AV14AJ18 rearrangements were easily detected by RT-PCR and the AV14-AJ18 rearrangement junction consisted of a stretch with three nucleotides encoding an alanine or a glycine. The predominance of the alanine codon (GCx) in the junction region can be explained by the germline nucleotides subsequent to all BN AV14 coding sequences which are GCC. The presence of glycine codons (GGx) can only be the result of the addition of N nucleotides since the adjacent nucleotides to the coding region of the AJ18 gene segment are two thymines. In mice and humans the predominant residue found in the junctional region of invariant α chains is also that

encoded by the germline DNA: glycine (GGC) in mouse and serine (AGC) in humans (Dellabona et al., 1994; Koseki et al., 1990). Analysis of the influence of alanine and glycine in the recognition of α -Gal-CD1d by rat iTCRs is underway.

Interestingly, among F344 thymocytes AV14-AJ18 rearrangements were easily detected by RT-PCR, but the size and the nucleotides of their junction regions were highly diverse, indicating that many thymocytes rearrange AV14 and AJ18 gene segments together in F344, but probably only in a low proportion of these rearrangements the junctional region is formed by three nucleotides encoding either alanine or glycine as observed in the invariant α chains of the periphery. These last results support the lack of the identification of a distinguishable population with rat α -Gal-loaded CD1d-IgG dimers in F344 thymocytes compared to splenocytes or intrahepatic lymphocytes. Among LEW thymocytes, AV14-AJ18 rearranged TCR α chain transcripts were hardly detected (Fig. 20). From three analyzed animals, only one successful sequence was obtained which also contained different junction regions. These results show that in comparison to F344, in LEW rats the proportion of thymocytes which rearrange these two particular gene segments is much lower. Rearrangement of TCR gene segments encoding the variable region occurs in an orderly manner: Proximal gene segments rearrange first and those which are distal require a prolonged lifespan of DP thymocytes (Guo et al., 2002). AJ18 is encoded close to the 3' end of the AJ loci and therefore is distal to the AV14 gene segment. Thus, various mouse models which lack - or have defective - factors that prolong thymocyte lifespan and sustained rearrangement such as ROR- γ t, BCL-X_L and c-Myb, have reduced iNKT cell numbers (Bezbradica et al., 2005; Egawa et al., 2005; Hu et al., 2010). Torres-Nagel and colleagues showed that in LEW rats, proximal AJ gene segments are also preferentially rearranged with the AV8S2 gene segment in comparison to distal AJ segments (Torres-Nagel et al., 1997). Moreover, direct comparison of the mouse and rat AJ loci by blasting the complete genomic region encoding the mouse AJ loci with the rat BN genome showed an overall conservation in the locations of the AJ gene segments in the rat (data not shown). Thus since both F344 and LEW rats have almost identical levels of CD1d at the cell surface of DP thymocytes and contain the genes (AV14-AJ18 rearrangements were found in both strains) necessary to form the invariant α chain, it may be possible that the reduced amounts of AV14-AJ18-containing TCR α transcripts in LEW thymocytes and also iNKT cells in the periphery are due to an decreased capacity to rearrange distal gene segments in comparison to F344 rats.

As previously mentioned, the much lower iNKT cell frequencies found in rats compared to mouse are close to the frequencies found in human. Among other reasons, this was surprising since rat and mouse DP thymocytes express very similar levels of CD1d at the cell surface. Nonetheless, rat and human thymocytes differ remarkably from their mouse counterparts least in one aspect: rat and human thymocytes express MHC class II molecules whereas mouse thymocytes do not (our own unpublished data and (Fukumoto et al., 1982; Li et al., 2005)). This difference is remarkable because Li et al. have recently shown that the expression of MHC-II molecules in mouse thymocytes suppress iNKT cell development in *trans* in a CD4-dependent manner (Li et al., 2009). More importantly, in mice whose thymocytes expressed MHC class II molecules, iNKT cells were not completely absent but their frequencies were dramatically reduced. The mechanism behind this phenomenon is not completely understood but the authors suggest that the reduction on iNKT cell numbers could be due an increased negative selection resulting from an augment in the strength of the TCR signalling caused by CD4 binding to MHC-II molecules. Another alternative which also should be considered for the unsuccessful detection of iNKT cells in the rat thymus is that rat iNKT cell development could take place in other site/sites other than the thymus. Thus it would be worth to analyze athymic nude rats as well as thymectomized animals. Nonetheless, unless iNKT cell biology in the rat differs very much from the mouse, this alternative hypothesis seems highly improbable.

4.8.1 NKR-P1 expression

iNKT cells own their name first, to the expression of the invariant AV14-AJ18 chain (AV24-AJ18 human homologues) and second, to the expression of NK1.1 (NKR-P1C) in C57BL/6 mice (Godfrey et al., 2004). As mentioned in the introduction, since not all iNKT cells express NK1.1 (NKR-P1C) in mice or CD161 (NKR-P1A) in humans and not all the NK1.1⁺/CD161⁺ T cells are iNKT cells, in order to unambiguously identify iNKT cells, α -Gal-loaded CD1d oligomers are needed (Godfrey et al., 2004; Gumperz et al., 2002; Hammond et al., 2001; Matsuda et al., 2000). Moreover, recent reports have shown that these receptors typical of NK cells used initially to identify iNKT cells are members of the same family but their orthology between mouse, rat and human is not clear due, in part, to the very high degree of polymorphism (Aust et al., 2009; Carlyle et al., 2008). As mentioned in the introduction, former attempts carried out to identify rat iNKT cells also relied in the co-expression of TCR/CD3 and two of these

NKR-P1 receptors (A and B) detected by the mAbs 3.2.3 or 10/78 (Knudsen et al., 1997; Li et al., 2003; Matsuura et al., 2000; Pyz et al., 2006; Ru and Peijie, 2009). Now, the identification of rat iNKT cells using α -Gal-loaded rat CD1d-IgG dimers in this study demonstrated that the expression of NKR-P1 is certainly not a suitable marker to identify rat iNKT cells. Indeed the frequencies of NKR-P1⁺ T cells in LEW rats, where iNKT cells were hardly detected if at all, do not differ from those of F344. These findings beg the reinterpretation of studies where rat TCR⁺ NKR-P1⁺ cells have been regarded as iNKT cells (Chopra et al., 2009; Kattan et al., 2008; Shao et al., 2003). In the spleen from F344 rats, iNKT cells are only a 1-2% of the NKR-P1⁺ T cells and in the liver where these cells accumulate they do not constitute more than a 10% of the NKR-P1⁺ T cells. These frequencies are much more reduced in comparison to C57BL/6 mice, where a 75% in the liver and thymus, and about 30% in the spleen of all NK1.1⁺ T cells are iNKTs (Matsuda et al., 2000). Frequencies of iNKT cells in humans are difficult to investigate due to the limited access to human samples other than blood and to the variations between individuals (Lee et al., 2002b). Nonetheless, the very low numbers of iNKT cells (1%) found among CD161⁺ T cells in PBMCs and the low frequencies of iNKT cells (~0.5%) compared to the high numbers of CD161⁺ CD3⁺ cells in the liver (40%) suggest, that also in this case, the frequencies observed in the rat resemble more those of humans than those of mice (Gumperz et al., 2002; Ishihara et al., 1999; Kenna et al., 2003).

In mice and humans, NK1.1 and CD161 negative iNKT cells are easily detectable among cells stained with α -Gal-loaded CD1d oligomers (Benlagha et al., 2000; Hammond et al., 2001; Lee et al., 2002b; Matsuda et al., 2000; Pellicci et al., 2002). Mouse NK1.1 negative iNKT cells are found in the thymus and in the periphery. NK1.1 negative NKT cells in the thymus are regarded as immature iNKT cells which nonetheless can secrete large amounts of cytokines (Coquet et al., 2008). These NK1.1⁺ and NK1.1⁻ iNKT cells can be further subdivided based on CD4 expression at the cell surface. Interestingly, it has been shown as these subsets also differ in the cytokine secretion and in the NK receptors expressed at the cell surface: NK1.1⁻ cells do not express NKG2D, NKG2A/C/E or Ly49C/I whereas NK1.1⁺ cells do (Coquet et al., 2008; McNab et al., 2007). In the rat, most, if not all, iNKT cells expressed NKR-P1 at intermediate levels (Fig. 18). Thus, if a mature NKR-P1 negative iNKT cell subset exists, this is more reduced in comparison to mice and humans.

In mice, cell surface NK1.1 is down modulated in iNKT cells after *in vitro* and *in vivo* activation (Crowe et al., 2003; Chen et al., 1997; Wilson et al., 2003) but all rat iNKT cells harvested after seven days of culture with the potent antigen α -Gal expressed considerable amounts of NKR-P1 at the cell surface (Fig. 34). Accordingly, it seems that rat iNKT cells do not down modulate NKR-P1 after activation.

In order to avoid a misinterpretation of the results where the expression of NKR-P1 receptors was analyzed, it should be considered that the receptors studied in each species are different molecules. Indeed, no orthologue of the mouse NKR-P1C (NK1.1) has been yet described in the rat (Kveberg et al., 2009). Therefore, the differences which are observed between species might result from the analysis of different NKR-P1 receptors.

4.8.2 CD4 and CD8 distribution

Based on the expression of CD4 at the cell surface, human iNKT cells can be divided into CD4⁺ and CD4⁻ cells. Most human CD4⁻ cells express CD8 $\alpha\alpha$ homodimers at the cell surface, but only a small fraction expresses CD8 $\alpha\beta$ heterodimers (Gadola et al., 2002; Gumperz et al., 2002; Takahashi et al., 2002). In contrast, whereas also CD4⁺ and CD4⁻ iNKT cells are found in the mouse, the CD4⁻ fraction expresses neither CD8 $\alpha\alpha$ nor CD8 $\alpha\beta$ at the cell surface. Due to the reduced iNKT cell numbers observed in mice in which all T cells expressed CD8 molecules as a transgene, it was formerly believed that expression of CD8 was incompatible with mouse iNKT cells due to CD8-mediated negative selection of iNKT cell precursors (Lantz and Bendelac, 1994) until Kronenberg and colleagues showed that the expression of CD8 $\alpha\beta$ at the cell surface does not drive negative selection of iNKT cells and is not incompatible with iNKT cell development and function. In contrast, the absence of CD8 at the cell surface of mouse iNKT cells is probably the result of the expression of the Th-POK transcription factor at the DP stage, which is necessary for the development of iNKT cells and which suppresses the expression of CD8 (Engel et al., 2010).

In this study we also analyzed CD4 and CD8 β distribution among rat iNKT cells. CD8 α was not included in the analysis because rat activated T cells and NK cells express CD8 $\alpha\alpha$ homodimers at the cell surface (Kenny et al., 2004). Most rat iNKT cells are DN or CD4. Similar as it has been shown for mouse iNKT cells, CD4 expression levels at the cell surface of rat iNKT cells are notably lower in comparison to those of $\alpha\beta$ T cells (Engel et al., 2010). Interestingly, in the rat, a small proportion of CD8 β positive cells

was constantly detected. Thus once more, rat iNKT cells appear more similar to human than to mouse iNKT cells.

Expansion of iNKT cells by seven days culture with α -Gal considerably reduced the proportion of CD4⁺ iNKT cells, whereas the percentage of CD8 β was more or less the same. It remains to be investigated whether this reduction in the frequencies of CD4⁺ iNKT cells in the cultures is due to a selective loss of CD4⁺ cells or to a down modulation of CD4 at the cell surface.

A lot of efforts have been made to distinguish between iNKT cell subsets with different effector functions to better understand how these cells with a semi-invariant TCR manage to enhance and also to suppress immune responses (Godfrey et al., 2010). In humans, CD4⁺ iNKT cells secrete both, Th1 and Th2, cytokines whereas CD4⁻ iNKT cells mainly produce Th1 cytokines (Gumperz et al., 2002; Lee et al., 2002b). In the mouse, although *ex vivo* analyses have not shown such a clear division between CD4⁺ and CD4⁻ iNKT cells, in an *in vivo* tumor model, transfer of liver CD4⁻ iNKT cells mediated tumor rejection whereas their CD4⁺ counterparts or iNKT cells from other tissues did not (Crowe et al., 2003; Godfrey et al., 2010). Moreover, in a recent study where these cells were further subdivided based on the expression of NK1.1 and tissue origin and where other cytokines than IL-4 and IFN- γ were measured, major differences have been found between the different subsets (Coquet et al., 2008). In this study Godfrey and colleagues also identified a new NK1.1⁻ CD4⁻ iNKT cell subset which produced large amounts of IL-17. IL-17 production by mouse NK1.1⁻ iNKT cells had been previously reported by Leite-de-Moreaes and colleagues (Michel et al., 2008); although in this case, in contrast to the subset described by Godfrey et al., the NK1.1⁻ iNKT cells did not secrete high amounts of IL-4 or IFN- γ .

Although not addressed in our study, analysis of cytokine profiles by different rat iNKT cells might help to understand the diverse functions of iNKT cells and it also may provide an animal model more similar to human than the mouse, beginning with the possibility to analyze cytokine secretion by CD8 β ⁺ iNKT cells.

4.8.3 BV usage

In humans and mice, iNKT cells show a marked bias in their BV repertoire. As previously mentioned, most human iNKT cells contain BV11 β chains, and among mouse iNKT cells the TCR β chains are principally formed by BV8S2, BV7 or BV2 comprising β chains (Dellabona et al., 1994; Lantz and Bendelac, 1994). The analysis of

F344 iNKT primary cells with the mAb R78, which in this strain binds to BV8S4 variable segments (Asmuss et al., 1996), revealed that about one-half of iNKT cells contained this particular BV. Supporting these data, among culture-expanded iNKT cells, about 50% of the cells were also stained with the R78 mAb.

The BV repertoire of the other half of rat iNKT cells still has to be analyzed in order to elucidate whether the rat iNKT cells which do not use BV8S4, use another member of the BV8 family, all BV8 members or other BVs than BV8. Nonetheless, *in vitro* experiments carried out by E. Pyz et al. demonstrated that BV8S2-containing invariant TCRs also recognize α -Gal presented by CD1d, although less efficiently than invariant TCRs with a β chain containing BV8S4 (with a L14V substitution) (Pyz et al., 2006). These results indicate that BV8S2 may form the rest or a part of the non-BV8S4 semi-invariant TCRs. In addition, it is likely that BV16-containing β chains do not form semi-invariant rat TCRs because this BV was not detected in cultured iNKT cells.

As shown by the crystal structures and mutagenesis analyses, the CDR2 β of BV8⁺ TCRs contributes to the recognition of α -Gal presented by CD1d (Borg et al., 2007; Mallevaey et al., 2009; Pellicci et al., 2009; Pyz et al., 2006; Scott-Browne et al., 2007; Wun et al., 2008). Particularly, as demonstrated by E. Pyz et al. (Pyz et al., 2006), the CDR2 β of BV8S4 is sufficient to enhance the reactivity to α -Gal-CD1d of a cell line expressing an AV14S8^F invariant α chain. Since rats have many different AV14 gene segments, it would be interesting to learn whether the BV repertoire changes depending on which AV14 gene segment is comprised in the invariant α chain. Different AV14 usage by rat iNKT cells is discussed in more detail in the discussion section 4.9.

Furthermore, it would be also very interesting to analyze the BV repertoire of iNKT cells in inbred rat strains which lack a functional BV8S4 (Asmuss et al., 1996), but showed a response to α -Gal such as BN rats (Results section 3.7.1).

4.8.4 Activation markers

After first antigen encounter, MHC-restricted $\alpha\beta$ T cells clonally expand and differentiate for several days before they can elicit their effector functions. In sharp contrast, iNKT cells after first antigen encounter are activated very rapidly and secrete large amounts of cytokines within hours. Moreover, iNKT cells have a phenotype that resembles activated or memory T cells. Mouse iNKT cells express cell surface molecules such of CD25, CD44, CD69 and CD122 (Matsuda et al., 2000; Park et al., 2000), and although most human iNKT cells in the peripheral blood do not express

CD69 or CD44, the majority of them are CD25 and CD45RO positive (Berzins et al., 2005; Gumperz et al., 2002). In contrast in the liver, human iNKT cells expressed CD69 but only a minority were CD25 positive (Kenna et al., 2003).

In addition, a considerable part of the iNKT pool also expresses other receptors typical of NK cells (apart from NKRP family members) such as CD94 or NKG2 family members or, in the mouse, Ly49 (Gumperz et al., 2002; Uldrich et al., 2005). Analysis of these activation markers and receptors typical of natural killer cells is still pending for rat iNKT cells.

4.9 AV14 gene segment usage in the rat

The intriguing expansion of the AV14 gene segments observed in the rat has not been described for any other mammal species in which AV14-AJ18 rearrangements have been detected (Kashiwase et al., 2003; Sim et al., 2003; Yasuda et al., 2009). As previously mentioned, the predicted amino acid sequences of all rat AV14 gene segments described up to date are highly similar with the exception of the CDR2 α region. According to the different sequences of the CDR2 α region, rat AV14 gene segments have been divided into two types ((Kinebuchi and Matsuura, 2004; Matsuura et al., 2000; Pyz et al., 2006) and this study). Interestingly, in the mouse two different genes differing exclusively in the CDR2 α region have also been found (Koseki et al., 1991). Nonetheless, most of the commonly used inbred mouse strains have only one of these two genes and probably therefore have been considered as alleles (Sim et al., 2003).

In contrast to the mode of recognition of peptide-MHC complexes, the CDR2 α of semi-invariant TCRs does not contribute with important interactions to the recognition of α -Gal-CD1d complexes (Borg et al., 2007; Godfrey et al., 2008; Pellicci et al., 2009). Consequently, single substitutions of the residues of this region by alanines did not affect the interaction of the semi-invariant TCR with CD1d tetramers loaded with α -Gal or with other lipidic antigens (Mallevaey et al., 2009; Scott-Browne et al., 2007). On the one hand, the variability in the CDR2 α region may reflect the lack of a selecting pressure in this region to maintain the semi-invariant TCR-CD1d interaction. In line with these findings, the two mouse AV14 alleles showed only minor differences in the binding kinetics to α -Gal-CD1d complexes (Sim et al., 2003). Nonetheless, on the other hand, it is also possible that the variability of the CDR2 α reflects the opposite situation:

The need of this region to recognize a wider spectrum of antigens of lipidic and/or protein origin.

We neither have studied the binding capacities of the different rat AV14s to α -Gal-CD1d oligomers, nor have we analyzed the AV14 repertoire of rat primary cells stained with rat α -Gal-loaded CD1d dimers yet. Nonetheless, among iNKT cells expanded in culture with α -Gal both AV14 types were observed after RT-PCR and direct sequencing, predicting that both AV14 types can participate in the recognition of α -Gal presented by CD1d. Moreover, both types of AV14s appeared with similar frequencies among AV14-AJ18 rearrangements of primary mature F344 lymphocytes. However, the BN genome contains only two type II versus seven type I AV14 gene segments and to date only one type II but four type I AV14 gene segments have been cloned from F344 rats (Fig. 22 and results section 3.6). Thus, the similar frequencies of both AV14 types in the periphery – of F344 rats – may indeed reflect the preferential usage of type II AV14s by iNKT cells. It would be worthwhile to analyze the usage of these diverse AV14 gene segments as well as the variable regions of the β chains which form α -Gal-CD1d-reactive TCRs in primary single cells, as this will provide information necessary to understand the basis of this variability in the rat. Moreover, in humans α -Gal-CD1d-reactive T cells with other AV and AJ gene segments than AV24 and AJ18 have been described (Gadola et al., 2002; Gadola et al., 2006a), therefore it also would be interesting to investigate whether such cells are also present among rat α -Gal-CD1d-reactive T cells.

In the first study where multiple AV14 genes were found in the rat, a tissue-specific distribution of the two different types was also proposed (Matsuura et al., 2000). After the analysis of several hundreds of clones pooled from three F344 rats, a preferential usage of type II AV14 gene segments was observed among invariant TCR α chains in the spleen and a bias in the usage of type I AV14 TCRs was detected in the thymus. In contrast, in the liver type II AV14 gene segments were more frequently found among invariant TCR α chains and in the bone marrow, a similar proportion of AV14 of either type was found to be rearranged with AJ18 (Matsuura et al., 2000). Although we also analyzed some cloned AV14-containing TCR α chains from F344 rats, in order to address the AV14 usage of invariant and any AV14-containing TCR in thymus, spleen and liver of F344 and LEW rats, we directly sequenced the pool of AV14-AJ18 rearrangements and AV14-comprising TCR α chains after amplification by RT-PCR. After having analyzed three animals of each inbred strain, in F344 we did not found a

tissue-specific usage of these two different AV14 types among AV14-containing or invariant TCRs, except in the thymus. Nonetheless, when the animals were analyzed individually, occasionally one AV14 type was more frequently found than the other. Therefore, the results obtained by Matsuura and colleagues do not disagree with our data.

In LEW rats, as previously pointed out (Results section 3.5.2), AV14-J18 rearrangements were hardly detectable and as a consequence, analysis of AV14 gene segment usage was only possible among non-invariant AV14 α chains. Interestingly, in contrast to F344 rats, where both AV14 types were detected with similar frequencies, in LEW, type I AV14 gene segments were preferentially used. Although the sequences of individual AV14 gene segments have not been determined yet in LEW rats, Southern blot analysis showed a pattern similar to that of BN rats (Matsuura et al., 2000), and despite at low frequencies, type II AV14 segments were also detected in LEW-derived RT-PCR sequences. Assuming, as discussed above, a bias towards type II AV14 segments among iNKT cells, the reduced usage of type II AV14 in LEW rats might be related to the low/absent iNKT cell frequencies in this inbred strain.

In this study only six cloned AV14-containing TCR α chains from F344 rats were analyzed (Results section 3.6.1). Nonetheless among these, a previously unidentified AV14 gene segment was detected. This AV14 gene segment was designed as AV14S5^F since the V-exon is identical to AV14S5 of BN rats. A premature stop codon was encoded in the cloned TCR α chain containing this novel AV14 gene. Since the TCR α chain does not undergo allelic exclusion, it is possible that this AV14S5 α chain was isolated from a T cell expressing another functional TCR α chain. Since no AV14S5^F or AV14S8^F gene segments have been yet found to be rearranged with AJ18 in single TCR α chains, it remains to be demonstrated whether these two segments can form invariant α chains in F344 rats.

4.10 α -Gal responsiveness in the rat

In this study, iNKT cell activation of five different inbred rat strains was analyzed by measuring cytokine release after *ex vivo* α -Gal stimulation of primary cells. We measured the secretion of IL-4 and IFN- γ into the supernatant after 24-hour stimulation by ELISA and of IL-4 by ELISPOT. Anti-CD1d mAbs were added to the cultures to demonstrate the CD1d restriction of such response. Nearly all isolated primary cells used in the stimulations express CD1d at the cell surface (Fig. 6) thus no supplementary

antigen presenting cells were included in the cultures. Despite that internalization and lysosomal processing is not necessary for α -Gal presentation (Prigozy et al., 2001), it should be considered that some differences in the cytokine production between rat inbred strains and/or tissues may result from variations in the number and efficiency of cells presenting α -Gal. Often, especially in intrahepatic lymphocytes cultures, very high amounts of IFN- γ were released into the supernatants even in cultures where only culture media was added. In contrast, IL-4 release was only observed when cells were stimulated with α -Gal or ConA (with the exception of PVG IHLs). The types and numbers of cells which secrete IL-4 within a few hours after activation are much more reduced compared to the cells which are able to secrete IFN- γ . Indeed, NK cells which were very abundant among the cultured cells (5 to 50%) respond very fast to IFN- γ released by iNKT cells by secreting more IFN- γ (Carnaud et al., 1999). In contrast, illustrating the more restricted sources of IL-4, the IL-4 levels reached after α -Gal stimulation were very similar to those reached after ConA stimulation. Thus IL-4 secretion reflects better than IFN- γ the presence of iNKT cells.

Among the inbred rat strains studied, a clear dose-dependent CD1d-restricted response to α -Gal was only observed among F344 and BN rats. In line with the homing of iNKT cells to the liver (Bendelac et al., 2007) among these inbred rat strains the amounts of cytokines released by IHLs were higher than by splenocytes. In contrast, no α -Gal-dependent cytokine release was measured in PVG- and LEW-derived cultures. This lack of α -Gal-dependent cytokine secretion is in line with the failure of iNKT cell expansion in LEW IHLs cultures with α -Gal (Results section 3.7.4). The absence of α -Gal responsiveness in PVG rats was surprising because NKR-P1⁺ T cell clones which expressed BV8S2, were either DN or CD4⁺ and secreted various cytokines had been isolated from PVG spleens (Knudsen et al., 1997). Intriguingly, ELISA results indicated that DA splenocytes and IHLs also contained cells which secrete IL-4 after α -Gal stimulation in a dose-dependent and CD1d-restricted manner but ELISPOT analyses showed an unspecific IL-4 production. These different outcomes may be explained by the differences between these two methodologies: In ELISPOT analyses the IL-4 secreted is continuously “captured” through the 24-hours of the culture whereas ELISA detect only the IL-4 contained in the supernatant at one specific time point, which in this case was after 24-hours of incubation.

Thymocytes derived from any of the studied inbred rat strains did not produced IL-4 in response to α -Gal stimulation. In part this was not surprising because we were not able

to visualize thymic iNKT cells with α -Gal-loaded CD1d-IgG dimers in F344 rats. After ConA stimulation some IL-4 production was observed, nonetheless it remains to be demonstrated whether it is released by iNKT cells. Importantly, it has been shown as α -Gal presented by dendritic cells is not the best stimulatory agent to induce cytokine production by thymic iNKT cells in the mouse (Coquet et al., 2008). Therefore, and since ConA may also not be sufficient to activate iNKT cells present in the thymus, cytokine secretion by rat thymocytes should be reinvestigated with stimulation protocols similar to those used in mice e.g. anti-CD3 and anti-CD28 stimulation (Coquet et al., 2008).

iNKT cell frequencies using rat CD1d-IgG dimers were studied in only two of these five inbred rat strains: F344 and LEW (a more detailed discussion about iNKT cell frequencies can be found in the discussion section 4.8). These analyses demonstrated that the numbers of iNKT cells correlate very well with the observed α -Gal response. The analysis of the other inbred rat strains is still pending but it will surely help to clarify unresolved questions such as the results observed in DA cultures.

As previously pointed out, iNKT cell frequencies are under genetic control (Esteban et al., 2003; Lee et al., 2002b; Rocha-Campos et al., 2006). Based on the α -Gal response pattern of these five inbred rat strains, at least we can say that in the rat iNKT cell frequencies neither correlate with *Tcra* nor with *Tcrb* haplotypes. Moreover, the CD1d allelism described in this study most likely does not affect iNKT cell numbers since BN rats responded to α -Gal and CD1d protein levels at the cell surface of thymocytes were the same regardless of the CD1d-allelic form.

The analysis of the F1 generation of F344 and LEW rats indicated a co-dominant effect of the genes controlling iNKT cell frequencies. Studies with congenic NOD mice were crucial to determine the role SLAM proteins in the development of iNKT cells (Jordan et al., 2007). Hence, further analysis of F344/LEW F2 generations and congenic animals selected for elevated iNKT cell numbers may reveal other genes important for iNKT cell biology.

iNKT cell frequencies and α -Gal response do not only correlate among the studied inbred rat strains but also between mice and rats. Hence, cytokine release by mouse primary cells after α -Gal stimulation was much more elevated than cytokine release by F344 rats. In the mouse, a role for iNKT cells in controlling autoimmune diseases and infection has been reported. Nonetheless, depending on the experimental model, iNKT cells can exert opposite functions (Godfrey and Kronenberg, 2004). For example, they

can control, aggravate or have no effect in experimental autoimmune encephalomyelitis (EAE) conducted in mice (Furlan et al., 2003; Jahng et al., 2001; Miyamoto et al., 2001; Pal et al., 2001; Singh et al., 2001). Among the inbred rat strains studied here, the strains which are commonly used in organ specific autoimmune disease models seem to have no or very few iNKT cells (LEW, PVG and DA). In contrast, F344 rats, which showed the most elevated response to α -Gal and where relatively high numbers of iNKT cells were detected, is a strain resistant to the induction of EAE (Sun et al., 1999). Nonetheless, this is a mere correlation between α -Gal responsiveness (in LEW and F344 rats also iNKT cell numbers) and autoimmune disease models established in these strains. Obviously, adequate experiments should be carried out to investigate whether rat iNKT cells play a role in such situations. Bortell and colleagues found that α -Gal had no therapeutic effect in virus-inducible models of Type 1 diabetes carried out in BBDR and LEW.1WR1 rats (Chopra et al., 2009). The authors addressed IL-4 and IFN- γ cytokine release after 48 and 72 hours of α -Gal *ex vivo* stimulation only in splenocytes, but they neither analyzed whether the observed response was CD1d-restricted nor stained iNKT cells appropriately (Chopra et al., 2009). Thus the presence of iNKT cells in these strains should be investigated in order to interpret the failure of α -Gal to alter the diabetes outcome in these experiments.

Several similarities between rat and human iNKT cells which are not conserved in the mouse have been previously pointed out (Discussion section 4.8). In a similar way rat iNKT cells derived from F344 intrahepatic lymphocytes could be easily expanded after 7 days in culture where only α -Gal, but not additional cytokines, was added similar as it has been described with human PBMC cultures. In contrast, the expansion of mouse iNKT cells *in vitro* is complicated and needs various cytokines apart from the addition of antigen presenting cells (Watarai et al., 2008). Therefore, the culture and expansion of rat iNKT cells is not only very important for the analysis of rat iNKT cell-specific features (as previously discussed) but also offers an animal model very similar to humans. Thus these cultures provide the possibility to simulate therapies in the rat which are currently being investigated such as the use of *in vitro* expanded human iNKT cells to treat various types of cancer (Kunii et al., 2009).

4.11 NKR-P1⁺ T cells

In this study we have demonstrated that in the rat the majority of NKR-P1⁺ T cells are not stained by α -Gal-loaded rat CD1d oligomers. Indeed, in LEW rats where iNKT cells

were hardly detected if at all, the numbers of NKR-P1⁺ T cells observed in the spleen and in the liver were very similar to those of F344 rats (Fig. 35 and 36).

The expression of NKR-P1 receptors by non α -Gal-CD1d-reactive T cells has extensively been reported in human and mice (Godfrey et al., 2004). These cells can be: i) CD1d-restricted T cells bearing TCR α chains with gene segments different than AV14 (AV24 in humans) and AJ18 which recognize glycolipid antigens other than α -Gal (type II NKT cells) ii) a distinct T cell subset with a different invariant TCR restricted to another MHC-I like molecule: MR1 (Kawachi et al., 2006), and iii) also “conventional” MHC-restricted cells (Iwabuchi et al., 1998; Legendre et al., 1999; Slifka et al., 2000). Thus it will be interesting to learn which is the restriction element or elements of the T cells expressing NKR-P1 in the rat which are not reactive to α -Gal presented by CD1d. Among all the inbred rat strains analyzed in this study we observed very similar frequencies of NKR-P1-expressing T cells in the spleen and the liver, with the only exception of DA where the percentage of NKR-P1⁺ T cells expressing was reduced.

The expression of CD4 and CD8 coreceptors by NKR-P1⁺ T cells differed from that of NKR-P1⁻ T cells; in all the inbred rat strains the majority of these cells expressed CD8 β , even in BN inbred rats, where most of the NKR-P1⁻ T cells are CD4 positive cells. Moreover the proportion of DN cells among NKR-P1⁺ T cells was also higher compared to NKR-P1⁻ T cells. This different phenotype may reflect a distinct T cell lineage.

BV8 and BV16 usage by these NKR-P1 positive and negative T cell subsets was also addressed. Only small differences in the usage of these BV segments between the NKR-P1⁺ and NKR-P1⁻ T cells in the spleen and in the liver of all the inbred rat strains analyzed, except in the liver of F344 NKR-P1A⁺ T cells where, as discussed in the results section 3.8.3, the frequency of BV8S4⁺ T cells was increased. These results are in agreement with previous reports where these cells also have been analyzed (Badovinac et al., 1998; Brissette-Storkus et al., 1994; Knudsen et al., 1997; Matsuura et al., 2000; Pyz et al., 2006). Nonetheless, apart from this phenotypic characterization and from some additional *in vitro* analyses where a cytolytic activity was only observed after IL-2-mediated activation (Brissette-Storkus et al., 1994), little is known about the functions of these cells *in vivo*. Evidence for a role of rat NKR-P1⁺ T cells in promoting allograft acceptance has been provided in only one study by Kiyomoto and colleagues. In this study, liver irradiated allografts survived for a longer period when they were

reconstituted with total or Ig-depleted donor spleen cells than when they were reconstituted with NKR-P1 or TCR-depleted spleen cells (Kiyomoto et al., 2005). Other studies, without taking into account the misinterpretation of NKR-P1⁺ T cells being regarded as iNKT cells, have shown variations of NKR-P1⁺ T cell frequencies under different pathological conditions (Altomonte et al., 2009; Iwakoshi et al., 1999; Kattan et al., 2008; Shao et al., 2003). Nonetheless, none of these studies directly demonstrated the implication of these cells in the different pathological conditions. Thus in order to elucidate the functions and origin of these cells further analysis are required, beginning with the identification of the restriction element (or elements) of these cells.

REFERENCES

Altman, J.D., Moss, P.A., Goulder, P.J., Barouch, D.H., McHeyzer-Williams, M.G., Bell, J.I., McMichael, A.J., and Davis, M.M. (1996). Phenotypic analysis of antigen-specific T lymphocytes. *Science* 274, 94-96.

Altomonte, J., Wu, L., Meseck, M., Chen, L., Ebert, O., Garcia-Sastre, A., Fallon, J., Mandeli, J., and Woo, S.L. (2009). Enhanced oncolytic potency of vesicular stomatitis virus through vector-mediated inhibition of NK and NKT cells. *Cancer Gene Ther* 16, 266-278.

Amano, M., Baumgarth, N., Dick, M.D., Brossay, L., Kronenberg, M., Herzenberg, L.A., and Strober, S. (1998). CD1 expression defines subsets of follicular and marginal zone B cells in the spleen: beta 2-microglobulin-dependent and independent forms. *J Immunol* 161, 1710-1717.

Amprey, J.L., Im, J.S., Turco, S.J., Murray, H.W., Illarionov, P.A., Besra, G.S., Porcelli, S.A., and Spath, G.F. (2004). A subset of liver NK T cells is activated during *Leishmania donovani* infection by CD1d-bound lipophosphoglycan. *J Exp Med* 200, 895-904.

Angenieux, C., Salamero, J., Fricker, D., Cazenave, J.P., Goud, B., Hanau, D., and de La Salle, H. (2000). Characterization of CD1e, a third type of CD1 molecule expressed in dendritic cells. *J Biol Chem* 275, 37757-37764.

Arrenberg, P., Halder, R., Dai, Y., Maricic, I., and Kumar, V. (2010). Oligoclonality and innate-like features in the TCR repertoire of type II NKT cells reactive to a beta-linked self-glycolipid. *Proc Natl Acad Sci U S A* 107, 10984-10989.

Arstila, T.P., Casrouge, A., Baron, V., Even, J., Kanellopoulos, J., and Kourilsky, P. (1999). A direct estimate of the human alphabeta T cell receptor diversity. *Science* 286, 958-961.

Asmuss, A., Hofmann, K., Hochgrebe, T., Giegerich, G., Hunig, T., and Herrmann, T. (1996). Alleles of highly homologous rat T cell receptor beta-chain variable segments 8.2 and 8.4: strain-specific expression, reactivity to superantigens, and binding of the mAb R78. *J Immunol* 157, 4436-4441.

Aust, J.G., Gays, F., Mickiewicz, K.M., Buchanan, E., and Brooks, C.G. (2009). The expression and function of the NKR1P1 receptor family in C57BL/6 mice. *J Immunol* 183, 106-116.

Badovinac, V., Boggiano, C., Trajkovic, V., Frey, A.B., Vujanovic, N.L., Gold, D.P., Mostarica-Stojkovic, M., and Vukmanovic, S. (1998). Rat NKR-P1+ CD3+ T cells: selective proliferation in interleukin-2, diverse T-cell-receptor-Vbeta repertoire and polarized interferon-gamma expression. *Immunology* 95, 117-125.

- Behar, S.M., and Cardell, S. (2000). Diverse CD1d-restricted T cells: diverse phenotypes, and diverse functions. *Semin Immunol* 12, 551-560.
- Bendelac, A. (1995). Positive selection of mouse NK1+ T cells by CD1-expressing cortical thymocytes. *J Exp Med* 182, 2091-2096.
- Bendelac, A., Lantz, O., Quimby, M.E., Yewdell, J.W., Bennink, J.R., and Brutkiewicz, R.R. (1995). CD1 recognition by mouse NK1+ T lymphocytes. *Science* 268, 863-865.
- Bendelac, A., Savage, P.B., and Teyton, L. (2007). The biology of NKT cells. *Annu Rev Immunol* 25, 297-336.
- Benlagha, K., Weiss, A., Beavis, A., Teyton, L., and Bendelac, A. (2000). In vivo identification of glycolipid antigen-specific T cells using fluorescent CD1d tetramers. *J Exp Med* 191, 1895-1903.
- Berzins, S.P., Cochrane, A.D., Pellicci, D.G., Smyth, M.J., and Godfrey, D.I. (2005). Limited correlation between human thymus and blood NKT cell content revealed by an ontogeny study of paired tissue samples. *Eur J Immunol* 35, 1399-1407.
- Bezbradica, J.S., Hill, T., Stanic, A.K., Van Kaer, L., and Joyce, S. (2005). Commitment toward the natural T (iNKT) cell lineage occurs at the CD4+8+ stage of thymic ontogeny. *Proc Natl Acad Sci U S A* 102, 5114-5119.
- Bleicher, P.A., Balk, S.P., Hagen, S.J., Blumberg, R.S., Flotte, T.J., and Terhorst, C. (1990). Expression of murine CD1 on gastrointestinal epithelium. *Science* 250, 679-682.
- Blumberg, R.S., Terhorst, C., Bleicher, P., McDermott, F.V., Allan, C.H., Landau, S.B., Trier, J.S., and Balk, S.P. (1991). Expression of a nonpolymorphic MHC class I-like molecule, CD1D, by human intestinal epithelial cells. *J Immunol* 147, 2518-2524.
- Bonish, B., Jullien, D., Dutronc, Y., Huang, B.B., Modlin, R., Spada, F.M., Porcelli, S.A., and Nickoloff, B.J. (2000). Overexpression of CD1d by keratinocytes in psoriasis and CD1d-dependent IFN-gamma production by NK-T cells. *J Immunol* 165, 4076-4085.
- Borg, N.A., Wun, K.S., Kjer-Nielsen, L., Wilce, M.C., Pellicci, D.G., Koh, R., Besra, G.S., Bharadwaj, M., Godfrey, D.I., McCluskey, J., *et al.* (2007). CD1d-lipid-antigen recognition by the semi-invariant NKT T-cell receptor. *Nature* 448, 44-49.
- Bradbury, A., Belt, K.T., Neri, T.M., Milstein, C., and Calabi, F. (1988). Mouse CD1 is distinct from and co-exists with TL in the same thymus. *EMBO J* 7, 3081-3086.
- Braud, V.M., Allan, D.S., O'Callaghan, C.A., Soderstrom, K., D'Andrea, A., Ogg, G.S., Lazetic, S., Young, N.T., Bell, J.I., Phillips, J.H., *et al.* (1998). HLA-E binds to natural killer cell receptors CD94/NKG2A, B and C. *Nature* 391, 795-799.

Brigl, M., and Brenner, M.B. (2004). CD1: antigen presentation and T cell function. *Annu Rev Immunol* 22, 817-890.

Brigl, M., and Brenner, M.B. (2010). How invariant natural killer T cells respond to infection by recognizing microbial or endogenous lipid antigens. *Semin Immunol* 22, 79-86.

Brissette-Storkus, C., Kaufman, C.L., Pasewicz, L., Worsey, H.M., Lakomy, R., Ildstad, S.T., and Chambers, W.H. (1994). Characterization and function of the NKR-P1^{dim}/T cell receptor-alpha beta⁺ subset of rat T cells. *J Immunol* 152, 388-396.

Brochet, X., Lefranc, M.P., and Giudicelli, V. (2008). IMGT/V-QUEST: the highly customized and integrated system for IG and TR standardized V-J and V-D-J sequence analysis. *Nucleic Acids Res* 36, W503-508.

Broeren, C.P., Wauben, M.H., Lucassen, M.A., Van Meurs, M., Van Kooten, P.J., Boog, C.J., Claassen, E., and Van Eden, W. (1995). Activated rat T cells synthesize and express functional major histocompatibility class II antigens. *Immunology* 84, 193-201.

Brossay, L., Jullien, D., Cardell, S., Sydora, B.C., Burdin, N., Modlin, R.L., and Kronenberg, M. (1997). Mouse CD1 is mainly expressed on hemopoietic-derived cells. *J Immunol* 159, 1216-1224.

Burke, S., Landau, S., Green, R., Tseng, C.C., Nattakom, T., Canchis, W., Yang, L., Kaiserlian, D., Gspach, C., Balk, S., *et al.* (1994). Rat cluster of differentiation 1 molecule: expression on the surface of intestinal epithelial cells and hepatocytes. *Gastroenterology* 106, 1143-1149.

Calabi, F., Jarvis, J.M., Martin, L., and Milstein, C. (1989). Two classes of CD1 genes. *Eur J Immunol* 19, 285-292.

Canchis, P.W., Bhan, A.K., Landau, S.B., Yang, L., Balk, S.P., and Blumberg, R.S. (1993). Tissue distribution of the non-polymorphic major histocompatibility complex class I-like molecule, CD1d. *Immunology* 80, 561-565.

Cardell, S., Tangri, S., Chan, S., Kronenberg, M., Benoist, C., and Mathis, D. (1995). CD1-restricted CD4⁺ T cells in major histocompatibility complex class II-deficient mice. *J Exp Med* 182, 993-1004.

Carlyle, J.R., Mesci, A., Fine, J.H., Chen, P., Belanger, S., Tai, L.H., and Makrigiannis, A.P. (2008). Evolution of the Ly49 and Nkrp1 recognition systems. *Semin Immunol* 20, 321-330.

Carnaud, C., Lee, D., Donnars, O., Park, S.H., Beavis, A., Koezuka, Y., and Bendelac, A. (1999). Cutting edge: Cross-talk between cells of the innate immune system: NKT cells rapidly activate NK cells. *J Immunol* 163, 4647-4650.

Casrouge, A., Beaudoin, E., Dalle, S., Pannetier, C., Kanellopoulos, J., and Kourilsky, P. (2000). Size estimate of the alpha beta TCR repertoire of naive mouse splenocytes. *J Immunol* *164*, 5782-5787.

Cerundolo, V., Silk, J.D., Masri, S.H., and Salio, M. (2009). Harnessing invariant NKT cells in vaccination strategies. *Nat Rev Immunol* *9*, 28-38.

Colgan, S.P., Hershberg, R.M., Furuta, G.T., and Blumberg, R.S. (1999). Ligation of intestinal epithelial CD1d induces bioactive IL-10: critical role of the cytoplasmic tail in autocrine signaling. *Proc Natl Acad Sci U S A* *96*, 13938-13943.

Coquet, J.M., Chakravarti, S., Kyparissoudis, K., McNab, F.W., Pitt, L.A., McKenzie, B.S., Berzins, S.P., Smyth, M.J., and Godfrey, D.I. (2008). Diverse cytokine production by NKT cell subsets and identification of an IL-17-producing CD4-NK1.1- NKT cell population. *Proc Natl Acad Sci U S A* *105*, 11287-11292.

Crocker, P.R., Jefferies, W.A., Clark, S.J., Chung, L.P., and Gordon, S. (1987). Species heterogeneity in macrophage expression of the CD4 antigen. *J Exp Med* *166*, 613-618.

Crowe, N.Y., Uldrich, A.P., Kyparissoudis, K., Hammond, K.J., Hayakawa, Y., Sidobre, S., Keating, R., Kronenberg, M., Smyth, M.J., and Godfrey, D.I. (2003). Glycolipid antigen drives rapid expansion and sustained cytokine production by NK T cells. *J Immunol* *171*, 4020-4027.

Cui, J., Shin, T., Kawano, T., Sato, H., Kondo, E., Toura, I., Kaneko, Y., Koseki, H., Kanno, M., and Taniguchi, M. (1997). Requirement for Valpha14 NKT cells in IL-12-mediated rejection of tumors. *Science* *278*, 1623-1626.

Chen, H., Huang, H., and Paul, W.E. (1997). NK1.1+ CD4+ T cells lose NK1.1 expression upon in vitro activation. *J Immunol* *158*, 5112-5119.

Chen, X., Walker, A.K., Strahler, J.R., Simon, E.S., Tomanicek-Volk, S.L., Nelson, B.B., Hurley, M.C., Ernst, S.A., Williams, J.A., and Andrews, P.C. (2006). Organellar proteomics: analysis of pancreatic zymogen granule membranes. *Mol Cell Proteomics* *5*, 306-312.

Chen, Y.H., Wang, B., Chun, T., Zhao, L., Cardell, S., Behar, S.M., Brenner, M.B., and Wang, C.R. (1999). Expression of CD1d2 on thymocytes is not sufficient for the development of NK T cells in CD1d1-deficient mice. *J Immunol* *162*, 4560-4566.

Chopra, P., Diiorio, P., Pino, S.C., Wilson, S.B., Phillips, N.E., Mordes, J.P., Rossini, A.A., Greiner, D.L., Shultz, L.D., and Bortell, R. (2009). Failure of alpha-galactosylceramide to prevent diabetes in virus-inducible models of type 1 diabetes in the rat. *In Vivo* *23*, 195-201.

Chun, T., Page, M.J., Gapin, L., Matsuda, J.L., Xu, H., Nguyen, H., Kang, H.S., Stanic, A.K., Joyce, S., Koltun, W.A., *et al.* (2003). CD1d-expressing dendritic cells but not

thymic epithelial cells can mediate negative selection of NKT cells. *J Exp Med* 197, 907-918.

Chung, B., Aoukaty, A., Dutz, J., Terhorst, C., and Tan, R. (2005). Signaling lymphocytic activation molecule-associated protein controls NKT cell functions. *J Immunol* 174, 3153-3157.

Dal Porto, J., Johansen, T.E., Catipovic, B., Parfiit, D.J., Tuveson, D., Gether, U., Kozlowski, S., Fearon, D.T., and Schneck, J.P. (1993). A soluble divalent class I major histocompatibility complex molecule inhibits alloreactive T cells at nanomolar concentrations. *Proc Natl Acad Sci U S A* 90, 6671-6675.

Darmoise, A., Teneberg, S., Bouzonville, L., Brady, R.O., Beck, M., Kaufmann, S.H., and Winau, F. (2010). Lysosomal alpha-galactosidase controls the generation of self lipid antigens for natural killer T cells. *Immunity* 33, 216-228.

de la Salle, H., Mariotti, S., Angenieux, C., Gilleron, M., Garcia-Alles, L.F., Malm, D., Berg, T., Paoletti, S., Maitre, B., Mourey, L., *et al.* (2005). Assistance of microbial glycolipid antigen processing by CD1e. *Science* 310, 1321-1324.

Dellabona, P., Padovan, E., Casorati, G., Brockhaus, M., and Lanzavecchia, A. (1994). An invariant V alpha 24-J alpha Q/V beta 11 T cell receptor is expressed in all individuals by clonally expanded CD4-8- T cells. *J Exp Med* 180, 1171-1176.

Egawa, T., Eberl, G., Taniuchi, I., Benlagha, K., Geissmann, F., Hennighausen, L., Bendelac, A., and Littman, D.R. (2005). Genetic evidence supporting selection of the Valpha14i NKT cell lineage from double-positive thymocyte precursors. *Immunity* 22, 705-716.

Engel, I., Hammond, K., Sullivan, B.A., He, X., Taniuchi, I., Kappes, D., and Kronenberg, M. (2010). Co-receptor choice by V alpha14i NKT cells is driven by Th-POK expression rather than avoidance of CD8-mediated negative selection. *J Exp Med* 207, 1015-1029.

Esteban, L.M., Tsoutsman, T., Jordan, M.A., Roach, D., Poulton, L.D., Brooks, A., Naidenko, O.V., Sidobre, S., Godfrey, D.I., and Baxter, A.G. (2003). Genetic control of NKT cell numbers maps to major diabetes and lupus loci. *J Immunol* 171, 2873-2878.

Exley, M., Garcia, J., Balk, S.P., and Porcelli, S. (1997). Requirements for CD1d recognition by human invariant Valpha24+ CD4-CD8- T cells. *J Exp Med* 186, 109-120.

Exley, M., Garcia, J., Wilson, S.B., Spada, F., Gerdes, D., Tahir, S.M., Patton, K.T., Blumberg, R.S., Porcelli, S., Chott, A., *et al.* (2000). CD1d structure and regulation on human thymocytes, peripheral blood T cells, B cells and monocytes. *Immunology* 100, 37-47.

Fujii, S., Motohashi, S., Shimizu, K., Nakayama, T., Yoshiga, Y., and Taniguchi, M. (2010). Adjuvant activity mediated by iNKT cells. *Semin Immunol* 22, 97-102.

Fukumoto, T., McMaster, W.R., and Williams, A.F. (1982). Mouse monoclonal antibodies against rat major histocompatibility antigens. Two Ia antigens and expression of Ia and class I antigens in rat thymus. *Eur J Immunol* 12, 237-243.

Furlan, R., Bergami, A., Cantarella, D., Brambilla, E., Taniguchi, M., Dellabona, P., Casorati, G., and Martino, G. (2003). Activation of invariant NKT cells by alphaGalCer administration protects mice from MOG35-55-induced EAE: critical roles for administration route and IFN-gamma. *Eur J Immunol* 33, 1830-1838.

Gadola, S.D., Dulphy, N., Salio, M., and Cerundolo, V. (2002). Valpha24-JalphaQ-independent, CD1d-restricted recognition of alpha-galactosylceramide by human CD4(+) and CD8alphabeta(+) T lymphocytes. *J Immunol* 168, 5514-5520.

Gadola, S.D., Koch, M., Marles-Wright, J., Lissin, N.M., Shepherd, D., Matulis, G., Harlos, K., Villiger, P.M., Stuart, D.I., Jakobsen, B.K., *et al.* (2006a). Structure and binding kinetics of three different human CD1d-alpha-galactosylceramide-specific T cell receptors. *J Exp Med* 203, 699-710.

Gadola, S.D., Silk, J.D., Jeans, A., Illarionov, P.A., Salio, M., Besra, G.S., Dwek, R., Butters, T.D., Platt, F.M., and Cerundolo, V. (2006b). Impaired selection of invariant natural killer T cells in diverse mouse models of glycosphingolipid lysosomal storage diseases. *J Exp Med* 203, 2293-2303.

Godfrey, D.I., and Berzins, S.P. (2007). Control points in NKT-cell development. *Nat Rev Immunol* 7, 505-518.

Godfrey, D.I., and Kronenberg, M. (2004). Going both ways: immune regulation via CD1d-dependent NKT cells. *J Clin Invest* 114, 1379-1388.

Godfrey, D.I., MacDonald, H.R., Kronenberg, M., Smyth, M.J., and Van Kaer, L. (2004). NKT cells: what's in a name? *Nat Rev Immunol* 4, 231-237.

Godfrey, D.I., Rossjohn, J., and McCluskey, J. (2008). The fidelity, occasional promiscuity, and versatility of T cell receptor recognition. *Immunity* 28, 304-314.

Godfrey, D.I., Stankovic, S., and Baxter, A.G. (2010). Raising the NKT cell family. *Nat Immunol* 11, 197-206.

Greten, T.F., Slansky, J.E., Kubota, R., Soldan, S.S., Jaffee, E.M., Leist, T.P., Pardoll, D.M., Jacobson, S., and Schneck, J.P. (1998). Direct visualization of antigen-specific T cells: HTLV-1 Tax11-19-specific CD8(+) T cells are activated in peripheral blood and accumulate in cerebrospinal fluid from HAM/TSP patients. *Proc Natl Acad Sci U S A* 95, 7568-7573.

- Griewank, K., Borowski, C., Rietdijk, S., Wang, N., Julien, A., Wei, D.G., Mamchak, A.A., Terhorst, C., and Bendelac, A. (2007). Homotypic interactions mediated by Slamf1 and Slamf6 receptors control NKT cell lineage development. *Immunity* 27, 751-762.
- Guex, N., and Peitsch, M.C. (1997). SWISS-MODEL and the Swiss-PdbViewer: an environment for comparative protein modeling. *Electrophoresis* 18, 2714-2723.
- Gumperz, J.E., Miyake, S., Yamamura, T., and Brenner, M.B. (2002). Functionally distinct subsets of CD1d-restricted natural killer T cells revealed by CD1d tetramer staining. *J Exp Med* 195, 625-636.
- Guo, J., Hawwari, A., Li, H., Sun, Z., Mahanta, S.K., Littman, D.R., Krangel, M.S., and He, Y.W. (2002). Regulation of the TCRalpha repertoire by the survival window of CD4(+)CD8(+) thymocytes. *Nat Immunol* 3, 469-476.
- Hamad, A.R., O'Herrin, S.M., Lebowitz, M.S., Srikrishnan, A., Bieler, J., Schneck, J., and Pardoll, D. (1998). Potent T cell activation with dimeric peptide-major histocompatibility complex class II ligand: the role of CD4 coreceptor. *J Exp Med* 188, 1633-1640.
- Hammond, K.J., Pellicci, D.G., Poulton, L.D., Naidenko, O.V., Scalzo, A.A., Baxter, A.G., and Godfrey, D.I. (2001). CD1d-restricted NKT cells: an interstrain comparison. *J Immunol* 167, 1164-1173.
- Hashim, G., Vandenbark, A.A., Gold, D.P., Diamanduros, T., and Offner, H. (1991). T cell lines specific for an immunodominant epitope of human basic protein define an encephalitogenic determinant for experimental autoimmune encephalomyelitis-resistant LOU/M rats. *J Immunol* 146, 515-520.
- Hebell, T., Ahearn, J.M., and Fearon, D.T. (1991). Suppression of the immune response by a soluble complement receptor of B lymphocytes. *Science* 254, 102-105.
- Hermans, I.F., Silk, J.D., Gileadi, U., Salio, M., Mathew, B., Ritter, G., Schmidt, R., Harris, A.L., Old, L., and Cerundolo, V. (2003). NKT cells enhance CD4+ and CD8+ T cell responses to soluble antigen in vivo through direct interaction with dendritic cells. *J Immunol* 171, 5140-5147.
- Hou, R., Goloubeva, O., Neubergh, D.S., Strominger, J.L., and Wilson, S.B. (2003). Interleukin-12 and interleukin-2-induced invariant natural killer T-cell cytokine secretion and perforin expression independent of T-cell receptor activation. *Immunology* 110, 30-37.
- Hu, T., Simmons, A., Yuan, J., Bender, T.P., and Alberola-Ila, J. (2010). The transcription factor c-Myb primes CD4+CD8+ immature thymocytes for selection into the iNKT lineage. *Nat Immunol* 11, 435-441.

Ichimiya, S., Kikuchi, K., and Matsuura, A. (1994). Structural analysis of the rat homologue of CD1. Evidence for evolutionary conservation of the CD1D class and widespread transcription by rat cells. *J Immunol* *153*, 1112-1123.

Im, J.S., Arora, P., Bricard, G., Molano, A., Venkataswamy, M.M., Baine, I., Jerud, E.S., Goldberg, M.F., Baena, A., Yu, K.O., *et al.* (2009). Kinetics and cellular site of glycolipid loading control the outcome of natural killer T cell activation. *Immunity* *30*, 888-898.

Im, J.S., Tapinos, N., Chae, G.T., Illarionov, P.A., Besra, G.S., DeVries, G.H., Modlin, R.L., Sieling, P.A., Rambukkana, A., and Porcelli, S.A. (2006). Expression of CD1d molecules by human schwann cells and potential interactions with immunoregulatory invariant NK T cells. *J Immunol* *177*, 5226-5235.

Ishihara, S., Nieda, M., Kitayama, J., Osada, T., Yabe, T., Ishikawa, Y., Nagawa, H., Muto, T., and Juji, T. (1999). CD8(+)NKR-P1A (+)T cells preferentially accumulate in human liver. *Eur J Immunol* *29*, 2406-2413.

Iwabuchi, C., Iwabuchi, K., Nakagawa, K., Takayanagi, T., Nishihori, H., Tone, S., Ogasawara, K., Good, R.A., and Onoe, K. (1998). Intrathymic selection of NK1.1(+)alpha/beta T cell antigen receptor (TCR)+ cells in transgenic mice bearing TCR specific for chicken ovalbumin and restricted to I-Ad. *Proc Natl Acad Sci U S A* *95*, 8199-8204.

Iwakoshi, N.N., Greiner, D.L., Rossini, A.A., and Mordes, J.P. (1999). Diabetes prone BB rats are severely deficient in natural killer T cells. *Autoimmunity* *31*, 1-14.

Jahng, A., Maricic, I., Aguilera, C., Cardell, S., Halder, R.C., and Kumar, V. (2004). Prevention of autoimmunity by targeting a distinct, noninvariant CD1d-reactive T cell population reactive to sulfatide. *J Exp Med* *199*, 947-957.

Jahng, A.W., Maricic, I., Pedersen, B., Burdin, N., Naidenko, O., Kronenberg, M., Koezuka, Y., and Kumar, V. (2001). Activation of natural killer T cells potentiates or prevents experimental autoimmune encephalomyelitis. *J Exp Med* *194*, 1789-1799.

Jordan, M.A., Fletcher, J.M., Pellicci, D., and Baxter, A.G. (2007). Slamf1, the NKT cell control gene Nkt1. *J Immunol* *178*, 1618-1627.

Josien, R., Heslan, M., Soulillou, J.P., and Cuturi, M.C. (1997). Rat spleen dendritic cells express natural killer cell receptor protein 1 (NKR-P1) and have cytotoxic activity to select targets via a Ca²⁺-dependent mechanism. *J Exp Med* *186*, 467-472.

Kampinga, J., Kroese, F.G., Pol, G.H., Nieuwenhuis, P., Haag, F., Singh, P.B., Roser, B., and Aspinall, R. (1989). A monoclonal antibody to a determinant of the rat T cell antigen receptor expressed by a minor subset of T cells. *Int Immunol* *1*, 289-295.

Karadimitris, A., Gadola, S., Altamirano, M., Brown, D., Woolfson, A., Klenerman, P., Chen, J.L., Koezuka, Y., Roberts, I.A., Price, D.A., *et al.* (2001). Human CD1d-glycolipid tetramers generated by in vitro oxidative refolding chromatography. *Proc Natl Acad Sci U S A* 98, 3294-3298.

Kasai, K., Matsuura, A., Kikuchi, K., Hashimoto, Y., and Ichimiya, S. (1997). Localization of rat CD1 transcripts and protein in rat tissues--an analysis of rat CD1 expression by in situ hybridization and immunohistochemistry. *Clin Exp Immunol* 109, 317-322.

Kashiwase, K., Kikuchi, A., Ando, Y., Nicol, A., Porcelli, S.A., Tokunaga, K., Omine, M., Satake, M., Juji, T., Nieda, M., *et al.* (2003). The CD1d natural killer T-cell antigen presentation pathway is highly conserved between humans and rhesus macaques. *Immunogenetics* 54, 776-781.

Kasmar, A., Van Rhijn, I., and Moody, D.B. (2009). The evolved functions of CD1 during infection. *Curr Opin Immunol* 21, 397-403.

Katabami, S., Matsuura, A., Chen, H.Z., Imai, K., and Kikuchi, K. (1998). Structural organization of rat CD1 typifies evolutionarily conserved CD1D class genes. *Immunogenetics* 48, 22-31.

Kattan, O.M., Kasravi, F.B., Elford, E.L., Schell, M.T., and Harris, H.W. (2008). Apolipoprotein E-mediated immune regulation in sepsis. *J Immunol* 181, 1399-1408.

Kawachi, I., Maldonado, J., Strader, C., and Gilfillan, S. (2006). MR1-restricted V alpha 19i mucosal-associated invariant T cells are innate T cells in the gut lamina propria that provide a rapid and diverse cytokine response. *J Immunol* 176, 1618-1627.

Kawano, T., Cui, J., Koezuka, Y., Toura, I., Kaneko, Y., Motoki, K., Ueno, H., Nakagawa, R., Sato, H., Kondo, E., *et al.* (1997). CD1d-restricted and TCR-mediated activation of valpha14 NKT cells by glycosylceramides. *Science* 278, 1626-1629.

Kenna, T., Golden-Mason, L., Porcelli, S.A., Koezuka, Y., Hegarty, J.E., O'Farrelly, C., and Doherty, D.G. (2003). NKT cells from normal and tumor-bearing human livers are phenotypically and functionally distinct from murine NKT cells. *J Immunol* 171, 1775-1779.

Kenny, E., Mason, D., Saoudi, A., Pombo, A., and Ramirez, F. (2004). CD8 alpha is an activation marker for a subset of peripheral CD4 T cells. *Eur J Immunol* 34, 1262-1271.

Kim, H.S., Garcia, J., Exley, M., Johnson, K.W., Balk, S.P., and Blumberg, R.S. (1999). Biochemical characterization of CD1d expression in the absence of beta2-microglobulin. *J Biol Chem* 274, 9289-9295.

- Kinebuchi, M., and Matsuura, A. (2004). Rat T-cell receptor TRAV11 (Valpha14) genes: further evidence of extensive multiplicity with homogeneous CDR1 and diversified CDR2 by genomic contig and cDNA analysis. *Immunogenetics* 55, 756-762.
- Kinjo, Y., Wu, D., Kim, G., Xing, G.W., Poles, M.A., Ho, D.D., Tsuji, M., Kawahara, K., Wong, C.H., and Kronenberg, M. (2005). Recognition of bacterial glycosphingolipids by natural killer T cells. *Nature* 434, 520-525.
- Kiyomoto, T., Ito, T., Uchikoshi, F., Ohkawa, A., Akamaru, Y., Miao, G., Komoda, H., Nishida, T., and Matsuda, H. (2005). The potent role of graft-derived NKR-P1+TCRalpha+ T (NKT) cells in the spontaneous acceptance of rat liver allografts. *Transplantation* 80, 1749-1755.
- Knabel, M., Franz, T.J., Schiemann, M., Wulf, A., Villmow, B., Schmidt, B., Bernhard, H., Wagner, H., and Busch, D.H. (2002). Reversible MHC multimer staining for functional isolation of T-cell populations and effective adoptive transfer. *Nat Med* 8, 631-637.
- Knodel, M., Kuss, A.W., Lindemann, D., Berberich, I., and Schimpl, A. (1999). Reversal of Blimp-1-mediated apoptosis by A1, a member of the Bcl-2 family. *Eur J Immunol* 29, 2988-2998.
- Knudsen, E., Seierstad, T., Vaage, J.T., Naper, C., Benestad, H.B., Rolstad, B., and Maghazachi, A.A. (1997). Cloning, functional activities and in vivo tissue distribution of rat NKR-P1+ TCR alpha beta + cells. *Int Immunol* 9, 1043-1051.
- Koseki, H., Asano, H., Inaba, T., Miyashita, N., Moriwaki, K., Lindahl, K.F., Mizutani, Y., Imai, K., and Taniguchi, M. (1991). Dominant expression of a distinctive V14+ T-cell antigen receptor alpha chain in mice. *Proc Natl Acad Sci U S A* 88, 7518-7522.
- Koseki, H., Imai, K., Nakayama, F., Sado, T., Moriwaki, K., and Taniguchi, M. (1990). Homogenous junctional sequence of the V14+ T-cell antigen receptor alpha chain expanded in unprimed mice. *Proc Natl Acad Sci U S A* 87, 5248-5252.
- Kovalovsky, D., Uche, O.U., Eladad, S., Hobbs, R.M., Yi, W., Alonzo, E., Chua, K., Eidson, M., Kim, H.J., Im, J.S., *et al.* (2008). The BTB-zinc finger transcriptional regulator PLZF controls the development of invariant natural killer T cell effector functions. *Nat Immunol* 9, 1055-1064.
- Kroese, F.G., Butcher, E.C., Lalor, P.A., Stall, A.M., and Herzenberg, L.A. (1990). The rat B cell system: the anatomical localization of flow cytometry-defined B cell subpopulations. *Eur J Immunol* 20, 1527-1534.
- Kumararatne, D.S., Bazin, H., and MacLennan, I.C. (1981). Marginal zones: the major B cell compartment of rat spleens. *Eur J Immunol* 11, 858-864.

- Kunii, N., Horiguchi, S., Motohashi, S., Yamamoto, H., Ueno, N., Yamamoto, S., Sakurai, D., Taniguchi, M., Nakayama, T., and Okamoto, Y. (2009). Combination therapy of in vitro-expanded natural killer T cells and alpha-galactosylceramide-pulsed antigen-presenting cells in patients with recurrent head and neck carcinoma. *Cancer Sci* *100*, 1092-1098.
- Kveberg, L., Dai, K.Z., Westgaard, I.H., Daws, M.R., Fossum, S., Naper, C., and Vaage, J.T. (2009). Two major groups of rat NKR-P1 receptors can be distinguished based on chromosomal localization, phylogenetic analysis and Clr ligand binding. *Eur J Immunol* *39*, 541-551.
- Lacasse, J., and Martin, L.H. (1992). Detection of CD1 mRNA in Paneth cells of the mouse intestine by in situ hybridization. *J Histochem Cytochem* *40*, 1527-1534.
- Lantz, O., and Bendelac, A. (1994). An invariant T cell receptor alpha chain is used by a unique subset of major histocompatibility complex class I-specific CD4+ and CD4-8- T cells in mice and humans. *J Exp Med* *180*, 1097-1106.
- Lebowitz, M.S., O'Herrin, S.M., Hamad, A.R., Fahmy, T., Marguet, D., Barnes, N.C., Pardoll, D., Bieler, J.G., and Schneck, J.P. (1999). Soluble, high-affinity dimers of T-cell receptors and class II major histocompatibility complexes: biochemical probes for analysis and modulation of immune responses. *Cell Immunol* *192*, 175-184.
- Lee, P.T., Benlagha, K., Teyton, L., and Bendelac, A. (2002a). Distinct functional lineages of human V(alpha)24 natural killer T cells. *J Exp Med* *195*, 637-641.
- Lee, P.T., Putnam, A., Benlagha, K., Teyton, L., Gottlieb, P.A., and Bendelac, A. (2002b). Testing the NKT cell hypothesis of human IDDM pathogenesis. *J Clin Invest* *110*, 793-800.
- Lefranc, M.P. (2001). Nomenclature of the human T cell receptor genes. *Curr Protoc Immunol Appendix 1*, Appendix 10.
- Legendre, V., Boyer, C., Guerder, S., Arnold, B., Hammerling, G., and Schmitt-Verhulst, A.M. (1999). Selection of phenotypically distinct NK1.1+ T cells upon antigen expression in the thymus or in the liver. *Eur J Immunol* *29*, 2330-2343.
- Leite-De-Moraes, M.C., Hameg, A., Arnould, A., Machavoine, F., Koezuka, Y., Schneider, E., Herbelin, A., and Dy, M. (1999). A distinct IL-18-induced pathway to fully activate NK T lymphocytes independently from TCR engagement. *J Immunol* *163*, 5871-5876.
- Li, D., Chen, N., McMichael, A.J., Screaton, G.R., and Xu, X.N. (2008). Generation and characterisation of CD1d tetramer produced by a lentiviral expression system. *J Immunol Methods* *330*, 57-63.

- Li, J., Rabinovich, B.A., Hurren, R., Shannon, J., and Miller, R.G. (2003). Expression cloning and function of the rat NK activating and inhibitory receptors NKR-P1A and -P1B. *Int Immunol* 15, 411-416.
- Li, W., Kim, M.G., Gourley, T.S., McCarthy, B.P., Sant'Angelo, D.B., and Chang, C.H. (2005). An alternate pathway for CD4 T cell development: thymocyte-expressed MHC class II selects a distinct T cell population. *Immunity* 23, 375-386.
- Li, W., Sofi, M.H., Wei, D.G., Du, W., Gervay-Hague, J., Renukaradhya, G.J., Brutkiewicz, R.R., and Chang, C.H. (2009). MHC class II-expressing thymocytes suppress invariant NKT cell development. *Immunol Cell Biol* 87, 186-189.
- Lotter, H., Gonzalez-Roldan, N., Lindner, B., Winau, F., Isibasi, A., Moreno-Lafont, M., Ulmer, A.J., Holst, O., Tannich, E., and Jacobs, T. (2009). Natural killer T cells activated by a lipopeptidophosphoglycan from *Entamoeba histolytica* are critically important to control amebic liver abscess. *PLoS Pathog* 5, e1000434.
- Luhder, F., Huang, Y., Dennehy, K.M., Guntermann, C., Muller, I., Winkler, E., Kerkau, T., Ikemizu, S., Davis, S.J., Hanke, T., *et al.* (2003). Topological requirements and signaling properties of T cell-activating, anti-CD28 antibody superagonists. *J Exp Med* 197, 955-966.
- Makowska, A., Faizunnessa, N.N., Anderson, P., Midtvedt, T., and Cardell, S. (1999). CD1^{high} B cells: a population of mixed origin. *Eur J Immunol* 29, 3285-3294.
- Mallevaey, T., Scott-Browne, J.P., Matsuda, J.L., Young, M.H., Pellicci, D.G., Patel, O., Thakur, M., Kjer-Nielsen, L., Richardson, S.K., Cerundolo, V., *et al.* (2009). T cell receptor CDR2 beta and CDR3 beta loops collaborate functionally to shape the iNKT cell repertoire. *Immunity* 31, 60-71.
- Mandal, M., Chen, X.R., Alegre, M.L., Chiu, N.M., Chen, Y.H., Castano, A.R., and Wang, C.R. (1998). Tissue distribution, regulation and intracellular localization of murine CD1 molecules. *Mol Immunol* 35, 525-536.
- Matsuda, J.L., and Gapin, L. (2005). Developmental program of mouse Valpha14i NKT cells. *Curr Opin Immunol* 17, 122-130.
- Matsuda, J.L., Naidenko, O.V., Gapin, L., Nakayama, T., Taniguchi, M., Wang, C.R., Koezuka, Y., and Kronenberg, M. (2000). Tracking the response of natural killer T cells to a glycolipid antigen using CD1d tetramers. *J Exp Med* 192, 741-754.
- Matsui, K., Boniface, J.J., Steffner, P., Reay, P.A., and Davis, M.M. (1994). Kinetics of T-cell receptor binding to peptide/I-Ek complexes: correlation of the dissociation rate with T-cell responsiveness. *Proc Natl Acad Sci U S A* 91, 12862-12866.

Matsuura, A., Kinebuchi, M., Chen, H.Z., Katabami, S., Shimizu, T., Hashimoto, Y., Kikuchi, K., and Sato, N. (2000). NKT cells in the rat: organ-specific distribution of NK T cells expressing distinct V alpha 14 chains. *J Immunol* *164*, 3140-3148.

Mattner, J., Debord, K.L., Ismail, N., Goff, R.D., Cantu, C., 3rd, Zhou, D., Saint-Mezard, P., Wang, V., Gao, Y., Yin, N., *et al.* (2005). Exogenous and endogenous glycolipid antigens activate NKT cells during microbial infections. *Nature* *434*, 525-529.

Matulis, G., Sanderson, J.P., Lissin, N.M., Asparuhova, M.B., Bommineni, G.R., Schumperli, D., Schmidt, R.R., Villiger, P.M., Jakobsen, B.K., and Gadola, S.D. (2010). Innate-like control of human iNKT cell autoreactivity via the hypervariable CDR3beta loop. *PLoS Biol* *8*, e1000402.

McNab, F.W., Pellicci, D.G., Field, K., Besra, G., Smyth, M.J., Godfrey, D.I., and Berzins, S.P. (2007). Peripheral NK1.1 NKT cells are mature and functionally distinct from their thymic counterparts. *J Immunol* *179*, 6630-6637.

Melian, A., Geng, Y.J., Sukhova, G.K., Libby, P., and Porcelli, S.A. (1999). CD1 expression in human atherosclerosis. A potential mechanism for T cell activation by foam cells. *Am J Pathol* *155*, 775-786.

Mendiratta, S.K., Martin, W.D., Hong, S., Boesteanu, A., Joyce, S., and Van Kaer, L. (1997). CD1d1 mutant mice are deficient in natural T cells that promptly produce IL-4. *Immunity* *6*, 469-477.

Michel, M.L., Mendes-da-Cruz, D., Keller, A.C., Lochner, M., Schneider, E., Dy, M., Eberl, G., and Leite-de-Moraes, M.C. (2008). Critical role of ROR-gammat in a new thymic pathway leading to IL-17-producing invariant NKT cell differentiation. *Proc Natl Acad Sci U S A* *105*, 19845-19850.

Miyamoto, K., Miyake, S., and Yamamura, T. (2001). A synthetic glycolipid prevents autoimmune encephalomyelitis by inducing TH2 bias of natural killer T cells. *Nature* *413*, 531-534.

Mizoguchi, A., Mizoguchi, E., Takedatsu, H., Blumberg, R.S., and Bhan, A.K. (2002). Chronic intestinal inflammatory condition generates IL-10-producing regulatory B cell subset characterized by CD1d upregulation. *Immunity* *16*, 219-230.

Monzon-Casanova, E., Steiniger, B., Schweigle, S., Clemen, H., Zdzieblo, D., Starick, L., Muller, I., Wang, C.R., Rhost, S., Cardell, S., *et al.* (2010). CD1d expression in paneth cells and rat exocrine pancreas revealed by novel monoclonal antibodies which differentially affect NKT cell activation. *PLoS One* *5*.

Morita, M., Motoki, K., Akimoto, K., Natori, T., Sakai, T., Sawa, E., Yamaji, K., Kozuka, Y., Kobayashi, E., and Fukushima, H. (1995). Structure-activity relationship of alpha-galactosylceramides against B16-bearing mice. *J Med Chem* *38*, 2176-2187.

Mosser, D.D., Duchaine, J., and Martin, L.H. (1991). Biochemical and developmental characterization of the murine cluster of differentiation 1 antigen. *Immunology* 73, 298-303.

Neudorfer, J., Schmidt, B., Huster, K.M., Anderl, F., Schiemann, M., Holzappel, G., Schmidt, T., Germeroth, L., Wagner, H., Peschel, C., *et al.* (2007). Reversible HLA multimers (Streptamers) for the isolation of human cytotoxic T lymphocytes functionally active against tumor- and virus-derived antigens. *J Immunol Methods* 320, 119-131.

Nichols, K.E., Hom, J., Gong, S.Y., Ganguly, A., Ma, C.S., Cannons, J.L., Tangye, S.G., Schwartzberg, P.L., Koretzky, G.A., and Stein, P.L. (2005). Regulation of NKT cell development by SAP, the protein defective in XLP. *Nat Med* 11, 340-345.

Nieuwenhuis, E.E., Matsumoto, T., Lindenbergh, D., Willemsen, R., Kaser, A., Simons-Oosterhuis, Y., Brugman, S., Yamaguchi, K., Ishikawa, H., Aiba, Y., *et al.* (2009). Cd1d-dependent regulation of bacterial colonization in the intestine of mice. *J Clin Invest* 119, 1241-1250.

Oi, V.T., Morrison, S.L., Herzenberg, L.A., and Berg, P. (1983). Immunoglobulin gene expression in transformed lymphoid cells. *Proc Natl Acad Sci U S A* 80, 825-829.

Paget, C., Mallevaey, T., Speak, A.O., Torres, D., Fontaine, J., Sheehan, K.C., Capron, M., Ryffel, B., Faveeuw, C., Leite de Moraes, M., *et al.* (2007). Activation of invariant NKT cells by toll-like receptor 9-stimulated dendritic cells requires type I interferon and charged glycosphingolipids. *Immunity* 27, 597-609.

Pal, E., Tabira, T., Kawano, T., Taniguchi, M., Miyake, S., and Yamamura, T. (2001). Costimulation-dependent modulation of experimental autoimmune encephalomyelitis by ligand stimulation of V alpha 14 NK T cells. *J Immunol* 166, 662-668.

Park, S.H., Benlagha, K., Lee, D., Balish, E., and Bendelac, A. (2000). Unaltered phenotype, tissue distribution and function of Valpha14(+) NKT cells in germ-free mice. *Eur J Immunol* 30, 620-625.

Park, S.H., Roark, J.H., and Bendelac, A. (1998). Tissue-specific recognition of mouse CD1 molecules. *J Immunol* 160, 3128-3134.

Pasquier, B., Yin, L., Fondaneche, M.C., Relouzat, F., Bloch-Queyrat, C., Lambert, N., Fischer, A., de Saint-Basile, G., and Latour, S. (2005). Defective NKT cell development in mice and humans lacking the adapter SAP, the X-linked lymphoproliferative syndrome gene product. *J Exp Med* 201, 695-701.

Pellicci, D.G., Hammond, K.J., Uldrich, A.P., Baxter, A.G., Smyth, M.J., and Godfrey, D.I. (2002). A natural killer T (NKT) cell developmental pathway involving a thymus-dependent NK1.1(-)CD4(+) CD1d-dependent precursor stage. *J Exp Med* 195, 835-844.

Pellicci, D.G., Patel, O., Kjer-Nielsen, L., Pang, S.S., Sullivan, L.C., Kyparissoudis, K., Brooks, A.G., Reid, H.H., Gras, S., Lucet, I.S., *et al.* (2009). Differential recognition of CD1d-alpha-galactosyl ceramide by the V beta 8.2 and V beta 7 semi-invariant NKT T cell receptors. *Immunity* 31, 47-59.

Pellicci, D.G., Uldrich, A.P., Kyparissoudis, K., Crowe, N.Y., Brooks, A.G., Hammond, K.J., Sidobre, S., Kronenberg, M., Smyth, M.J., and Godfrey, D.I. (2003). Intrathymic NKT cell development is blocked by the presence of alpha-galactosylceramide. *Eur J Immunol* 33, 1816-1823.

Pietschmann, T., Heinkelein, M., Heldmann, M., Zentgraf, H., Rethwilm, A., and Lindemann, D. (1999). Foamy virus capsids require the cognate envelope protein for particle export. *J Virol* 73, 2613-2621.

Porubsky, S., Speak, A.O., Luckow, B., Cerundolo, V., Platt, F.M., and Grone, H.J. (2007). Normal development and function of invariant natural killer T cells in mice with isoglobotrihexosylceramide (iGb3) deficiency. *Proc Natl Acad Sci U S A* 104, 5977-5982.

Prigozy, T.I., Naidenko, O., Qasba, P., Elewaut, D., Brossay, L., Khurana, A., Natori, T., Koezuka, Y., Kulkarni, A., and Kronenberg, M. (2001). Glycolipid antigen processing for presentation by CD1d molecules. *Science* 291, 664-667.

Pyz, E. (2004). Identification of rat NKT cells and molecular analysis of their surface receptor mediated activation In Institute for Virology and Immunobiology (Würzburg, University of Würzburg).

Pyz, E., Naidenko, O., Miyake, S., Yamamura, T., Berberich, I., Cardell, S., Kronenberg, M., and Herrmann, T. (2006). The complementarity determining region 2 of BV8S2 (V beta 8.2) contributes to antigen recognition by rat invariant NKT cell TCR. *J Immunol* 176, 7447-7455.

Rindler, M.J., Xu, C.F., Gumper, I., Smith, N.N., and Neubert, T.A. (2007). Proteomic analysis of pancreatic zymogen granules: identification of new granule proteins. *J Proteome Res* 6, 2978-2992.

Roark, J.H., Park, S.H., Jayawardena, J., Kavita, U., Shannon, M., and Bendelac, A. (1998). CD1.1 expression by mouse antigen-presenting cells and marginal zone B cells. *J Immunol* 160, 3121-3127.

Rocha-Campos, A.C., Melki, R., Zhu, R., Deruytter, N., Damotte, D., Dy, M., Herbelin, A., and Garchon, H.J. (2006). Genetic and functional analysis of the Nkt1 locus using congenic NOD mice: improved Valpha14-NKT cell performance but failure to protect against type 1 diabetes. *Diabetes* 55, 1163-1170.

Rodgers, J.R., and Cook, R.G. (2005). MHC class Ib molecules bridge innate and acquired immunity. *Nat Rev Immunol* 5, 459-471.

Roy, K.C., Maricic, I., Khurana, A., Smith, T.R., Halder, R.C., and Kumar, V. (2008). Involvement of secretory and endosomal compartments in presentation of an exogenous self-glycolipid to type II NKT cells. *J Immunol* 180, 2942-2950.

Ru, W., and Peijie, C. (2009). Modulation of NKT cells and Th1/Th2 imbalance after alpha-GalCer treatment in progressive load-trained rats. *Int J Biol Sci* 5, 338-343.

Rymarchyk, S.L., Lowenstein, H., Mayette, J., Foster, S.R., Damby, D.E., Howe, I.W., Aktan, I., Meyer, R.E., Poynter, M.E., and Boyson, J.E. (2008). Widespread natural variation in murine natural killer T-cell number and function. *Immunology* 125, 331-343.

Sagiv, Y., Hudspeth, K., Mattner, J., Schrantz, N., Stern, R.K., Zhou, D., Savage, P.B., Teyton, L., and Bendelac, A. (2006). Cutting edge: impaired glycosphingolipid trafficking and NKT cell development in mice lacking Niemann-Pick type C1 protein. *J Immunol* 177, 26-30.

Salamone, M.C., Rabinovich, G.A., Mendiguren, A.K., Salamone, G.V., and Fainboim, L. (2001). Activation-induced expression of CD1d antigen on mature T cells. *J Leukoc Biol* 69, 207-214.

Salio, M., Speak, A.O., Shepherd, D., Polzella, P., Illarionov, P.A., Veerapen, N., Besra, G.S., Platt, F.M., and Cerundolo, V. (2007). Modulation of human natural killer T cell ligands on TLR-mediated antigen-presenting cell activation. *Proc Natl Acad Sci U S A* 104, 20490-20495.

Savage, A.K., Constantinides, M.G., Han, J., Picard, D., Martin, E., Li, B., Lantz, O., and Bendelac, A. (2008). The transcription factor PLZF directs the effector program of the NKT cell lineage. *Immunity* 29, 391-403.

Scott-Browne, J.P., Matsuda, J.L., Mallevaey, T., White, J., Borg, N.A., McCluskey, J., Rossjohn, J., Kappler, J., Marrack, P., and Gapin, L. (2007). Germline-encoded recognition of diverse glycolipids by natural killer T cells. *Nat Immunol* 8, 1105-1113.

Scriba, A., Schneider, M., Grau, V., van der Meide, P.H., and Steiniger, B. (1997). Rat monocytes up-regulate NKR-P1A and down-modulate CD4 and CD43 during activation in vivo: monocyte subpopulations in normal and IFN-gamma-treated rats. *J Leukoc Biol* 62, 741-752.

Schatz, P.J. (1993). Use of peptide libraries to map the substrate specificity of a peptide-modifying enzyme: a 13 residue consensus peptide specifies biotinylation in *Escherichia coli*. *Biotechnology (N Y)* 11, 1138-1143.

Schiemann, M. (2005). Ex-vivo-Analyse antigen-spezifischer CD4-1hn+-T-Zell-Antworten im Infektionsmodell der murinen Listeriose (Technische Universitaet Bergakademie Freiberg).

Schneck, J., Slansky, J. E., O'Herrin, S.M. and Greten, T. F. (2000). Current protocols in immunology Vol 5 (John Wiley & Sons, Inc.).

Schneider, C., Newman, R.A., Sutherland, D.R., Asser, U., and Greaves, M.F. (1982). A one-step purification of membrane proteins using a high efficiency immunomatrix. *J Biol Chem* 257, 10766-10769.

Schrantz, N., Sagiv, Y., Liu, Y., Savage, P.B., Bendelac, A., and Teyton, L. (2007). The Niemann-Pick type C2 protein loads isoglobotrihexosylceramide onto CD1d molecules and contributes to the thymic selection of NKT cells. *J Exp Med* 204, 841-852.

Schumann, J., Voyle, R.B., Wei, B.Y., and MacDonald, H.R. (2003). Cutting edge: influence of the TCR V beta domain on the avidity of CD1d:alpha-galactosylceramide binding by invariant V alpha 14 NKT cells. *J Immunol* 170, 5815-5819.

Shao, H., Van Kaer, L., Sun, S.L., Kaplan, H.J., and Sun, D. (2003). Infiltration of the inflamed eye by NKT cells in a rat model of experimental autoimmune uveitis. *J Autoimmun* 21, 37-45.

Silk, J.D., Salio, M., Brown, J., Jones, E.Y., and Cerundolo, V. (2008). Structural and functional aspects of lipid binding by CD1 molecules. *Annu Rev Cell Dev Biol* 24, 369-395.

Sim, B.C., Holmberg, K., Sidobre, S., Naidenko, O., Niederberger, N., Marine, S.D., Kronenberg, M., and Gascoigne, N.R. (2003). Surprisingly minor influence of TRAV11 (Valpha14) polymorphism on NK T-receptor mCD1/alpha-galactosylceramide binding kinetics. *Immunogenetics* 54, 874-883.

Singh, A.K., Wilson, M.T., Hong, S., Olivares-Villagomez, D., Du, C., Stanic, A.K., Joyce, S., Sriram, S., Koezuka, Y., and Van Kaer, L. (2001). Natural killer T cell activation protects mice against experimental autoimmune encephalomyelitis. *J Exp Med* 194, 1801-1811.

Slifka, M.K., Pagarigan, R.R., and Whitton, J.L. (2000). NK markers are expressed on a high percentage of virus-specific CD8+ and CD4+ T cells. *J Immunol* 164, 2009-2015.

Smith, L.R., Kono, D.H., and Theofilopoulos, A.N. (1991). Complexity and sequence identification of 24 rat V beta genes. *J Immunol* 147, 375-379.

Smyth, M.J., Crowe, N.Y., Hayakawa, Y., Takeda, K., Yagita, H., and Godfrey, D.I. (2002). NKT cells - conductors of tumor immunity? *Curr Opin Immunol* 14, 165-171.

Soneoka, Y., Cannon, P.M., Ramsdale, E.E., Griffiths, J.C., Romano, G., Kingsman, S.M., and Kingsman, A.J. (1995). A transient three-plasmid expression system for the production of high titer retroviral vectors. *Nucleic Acids Res* 23, 628-633.

Spada, F.M., Borriello, F., Sugita, M., Watts, G.F., Koezuka, Y., and Porcelli, S.A. (2000). Low expression level but potent antigen presenting function of CD1d on monocyte lineage cells. *Eur J Immunol* 30, 3468-3477.

Stanic, A.K., De Silva, A.D., Park, J.J., Sriram, V., Ichikawa, S., Hirabayashi, Y., Hayakawa, K., Van Kaer, L., Brutkiewicz, R.R., and Joyce, S. (2003). Defective presentation of the CD1d1-restricted natural Va14Ja18 NKT lymphocyte antigen caused by beta-D-glucosylceramide synthase deficiency. *Proc Natl Acad Sci U S A* 100, 1849-1854.

Steiniger, B., Timphus, E.M., and Barth, P.J. (2006). The splenic marginal zone in humans and rodents: an enigmatic compartment and its inhabitants. *Histochem Cell Biol* 126, 641-648.

Sun, D., Whitaker, J.N., and Wilson, D.B. (1999). Regulatory T cells in experimental allergic encephalomyelitis. III. Comparison of disease resistance in Lewis and Fischer 344 rats. *Eur J Immunol* 29, 1101-1106.

Takahashi, T., Chiba, S., Nieda, M., Azuma, T., Ishihara, S., Shibata, Y., Juji, T., and Hirai, H. (2002). Cutting edge: analysis of human V alpha 24+CD8+ NK T cells activated by alpha-galactosylceramide-pulsed monocyte-derived dendritic cells. *J Immunol* 168, 3140-3144.

Torres-Nagel, N., Deutschlander, A., Herrmann, T., Arden, B., and Hunig, T. (1997). Control of TCR V alpha-mediated positive repertoire selection and alloreactivity by differential J alpha usage and CDR3 alpha composition. *Int Immunol* 9, 1441-1452.

Torres-Nagel, N.E., Gold, D.P., and Hunig, T. (1993). Identification of rat Tcrb-V8.2, 8.5, and 10 gene products by monoclonal antibodies. *Immunogenetics* 37, 305-308.

Uldrich, A.P., Crowe, N.Y., Kyparissoudis, K., Pellicci, D.G., Zhan, Y., Lew, A.M., Bouillet, P., Strasser, A., Smyth, M.J., and Godfrey, D.I. (2005). NKT cell stimulation with glycolipid antigen in vivo: costimulation-dependent expansion, Bim-dependent contraction, and hyporesponsiveness to further antigenic challenge. *J Immunol* 175, 3092-3101.

van den Berg, T.K., Puklavec, M.J., Barclay, A.N., and Dijkstra, C.D. (2001). Monoclonal antibodies against rat leukocyte surface antigens. *Immunol Rev* 184, 109-116.

Venkataswamy, M.M., and Porcelli, S.A. (2010). Lipid and glycolipid antigens of CD1d-restricted natural killer T cells. *Semin Immunol* 22, 68-78.

Wang, Z., Raifu, M., Howard, M., Smith, L., Hansen, D., Goldsby, R., and Ratner, D. (2000). Universal PCR amplification of mouse immunoglobulin gene variable regions: the design of degenerate primers and an assessment of the effect of DNA polymerase 3' to 5' exonuclease activity. *J Immunol Methods* 233, 167-177.

Watarai, H., Nakagawa, R., Omori-Miyake, M., Dashtsoodol, N., and Taniguchi, M. (2008). Methods for detection, isolation and culture of mouse and human invariant NKT cells. *Nat Protoc* 3, 70-78.

Wei, D.G., Lee, H., Park, S.H., Beaudoin, L., Teyton, L., Lehuen, A., and Bendelac, A. (2005). Expansion and long-range differentiation of the NKT cell lineage in mice expressing CD1d exclusively on cortical thymocytes. *J Exp Med* 202, 239-248.

Wilson, M.T., Johansson, C., Olivares-Villagomez, D., Singh, A.K., Stanic, A.K., Wang, C.R., Joyce, S., Wick, M.J., and Van Kaer, L. (2003). The response of natural killer T cells to glycolipid antigens is characterized by surface receptor down-modulation and expansion. *Proc Natl Acad Sci U S A* 100, 10913-10918.

Wun, K.S., Borg, N.A., Kjer-Nielsen, L., Beddoe, T., Koh, R., Richardson, S.K., Thakur, M., Howell, A.R., Scott-Browne, J.P., Gapin, L., *et al.* (2008). A minimal binding footprint on CD1d-glycolipid is a basis for selection of the unique human NKT TCR. *J Exp Med* 205, 939-949.

Yanaba, K., Bouaziz, J.D., Haas, K.M., Poe, J.C., Fujimoto, M., and Tedder, T.F. (2008). A regulatory B cell subset with a unique CD1dhiCD5+ phenotype controls T cell-dependent inflammatory responses. *Immunity* 28, 639-650.

Yasuda, N., Masuda, K., Tsukui, T., Teng, A., and Ishii, Y. (2009). Identification of canine natural CD3-positive T cells expressing an invariant T-cell receptor alpha chain. *Vet Immunol Immunopathol* 132, 224-231.

Yuan, W., Qi, X., Tsang, P., Kang, S.J., Illarionov, P.A., Besra, G.S., Gumperz, J., and Cresswell, P. (2007). Saposin B is the dominant saposin that facilitates lipid binding to human CD1d molecules. *Proc Natl Acad Sci U S A* 104, 5551-5556.

Yue, S.C., Shaulov, A., Wang, R., Balk, S.P., and Exley, M.A. (2005). CD1d ligation on human monocytes directly signals rapid NF-kappaB activation and production of bioactive IL-12. *Proc Natl Acad Sci U S A* 102, 11811-11816.

Zhang, P., Li, D., Stewart-Jones, G., Shao, X., Zhang, Y., Chen, Q., Li, Y., He, Y.W., Xu, X.N., and Zhang, H.T. (2009). A single amino acid defines cross-species reactivity of tree shrew (*Tupaia belangeri*) CD1d to human invariant natural killer T (iNKT) cells. *Immunology* 128, 500-510.

Zhou, D., Cantu, C., 3rd, Sagiv, Y., Schrantz, N., Kulkarni, A.B., Qi, X., Mahuran, D.J., Morales, C.R., Grabowski, G.A., Benlagha, K., *et al.* (2004a). Editing of CD1d-bound lipid antigens by endosomal lipid transfer proteins. *Science* 303, 523-527.

Zhou, D., Mattner, J., Cantu, C., 3rd, Schrantz, N., Yin, N., Gao, Y., Sagiv, Y., Hudspeth, K., Wu, Y.P., Yamashita, T., *et al.* (2004b). Lysosomal glycosphingolipid recognition by NKT cells. *Science* 306, 1786-1789.

Zimmer, M.I., Colmone, A., Felio, K., Xu, H., Ma, A., and Wang, C.R. (2006). A cell-type specific CD1d expression program modulates invariant NKT cell development and function. *J Immunol* *176*, 1421-1430.

Zimmer, M.I., Nguyen, H.P., Wang, B., Xu, H., Colmone, A., Felio, K., Choi, H.J., Zhou, P., Alegre, M.L., and Wang, C.R. (2009). Polymorphisms in CD1d affect antigen presentation and the activation of CD1d-restricted T cells. *Proc Natl Acad Sci U S A* *106*, 1909-1914.

Zinkernagel, R.M., and Doherty, P.C. (1974). Restriction of in vitro T cell-mediated cytotoxicity in lymphocytic choriomeningitis within a syngeneic or semiallogeneic system. *Nature* *248*, 701-702.

ABBREVIATIONS

Ab	Antibody
α -Gal	α -Galactosylceramide
APC	Antigen presenting cell
APCy	Allophycocyanin
β 2m	β 2-microglobulin
β -Gal	β -Galactosylceramide
BSA	Bovine serum albumin
BSS	Balanced salt solution
CD	Cluster of differentiation
cDNA	Complementary DNA
CDR	Complementary determining region
ConA	Concanavalin A
Ct	Cycle threshold
cTECs	Cortical thymic epithelial cells
D α M-PE	PE labeled donkey anti-mouse IgG F(ab') ₂ fragment
D α M-FITC	FITC labeled donkey anti-mouse IgG F(ab') ₂ fragment
ddNTP	Dideoxynucleotide
DMSO	Dimethyl sulfoxide
DN	Double negative
DNA	Deoxyribonucleic acid
dNTP	Deoxynucleotide
DP	Double positive
EAE	Experimental autoimmune encephalomyelitis
FACS	Fluorescence activated cell scan
FCS	Fetal calf serum
FITC	Fluorescein Isothiocyanate
FSC	Forward scatter
GBN	GenBank accession number
HRP	Horseradish peroxidase
IFN	Interferon
Ig	Immunoglobulin
IHLs	Intrahepatic lymphocytes

IL	Interleukin
kDa	Kilo dalton
M	Molar
mAb	Monoclonal antibody
MFI	Mean fluorescence intensity
MHC	Major histocompatibility complex
min	Minutes
mRNA	Messenger RNA
NK cell	Natural killer cell
PBCs	Peripheral blood cells
PBS	Phosphate buffered saline
PBMCs	Peripheral blood mononuclear cells
PCR	Polymerase chain reaction
PE	Phycoerythrin
rcf	Relative centrifugal force
RNA	Ribonucleic acid
rpm	Revolutions per minute
RT	Reverse transcriptase
SA	Streptavidin
SAP	SLAM adaptor protein
SD	Standard deviation
SLAM	Signaling lymphocytic activation molecules
SSC	Side scatter
TCR	T cell receptor

CURRICULUM VITAE

Personal Data

Name: Elisa Monzón Casanova
Place and date of birth: Huesca, Spain; September 12th, 1982
Nationality: Spanish
Marital Status: Single

Contact Information

Address: Institute for Virology and Immunobiology
University of Würzburg
Versbacher Str. 7
97078 Würzburg
Germany
Phone number: +49 (0)931 201 49124
Email address: elisa.monzon-casanova@uni-wuerzburg.de

Education

Sept. 2000 - Sept. 2005 Graduate in Biology, Specialised in Sanitary Biology
University of Barcelona, Barcelona, Spain
Sept. 2005 - July 2006 Master in Experimental Biology
Degree obtained from the University of Barcelona,
Barcelona, Spain; work performed in the University of
Würzburg, Würzburg, Germany; under the direction of
Prof. Dr. Thomas Herrmann
Thesis title: Analysis of the expression of rat MHC class II
molecules
Since Aug. 2006 PhD
University of Würzburg, Würzburg, Germany
Thesis title: Rat iNKT cells: phenotype and function
Thesis advisor: Prof. Dr. Thomas Herrmann

Publications

Monzon-Casanova, E., Steiniger, B., Schweigle, S., Clemen, H., Zdzieblo, D., Starick, L., Muller, I., Wang, C.R., Rhost, S., Cardell, S., Pyz, E. and Herrmann, T. (2010). CD1d expression in paneth cells and rat exocrine pancreas revealed by novel monoclonal antibodies which differentially affect NKT cell activation. *PLoS One* 5 (9): e13089

Dlaske, H., Karauzum, H., **Monzon-Casanova, E.**, Rudolf, R., Starick, L., Muller, I., Wildner, G., Diedrichs-Mohring, M., Koch, N., Miyoshi-Akiyama, T., Uchiyama, T., Wonigeit, K., Fleischer, B., Overbeck, S., Rink, L. and Herrmann, T. (2009). Superantigen-presentation by rat major histocompatibility complex class II molecules RT1.B1 and RT1.D1. *Immunology* 128, e572-581

Stipends and Grants

Sept. 2004 - July 2005	ERASMUS Stipend
Aug. 2006 - Aug. 2009	Doctoral Stipend from the DFG (German Research Foundation)-sponsored the Graduate College 520 Immunomodulation
Sept. 2009 - Feb. 2010	DAAD-STIBET Stipend
Aug. 2010	Travel Grant from the German Society of Immunology to attend the 40 th Annual Conference of the German Society of Immunology, in Leipzig, Germany
Nov. 2010	Travel Grant from the German Society of Immunology to attend the Keystone Symposia: NK and NKT Cell Biology: Specificity and Redundancy of Innate Responses

Participation in Scientific Conferences

3 - 6 Sept. 2006	1 st Joint Meeting of European National Societies of Immunology; Paris, France Talk: RT1-Db2: Identification and first functional analysis of a new non-polymorphic MHC class II molecule
26 - 28 Feb. 2007	2 nd Göttingen Workshop on Immunogenetics; Göttingen, Germany Talk: RT1-Db2: Identification and first functional analysis of a new non-polymorphic MHC class II molecule
5 - 8 Sept. 2007	37 th Annual Meeting of the German Society of Immunology; Heidelberg, Germany Poster: RT1-Db2: Identification and first functional analysis of a new non-polymorphic MHC class II molecule
4 - 11 May 2008	3 rd ENII-MUGEN Immunology Summer School; Sardinia, Italy Talk and Poster: RT1-Db2: Identification and first functional analysis of a new non-polymorphic MHC class II molecule

3 - 6 Sept. 2008	<p>Joint Annual Meeting of the German and Austrian Societies of Immunology; Vienna, Austria</p> <p>Poster 1: Rat and mouse CD1d: a comparison using novel monoclonal antibodies</p> <p>Poster 2: Identification and first functional analysis of novel MHC class II molecules: RT1-Db2 and H2-Eb2</p>
26 - 27 Mar. 2009	<p>4th International Symposium organized by the Students of GSLS of the University of Würzburg; Würzburg, Germany</p> <p>Talk: iNKT cells: a rat is a rat and not a big mouse</p>
20 - 24 Apr. 2009	<p>EMBO Conference: Tackling and Imaging the Complexity of the Immune Systems; Sardinia, Italy</p> <p>Poster: Rat iNKT cells: phenotype and function</p>
13 - 16 Sept. 2009	<p>2nd European Congress of Immunology; Berlin, Germany</p> <p>Talk and Poster 1: Identification and first functional analysis of novel MHC class II molecules: RT1-Db2 and H2-Eb2</p> <p>Poster 1: Rat vs. Mouse iNKT cells: alike <i>in silico</i> but different <i>in vivo</i></p>
22 - 25 Sept. 2010	<p>40th Annual Conference of the German Society of Immunology; Leipzig, Germany</p> <p>Poster: Direct identification of iNKT cells and analysis of expression and function of CD1d in the rat</p>

Additional activities

July - Aug. 2004	<p>Practical training</p> <p>Clinic Hospital Lozano Bielsa, Unidad Mixta de Investigación</p> <p>University of Zaragoza, Zaragoza, Spain</p>
Sept. 2004 - July 2005	<p>ERASMUS study exchange</p> <p>University of Würzburg, Würzburg, Germany</p>
Sept. 2006 - Oct. 2007	<p>Organization of the 3rd International Symposium</p> <p>Organized by the Students of the Graduate School of Life Sciences: "Drilling into Life's Depths – Innovative Techniques in Molecular Biology"</p> <p>University of Würzburg, Würzburg, Germany</p>
May 2007 - May 2009	<p>Student Speaker of the DFG (German Research Council)-sponsored Graduate College 520 Immunomodulation</p>
Since Dec. 2007	<p>Member of the German Society for Immunology</p>

Affidavit
(Eidesstattliche Erklärung)

I hereby declare that my thesis entitled Rat iNKT Cells: Phenotype and Function is the result of my own work. I did not receive any help or support from commercial consultants. All sources and / or materials applied are listed and specified in the thesis.

Furthermore, I verify that this thesis has not yet been submitted as part of another examination process neither in identical nor in similar form.

Würzburg.....

Date

Signature